

**UCLA**

**UCLA Electronic Theses and Dissertations**

**Title**

Quantum Chain Reactions and  $\delta$ -Hydrogen Abstraction of Aromatic Ketones: Insights into Solid to Solid Transformations and Efficiency in Crystals

**Permalink**

<https://escholarship.org/uc/item/71v943nz>

**Author**

Nielsen, Amy

**Publication Date**

2014

Peer reviewed|Thesis/dissertation

UNIVERSITY OF CALIFORNIA

Los Angeles

Quantum Chain Reactions and  $\delta$ -Hydrogen Abstraction of Aromatic Ketones:  
Insights into Solid to Solid Transformations and Efficiency in Crystals

A dissertation submitted in partial satisfaction of the  
requirements for the degree Doctor of Philosophy  
in Chemistry

by

Amy Nielsen

2014



## ABSTRACT OF THE DISSERTATION

Quantum Chain Reactions and  $\delta$ -Hydrogen Abstraction of Aromatic Ketones:  
Insights into Solid to Solid Transformations and Efficiency in Crystals

By

Amy Esther Nielsen

Doctor of Philosophy in Chemistry

University of California, Los Angeles 2014

Professor Miguel A. Garcia-Garibay, Chair

Solid state photoreactions of ketones have long been of equal fascination and frustration for researchers. In the 19<sup>th</sup> century, Trommsdorff reported on his observations of the yellowing and cracking of crystals of  $\alpha$ -santonin when they were exposed to ambient sunlight. While this reaction took place with great visual effect, it was not until many years later that the cause of the bursting of the crystals was more fully elucidated. Solid-state photochemistry has generally been plagued with issues stemming from an inability to rationally design photoreactions as, until recently, few analytical methods were available for analysis of reactions in the solid state that are analogous to those commonly used to analyze solution phase experiments. As a result, solid state photochemistry has historically been heavily reliant on product analysis for investigations into mechanisms. This usually involves dissolving the crystal in solution. While this is adequate for solution phase experiments, reaction outcomes in crystals are impacted by the crystalline environment in which the reaction occurs, and dissolving the crystal effectively erases any de novo crystallographic information inherent to the reaction. Research in the Garcia-Garibay group has

found a way to circumvent many of these issues via the utilization of nanocrystalline suspensions for solid state photoreaction studies, an advance which has already expanded our insight into the mechanisms of organic reactions in crystals. Analysis of solid state photochemistry via nanocrystalline suspensions offers the opportunity to gain more detailed knowledge into reaction mechanisms by providing a method to conduct spectroscopic and actinometric analysis into solid state reactions without losing any of the structural information contained in the crystal lattice.

Chapter 2 of this thesis will discuss a solid state photochemical study originally reported by Wagner and co-workers in 1989. In their original study, the Norrish-Yang-like photochemical cyclization of  $\alpha$ -*o*-tolyl and  $\alpha$ -mesityl acetophenones to the corresponding 2-indanols was explored in both solution phase and the bulk solid, though a lack of methodology for spectroscopic and kinetic analysis at the time made it difficult to gain understanding of the mechanisms at work in the solid state reaction. Utilizing our methodology of photolysis of nanocrystalline suspensions, we were able to analyze the efficiency of the cyclization reaction in the solid state, and discovered a unique trend that correlated with the steric bulk of  $\alpha$ -*o*-tolyl acetophenones, but showed the inverse trend in  $\alpha$ -mesityl acetophenones under identical conditions.

Chapters 3 and 4 will discuss a quantum chain reaction known to take place in the conversion of diarylcyclopropanones to diarylacetylenes, stemming from work that was previously published in our group. In Chapter 3, in work done in collaboration with Dr. Gregory Kuzmanich, the photochemical decarbonylation of alkyl-tethered diphenylcyclopropanone dimers to form tethered diphenylacetylenes will be discussed. Both solution and solid state photolysis are explored, and evidence is shown for a Dexter mediated energy transfer mechanism. In Chapter 4, as an extension to this preliminary study, the reactions of aryl-tethered diphenylcyclopropanones

have also been examined, with respect to applications in materials chemistry; in this system we demonstrate evidence of a through bond energy transfer mechanism.

In Chapter 5, in work done in collaboration with Dr. Antoine Stopin, the reactions of biarylcyclopropenones with substituents of varying steric bulk are described, in an effort to better understand and test the limitations of the topochemical postulate in solid state photochemistry, which indicates that reaction in crystals may only occur with a minimum amount of molecular movement without rupturing the crystal lattice. In two cases shown here, evidence is shown for the occurrence of solid-to-solid reconstructive phase transformations taking place, despite steric bulk. This indicates that, even though there are structural limits to the strength of the crystal lattice, reactions can take place in a solid-to-solid manner in some substrates that can be activated to have a high potential energy.

The dissertation of Amy Esther Nielsen is approved.

Neil K. Garg

Andrea M. Kasko

Miguel A. Garcia-Garibay, Committee Chair

University of California, Los Angeles

2014

*Not all those who wander are lost.*



## Table of Contents

Abstract of the Dissertation.....	ii
List of Schemes.....	x
List of Figures.....	xi
List of Tables.....	xii
List of Charts.....	xii
List of Abbreviations.....	xiii
Acknowledgements.....	xv
Vita.....	xvi
Publications and Presentations.....	xvii

### **Chapter 1. Introduction: Solid-State Photochemistry and Crystal Engineering**

1.1	Introduction.....	2
1.2	The Topochemical Postulate.....	3
1.3	The Crystal Structure Reactivity Correlation Method.....	5
1.4	The Current State of Reactions in Crystals.....	7
1.5	Conclusions.....	9

### **Chapter 2. Studies on the Solid State Photocyclization of Sterically Congested $\alpha$ -o-Tolyl and Mesityl Ketones**

2.1	Introduction.....	11
-----	-------------------	----

2.2	Results and Discussion.....	19
2.3	Photochemical Reactivity of 4-5 and 8-11 in Nanocrystalline Suspensions.....	22
2.4	Conclusions.....	27
2.5	Experimental.....	28
2.6	Appendix.....	31

**Chapter 3. Quantum Chain Reaction of Tethered Diarylcyclopropenones in the Solid State and Their Distance-Dependence in Solution Reveal a Dexter S<sub>2</sub>-S<sub>2</sub> Energy Transfer**

**Mechanism**

3.1	Introduction.....	42
3.2	Results and Discussion.....	45
3.3	Conclusions.....	54
3.4	Experimental.....	55
3.5	Appendix.....	63

**Chapter 4. Photochemistry of Aryl-Tethered Diarylcyclopropenones in the Solid State and Application to Materials Development**

4.1	Introduction.....	113
4.2	Results and Discussion.....	119

4.3	Photochemical Reactivity of Aryl-Linked Diarylcyclopropenone Derivatives.....	120
4.4	Conclusions.....	123
4.5	Experimental.....	124
4.6	Appendix.....	130

**Chapter 5. Photo-Induced Decarbonylation of Crystalline Biaryl Cyclopropenones with Bulky Substituents: Insights into Reactions that Challenge the Topochemical Postulate**

5.1	Introduction.....	141
5.2	Results and Discussion.....	146
5.3	Conclusions.....	157
5.4	Experimental.....	158
5.4	Appendix.....	161
	<b>References.....</b>	<b>173</b>

## List of Schemes

<b>Scheme 1. 1.</b> The light initiated rearrangement of $\alpha$ -santonin to Lumisantonin.....	2
<b>Scheme 1. 2.</b> The solid state [2+2] photodimerization of <i>trans</i> -cinnamic acid.....	4
<b>Scheme 2. 1. 1.</b> Norrish Type II Photoelimination and Yang Cyclization Mechanism.....	11
<b>Scheme 2. 1. 2.</b> Norrish Type II - Yang cyclization pathway.....	13
<b>Scheme 2. 1. 3.</b> The photochemical cyclization of $\alpha$ - <i>o</i> -tolyl and $\alpha$ -mesityl acetophenones.....	16
<b>Scheme 2. 1. 4.</b> Photoproducts of solution phase photolysis of acetophenones.....	17
<b>Scheme 2. 2. 1.</b> Synthesis of ketones <b>4</b> and <b>5</b> .....	19
<b>Scheme 2. 2. 2.</b> Synthesis of ketones <b>8</b> , <b>9</b> , <b>10</b> , and <b>11</b> .....	20
<b>Scheme 3. 1.</b> Synthesis of alkyl-tethered DPCP dimers.....	43
<b>Scheme 3. 2.</b> Mechanism of photoexcitation and reaction of DPCP derivatives.....	45
<b>Scheme 3. 4. 1.</b> Synthesis of tethered diarylcyclopropenones.....	56
<b>Scheme 4. 1. 1.</b> The mechanism of a quantum chain reaction.....	115
<b>Scheme 4. 1. 2.</b> Mechanism of quantum chain reaction in diphenylcyclopropenone.....	117
<b>Scheme 4. 1. 3.</b> Mechanism of energy transfer via a quantum chain in alkyl-tethered DPCP dimers...118	
<b>Scheme 4. 2. 1.</b> Synthesis of aryl-tethered DPCP dimers.....	119
<b>Scheme 4. 2. 2.</b> Synthesis of aryl-tethered DPCP trimer.....	120
<b>Scheme 5. 1. 1.</b> Solid-state dimerization of <i>trans</i> -cinnamic acid.....	142
<b>Scheme 5. 1. 2.</b> Photoinduced decarbonylation of diphenylcyclopropenone.....	144
<b>Scheme 5. 1. 3.</b> Solid-state photolysis of cyclopropenones.....	145
<b>Scheme 5. 2. 1.</b> Synthesis of tritylbenzene, the largest substituent utilized in this study.....	146
<b>Scheme 5. 2. 2.</b> Predicted attack on cyclopropenium cation.....	147
<b>Scheme 5. 2. 3.</b> Synthetic route to cyclopropenones with bulky substituents.....	149

## List of Figures

<b>Figure 2. 3. 1.</b> Calculations of the hydrogen abstraction geometry for acetophenones <b>5</b> and <b>11</b> .....	25
<b>Figure 2. 3. 2.</b> Wagner's proposed geometry of solution phase hydrogen abstraction.....	26
<b>Figure 3. 2. 1.</b> S <sub>2</sub> -S <sub>0</sub> fluorescence spectrum of <b>2</b> and <b>13</b> .....	47
<b>Figure 3. 2. 2.</b> PXRD as a measure of sample crystallinity as a function of conversion.....	48
<b>Figure 3. 2. 3.</b> Plot of calculated energy transfer efficiency vs. intrachromophore distance.....	53
<b>Figure 4. 3. 1.</b> Photolysis of <i>ortho</i> -tethered dimer, monitored via benzylic peak shift.....	121
<b>Figure 5. 1. 2.</b> Solid-state de-nitrogenation of triazolines with bulky substituents.....	143
<b>Figure 5. 1. 3.</b> Phase diagram of solid state triazoline denitrogenation reaction progress.....	144
<b>Figure 5. 2. 1.</b> PXRD of cyclopropenone <b>3</b> as a function of conversion.....	150
<b>Figure 5. 2. 2.</b> Crystal structure of cyclopropenone <b>3</b> and the corresponding alkyne.....	151
<b>Figure 5. 2. 3.</b> PXRD of cyclopropenone <b>2</b> as a function of conversion .....	152
<b>Figure 5. 2. 4.</b> Crystal structure and packing of cyclopropeone <b>2</b> .....	153
<b>Figure 5. 2. 5.</b> PXRD of cyclopropenone <b>2</b> illustrating a reconstructive phase transformation.	153
<b>Figure 5. 2. 6.</b> PXRD of cyclopropenone <b>4</b> as a function of conversion.....	154
<b>Figure 5. 2. 7.</b> PXRD of cyclopropenone <b>4</b> , illustrating a reconstructive phase transformation.....	155
<b>Figure 5. 2. 8.</b> Crystal structure and packing for cyclopropenone <b>4</b> .....	156

## List of Tables

<b>Table 2.1.1.</b> Relative quantum yields for the photoreaction of bulky acetophenones.....	18
<b>Table 3. 2. 1.</b> Quantum yields for decarbonylation for <b>2</b> and <b>4 – 6</b> in benzene and as nanocrystals.....	49
<b>Table 3. 2. 2.</b> Calculated aryl edge-to-edge inter-chromophore distances in <b>4 – 6</b> .....	53
<b>Table 4. 3. 1.</b> Energy transfer efficiencies in solution and solid state studies.....	122

## List of Charts

<b>Chart 1. 1.</b> The four geometric parameters of The CSRCM for Norrish Type II reactions.....	7
<b>Chart 2. 1. 1.</b> The four defining parameters of “ideal” hydrogen abstraction geometry.....	15
<b>Chart 5. 2. 1.</b> Set of cyclopropanones designed to test the limits of the topochemical postulate.....	148

## List of Abbreviations

Ar	aryl
Bn	benzyl
ca	approximately
CDCl <sub>3</sub>	deuterated chloroform
Cl	chloro
CO	carbon monoxide
d	doublet (NMR)
dd	doublet of doublets (NMR)
DtBPF	1,1'-bis(di-tert-butylphosphino)ferrocene
DMF	dimethylformamide
DPA	diphenylacetylene
DPCP	diphenylcyclopropenone
et al.	and others
FT-IR	fourier transform infrared (spectroscopy)
GC	gas chromatography
HRMS	high resolution mass spectrometry
Hz	hertz
ISC	intersystem crossing
IR	infrared (spectroscopy)
m	multiplet (NMR)
Me	methyl
MeO	methoxy

MHz	megahertz
min	minute
mmol	millimol
mp	melting point
MS	mass spectrometry
NMR	nuclear magnetic resonance (spectroscopy)
Ph	phenyl
ppm	parts per million
q	quartet (NMR)
rt	room temperature
s	singlet (NMR)
t	triplet (NMR)
THF	tetrahydrofuran
TLC	thin layer chromatography
UV-Vis	ultraviolet-visible (spectroscopy)
PXRD	powder x-ray diffraction
Å	angstrom
Φ	quantum yield



## Acknowledgements

First and foremost, I would like to thank my family and especially Rock Mancini. Although the following individuals may have played a larger role in me obtaining my Ph. D., none of them had to live with me. Second, I would like to thank my research advisor, Professor Miguel A. Garcia-Garibay for guiding me through five years of graduate study and molding me into the scientist that I am today. I must also thank Dr. Gregory Kuzmanich for teaching me everything about photochemistry and more than I ever wanted to know about the digestive tract of hibernating bears. I thank the following people for their collaborative efforts in this dissertation: Dr. Gregory Kuzmanich (Chapter 3 and Chapter 4), Dr. Antoine Stopin (Chapter 5), and Saeed Khan (Chapter 5). I would also like to thank the past and present members of the Garcia-Garibay Lab, Patty and Geeta in particular, for excellent companionship, snacks, and more coffee breaks than I can count. Lastly, I would like to acknowledge the NSF for project funding.

## VITA

- 2005-2007 Undergraduate Research Assistant  
Iowa State University, Ames, IA  
Department of Chemistry  
Advisor: Dr. Nicola Pohl
- 2007 Undergraduate Research Assistant  
Iowa State University, Ames, IA  
Department of Chemistry  
Advisor: Dr. Walter Trahanovsky
- 2007 Bachelor of Science in Chemistry  
Iowa State University
- 2007-2013 Teaching Assistant  
Department of Chemistry and Biochemistry  
University of California, Los Angeles

## Publications and Presentations

Nielsen, A., Kuzmanich, G. Garcia-Garibay, M. A. “*Quantum Chain Reaction of Tethered Diarylcyclopropenones in the Solid State and Their Distance-Dependence in Solution Reveal a Dexter  $S_2$ - $S_2$  Energy Transfer Mechanism*” J. Phys. Chem. A. **2014**, *118*, 1858-1863.

Nielsen, A., Kuzmanich, G., Garcia-Garibay, M. A. (2012, March) Energy Transfer in a Quantum Chain Reaction of Aryl- and Alkyl-Linked Diarylcyclopropenone Dimers Takes Place Through a Dexter or Linker-Dependent Super-Exchange Mechanism, Depending on the Nature of the Linker. Presented at 243<sup>rd</sup> American Chemical Society Meeting, San Francisco, CA.

Nielsen, A., Garcia-Garibay, M. A. (2010, July) Photodecarbonylation Reactions to Form Adjacent Stereogenic Quaternary Centers: Applications Toward the Synthesis of Hexahydropyrroloindole Alkaloids. Gordon Conference on Green Chemistry, Davidson, NC.

## **Chapter 1**

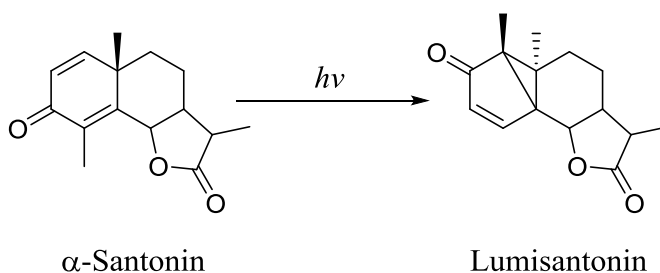
### **Introduction:**

### **Solid-State Photochemistry and Crystal Engineering**

## 1.1. Introduction

From as early as the 19<sup>th</sup> century, when Trommsdorff observed that crystals of  $\alpha$ -santonin yellowed and shattered when exposed to ambient sunlight (**Scheme 1. 1**),<sup>1</sup> the photoreactions of crystals have fascinated and frustrated chemists. Reactions in the solid state are attractive due to the distinct advantages they offer in contrast to reactions in solution, including greater stereochemical control,<sup>2</sup> correlation of chemical behavior and reactivity with structural information,<sup>3</sup> solvent-free “green” synthesis,<sup>4</sup> ease of handling,<sup>5</sup> and pathways to reactivity that deviate from solution phase behavior.<sup>6</sup>

**Scheme 1. 1.** The light initiated rearrangement of  $\alpha$ -santonin to Lumisantonin.



Despite these advantages, there is a paucity of analytical techniques available for solid state photochemical reactions, particularly chemical actinometry.<sup>7</sup> This lacking analytical toolbox has prevented the widespread use of solid state photochemistry in synthetic preparations. This introductory chapter will highlight the issues that have historically plagued solid state photochemistry and how methods such as the photolysis of nanocrystalline suspensions and powder x-ray diffraction are emerging to shed light on reactions in crystals by providing an in situ “snapshot” of reaction progress. With these methods at hand, it is possible to further develop and advance an already rich field of organic chemistry, and simultaneously revisit studies conducted at a time when analytical methods were lacking.

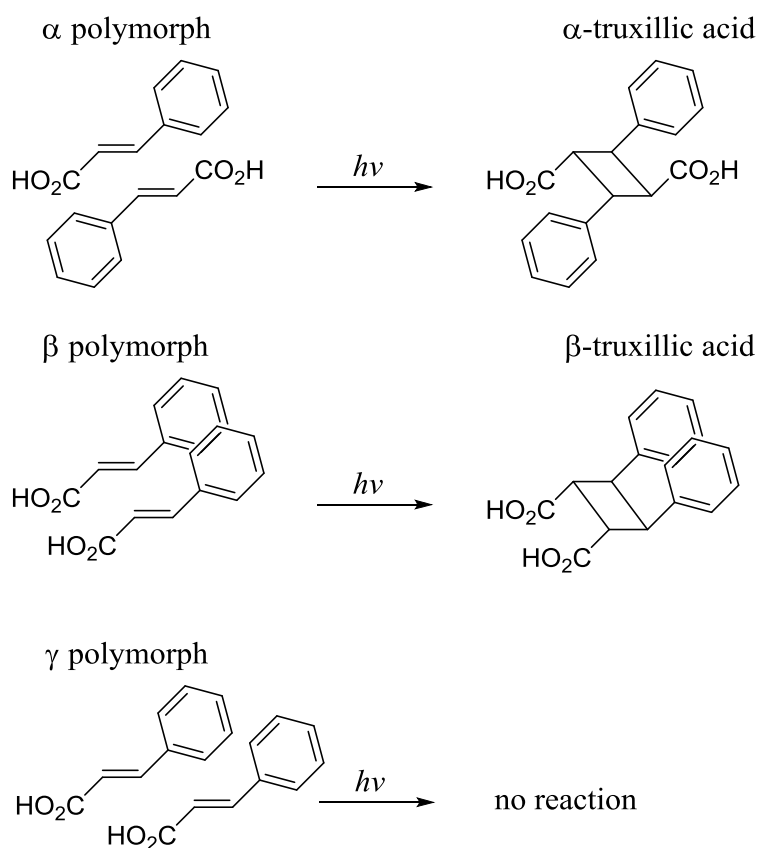
There has been interest in reactions in crystals for many years, but their utilization in synthesis and, consequentially, the overall growth of the field of solid state photochemistry have remained sluggish. This is largely because analysis of solid state reactions previously required that crystals be dissolved and studied in solution,<sup>8</sup> with only product analysis to guide mechanistic interpretation. While this is the standard procedure for solution phase reactions, and does provide important data, it loses one of the most important pieces of information that guides and sometimes dictates the progress of reactions in the solid state - the crystal lattice. It was not until the experiments of Schmidt and Cohen,<sup>9</sup> aided by the newly widespread use of single crystal x-ray crystallography, that the magnitude of impact the crystalline environment had on reaction outcomes was recognized. It soon became clear that the ability to analyze and monitor a solid state reaction as it progressed from starting material to product within the crystal lattice would provide the key to understand and engineer crystal reactivity in the future.

## **1. 2. The Topochemical Postulate**

In the 1960s, the use of single crystal x-ray crystallography for structural determination was recently introduced, and, for the first time, chemists were able to observe solid state photoreactions within their native environment. Around the same time, Schmidt and Cohen conducted a series of experiments<sup>10</sup> on the [2+2] photodimerization of the three crystalline polymorphs of *trans*-cinnamic acid ( $\alpha$ ,  $\beta$ , and  $\gamma$ ) each of which varied in both distance to nearest neighbor and orientation in the crystal lattice. Armed with the knowledge that each polymorph of *trans*-cinnamic acid had different photophysical properties, they speculated that this was caused by their varying orientation in the crystal lattice, and designed their study to test the impact that these varying orientations and distances would have on the reaction outcomes. With the aid of single crystal X-ray crystallography, which at the time was utilized primarily for structure

determination, they found that product distributions varied widely among the three polymorphs. The molecules in adjacent stacks in the  $\alpha$  polymorph (with an intermolecular distance of 4.2 Å) reacted to form  $\alpha$ -truxillic acid when irradiated. The  $\beta$  polymorph formed  $\beta$ -truxillic acid from the reaction within the stacks (with an intermolecular distance of 3.5 Å) under identical conditions. The  $\gamma$  polymorph, in which the intermolecular distance was greater than 4.8 Å, did not react to give [2+2] dimerization products, and the authors speculated that the [2+2] dimerization could only take place at an intermolecular distance of less than 4.1 Å. This hypothesis was further confirmed when structural analogues of *trans*-cinnamic acid that packed in the same three polymorphs ( $\alpha$ ,  $\beta$ , and  $\gamma$ ) showed the same product distributions observed in *trans*-cinnamic acid (**Scheme 1. 2**).<sup>11</sup>

**Scheme 1. 2.** The solid state [2+2] photodimerization of *trans*-cinnamic acid.



This data presents an example where the crystalline environment of the solid state reaction dominates over the molecules inherent reactivity in determining the outcome of a photochemical reaction. Aided by the single crystal x-ray structure data obtained from their studies of *trans*-cinnamic acid, Schmidt and Cohen refined these observations into what is now referred to as the topochemical postulate,<sup>11</sup> as was first suggested by Kohlschutter,<sup>12</sup> who noted the relation between reactions occurring in the solid state and the spatial orientation of the products in 1918. The topochemical postulate stated that reactions in crystals took place only with a limited amount of atomic or molecular movement. Furthermore, the geometry and packing of a molecule in the crystal lattice was potentially of greater importance than its inherent reactivity. This was largely based on evidence that product distributions were widely different for different polymorphs, and solid phase reactions could be more selective than comparable reactions observed in solution. The study by Schmidt and Cohen was one of the first documented instances of directly probing the relationship between the orientation of molecules in the crystal lattice and the geometry of reaction products; seminal work that hinted at the beginnings of engineering reactions in crystals. The concept of this correlation, as laid out in the topochemical postulate, was so ubiquitous that today it remains the motivation behind the development of crystals engineered specifically for their reactivity.<sup>13</sup>

### **1.3. The Crystal Structure Reactivity Correlation Method**

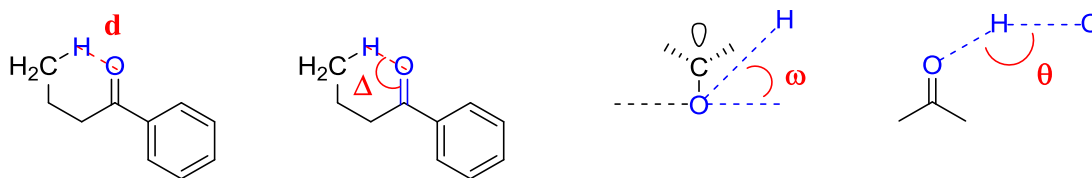
The photoreaction of aryl or alkyl ketones with a  $\gamma$ -hydrogen via a Norrish Type II mechanism is one of the most studied and, therefore, well understood photoreactions.<sup>14</sup> Susceptible substrates, when irradiated, will exhibit an intramolecular 1,5-hydrogen abstraction to form a 1,4 biradical, which may progress to reverse hydrogen abstraction to reform the reactant, elimination to form an alkene and enol (Norrish Type I), or Yang cyclization via coupling of the triplet 1,4



biradical intermediate. The Norrish Type II hydrogen abstraction has been extensively studied, but there had been a debate in regards to the geometry of excited state molecules during the reaction.<sup>15</sup> While studying the Norrish Type II hydrogen abstraction reaction, Scheffer and co-workers developed the idea of relating the geometric parameters of a molecule, as determined by single crystal x-ray crystallography, to the success or failure of a photochemical hydrogen abstraction in a Norrish Type II process.<sup>16</sup> They referred to the model as The Crystal Structure Reactivity Correlation Method,<sup>17</sup> which defined four parameters that correlated with reaction success ( $d$ ,  $\Delta$ ,  $\omega$ , and  $\theta$ ) and found that the majority of substrates tested in the solid state behaved as the model had predicted (**Chart 1.1**). An “ideal” value of  $d$ , the distance between the carbonyl oxygen and the hydrogen, was estimated to be within 0.2 Å of the sum of the van der Waals radii, 2.72 Å.<sup>18</sup>  $\Delta$ , the angle between the hydrogen and the carbonyl was predicted to result in success when it fell between 90° and 120°.<sup>19</sup> The angle between the reacting CH bond and the carbonyl oxygen,  $\theta$ , was closest to “ideal” at 180°. Finally  $\omega$ , the out-of-plane angle of the hydrogen (relative to the plane defined by the carbonyl) optimized the reaction at 0°. These four parameters were defined and refined by studying the photo-initiated hydrogen abstraction reactions of a large number of ketones. However, there were several examples that reacted in “violation” to what was predicted by the model. It was observed that some ketones, despite having less than “ideal” geometric parameters, reacted readily under photochemical conditions. Additionally, other ketones, with almost “ideal” geometry, as predicted by the model, failed to react as anticipated.<sup>20</sup> Though the bulk of crystalline ketones studied reacted as the model predicted, the implications suggested by the examples in violation of the model were surprising. This small portion of crystalline ketones that did not follow the model indicated that, while there were some parameters that were close to “ideal” for hydrogen abstraction, there were other factors at hand that also played a role in reaction

outcomes. While this model represented a huge step forward in solid state photochemistry, it also revealed that there was potentially a great need to be able to observe the excited states and transient intermediates in the solid state as a way of learning how to predict crystal reactivity. This might allow application to crystal design; current methods of analysis were simply inadequate to tell the whole story.

**Chart 1. 1.** The four geometric parameters of The CSRCM for Norrish Type II reactions.



#### 1.4. The Current State of Reactions in Crystals

Research in our lab has focused on the use of nanocrystalline suspensions to study the mechanisms and photophysical properties of reactions taking place in the solid state.<sup>21</sup> Nanocrystalline suspensions are prepared via the reprecipitation method developed by Kasai,<sup>22</sup> which gives aqueous suspensions of organic crystals with an average particle size of 200 nm. Though bulk solids can exhibit large dichroism, light scattering, and high optical density, nanocrystalline suspensions are able to partially circumvent these issues, as the average particle size is smaller than the wavelength of light typically utilized in photoreactions.<sup>23</sup> Nanocrystalline suspensions are homogeneous and free flowing, which makes analysis via a number of spectroscopic methods possible. These nanocrystalline suspensions provide a unique opportunity for direct observation of reactive intermediates in crystals via transient absorption spectroscopy, and make it possible to begin to visualize the geometry of excited state intermediates in solid state photoreactions.<sup>24</sup> The use of these suspensions will almost certainly play a role in the further

development and understanding of solid state photoreactions and their mechanisms in their native crystalline reaction environment.

Powder x-ray diffraction (PXRD) has also become a powerful tool in furthering the understanding of reactions in the solid state. In work recently published by our group,<sup>25</sup> the photochemically induced de-nitrogenation of triazolines to form aziridines in the solid state was studied. The photoreaction of triazolines to form aziridines is quite general, and ideal in the sense that it rarely results in other products, due to the limited amount of motion of the intermediate 1,3-biradical in the crystals. This particular work featured the synthesis of a set of triazolines substituted at varying positions with large, sterically bulky substituents. It was speculated that, in accordance with the topochemical postulate, reactions in the solid state could only take place with a minimum amount of molecular motion. However, considering the large amount of potential energy available in the 1,3-biradicals, it was of interest to determine if the biradicals would be trapped in the crystals or the reaction would occur despite requiring a large change in volume. It was shown that the reaction proceeded despite the disruption of the crystal lattice, which led to its amorphization. By utilizing powder x-ray diffraction (PXRD) as a method to monitor the sample crystallinity as a function of reaction progress, it was determined that solid to solid reactions were able to progress via metastable phases that were susceptible to amorphization or by reaction pathways that involve reconstructive phase transitions that result in the formation of a stable phase of the product.<sup>26</sup> It was additionally observed that reactions that progressed through metastable phases or by reconstructive phase transitions were dependent on the glass transition temperature. This led to a proposed modification of the topochemical postulate from a more energetic standpoint: reactions in crystals are limited by the constraints of the crystal lattice in molecular and atomic movement, but reaction barriers can be overcome by substrates that either have or are

able to acquire a large enough amount of potential energy. In this thesis, a similar study was explored, featuring a highly strained and photochemically sensitive cyclopropanone with substituents of varying steric bulk to further test the limits of the topochemical postulate.

## **1.5. Conclusions**

As illustrated here, solid state photoreactions, particularly those of ketones, have long been of interest to scientists despite the historical lack of analytical methods available to determine reaction mechanisms. With the development of powder x-ray diffraction and single crystal x-ray crystallography, it became possible to probe the molecular and packing structures that allow for chemical reactivity in crystals and to formulate predictions for reaction outcomes based upon solid state models; the first step toward the engineering of crystals for specific photochemical reactivity. However, these new models revealed that structural analysis alone does not give a complete picture of the reaction progress in crystals. Other factors, such as energetics and the geometry of transient intermediates may also have significant impact on reaction outcomes, and would require more in depth methods of analysis. The use of nanocrystalline suspensions in our lab presents one of the most promising solutions to this issue, as their small crystal size and free flowing nature make them more amenable to analytical techniques traditionally used for solution phase chemistry. Additionally, these suspensions are excellent candidates for methods such as transient absorption spectroscopy that can be used to probe the kinetics and reactivity of excited state photochemical intermediates.

## **Chapter 2**

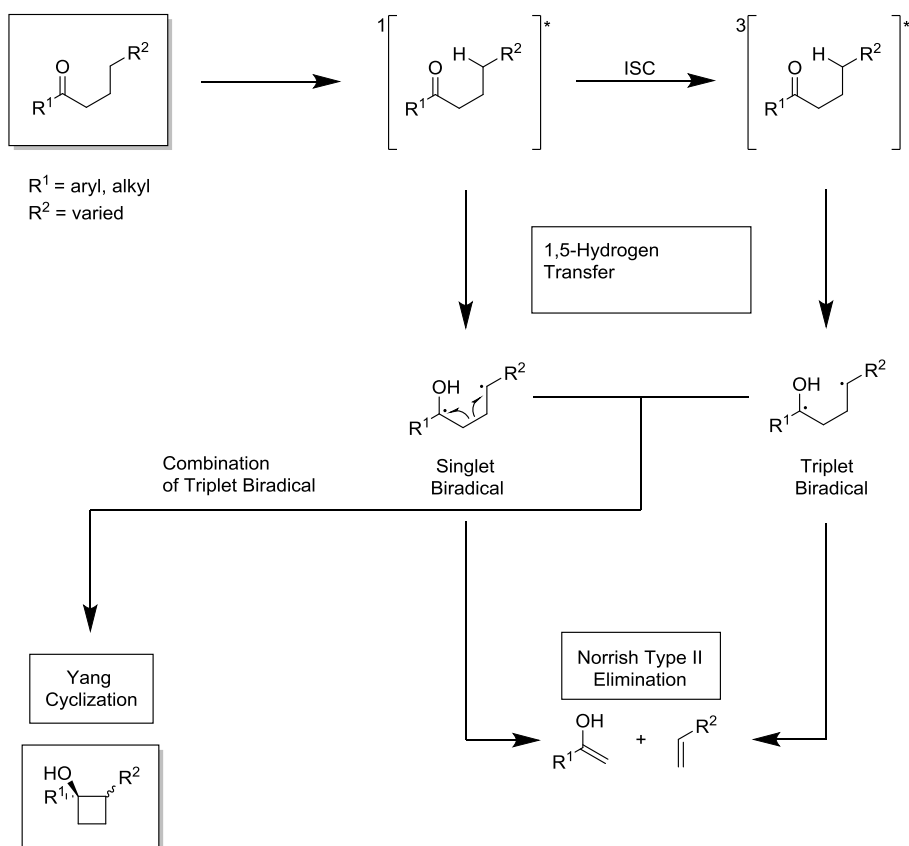
**Studies on the Solid State Photocyclization of Sterically**

**Congested  $\alpha$ -*o*-Tolyl and Mesityl Ketones**

## 2. 1. Introduction

The photo-induced intramolecular  $\gamma$ -hydrogen abstraction reaction to form 1-hydroxy-1,4-biradicals, has been known to take place in a wide variety of carbonyl compounds.<sup>27</sup> The reaction initiates three subsequent competing reactions: 1) combination of the 1,4 biradical intermediate to form cyclic alcohols<sup>28</sup>, 2) regeneration of the starting material via reverse hydrogen abstraction,<sup>29</sup> and 3) elimination, which results in the formation of an enol and the corresponding alkene, and is known as the Norrish Type II Elimination.<sup>30</sup>

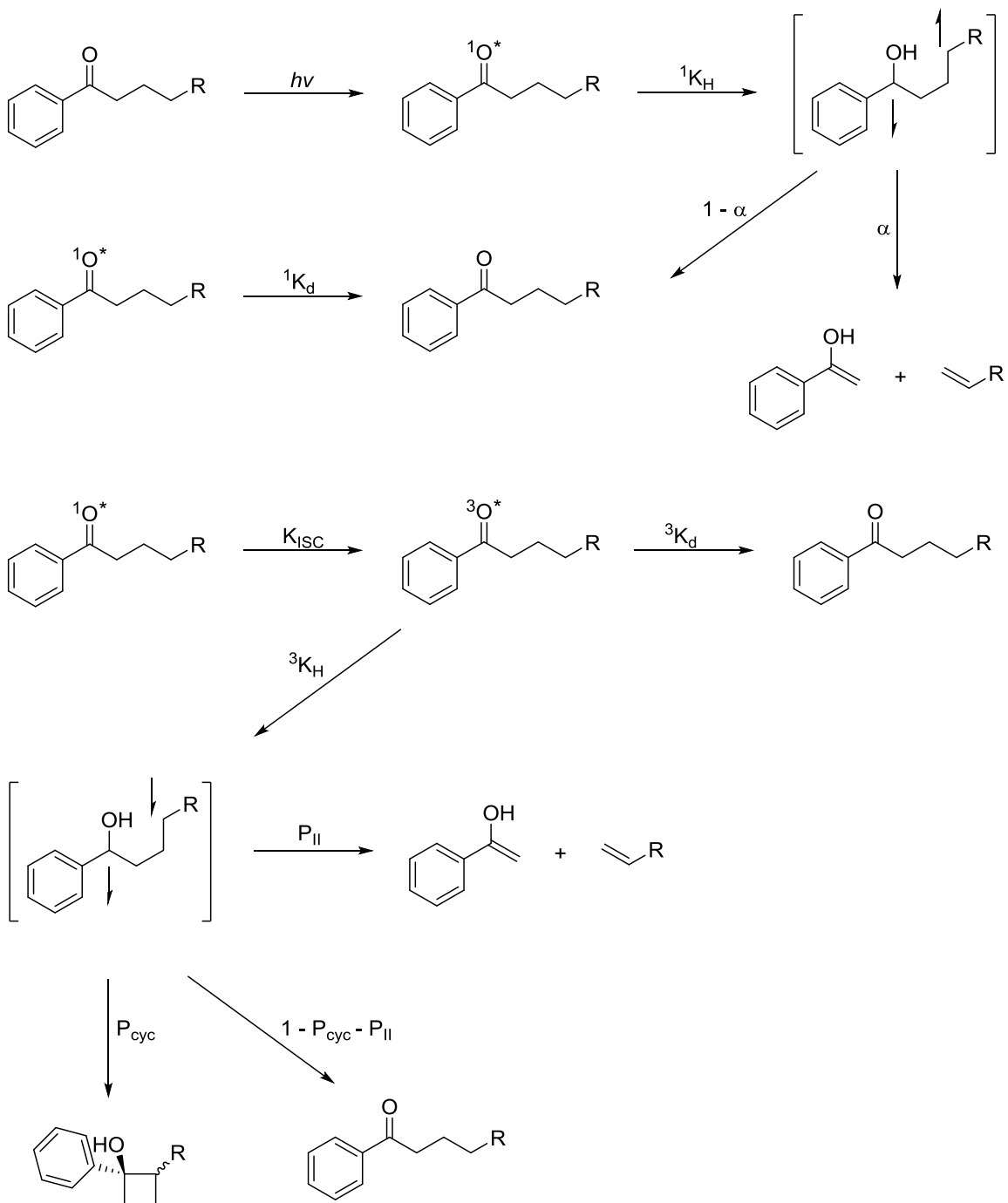
**Scheme 2. 1. 1.** Norrish Type II Photoelimination and Yang Cyclization Mechanism.



The earliest and most recognized example of this occurrence, referred to as a Type II photoelimination,<sup>31</sup> was observed by Norrish,<sup>32</sup> who discovered that upon irradiation the  $\gamma$ -CH bonds associated with ketones would cleave to alkenes and methyl ketones rather than alkyl or acyl radicals, which was observed to take place in the Norrish Type I reaction (**Scheme 2. 1. 1**).<sup>33</sup> It was originally thought that the reaction was a concerted 1,5-hydrogen transfer simultaneous with a carbon-carbon bond cleavage emerging from a six-membered cyclic transition state, in similar mechanistic fashion to a retro-ene reaction.<sup>34</sup> It was later discovered by Yang et al.,<sup>35</sup> that the observed carbon-carbon bond cleavage reaction was accompanied by cyclobutanol formation which led to the inference that both events (cleavage and cyclization) arose from a single common biradical intermediate.<sup>36</sup> Though a number of hydrogen abstraction processes are possible in ketones,  $\gamma$ -hydrogen abstraction to form 1,4-biradicals has been the most extensively researched,<sup>37</sup> due to the high reactivity of the ketones that undergo this reaction and the well-known preference of 1-5 hydrogen transfers in radical chemistry.<sup>38</sup> Studying the reactions of photochemically induced 1,4-biradicals is attractive as 1,4-biradicals are capable of cleavage to form two alkenes, and thus can form products from almost any conformation.<sup>39</sup> Additionally, the cleavage process of 1,4-biradicals is simple to measure and quantify. By contrast, biradicals formed by hydrogen abstraction at non- $\gamma$  positions may cyclize, but cannot cleave in the same fashion as a 1,4-biradical, thereby complicating analysis.

What are now termed the Norrish Type II elimination and the Norrish-Yang cyclization, take place from the lowest excited state of a ketone, typically a singlet or triplet  $n, \pi^*$  state.<sup>40</sup> The formation of products from the triplet state is more common (**Scheme 2. 1. 2**), as the singlet reaction takes place on a time scale that is typically too slow to compete with intersystem crossing (ISC).

**Scheme 2. 1. 2.** Norrish Type II - Yang cyclization pathway.



The bulk of studies into the Norrish-Yang cyclization have been focused on the mechanism of the formation and subsequent reactions of 1,4-biradicals in solution, but the formation of other biradical species has also been addressed, though these species are much less common.

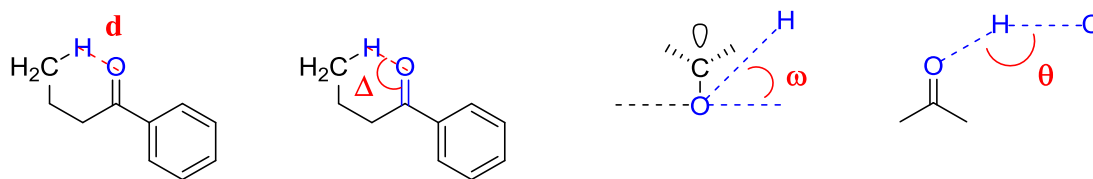


$\delta$ -Hydrogen abstraction is interesting because it requires either the absence of  $\gamma$ -hydrogens, or  $\gamma$ -hydrogens in molecules that have high barriers for optimal orientation, or a corresponding  $\gamma$ -C-H bond dissociation energy that is too elevated for the reaction to proceed.<sup>41</sup> The photochemical formation of 1,5-biradical species can result in the formation of synthetically useful five-membered rings.<sup>42</sup> The overall reaction is attractive, as an acyclic ketone can be readily transformed into a cyclic compound with a chiral or pro-chiral center.<sup>43</sup> There are, however, significant drawbacks. In solution there are few ways to provide stereochemical control for the formation of the five-membered ring.<sup>44</sup> It is also difficult to minimize or eliminate the formation of side-products, which tend to be characteristic in this class of reaction.<sup>45</sup>

For many years the “ideal” geometry necessary for hydrogen abstraction<sup>46</sup> for  $n, \pi^*$  ketone triplets has been debated, the most noteworthy advance being the Crystalline Structure-Reactivity Correlation Method (CSRCM).<sup>47</sup> Developed by Scheffer, the CSRCM was intended as a model for the Norrish Type II reaction that sought to correlate geometric parameters of crystalline ketones with their success or failure in the reaction, as defined by  $\gamma$ -hydrogen abstraction. A large number of crystalline ketones that could potentially react in a Norrish Type II reactions were studied, and four crucial parameters were defined ( $d, \Delta, \omega, \theta$ ) as the major determining factors in the success of hydrogen abstraction. The parameter  $d$ , the distance between the carbonyl and the  $\gamma$ -hydrogen to be abstracted, was expected to be optimized when the hydrogen was within 0.2 Å of the sum of the van der Waals radii of 2.72 Å. The parameter  $\Delta$  was defined as the angle between the hydrogen and the carbon-oxygen bond of the carbonyl. Hydrogen abstraction in Scheffer’s model was anticipated to proceed readily when  $\Delta$  was between 90° and 120°. The third factor,  $\omega$ , was defined as the out of plane angle of the hydrogen relative to the plane of the carbonyl. 0° was assumed to be the optimum angle for  $\omega$ . The last parameter,  $\theta$ , the angle defined by CH-O, was expected to

be optimal at an  $180^\circ$  angle. However, in Scheffer's study, ketones were biased towards forming hydrogen abstraction products along a range of values for all of these parameters, and some varied widely from the predicted "more-ideal" values. In particular, the parameters  $\omega$  and  $\theta$  were shown to display large deviations from the "ideal" measured in compounds that readily reacted in Norrish Type II fashion. Additionally, Scheffer's study indicated that a large number of compounds with nearly "ideal" geometry failed to undergo  $\gamma$ -hydrogen abstraction. The study focused on the Norrish Type II abstraction of  $\gamma$ -hydrogens, but it is a clear indicator that, in general, reactive intermediates in crystals and their geometries have a larger impact on the outcome reactions than what was previously thought (**Chart 2. 1. 1**).

**Chart 2. 1. 1.** The four defining parameters of "ideal" hydrogen abstraction geometry.

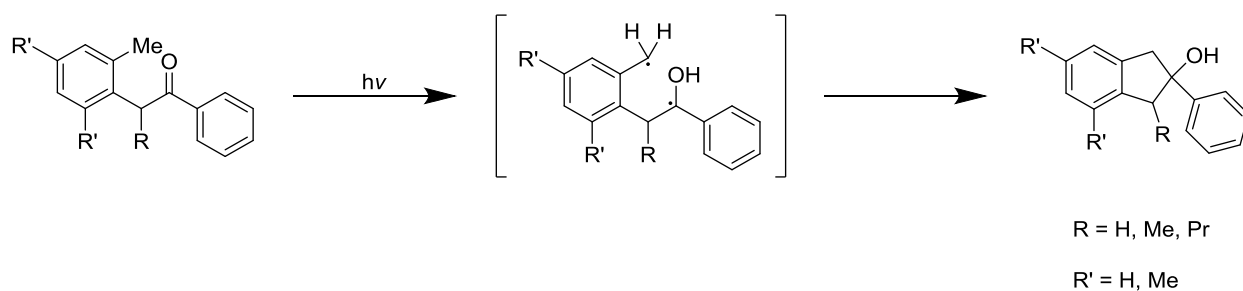


By utilizing the "cage-effect", the rigid environment of reactions in crystals prevents the formation of many side-products that can form in solution due to greater restriction of molecular motion and can often take place with great stereo-selectivity.<sup>48</sup> The development and application of photoreactions in crystals has been slow to progress, however, as there are few methods for gaining mechanistic insights that are analogous to those available in solution. To date, the majority of mechanisms in the solid state have been based upon inferences from product analysis.<sup>49</sup> Research in the Garcia-Garibay lab has revealed that photochemical reactions in nanocrystalline solids have the potential for applications in solvent-free, green chemical synthesis<sup>50</sup> and materials science, while simultaneously combining the ease of solution phase reactions with the stereochemical control possible in bulk solids.<sup>51</sup> We have recently disclosed a method for analysis

of solid state reactions via the utilization of nanocrystalline suspensions, which makes it possible to conduct solid state chemical actinometry, the study of the efficiency of a photoreaction.<sup>52</sup> This methodology has shed light on a number of photophysical processes, and we felt there was valuable information to be obtained from revisiting Wagner's study of the photocyclization of sterically congested  $\alpha$ -*o*-tolyl and mesityl ketones.<sup>21</sup>

In 1989 Wagner published on the Norrish-Yang-like photochemical cyclization of  $\alpha$ -*o*-tolyl and  $\alpha$ -mesityl acetophenones to the corresponding 2-indanols (**Scheme 2. 1. 3**).<sup>53</sup> The cyclization involved  $\delta$ -hydrogen atom abstraction from the n,  $\pi^*$  ketone triplet to form a 1,5-biradical species from a sterically hindered substrate with what was considered to be "less than ideal" hydrogen abstraction geometry.<sup>54</sup>

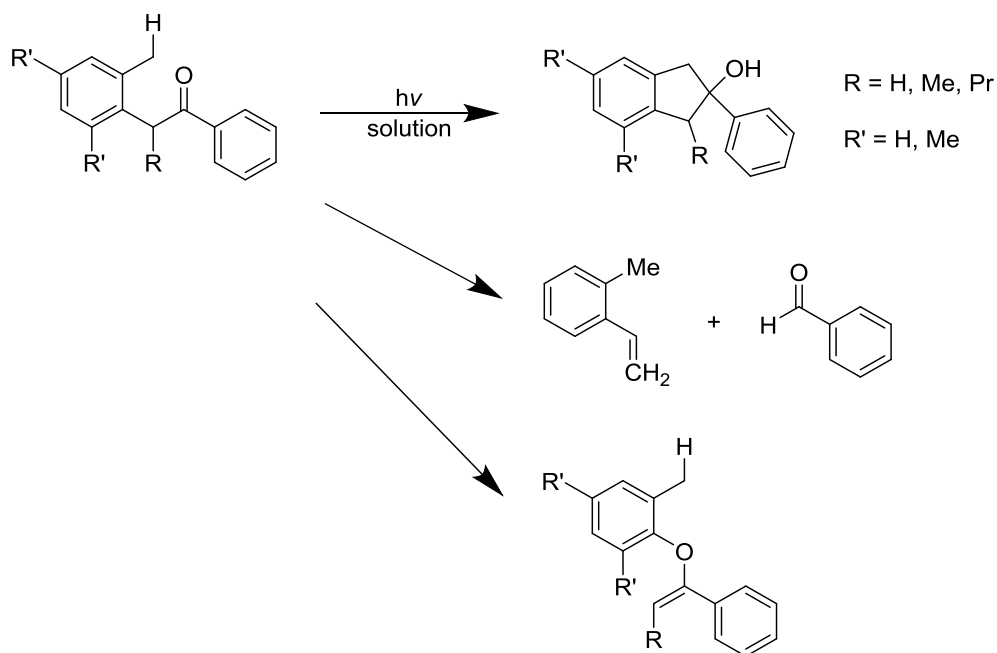
**Scheme 2. 1. 3.** The photochemical cyclization of  $\alpha$ -*o*-tolyl and  $\alpha$ -mesityl acetophenones.



Their findings revealed that the acetophenones cyclized to the corresponding indanols with good efficiency in the bulk solid and in benzene, as determined by quantum yield calculations, despite having bulky substituents and what were typically considered "poor" H-abstraction geometries<sup>55</sup> that should have hindered the reaction progress. Analysis of the results revealed that photochemical cyclization in benzene additionally resulted in the formation of undesired photoproducts (**Scheme 2. 1. 4**). Chemical actinometry of the solution phase experiments showed that the reaction proceeded with reasonable efficiency, particularly considering the steric bulk of

the substituents immediately neighboring the carbonyl. By contrast, in the bulk solid the reactants progressed to the products with 100% chemical yield, and the formation of side products was not observed. This was likely due to a constraint on translational and rotational movement in the crystal lattice, which has been observed in numerous other solid state photoreactions.<sup>56</sup> At the time, the technology to perform chemical actinometry on solid state reactions was not available, and the efficiency of the solid state reaction was not reported. This inspired us to pursue the solid state actinometry of nanocrystalline suspensions of these compounds to further explore this phenomenon.<sup>57</sup>

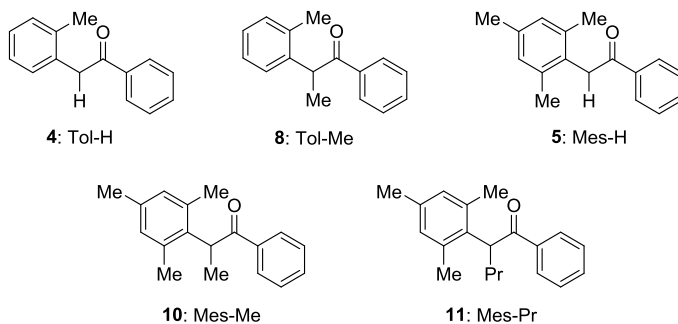
**Scheme 2. 1. 4.** Photoproducts of solution phase photolysis of acetophenones. In the solid state, only the formation of the cyclization product is observed.



Our lab has previously revealed the actinometry of a solid state reactions can be performed via photolysis of nanocrystalline suspensions. Typically, reactions of large single crystals or bulk powders are difficult to analyze using traditional optical methods, as a result of their high optical densities and strong light scattering capabilities.<sup>58</sup> These limitations can be overcome by utilizing

aqueous suspensions of nanocrystals (averaging 200 nm in size) synthesized via the reprecipitation method developed by Kasai.<sup>22</sup> We recognized that, as particle size approached the wavelength of the irradiation source, samples could be photochemically excited in a nearly uniform manner.<sup>59</sup> We applied this methodology to study the ketones synthesized by Wagner and found that the reaction not only proceeded efficiently, but without formation of the undesired photoproducts observed in solution (**Table 2. 1. 1**).

**Table 2. 1. 1.** Relative quantum yields for the photoreaction of bulky acetophenones.



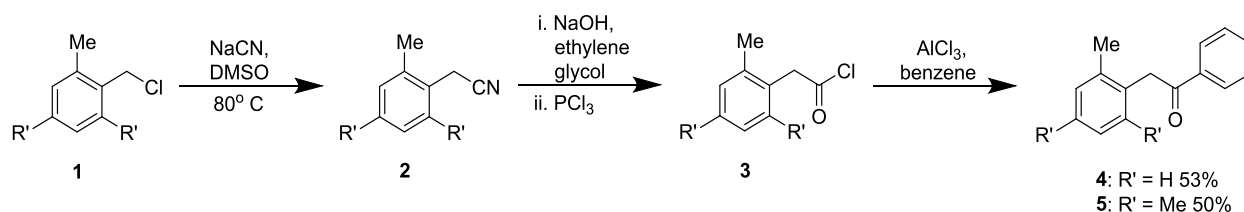
Compound	$\Phi_{\text{soln}}$	$\Phi_{\text{other}}$	%Cyc <sub>soln</sub>	$\Phi_{\text{NC}}$
Tol-H ( <b>4</b> )	1.0	-	100	0.98
Tol-Me ( <b>8</b> )	0.05	0.28	67	0.21
Mes-H ( <b>5</b> )	0.55	-	-	0.096
Mes-Me ( <b>10</b> )	0.24	0.03	100	0.13
Mes-Pr ( <b>11</b> )	0.12	0.025	94	0.35

## 2. 2. Results and Discussion

### Synthesis of Ketones 4 and 5

Following a procedure reported by Wagner,<sup>60</sup> 2, 4, 6-Trimethylbenzyl chloride or 2-Methylbenzyl chloride was transformed into the product ketones in three steps. As indicated in **Scheme 2. 2. 1.**, isolated yields ranged from 50-53%. The purified products were recrystallized from DCM: hexanes 1:10. All ketones were characterized by <sup>1</sup>H and <sup>13</sup>C NMR, IR, UV-Vis, and mass spectrometry (**Scheme 2. 2. 1**).

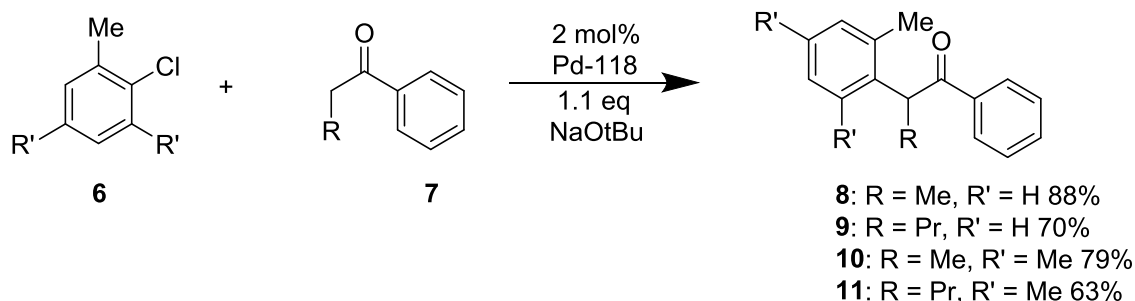
#### Scheme 2. 2. 1. Synthesis of ketones 4 and 5.



### Synthesis of Ketones 8-11

Ketones 8-11 were synthesized following a modified procedure by Grassa<sup>61</sup> in one step utilizing 1,1'-bis(di-tert-butylphosphino)ferrocene (DtBPF)PdCl<sub>2</sub>. When complete, the reaction mixture was purified via flash chromatography and recrystallized from DCM: hexanes 1:10, with yields of pure ketone ranging from 63-88%, as shown in **Scheme 2. 2. 2**. All ketone products were characterized by <sup>1</sup>H and <sup>13</sup>C NMR, IR, UV-Vis, and mass spectrometry. Ketone 9 ( $\alpha$ -mesityl,  $\alpha$ -propyl-acetophenone) was an oil, and, as such, was not a candidate for solid-state actinometry in nanocrystalline suspensions (**Scheme 2. 2. 2**).

**Scheme 2. 2. 2. Synthesis of ketones 8, 9, 10, and 11.**



All ketones synthesized had been previously published and characterization by conventional methods was simple. The Mes-H ketone (**5**) and the Tol-H ketone (**4**) both had a common quartet at 8.03 ppm in the  $^1\text{H}$ NMR, with a  $J$  value equal to 1.5 Hz. Toly ketones (**4**, **8**, and **9**) were characterized by the shift of the aromatic methyl singlet at 2.30 ppm integrating to 3H, while for mesityl ketones (**4**, **10**, and **11**) the mesityl methyl hydrogens showed a shift of 2.20 ppm and integrated for 9H. The solid state IR for all compounds showed a characteristic carbonyl peak at  $1680 \text{ cm}^{-1}$ .

**Preparation and Characterization of Nanocrystalline Suspensions**

As was previously stated, our lab has shown that photochemical reactions in nanocrystalline suspensions can be analyzed via traditional optical methods that cannot be utilized with large single crystals or bulk powders. The easiest method for the preparation of nanocrystalline suspensions is by the reprecipitation method, first developed by Kasai.<sup>22</sup> This method typically is able to produce nanocrystals averaging 200 nm in size for numerous crystalline chemical compounds. In order to determine the solid state reactivity and quantum yields of reaction for the derivatives shown in **Table 2. 1. 1**, 0.012 mmol of synthesized ketone and dicumyl ketone (used as an internal actinometer) were dissolved separately in a minimal amount of acetone. These solutions of ketone or dicumyl ketone were injected via micropipette into culture tubes of rapidly

vortexing millipore water (8 mL). The resulting co-suspension of ketone and actinometer were further vortexed and sonicated to ensure that no acetone remained in the sample, and were combined just prior to photolysis. The solid ketones studied readily formed nanocrystals under these conditions and no surfactant was needed to aid in their formation.

### **Relative Quantum Yield Determination in Nanocrystalline Suspensions**

Quantum yield determinations require knowledge of the number of photons absorbed by the sample and by the actinometer in order to determine the number of product molecules formed per photon in each case and relate that to the quantum yield of the actinometer. Simply put, if the absorbances are equivalent and the amount of product formed in each case is identical, the quantum yield of the reactant is the same as that of the actinometer. Differences in the amount of product formed under these conditions are directly proportional to the differences in quantum yields. In the experiments reported in this chapter, we used equimolar amounts of the dicumyl ketone actinometer and of each of the hindered ketones shown in **Table 2. 1. 1**. Since all of the hindered ketones have the same chromophore, it is reasonable to assume that equimolar concentrations will have the same absorbance, and that comparisons of the quantum yields values obtained in the solid state will be accurate. However, to determine the absolute quantum yield values in a rigorous manner, it will be necessary to determine the relative absorbance of dicumyl ketones and the hindered ketones under the conditions of the experiment. Considering this uncertainty, the quantum yields reported here should be considered relative, rather than absolute. It will be possible to make a systematic correction in the future.

The absolute quantum yields in benzene for all compounds in **Table 2. 1. 1** had been previously published by Wagner in 1989. Therefore, our experimentation focused exclusively on the reactions of nanocrystalline suspensions. Relative quantum yield determinations were



performed in triplicate or quadruplicate, utilizing dicumyl ketone ( $\Phi_{\text{NC}} = 0.18$ ) as an internal actinometer. Photochemical experiments were conducted in a Rayonet photochemical reactor using 312 nm lamps (BLE-8T312). Relative quantum yields were determined with equimolar, optically dense nanocrystalline suspensions. Samples of actinometer and substrate were suspended independently, and then combined immediately prior to irradiation in a culture tube and irradiated for a total time of 10 minutes. A 2 mL aliquot was removed every 2.5 minutes, to give a total of 4 aliquots sampled over the time period of the experiment. Each aqueous aliquot was extracted with DCM, and dried over sodium sulfate prior to evaporating to dryness. Each resulting sample, containing both actinometer, ketone, and their respective photoproducts, was dissolved in a minimal amount of acetone, and subjected to gas chromatography to determine the extent of reaction for actinometer and substrate for the given time point. For all ketones studied in nanocrystalline suspensions, conversion to the product occurred without formation of undesired products.

### **2. 3. Photochemical Reactivity of 4-5 and 8-11 in Nanocrystalline Suspension**

Nanocrystalline suspensions of all ketones were prepared as stated above, and photolysis was performed at 312 nm. The result of these experiments were as follows. As was anticipated, based upon Wagner's findings and our understanding of photoreactions in the solid state, all of the ketones in the study cyclized to form the corresponding 2-indanols without the formation of undesired photoproducts. The solid state relative quantum yields range from up to 0.98 for compound **4** to 0.096 for compound **5** (**Table 2. 1. 1**). In Wagner's previous study, ketone **5** did not show appreciable formation of the corresponding 2-indanol in the bulk solid. However, under our conditions, cyclization to the 2-indanol was observed for ketone **5**. The lack of cyclization observed by Wagner could have been due to a number of factors. At the time of publication in

1989, the conditions for photolysis of the bulk solid in this study were not described in detail. It is possible with knowledge of solid state reactions being limited at the time that cyclization in the bulk solid did occur, but to such a small degree that it was virtually undetectable by the methods available at the time. It is well documented that reactions in bulk solids are inherently plagued by issues of penetration depth and filtering effects by strongly absorbing photoproducts.<sup>62</sup> It is possible that cyclization did occur in Wagner's study of ketone **5**, but the desired photoproduct was undetectable. It is also a possibility that these ketones exhibit polymorphism, which may explain the differences in observed reactivity.

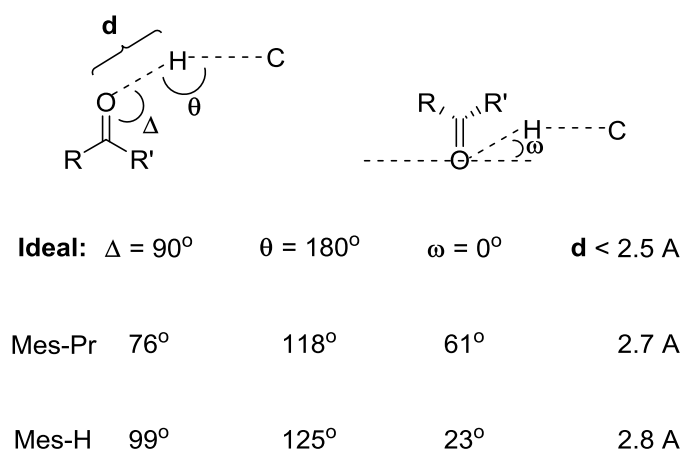
An interesting result was also observed in the trend in the quantum yields of the mesityl substituted compounds, ketones **5**, **10**, and **11**. Wagner's solution phase studies (in benzene) of these three compounds showed a decrease in quantum yield with respect to increasing steric bulk at the  $\alpha$  position of the ketone. This result was intuitive, as steric bulk at that position would be anticipated to effectively block the carbonyl from reaction, and therefore reduce the efficiency of the hydrogen abstraction. Additionally, the ketones in question were anticipated to have "less than ideal" geometry for hydrogen abstraction, so it made sense that increased steric bulk would be a significant factor in preventing hydrogen abstraction from taking place. So it was remarkable that in nanocrystalline suspensions of the same ketones, where individual molecules are more restricted in their movements by the crystal lattice, the quantum yields of cyclization showed an inverted trend of increasing quantum yield with respect to the increase in steric hindrance at the  $\alpha$  position of the ketone.

While this trend was surprising, there are numerous explanations for this inversion, the most likely being the following: In solution, isolated molecules of the ketone are in constant motion. In the solid state, this is not the case – ketone molecules are held in place by the confining

structure of the crystal lattice. When irradiated and a photon is absorbed, molecules will be excited from the ground state to an excited state. In solution, a single molecule of the ketone is in constant motion to minimize negative external and internal interactions. In the solid state, this is not the case. A single molecule of the ketone is held in place by the confining structure of the crystal lattice. When a photon of adequate energy is absorbed, a single molecule of the ketone, in either solution or solid, will be excited from the ground state to an excited state. In solution, the excited state ketone has rotational freedom to maneuver into the lowest energy conformation, which may or may not be the optimal geometry for reaction. In the solid, this geometric change to the lowest energy conformation is less likely. The topochemical postulate for reactions in solids, first formulated by Kohlschutter in 1918, suggests the following: crystalline phase reactions occur with a minimum of atomic and molecular motion. Both are inhibited by the reaction cavity as contained within the crystal lattice. It can be inferred from this that molecular packing in the crystal lattice can play a substantial role in solid state reactivity, and can over-ride inherent reactivity.<sup>63</sup> It is plausible to consider that, in solution, the excited state of the ketone may adopt a different geometry than that of the ground state ketone. In the solid state, however, the topochemical postulate applies and this is more difficult to achieve. In the solid phase, the excited state ketone is held in a more reactant-like reaction cavity by the structure of the crystal lattice. Utilizing this information, one could begin theorize that the geometry of the excited state of this particular subset of ketones is different in the solid state than in solution. While it is impossible to determine which is more “favorable” for the formation of the desired indanols, product analysis and actinometry indicate that the reaction in the solid state is generally more efficient in the formation of desired products.

Our study contrasts greatly with the analysis performed by Wagner. Research and calculations on the subject formerly indicated that when the reacting C-H bond lied along the axis of the n orbital ( $\Delta = 90^\circ$ ) hydrogen abstraction geometry was optimized, as indicated by the rate constant for abstraction being at the maximum.<sup>64</sup> Based upon this, ketones lacking an additional  $\alpha$  substituent should be able to adopt a nearly “ideal” geometry for hydrogen abstraction, and this was effectively illustrated by calculations performed by Wagner.

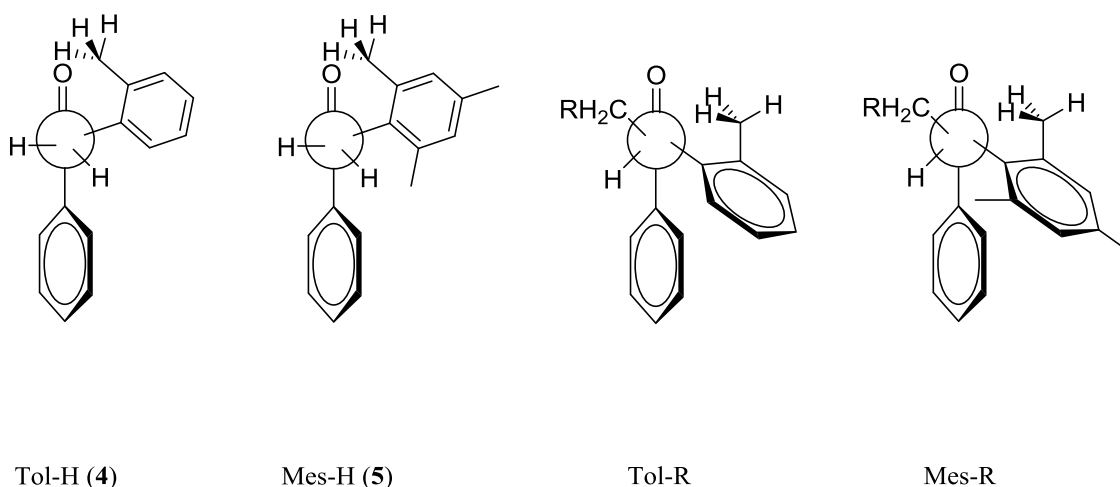
**Figure 2. 3. 1.** Calculations of the hydrogen abstraction geometry for acetophenones **5** and **11**.



As illustrated in **Figure 2. 3. 1**, the Mes-H ketone (**5**) was calculated to have a “more ideal” hydrogen abstraction geometry than the bulkier Mes-Pr ketone (**11**). However, in ketones with an additional  $\alpha$  substituent, the  $\alpha$  aromatic substituent, in the lowest energy conformation, is forced to twist out of the “more-ideal” conformation and angle for hydrogen atom abstraction.<sup>66</sup> The most logical conclusion to draw from this is that ketones with less steric bulk at the  $\alpha$  position are able to adopt a more ideal geometry for hydrogen abstraction in solution, and Wagner’s quantum yield data in solution supports this. However, our solid state actinometry studies of the same crystalline ketones illustrated that some of the more sterically congested ketones were able to react from what was presumed to be a “less-ideal” geometry, an indication that the environment of the crystal

structure may play a greater role in the outcome of the reaction than was previously suspected. In the previous publication, Wagner calculated the lowest energy conformation for both the mesityl and *o*-tolyl compounds (based upon MMPMI calculations) (**Figure 2. 3. 2**), but the calculated structures do not give an indication as to what might be the cause of the trends observed in our solid state quantum yield data. Wagner was able to obtain a crystal structure of ketone **11** which illustrated the twisting of the aryl group away from the ketone to obtain what was considered a “more ideal” geometry. However, without a crystal structure of the less-substituted ketone **5**, it would be difficult to draw conclusions about the ideal geometry for hydrogen abstraction in these ketones. Even more difficult would be to determine how the ideal geometry would be obtained in the solid state where movement within the crystal lattice is limited compared to solution phase experiments. In addition to this, the presence of polymorphism in the compounds, which has not been observed but could be possible, could have an enormous impact on the outcomes of the photoreaction. A crystal structure cannot accurately be utilized to make assumptions about the mechanism for cyclization in solution when the environment in which the reaction takes place can have such an enormous impact on reactivity and reaction outcomes.

**Figure 2. 3. 2.** Wagner’s proposed geometry of solution phase hydrogen abstraction.



## 2. 4. Conclusions

In this study, we have shown that the solid state cyclization of this small set of crystalline ketones to the corresponding 2-indanols takes place with reasonable efficiency, despite what has traditionally been considered to be “less-ideal” geometry to do so. However, studies by Scheffer and others into the mechanism of the Norrish Type II reaction in crystals indicate that reaction efficiency depends upon more than just the geometry of hydrogen abstraction. Observation of excited state intermediates via spectroscopic methods may give greater insight into the mechanism of the reaction and the effect that geometric constraints have on the outcome. Our study also highlighted the discovery of a surprising trend in the efficiency of a solid state reaction, which may help to illuminate the mechanism of the formation and reactions of 1 – 5 biradicals in the solid state.

## 2. 5. Experimental

### General Methods

All chemicals were purchased from Sigma-Aldrich Co. Inc. and Fisher Scientific Co. Inc. and used without further purification. Anhydrous solvents were acquired by distillation from sodium, distillation over calcium chloride, or drying over Potassium Carbonate. Purification was carried out using Silica-P flash silica gel (40-62 angstrom) purchased from SiliCycle Inc.  $^1\text{H}$  and  $^{13}\text{C}$  spectra were obtained on a Bruker Advance AV300. IR spectra were collected using a Perkin-Elmer Spectrum instrument equipped with a universal attenuated total reflectance (ATR) accessory. Mass spectra were obtained using an Applied Biosystems Voyager DE-STR-MALDI-TOF. UV-Vis spectra were collected with an Ocean Optics USB2000. Gas chromatography data was acquired on a Hewlett-Packard 5890 series II gas chromatograph equipped with an HP3396 series II integrator and an HP-5 capillary column of dimensions 25 m x 0.2 mm with a film thickness of 0.11 mm. Dynamic light scattering experiments were conducted on a Beckman-Coulter N4 Plus submicron particle size analyzer.

### Synthesis of Crystalline Ketones 4 and 5

Following a procedure by Wagner, 2, 4, 6-Trimethylbenzyl chloride or 2-Methylbenzyl chloride was heated to 80°C overnight with an excess of NaCN in DMSO, which, upon workup, gave crude  $\alpha$ -mesityl or  $\alpha$ -tolylacetonitrile. The crude acetonitrile was hydrolyzed by heating to 155°C with KOH and ethylene glycol for 6 hours, followed by cooling. After cooling, the solution was acidified using concentrated HCl, which gave a solid. Recrystallization from acetone was followed by treatment with  $\text{PCl}_3$  to give the acid chloride. Friedel-Crafts acylation with  $\text{AlCl}_3$  in benzene gave the desired ketones in the yields of 50-53%. Ketones were recrystallized from DCM: hexanes 1:10.

**$\alpha$ -(*o*-tolyl)acetophenone (4).** Yield 53%; m.p. 167-168 °C;  $^1\text{H}$  NMR (300 MHz,  $\text{CDCl}_3$ )  $\delta$  8.03 (m, 2H, **CH**), 7.57 (m, 1H, **CH**), 7.46 (m, 2H, **CH**), 7.17 (m, 4H, **CH**), 4.31 (s, 2H, **CH<sub>2</sub>CO**), 2.26 (s, 3H, **CCH<sub>3</sub>**);  $^{13}\text{C}$  NMR (75MHz,  $\text{CDCl}_3$ )  $\delta$  197.52 (**CO**), 136.93(**CHCH**), 136.91(**CHCH**), 133.48(**CHCH**), 133.19(**CHCH**), 130.39(**CHCH**), 130.31(**CHCH**), 128.70(**CHCH**), 128.37(**CHCH**), 127.26(**CHCH**), 126.14(**CHCH**), 43.51 (**CH<sub>2</sub>CO**), 19.81(**CH<sub>3</sub>C**). FTIR (solid, HATR,  $\text{cm}^{-1}$ ): 2900, 1684, 1447, 1337, 1210, 997.

**$\alpha$ -(*mesityl*)acetophenone (5).** Yield 50%; m.p. 164-165 °C;  $^1\text{H}$  NMR (300 MHz,  $\text{CDCl}_3$ )  $\delta$  8.07 (m, 2H, **CH**), 7.59 (m, 1H, **CH**), 7.50 (m, 2H, **CH**), 6.91 (s, 2H, **CH**), 4.16 (s, 2H, **CH<sub>2</sub>CO**), 2.2 (s, 9H, **CCH<sub>3</sub>**);  $^{13}\text{C}$  NMR (75MHz,  $\text{CDCl}_3$ )  $\delta$  196.52 (**CO**), 137.63(**CHCH**), 136.51(**CHCH**), 133.68(**CHCH**), 132.89(**CHCH**), 130.38(**CHCH**), 130.35(**CHCH**), 128.61(**CHCH**), 128.38(**CHCH**), 41.31(**COCH<sub>2</sub>**), 21.81(**CCH<sub>3</sub>**), 17.80(**CCH<sub>3</sub>**). FTIR (solid, HATR,  $\text{cm}^{-1}$ ): 2920, 1684, 1448, 1221, 990.

### Synthesis of Crystalline Ketones 8 - 11

Following a modified procedure by Grassa, 1,1'-bis(di-*tert*-butylphosphino)ferrocene palladium chloride ((DtBPF)PdCl<sub>2</sub>) (2 mol %) and NaO<sup>t</sup>Bu (2.2 mmol) were placed in a clean, flame dried Schlenk tube under argon. Anhydrous, degassed THF was added, followed by addition of the tolyl or mesityl aryl hydride (2 mmol) and ketone (2 mmol). The resulting mixture was stirred at 60° C and monitored via GC. When complete, the reaction mixture was purified via flash chromatography to give yields of 63-88%. The products were recrystallized from DCM: hexanes 1:10.

**$\alpha$ -(*o*-tolyl)propiophenone (8).** Yield 88%; m.p. 154.4-155 °C;  $^1\text{H}$  NMR (300 MHz,  $\text{CDCl}_3$ )  $\delta$  7.83 (m, 2H, **CH**), 7.46 (m, 1H, **CH**), 7.32 (m, 2H, **CH**), 7.21 (m, 1H, **CH**), 7.08 (m, 3H, **CH**), 4.76 (q,  $J = 6.7$  Hz, 1H, **CHCH<sub>3</sub>**), 2.49 (s, 3H, **CH<sub>3</sub>C**), 1.47(d,  $J = 6.7$ , 3H, **CHCH<sub>3</sub>**);  $^{13}\text{C}$  NMR (75MHz,



CDCl<sub>3</sub>)  $\delta$  201.03 (CO), 140.18(CHCH), 136.64(CHCH), 134.55(CHCH), 132.68(CHCH), 130.95(CHCH), 128.50(CHCH), 127.01(CHCH), 126.88(CHCH), 126.77(CHCH), 44.59(CHCO), 19.63(CH<sub>3</sub>C), 18.05(CH<sub>3</sub>CH). FTIR (solid, HATR, cm<sup>-1</sup>): 2930, 1677, 1446, 1324, 1225, 949.

**$\alpha$ -(mesityl)propiofenone (10).** Yield 79%; m.p. 179-180 °C; <sup>1</sup>H NMR (300 MHz, CDCl<sub>3</sub>)  $\delta$  7.72 (m, 2H, CHCH), 7.40 (m, 1H, CHCH), 7.27 (m, 2H, CHCH), 6.78 (s, 2H, CHCH), 4.49 (q, J = 6.8 Hz, 1H, CHCH<sub>3</sub>), 2.23 (s, 9H, CH<sub>3</sub>C), 1.49 (d, J = 6.8, 3H, CH<sub>3</sub>CH); <sup>13</sup>C NMR (75MHz, CDCl<sub>3</sub>)  $\delta$  199.32(CO), 137.23(CHCH), 137.22(CHCH), 136.85(CHCH), 133.11(CHCH), 130.67(CHCH), 128.83(CHCH), 126.71(CHCH), 41.25(CHCO), 22.34(CH<sub>3</sub>CCH), 20.00(CH<sub>3</sub>CH), 17.01(CH<sub>3</sub>CHC). FTIR (solid, HATR, cm<sup>-1</sup>): 2926, 1683, 1445, 1228, 1026, 991.

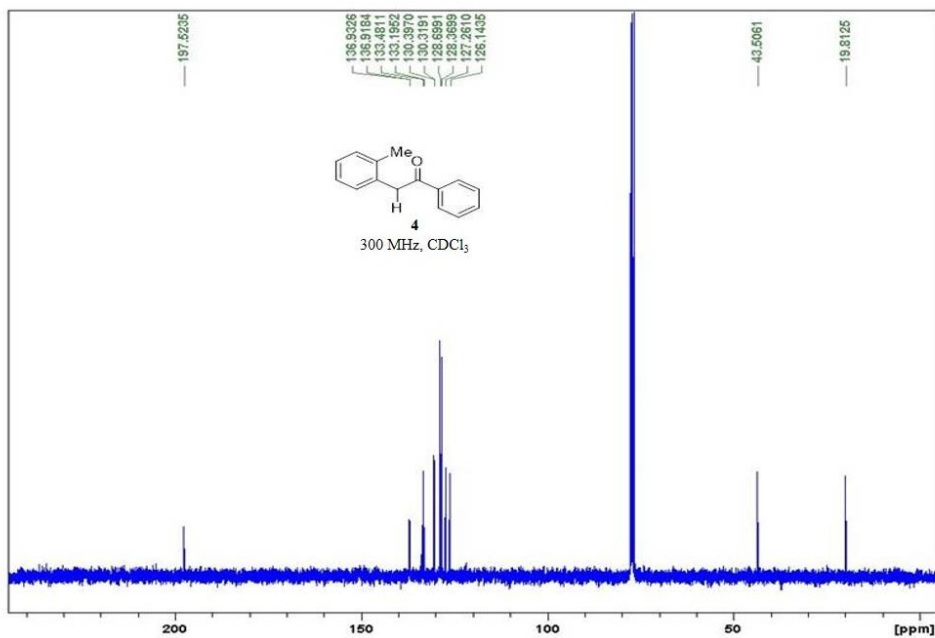
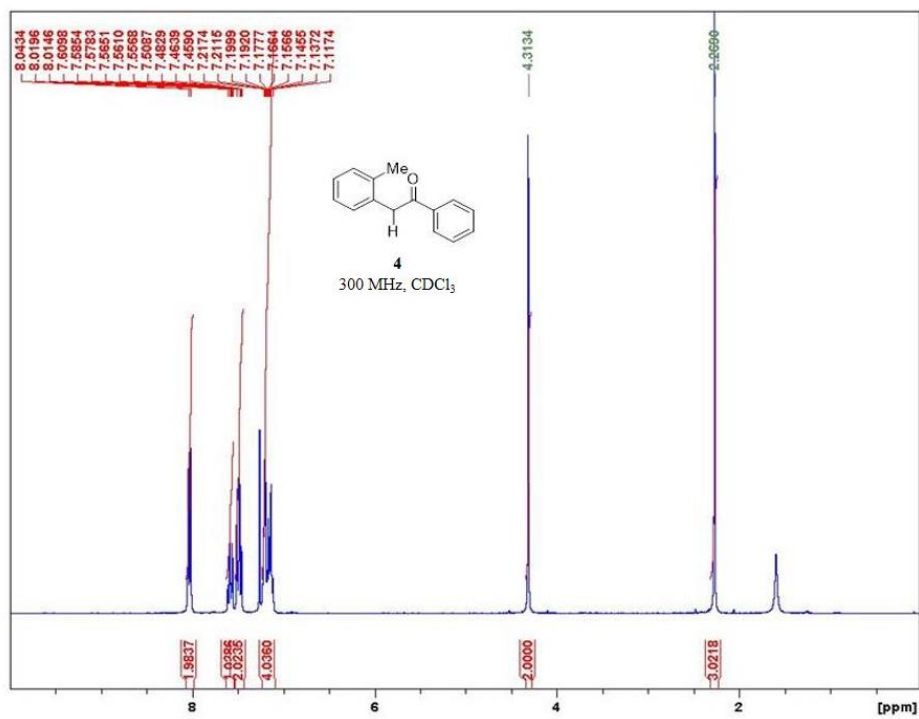
**$\alpha$ -propyl- $\alpha$ -mesityl-acetophenone (11).** Yield 63%; m.p. 167-168 °C; <sup>1</sup>H NMR (300 MHz, CDCl<sub>3</sub>)  $\delta$  8.05 (m, 2H, CHCH), 7.67 (m, 1H, CHCH), 7.56 (m, 2H, CHCH), 6.81 (s, 2H, CHCH), 4.28 (q, J = 6.7, 1H, CHCO), 2.36 (s, 9H, CH<sub>3</sub>C), 1.77 (m, 2H, CH<sub>2</sub>CH<sub>2</sub>), 1.34 (m, 2H, CH<sub>3</sub>CH<sub>2</sub>), 1.1 (t, 3H, CH<sub>3</sub>CH<sub>2</sub>); <sup>13</sup>C NMR (75MHz, CDCl<sub>3</sub>)  $\delta$  201.78 (CO), 137.63(CHCH), 136.02(CHCH), 135.89(CHCH), 132.32(CHCH), 130.59(CHCH), 128.24(CHCH), 128.12(CHCH), 51.03 (CHCO), 32.71(CHCH<sub>2</sub>), 21.54(CH<sub>3</sub>CCH), 20.90(CH<sub>2</sub>CH<sub>2</sub>), 20.72(CH<sub>3</sub>C), 14.49(CH<sub>3</sub>CH<sub>2</sub>). FTIR (solid, HATR, cm<sup>-1</sup>): 2952, 1675, 1596, 1446, 1209, 1025, 848.

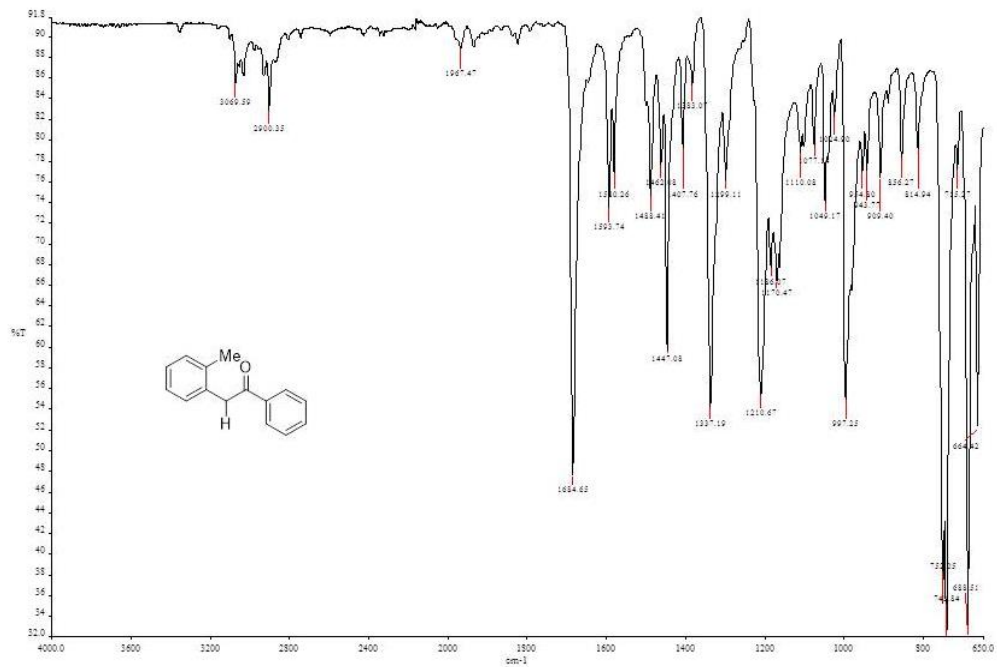
## 2. 6. Appendix

### Characterization for Chapter 2

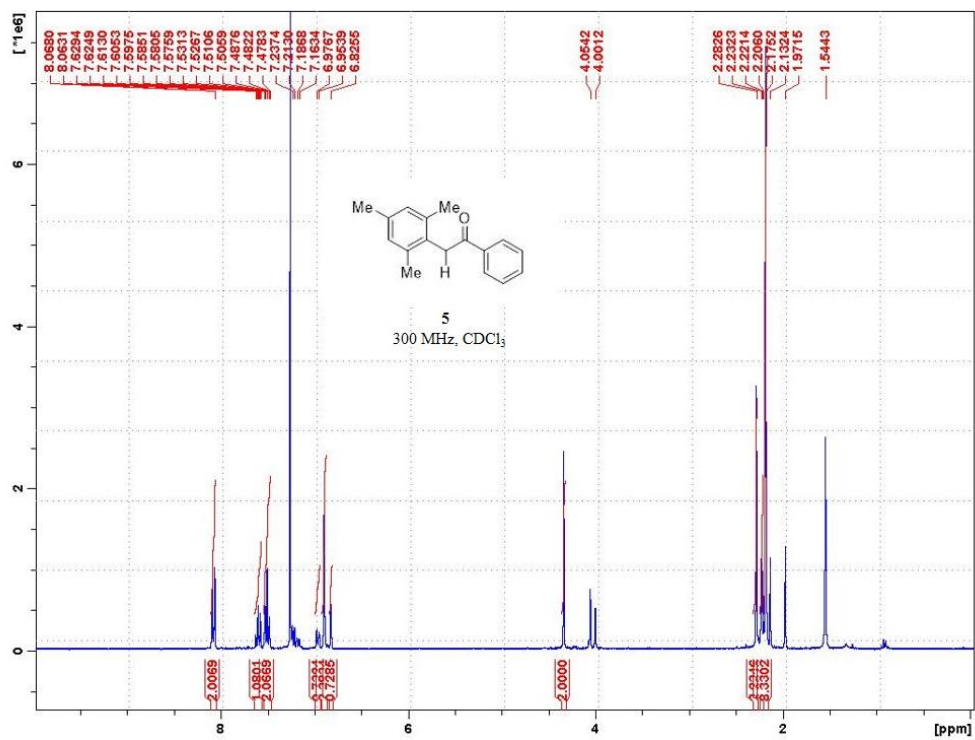
$^1\text{H}$ , $^{13}\text{C}$ , and IR data for <b>4</b> .....	32
$^1\text{H}$ , $^{13}\text{C}$ , and IR data for <b>5</b> .....	33
$^1\text{H}$ , $^{13}\text{C}$ , and IR data for <b>8</b> .....	35
$^1\text{H}$ , $^{13}\text{C}$ , and IR data for <b>10</b> .....	36
$^1\text{H}$ , $^{13}\text{C}$ , and IR data for <b>11</b> .....	38
DLS Data – Representative Sample ( <b>4</b> ).....	40

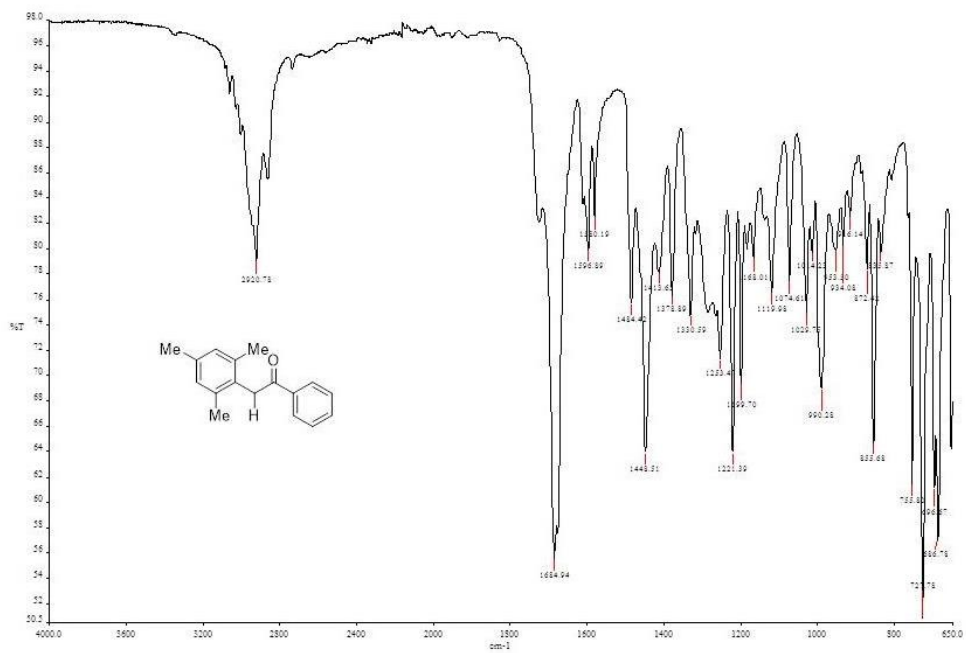
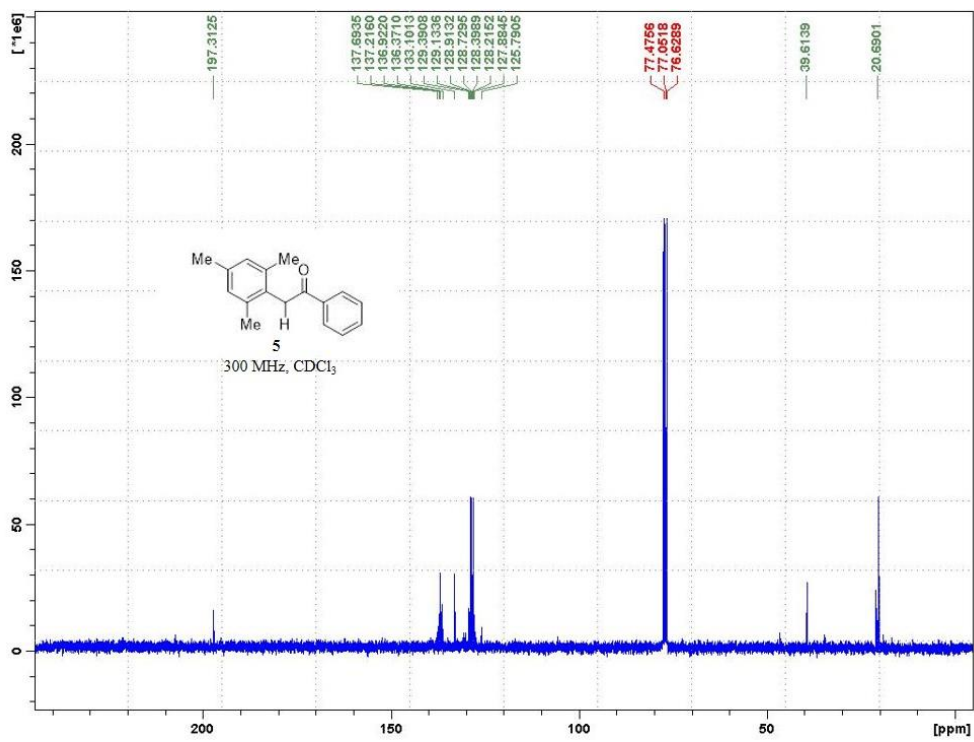
$\alpha$ -(o-tolyl)acetophenone (4)



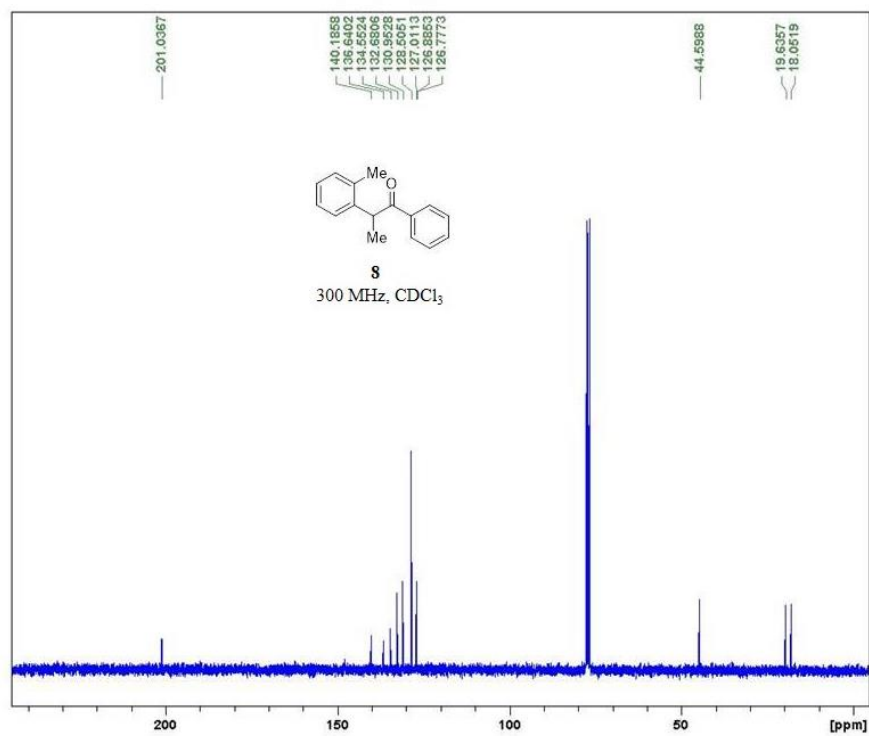
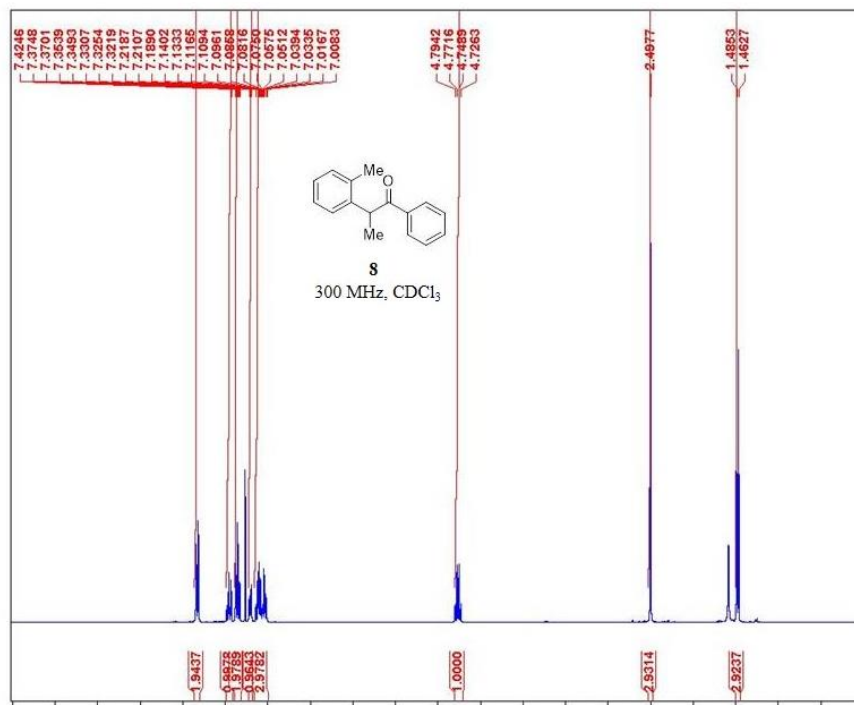


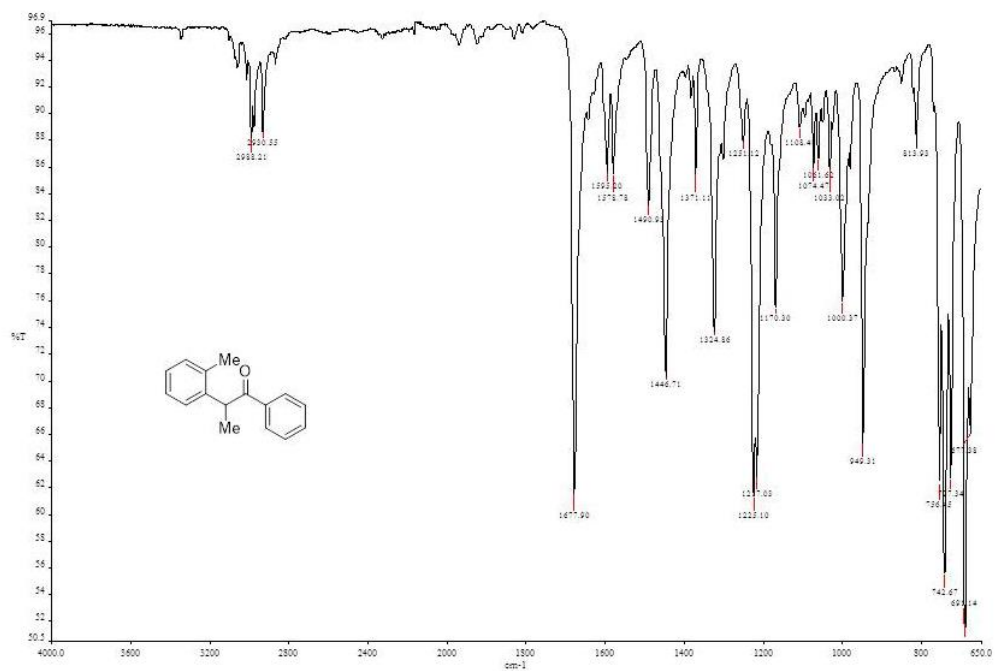
$\alpha$ -(mesityl)acetophenone (5)



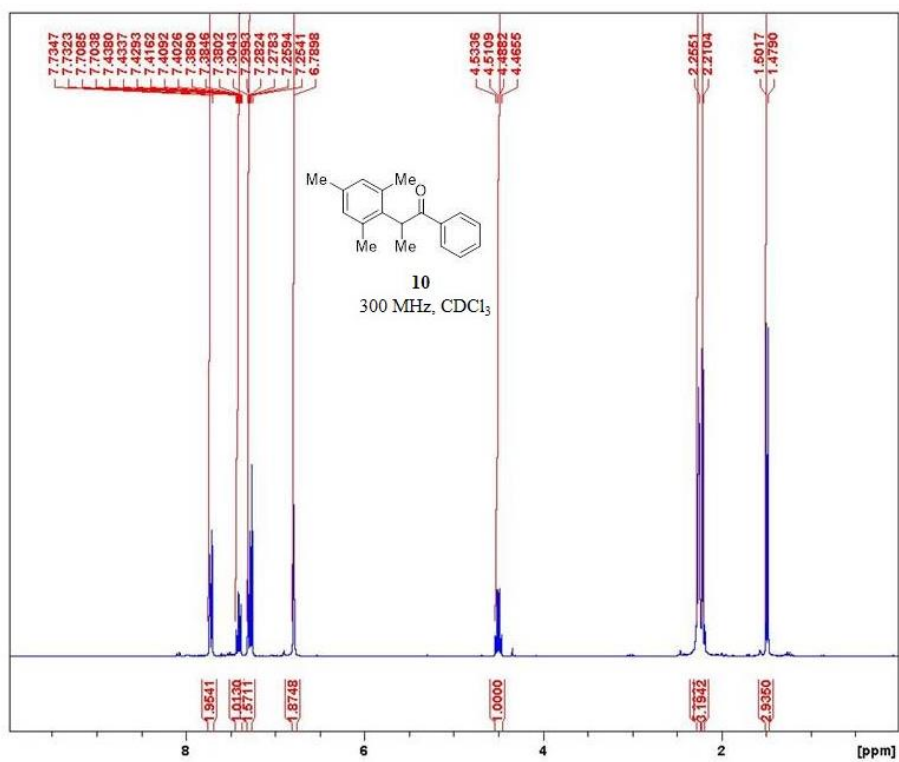


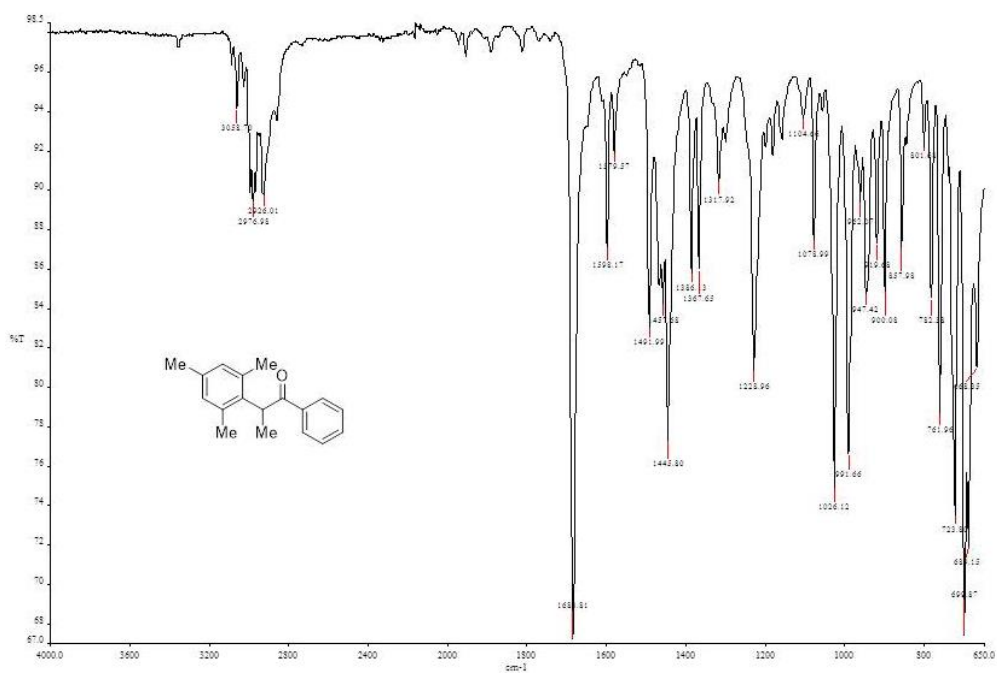
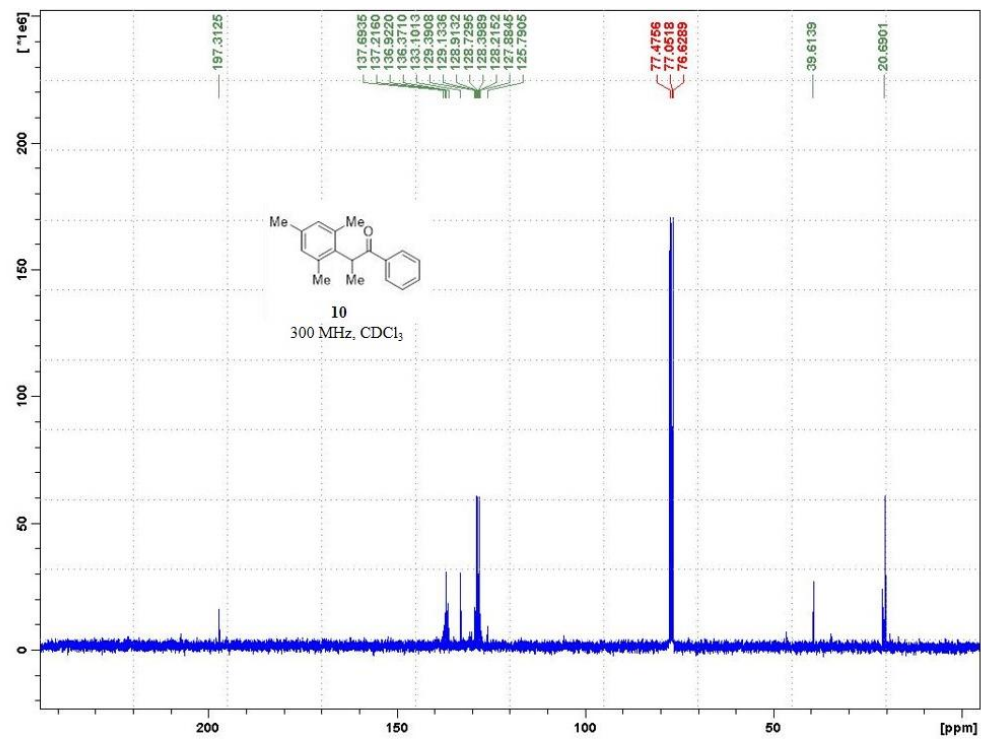
$\alpha$ -(o-tolyl)propiophenone (**8**)





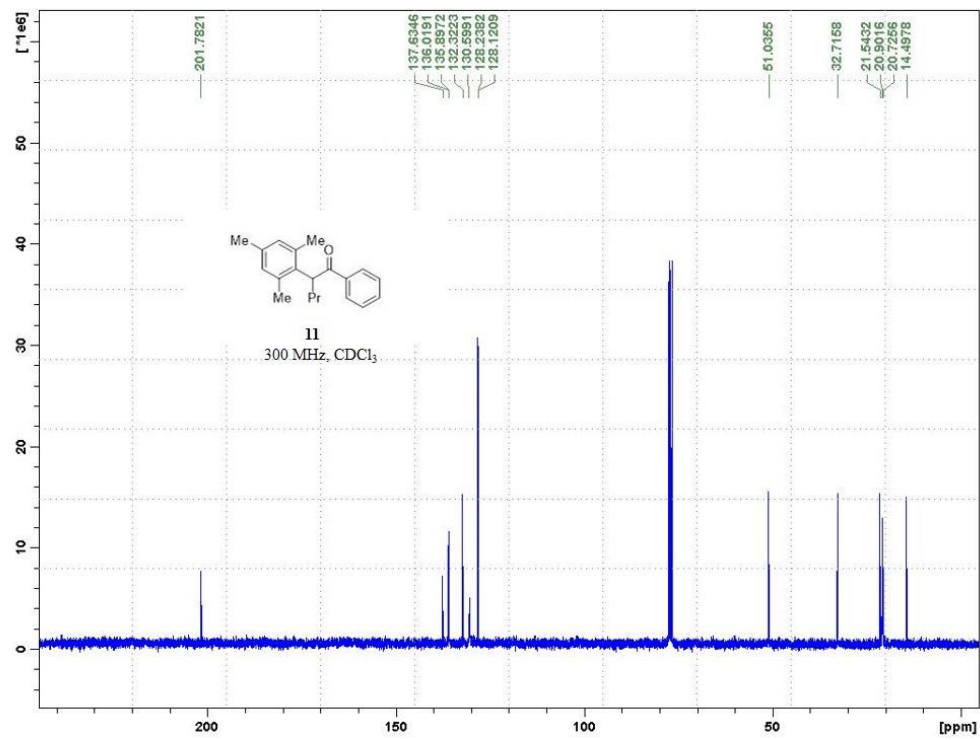
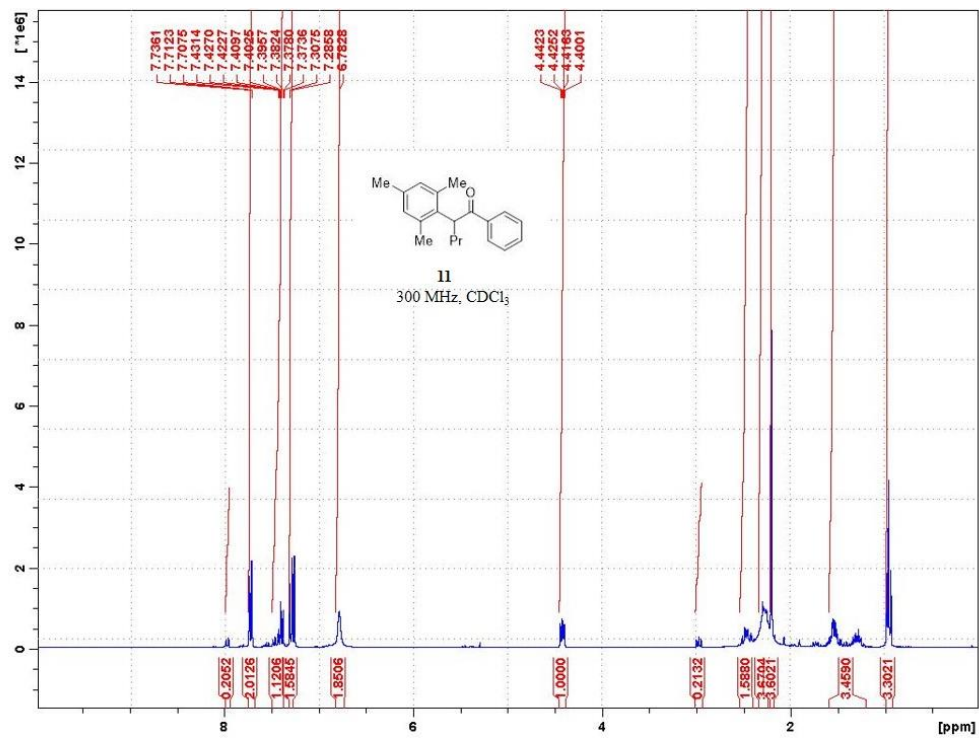
$\alpha$ -(mesityl)propiofenone (10)

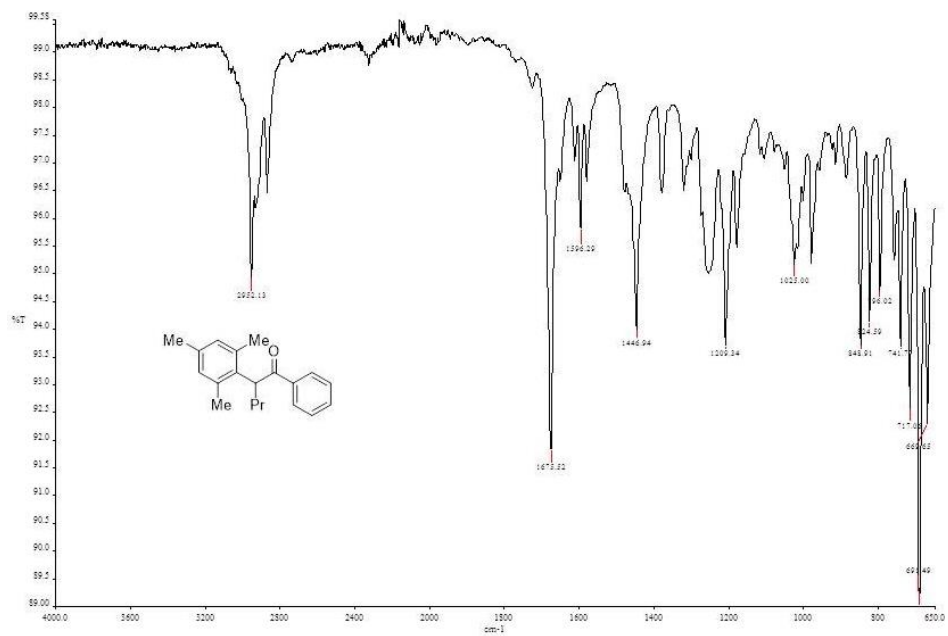




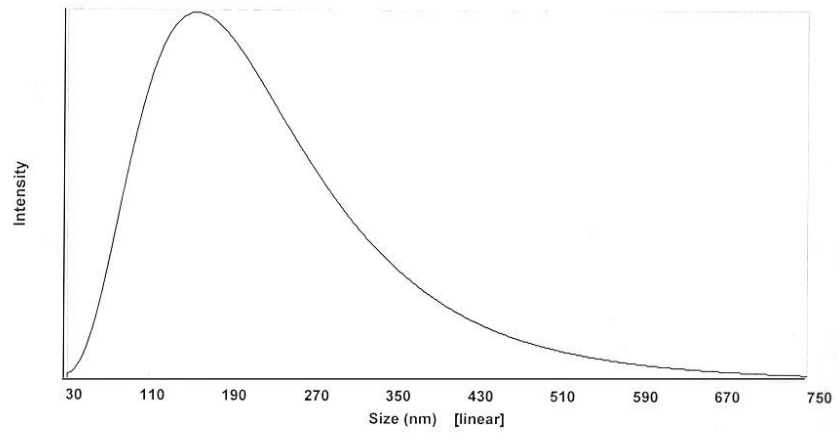


# $\alpha$ -propyl- $\alpha$ -mesityl-acetophenone (11)





**Dynamic Light Scattering – Representative Example ( $\alpha$ -(o-tolyl)acetophenone (4))**



**$\alpha$ -(o-tolyl)acetophenone (4)**

## **Chapter 3**

### **Quantum Chain Reaction of Tethered Diarylcyclopropenones in the Solid State and Their Distance-Dependence in Solution Reveal a Dexter S<sub>2</sub>-S<sub>2</sub> Energy Transfer Mechanism**

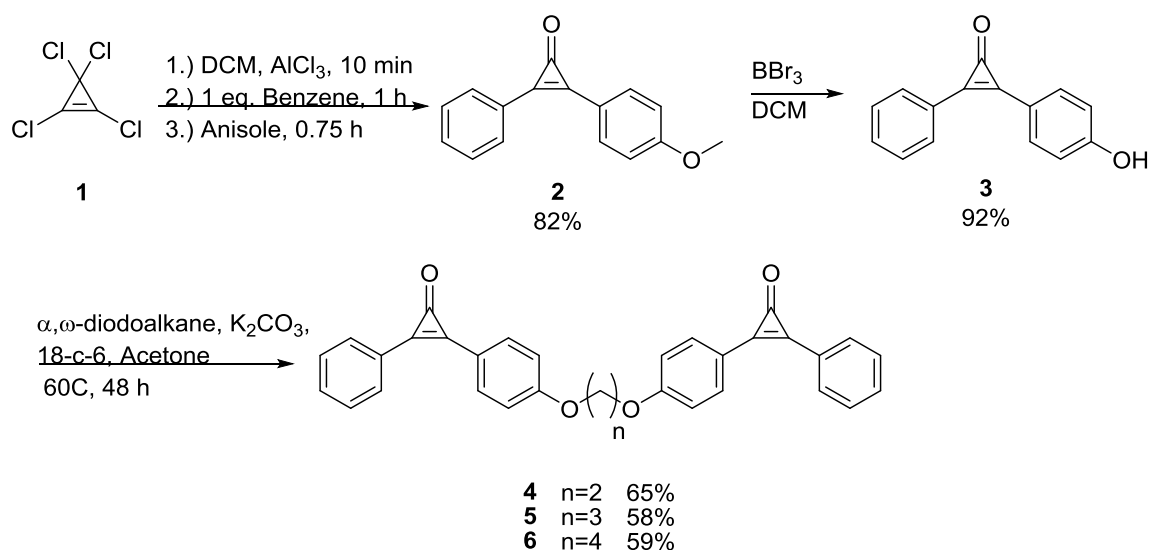
### 3. 1. Introduction

Fundamental knowledge of energy transfer mechanisms over short and long range distances, and in the solid state, is essential to the development of optoelectronic materials and sensors that rely on photon collection and transport.<sup>65</sup> While high-energy transitions are common in absorption processes, it is generally assumed that energy transfer is only important between the lowest singlet ( $S_1$ ) or triplet ( $T_1$ ) states. Energy transfer from upper excited states ( $S_n$ ,  $n \geq 2$ ) is generally not considered because literature precedent suggests that internal conversion to  $S_1$  should be dominant. In fact, it appears that only a few compounds have been shown to exhibit efficient energy transfer from upper excited singlet states in solution. Among them are the natural purple bacteria light-harvesting complex II, some synthetic porphyrin dyads,<sup>66</sup> and azulene-porphyrin systems.<sup>67</sup>

Suggesting that energy transfer from upper excited states in the solid state may be more important than suspected, we recently disclosed an efficient singlet state quantum chain reaction that is propagated by a  $S_2(\text{Donor}) \rightarrow S_2(\text{Acceptor})$  energy transfer process. In this reaction, the absorption of a single photon by a diarylcyclopropanone molecule in the solid state unveils several diarylacetylene photoproducts in a process that may be suited for the development of materials applications based on photochemical amplification with a gain.<sup>68,69</sup> As initially described,<sup>70</sup> the reaction starts by excitation of a diarylcyclopropanone (DACP) to its second excited state ( $S_2\text{-DACP}^*$ ) where it undergoes an adiabatic decarbonylation within ca. 200 fs to form a diarylacetylene in its second excited state ( $S_2\text{-DAA}^*$ ).<sup>6</sup> Although the detailed nature of the excited state species formed immediately after reaction has been a matter of debate (henceforth indicated as  $S_2\text{-I}^*$ ),<sup>71,72</sup> it has a relatively long lifetime (ca. 8 ps)<sup>73</sup> and, under favorable

circumstances, it can transfer its energy to a new diarylcyclopropenone DACP molecule before going to the ground state of diarylacetylene DAA.<sup>74</sup>

**Scheme 3. 1.** Synthesis of alkyl-tethered DPCP dimers.



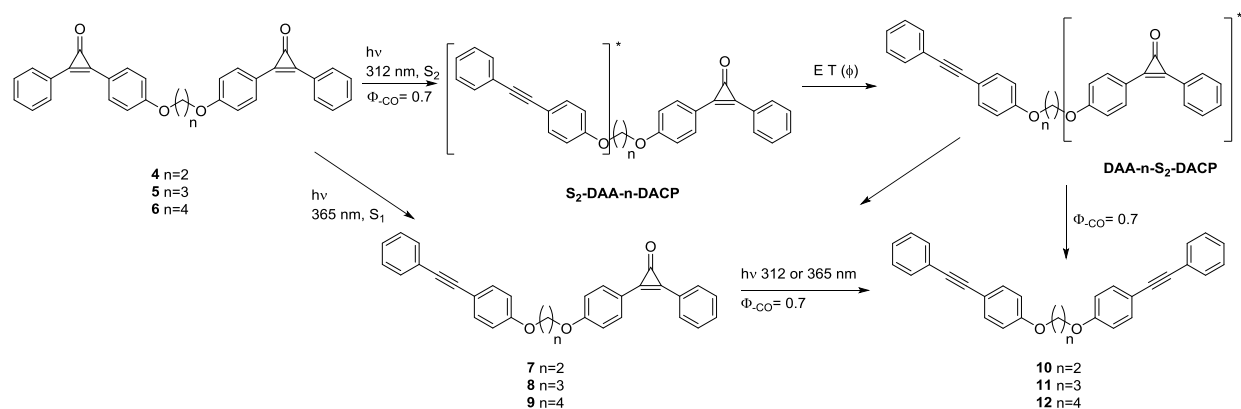
While diffusion-controlled energy transfer in solution is too slow to mediate a quantum chain, we have shown that fast energy transfer in crystals ( $k_{ET} \approx 10^{12}$ )<sup>75</sup> allows for efficient energy transfer from the S<sub>2</sub>-I\* species to S<sub>2</sub>-DACP\*. The sensitization of new reactants by the newly formed excited state products allows for a chain process with more than one reaction per photon to take place. We have shown that the quantum chain reaction in crystals is quite general. Examples were found where the quantum yield of reaction increases by as much as 1100% with absolute quantum yields as high as  $\Phi_{rxn}=3.3$ .<sup>4</sup> Furthermore, to investigate the proposed reaction mechanism and to address the nature of the excited state chain carrier (S<sub>2</sub>-I\*), we recently performed femtosecond pump-probe measurements with samples of nanocrystalline diphenylcyclopropenone (DPCP) suspended in water.<sup>76</sup> We were able to confirm that solid state photoexcitation of S<sub>2</sub>-DPCP leads to the formation of the postulated excited state intermediate S<sub>2</sub>-I\*, and that the corresponding transient is spectroscopically similar, but not identical to the one

that is optically accessible for the second excited state of the photoproduct ( $S_2$  diphenylacetylene).<sup>12</sup>

In order to test the nature of the excited state carrier ( $S_2-I^*$ ), and on the way to extending this process to polymer matrices and other solid state materials, we decided to explore the key  $S_2-I^*-S_0$ -DACP energy transfer step by simple energy transfer studies. Assuming that coherent excitation with simultaneous reactions of the two reaction sites is not the dominant mechanism, we set out to analyze the distance-dependence of energy transfer by measuring the quantum yields of the DACP- $n$ -DACP tethered dimers **4** - **6** shown in **Scheme 3.1**. Ether tethers with  $n=2$  (**4**),  $n=3$  (**5**) and  $n=4$  carbons (**6**) were selected because they are likely to minimize a linker-dependent super-exchange-mediated energy transfer processes.<sup>77</sup> As indicated in **Scheme 3. 2**, excitation with a 312 nm source is expected to initiate the adiabatic reaction in  $S_2$  at one of the two termini ( $S_2$ -DACP\*- $n$ -DACP) to generate an excited state chain carrier ( $S_2-I^*-n$ -DACP). This can decay to monoreacted structures **7** - **9** (DAA- $n$ -DACP), or transfer energy to the other end (DAA- $n$ - $S_2$ -DACP\*), which is enabled to undergo a second reaction to form doubly reacted products **10** - **12** (DAA- $n$ -DAA). By measuring the singlet-state quantum efficiency for decarbonylation of **4** - **6** in solution it is possible to determine the efficiency of the energy transfer step,  $\phi_{ET}$ . To analyze the mechanism of energy transfer, we estimated the approximate distances between the linked  $S_2-I^*$  donors and DACP acceptors and we determined the critical distance ( $R_0$ ) for a resonance (Förster)<sup>78</sup> energy transfer process using the measured spectroscopic properties of the  $S_2$ -DAA\* and  $S_2$ -DACP\* states. Despite an estimated critical distance of ca.  $R_0=30$  Å, we found that the singlet-state quantum chain vanishes beyond distances of ca. 6 Å. As described in detail below, an exponential decay of the energy transfer efficiency as a function of the donor-acceptor distance indicated that, as suggested by Popik,<sup>7</sup> and in agreement with our recent transient absorption

studies,<sup>12</sup> the S<sub>2</sub>-S<sub>2</sub> energy transfer involves an intermediate that is different from the spectroscopic S<sub>2</sub>-DAA\*, and that energy transfer is likely to proceed by an exchange, Dexter mechanism.<sup>79</sup>

**Scheme 3. 2.** Mechanism of photoexcitation and reaction of DPCP derivatives.



## 3. 2. Results and Discussion

### Tethered Dimer Preparation and Crystallization.

The crystalline tethered dimers **4 - 6** were synthesized (**Scheme 3. 1**) from commercially available tetrachlorocyclopropene **1** in a three-step procedure with overall yields ranging from 58-65% and were characterized by <sup>1</sup>H and <sup>13</sup>C NMR, IR, UV-Vis and MALDI-TOF mass spectrometry (SI). All dimers were purified via column chromatography (1:2 acetone:hexanes) R<sub>f</sub> = 0.2 – 0.3. The crystalline products were then recrystallized from DCM: methylcyclohexane (1:9). All three dimers (**4 – 6**) were crystalline solids with similar melting points. The recrystallized dimers were analyzed via Thermogravimetric Analysis (TGA), Dynamic Scanning Calorimetry (DSC), and Powder X-Ray Diffraction (PXRD). TGA and DSC analysis indicated that decarbonylation took place under thermal conditions starting at 50 °C, while PXRD analysis revealed that the samples were highly crystalline. Solid state quantum yield determinations of the linked dimers described below were carried with aqueous nanocrystalline suspensions prepared with the reprecipitation method.<sup>80</sup> A known amount of sample in acetone was injected into rapidly

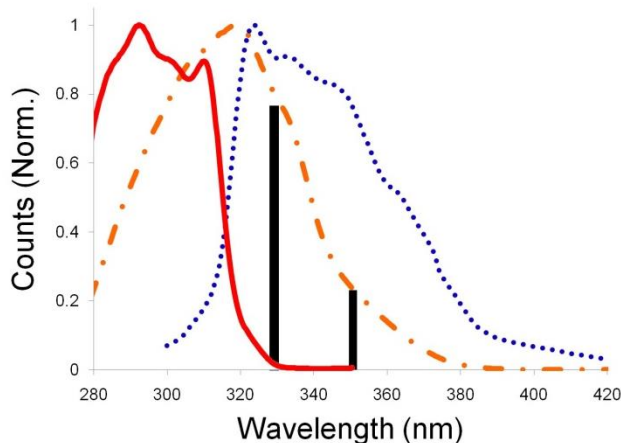


vortexing millipore water and sonicated at room temperature multiple times prior to reaction. Nanocrystals ranged in size from 50 to 200 nm as determined by Dynamic Light Scattering (DLS) analysis.

### **DACP UV Absorption, DAA Emission and Estimation of the Förster Distance.**

Compared to the UV spectrum of monomer **2** measured in benzene (**Figure 3.2.1**), those of tethered dimers **4–6** displayed small shifts in  $\lambda_{\text{max}}$  (290 nm to 292 nm) with molar absorptivities that are twice as large, and a slight increase in molar absorptivity of the weak  $S_1$  transition at  $\lambda > 350$  nm.<sup>81</sup> These results suggest that there are small electronic interactions between the two cyclopropanone units in the ground state.<sup>82</sup> The characteristic  $S_2$ - $S_0$  fluorescence of the monomeric 1-methoxy-4-(phenylethynyl)benzene **13** (dotted blue line in **Figure 3.2.1**) has a smaller vibrational resolution than that of the parent diphenyl acetylene but it also has a relatively small emission quantum yield of  $\Phi=0.032$ . The  $S_2$ - $S_0$  emission spectrum of the dialkyne has a good overlap with the  $S_0$ - $S_2$  absorption of methoxy-cyclopropanone **2** (dashed orange line), suggesting that the acetylene has enough energy to sensitize the subsequent reaction (**Figure 3.2.1**).<sup>83</sup> From the spectral overlap in **Figure 3.2.1**, a reported lifetime of ca. 10 ps for the  $S_2$  of **2**, a measured quantum yield of 0.032, and estimated orientation factors between 1.16 and 2.60 (see below) one can estimate a critical Förster distance of ca.  $R_0 = 30 \text{ \AA}$ . While this estimate is based on a point dipole approximation that is known to break down at short distances, it suggests that Förster energy transfer involving  $S_2$ -DAA\* should be effective to relatively long distances, which turned out not to be the case.

**Figure 3. 2. 1.** S<sub>2</sub>-S<sub>0</sub> fluorescence spectrum of **2** and **13**.

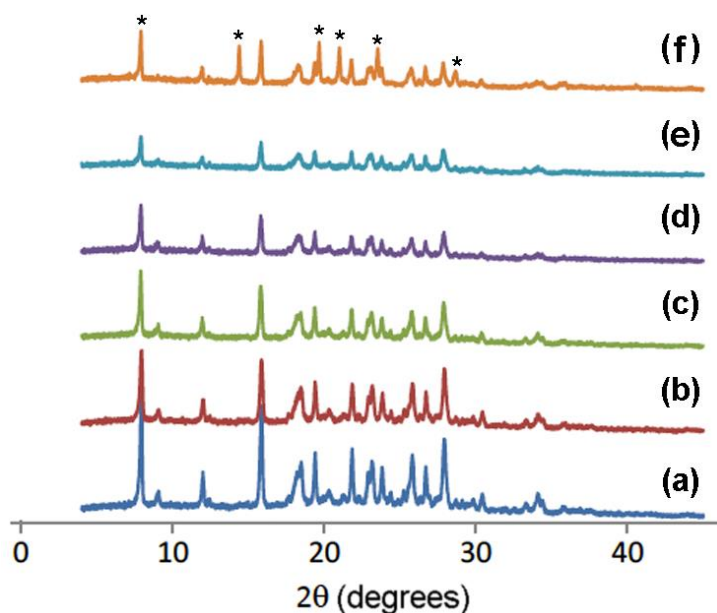


### Photochemical Reactivity in Solution and in Crystals.

Photochemical experiments were carried out in benzene by excitation at 312 nm and 365 nm to establish the reactivity of the S<sub>1</sub> and S<sub>2</sub> states. Samples of the methoxy-monomer **2** and tethered dimers **4 - 6** were found to decarbonylate with a 100% chemical yield to give the corresponding 1-methoxy-4-(phenylethynyl)benzene **13** and DAA dimers **10 - 12**, respectively, at both wavelengths. Solution phase photochemical experiments were monitored using <sup>1</sup>H NMR analysis of samples irradiated in *d*<sub>6</sub>-benzene. Solid state experiments were monitored via <sup>1</sup>H NMR analysis of extracted aliquots of aqueous nanocrystalline suspensions. Irradiated samples were separated via column chromatography, as necessary, and subsequently characterized via <sup>1</sup>H NMR, <sup>13</sup>C NMR, and IR analysis. For samples exposed to extended irradiation times there were no byproducts detected by gas chromatography or <sup>1</sup>H NMR. Similar results were obtained upon photolysis of bulk crystals and nanocrystalline suspensions.<sup>15</sup> Thermal decarbonylation in the solid state was observed by TGA analysis over a range of 50 -100 °C for all three linked dimers, and this was confirmed via DSC and thin layer chromatography analysis. Compounds **4 - 6** had melting points within a similar range (150 - 160 °C) and were not observed to degrade at

temperatures of up to 200 °C. Photolysis of the bulk crystalline solid was monitored over time via PXRD analysis at varying extents of conversion to product, as determined by  $^1\text{H}$  NMR analysis. All three dimers display high crystallinity, even after extended irradiation times and high conversion values, as shown in **Figure 3. 2. 2** for tethered dimer **5**. It could be shown that PXRD measured at high conversion values retains the characteristics of the reactant phase, with the late appearance of diffraction peaks assigned to the phase of the product, suggesting that reaction proceeds via a metastable phase with the characteristics of reactant, rather than by a more demanding single crystal to single crystal transformation, or by melting or amorphization, as discussed in recently published work.<sup>121</sup>

**Figure 3. 2. 2.** PXRD as a measure of sample crystallinity as a function of conversion.



### Solid State Photochemistry and Confirmation of a Quantum Chain.

Quantum yield measurements in the solid state using nanocrystalline suspensions of compounds **2** and **4 - 6** were carried out using suspended dicumylketone nanocrystals as a chemical actinometer ( $\Phi_{\text{Rxn}} = 0.18$ ).<sup>84</sup> The extent of reaction upon irradiation at 312 nm ( $S_2$ ) and at 365 nm

(S<sub>1</sub>) was determined from the disappearance of the starting material by <sup>1</sup>H NMR. As indicated in Table 1, the results in the solid state are essentially identical for all compounds. Irradiation of S<sub>1</sub> at 365 nm resulted in Φ<sub>Rxn</sub> values between 0.69 and 0.78, and experiments carried out by excitation of S<sub>2</sub> at 312 nm gave values between 2.4 and 2.7, which confirm that a quantum chain take place in the crystalline state.

### Adiabatic Reaction and Energy Transfer in Solution.

Having confirmed that nanocrystalline suspensions of DACPs **2** and **4 - 6** can undergo a quantum chain reaction when excited to S<sub>2</sub>, the quantum yields of reaction in benzene solutions were measured at 312 and 365 nm (**Table 3.2**). The quantum yields for decarbonylation per cyclopropanone moiety at 365 nm (S<sub>1</sub>) are nearly identical for all compounds (Φ<sub>Rxn</sub> 0.72-0.74), indicating that the tethered dimers act as two individual chromophores.

**Table 3. 2. 1.** Quantum yields for decarbonylation for **2** and **4 – 6** in benzene and as nanocrystals.

	Φ <sub>CO</sub> Benzene		Φ <sub>CO</sub> Nanocrystals		Φ <sub>ET</sub>
	365 nm	312 nm	365 nm	312 nm	
<b>2</b>	0.72± 0.06	0.70± 0.05	0.78± 0.1	2.74± 0.31	N/A
<b>4</b>	0.73± 0.03	1.14± 0.03	0.71± 0.1	2.52± 0.29	89.7± 6.0
<b>5</b>	0.74± 0.06	1.02± 0.04	0.69± 0.1	2.39± 0.33	65.3± 8.1
<b>6</b>	0.74± 0.04	0.70± 0.04	0.76± 0.1	2.47± 0.28	0.00± 7.9

To show that energy transfer and a quantum chain do not occur by irradiation at 365 nm, we detected, isolated, and fully characterized all the half-reacted (DAA-n-DACP) compounds **7 - 9** from reactions carried out to moderate conversion values (ca. 40%, SI). We also showed that isolated samples of **7 - 9** react to form **10 - 12** with quantum yields of Φ<sub>rxn</sub>=0.70, indicating that the tethered-DAA does not affect the photochemical properties of the DACP chromophore.

Subsequent experiments with linked dimers **4** - **6** at 312 nm ( $S_2$ ) in benzene revealed an increased quantum yield of decarbonylation relative to monomer **2** ( $\Phi_{Rxn}=0.70$ ) for ethylenedioxy tethered dimer **4** ( $\Phi_{Rxn}=1.14$ ) and propylenedioxy linked dimer **5** ( $\Phi_{Rxn}=1.02$ ). The butylenedioxy tethered dimer **6** showed no increase in quantum yield relative to **2** (Table 1). Experiments carried out independently with product detection using  $^1H$  NMR or UV-Vis analysis gave consistent results.

### **$S_2$ - $S_2$ Energy Transfer Efficiency.**

To determine the efficiency of energy transfer in solution,  $\phi_{ET}$ , we assume that excitation to  $S_2$ -DACP\*-DACP at 312 nm follows by adiabatic reaction to  $S_2$ -I\*-DACP with a quantum yield of  $\Phi_{Rxn}=0.7$ , as is the case of compound **2**. The excitation in  $S_2$ -I\*-DACP, residing in one half of the tethered dimer, can decay to the ground state to give DAA-n-DACP products **7** - **9**, or it can undergo an energy transfer process with a quantum efficiency  $\phi_{ET}$  to form the second reactant excitation, DAA- $S_2$ -DACP\* (**Scheme 3.2**). If we assume that the latter reacts to give DAA-n-DAA linked dimer with a quantum yield of 0.7 we can formulate the efficiency of energy transfer,  $\phi_{ET}$ , as given by Equation 1.

$$\Phi_{Dimer} = \Phi_{Monomer} + \phi_{ET} (\Phi_{Monomer})^2 \quad (1)$$

The value  $\Phi_{Dimer}$  is the quantum yield for decarbonylation of **4-6** with respect to the each cyclopropanone moiety, which could be as high as 2.0, and  $\phi_{ET}$  is the quantum efficiency for energy transfer. The  $\phi_{ET}$  values calculated with Eq. 1 for **4**, **5**, and **6** are 90, 63, and 0%, respectively. These results indicate that the efficiency of the quantum chain reaction falls off rapidly with increasing chain length, indicating that close proximity is needed for efficient  $S_2$ - $S_2$  energy transfer.

In qualitative terms, and in the absence of super-exchange or coherent excitation, we can assume that the rate of excited state energy transfer ( $k_{ET}$  in Eq. 2) is determined by exchange ( $k_{Exch}$ )<sup>xv</sup> and dipole-dipole ( $k_{Coul}$ ) interactions, which are associated with the models originally proposed by Dexter and Förster. While the rate of energy transfer by the two mechanisms in Eqs 3 and 4 are based on approximations that are difficult to separate when they are competing at short distances, it is well known that Förster energy transfer dominates at long distances and that Dexter energy transfer is only effective under conditions where there is significant orbital overlap. The Förster mechanism is based on a point-dipole approximation and has a distance dependence of  $1/R^6$  (Eq. 3) for donor-acceptor (DA) separations that are larger than the size of the donor and acceptor.<sup>85</sup> The rate constant for excited state energy transfer by a Dexter mechanism decays exponentially as a function of distance  $R_{DA}$  with a maximum rate constant when the donor and the acceptor are within van der Waals contact (i.e.,  $R_{DA} = L$  in Eq. 4). While the efficiency of the exchange mechanism decays exponentially with distance, the dipole approximation breaks down at separations comparable to the chromophore size and its distance-dependence varies in a manner that depends upon the details of each system.<sup>86</sup>

$$k_{ET} = k_{Coul} + k_{Exch} \quad (2)$$

$$k_{Coul} = \frac{K^2 k_d}{R_{DA}^6} J(\epsilon_A) \quad (3)$$

$$k_{Exch} = K J_{exp} \frac{-2R_{DA}}{L} \quad (4)$$

Both mechanisms have efficiencies that depend on the relative orientation of the donor and the acceptor, expressed in the terms  $\kappa^2$  (Förster) and  $K$  (Dexter) respectively, and they both require energy to be conserved, which is experimentally determined by the spectral overlap [ $J(\epsilon_A)$  and  $J$ ].

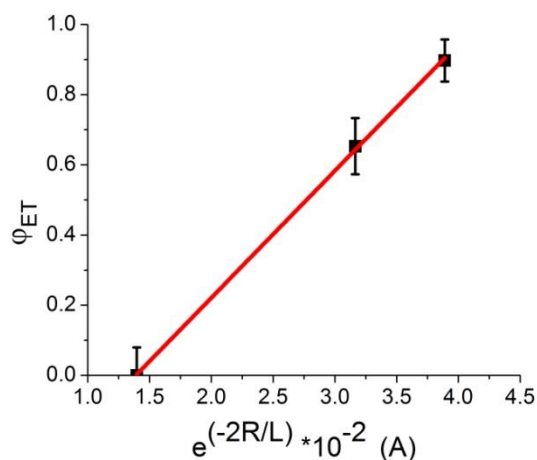
In general, it is well known that Dexter energy transfer is not significant beyond ca. 5 Å<sup>87</sup> and that the Förster mechanism can reach out to ca. 100 Å for suitable donor and acceptor pairs.

While the role of specific orientations is generally difficult to assess for non-rigid DA pairs, we decided to explore qualitatively the distances involved in link dimers **4** – **6**. Considering that reaction and energy transfer in S<sub>2</sub>-I\*-DACP must occur within a few picoseconds to compete with internal conversion, we assume that there is no equilibration in the excited state and that energy transfer occurs from conformations that are analogous to those populated in the ground state. With that in mind, we carried out a Monte Carlo search for all conformers within 5 kcal/mol of the global minimum of linked dimers **4** – **6** using the Optimized Potentials for Liquid Simulations (OPLS) force field as implemented in MacroModel.<sup>88</sup> With ca. 30 conformers generated for each of compounds **4** – **6** we carried out single point energy minimizations in benzene using the CPCM model at the B3LYP/6-31G\* level of theory in Gaussian 10.<sup>89</sup> The closest aryl edge-to-edge interchromophore distances in **4** - **6** varied between 4.4 and 6.1 Å and the maxima varied between 6.0 and 8.6 Å (**Table 3.2.2**). In order to gain some insight into the orientation factor  $\kappa^2$  in the Förster mechanism, we determined the angle formed by the long axes of the two chromophores. Recognizing that energy transfer may occur from all conformations, we calculated a Boltzmann-weighted average of the distances and orientation factors as a reasonable representatives for the samples in solution.<sup>90</sup>

**Table 3. 2. 2.** Calculated aryl edge-to-edge inter-chromophore distances in **4 – 6**.

Compound	D-A Distance (Å) <sup>a</sup>			Orientation <sup>b,c</sup> $\kappa^2$
	Min	Max	Avg <sup>d</sup>	
<b>4</b>	4.4	6.0	5.5	2.02
<b>5</b>	5.7	6.6	6.0	1.16
<b>6</b>	6.1	8.6	7.2	2.6

**Figure 3. 2. 3.** Plot of calculated energy transfer efficiency vs. intrachromophore distance.



In agreement with the exchange (Dexter) mechanism, a plot of  $\phi_{ET}$  vs.  $e^{-2} R_{DA}$  in **Figure 3. 2. 3** revealed a good linear relationship ( $R^2=0.994$ ). While conclusions from three data points should be made with caution, a weighted average distance of 7.2 Å between the two cyclopropanone moieties with a butanedioxy linker in the case of **6** should be close enough for Coulombic energy transfer by the point-dipole approximation, if it were active.



### 3. 3. Conclusions.

Quantum yields of decarbonylation of 2.4-2.7 in crystals of linked diarylcyclopropanone dimers reveal a quantum chain reaction consistent with those previously observed for monomeric diarylcyclopropanones.<sup>4,5</sup> Studies carried out in solution confirm that the quantum chain reaction is also possible by excitation to the  $S_2$  state of diarylcyclopropanones linked by two and three carbon alkyldioxy tethers which are able to display an efficient adiabatic decarbonylation followed by energy transfer and a second decarbonylation. Having preformed an analysis of the conformational populations determined by single point energy calculations of a Monte Carlo search, we correlated the efficiency of energy transfer to ground state geometries. Noting that a very close approach of the two diarylcyclopropanones is needed for energy transfer we determined that a Dexter or exchange mechanism is most likely to operate. We believe that this work will open avenues for singlet-state quantum chain reactions of diarylcyclopropanones and one of our goals will be to embed these chromophores into a polymers in order to explore their use in signal amplification materials.

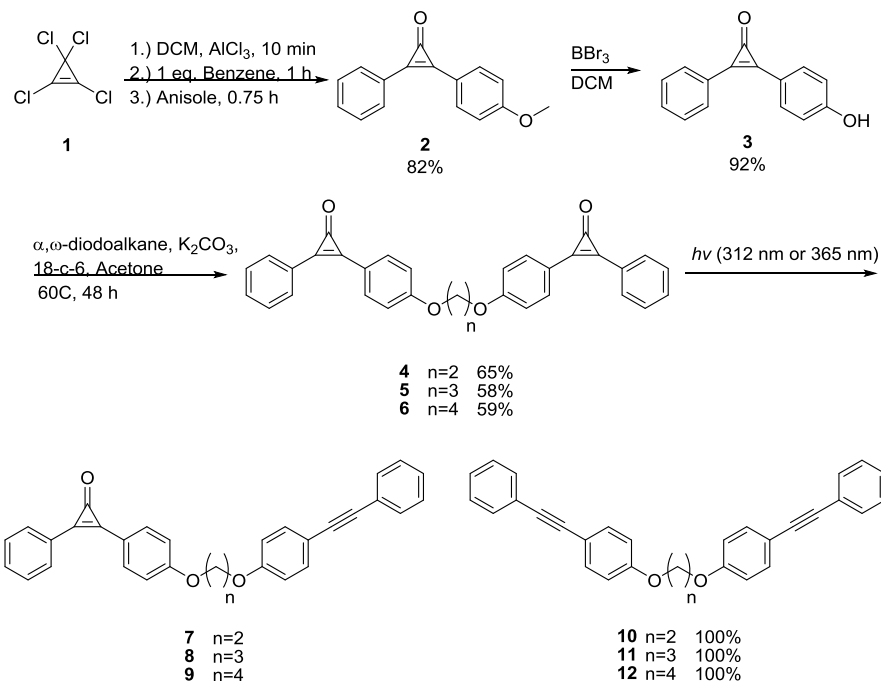
### 3. 4. Experimental

#### Synthesis of 2

Following a modified procedure by Wadsworth,<sup>91</sup> in a flame-dried, argon filled three neck flask, AlCl<sub>3</sub> (4 eqs.) was charged to dry dichloromethane (DCM). The flask was then cooled to 0 °C. To this stirring suspension, tetracyclopropenone, (1eqs.) was added dropwise over the course of 30 minutes. The resulting suspension turned yellow, and was allowed to stir at 0 °C for an additional 10 minutes. To this stirring yellow suspension, benzene (1 eqs.) was added. This resulted in a further color change in the solution to a deep red or orange. This was allowed to stir at 0 °C for 90 min. To this stirring red suspension, anisole (1 eqs.) was added and the solution was allowed to warm to room temperature until complete consumption of anisole was indicated by TLC analysis, ca. 1 hour. The suspension was then quenched slowly with satd. ammonium chloride solution and extracted with DCM and washed with brine. The solvents were removed under reduced pressure, and subjected to column chromatography (1:2 acetone:hexane) R<sub>f</sub> = 0.4. The resulting crystalline solid (85% yield) was recrystallized from a ca. 20:1 hexane:acetone solution.

**(4-methoxyphenyl)-phenylcyclopropenone (2).** Yield 85%; m.p. 128 °C;  $\lambda_{\max}$  =330 (log  $\epsilon$ =4.70), 315 (log  $\epsilon$ =4.76), 303 (log  $\epsilon$ =4.63) nm; <sup>1</sup>H NMR (300 MHz, CDCl<sub>3</sub>)  $\delta$  7.84 (d,  $J$  = 2.7 Hz, 2H, CCH<sub>2</sub>CH<sub>2</sub>), 7.84 (d,  $J$  = 5.4 Hz, 2H, CCH<sub>2</sub>CH<sub>2</sub>), 7.47 (m, 3H, CHCH), 6.969 (d,  $J$  = 5.4 Hz, 2H, CHCH), 3.80 (s, 3H, CH<sub>3</sub>); <sup>13</sup>C NMR (75 MHz, CDCl<sub>3</sub>)  $\delta$  163.17(CO), 155.61(CCO), 147.56(OCCH), 144.15(CHCH), 133.90(CHCH), 131.22(CHCH), 129.26(CHCH), 124.15(CHCH), 116.59(CHCH), 114.88(CHCH), 111.47(CHCH), 55.61(CH<sub>3</sub>). FTIR (solid, HATR, cm<sup>-1</sup>): 2926, 1847, 1722, 1599, 1508, 1487, 1447. HRMS (MALDI-TOF) Formula: C<sub>16</sub>H<sub>12</sub>O<sub>2</sub> calcd 236.0837; found (M + Na<sup>+</sup>) 259.1239.

### Scheme 3. 4. 1. Synthesis of tethered diarylcyclopropenones.



### Synthesis of 3

In a flame-dried, argon-filled, three neck flask fitted with a reflux condenser, **2** was dissolved in 20 mL of dry DCM. The flask was then cooled to 0 °C. To this stirring suspension, 1M  $\text{BBr}_3$  in DCM (2.25 eqs.) was added dropwise over the course of 20 minutes. This resulted in a color change in the solution to a deep red. This was stirred at 0 °C for 1 hours, and then allowed to warm to room temperature and stir overnight. The suspension was then quenched slowly with satd. ammonium chloride solution and extracted with DCM and washed with brine. The solvents were removed under reduced pressure, and subjected to column chromatography (1:2 acetone:hexane)  $R_f = 0.2$ . The resulting crystalline solid (90% yield) was not further purified.

**(4-hydroxyphenyl)-phenylcyclopropenone (3)**. Yield 90%; m.p. 181 °C (decomp.);  $^1\text{H}$  NMR (300 MHz,  $\text{CDCl}_3$ )  $\delta$  7.96 (d,  $J = 2.7$  Hz, 2H,  $\text{CCH}_2\text{CH}_2$ ), 7.88 (d,  $J = 4.8$  Hz, 2H,  $\text{CCH}_2\text{CH}_2$ ), 7.58 (m, 3H,  $\text{CHCH}$ ), 7.10 (d,  $J = 4.8$  Hz, 2H,  $\text{CHCH}$ );  $^{13}\text{C}$  NMR (75 MHz,  $\text{CDCl}_3$ )  $\delta$  165.32,

155.46, 143.46, 138.40, 137.06, 135.46, 133.60, 130.13, 120.80, 117.86, 111.46. FTIR (solid, HATR,  $\text{cm}^{-1}$ ): 3069, 2817, 2686, 1853, 1551, 1443. HRMS (MALDI-TOF) Formula: calcd. 222.0681; found ( $\text{M} + \text{Na}^+$ ) 244.0437.

### Synthesis of Tethered Dimers 4-6

In a flame-dried, argon filled three neck flask fitted with a reflux condenser, **2** (2.5 eqs) was dissolved in 10 mL of dry acetone (**Scheme 3. 4. 1**). To this, potassium carbonate (3.5 eqs.), 18-crown-6 (0.15 eqs.), and the corresponding  $\alpha,\omega$ -diiodoalkane was added to the stirring solution. The flask was covered in aluminum foil and refluxed for 48 hours. The acetone was removed under reduced pressure, and the resulting solid was dissolved in DCM and water. The aqueous layer was extracted with DCM, and the combined organic layer was washed with brine. The solvents were removed under reduced pressure, and subjected to column chromatography (1:2 acetone:hexane)  $R_f = 0.2$ . The resulting solid was recrystallized from DCM: acetone (ca. 20:1).

**1,2 di(4-phenoxy (phenylcyclopropenone)) ethane (4)**. Yield 65%; m.p. 160 °C;  $\lambda_{\text{max}} = 328$  (log  $\epsilon = 4.94$ ), 314 (log  $\epsilon = 5.069$ ), 303 (log  $\epsilon = 5.00$ ) nm;  $^1\text{H}$  NMR (300 MHz,  $\text{CDCl}_3$ )  $\delta$  7.91 (m, 8H, CHCH), 7.54 (m, 6H, CHCH), 7.03 (d,  $J = 5.1$  Hz, 2H, CHCH), 4.65 (s, 4H,  $\text{CH}_2\text{O}$ );  $^{13}\text{C}$  NMR (75 MHz,  $\text{CDCl}_3$ )  $\delta$  160.86(CO), 155.36(CCO), 147.29(OCCH), 145.23(CHCH), 133.7(CHCH), 132.30(CHCH), 131.14(CHCH), 129.23(CHCH), 124.03(CHCH), 117.67(CHCH), 115.22(CHCH), 72.66( $\text{OCH}_2$ ). FTIR (solid, HATR,  $\text{cm}^{-1}$ ): 2924, 1849, 1732, 1600, 1509, 1447. HRMS (MALDI-TOF) Formula: calcd. 470.5147; found ( $\text{M} - \text{CO}$ ) 443.6214.

**1,3 di(4-phenoxy (phenylcyclopropenone)) propane (5)**. Yield 58%; m.p. 149 °C;  $\lambda_{\text{max}} = 329$  (log  $\epsilon = 4.94$ ), 317 (log  $\epsilon = 5.069$ ), 303 (log  $\epsilon = 5.00$ ) nm;  $^1\text{H}$  NMR (300 MHz,  $\text{CDCl}_3$ )  $\delta$  7.93 (m, 8H, CHCH), 7.88 (d,  $J = 4.8$  Hz, 2H, CHCH), 7.55 (m, 6H CHCH), 7.07 (d,  $J = 8.4$  Hz, 2H, CHCH), 4.28 (t,  $J = 5.9$  Hz, 4H,  $\text{OCH}_2$ ), 2.36 (t,  $J = 5.9$  Hz, 2H,  $\text{CH}_2\text{CH}_2$ );  $^{13}\text{C}$  NMR (75 MHz,  $\text{CDCl}_3$ )  $\delta$

162.27(CO), 155.60(CCO), 147.70(OCCH), 133.87(CHCH), 132.28(CHCH), 131.23(CHCH), 129.34(CHCH), 117.05(CHCH), 115.29(CHCH), 64.61(OCH<sub>2</sub>), 29.00(CH<sub>2</sub>CH<sub>2</sub>). FTIR (solid, HATR, cm<sup>-1</sup>): 2924, 1848, 1722, 1601, 1509. HRMS (MALDI-TOF) Formula: calcd. 484.5413; found (M + Na<sup>+</sup>) 501.5997.

**1,4 di(4-phenoxy (phenylcyclopropenone)) butane (6).** Yield 90%; m.p. 151 °C;  $\lambda_{\max}$  =329 (log  $\epsilon$ =4.94), 317 (log  $\epsilon$ =5.069), 303 (log  $\epsilon$ =5.00) nm; <sup>1</sup>H NMR (300 MHz, CDCl<sub>3</sub>)  $\delta$  7.94 (m, 8H, CHCH), 7.56 (m, 6H, CHCH), 7.06 (d, *J* = 8.4 Hz, 2H, CHCH), 4.16 (t, *J* = 5.9 Hz, 4H, CH<sub>2</sub>O), 2.06 (t, *J* = 5.9 Hz, 4H, CH<sub>2</sub>CH<sub>2</sub>); <sup>13</sup>C NMR (75 MHz, CDCl<sub>3</sub>)  $\delta$  162.46(CO), 155.68(CCO), 155.61(OCCH), 144.54(CHCH), 133.93(CHCH), 132.29(CHCH), 131.25(CHCH), 129.39(CHCH), 124.40(CHCH), 116.91(CHCH), 115.28(CHCH), 67.87(OCH<sub>2</sub>), 25.86(CH<sub>2</sub>CH<sub>2</sub>). FTIR (solid, HATR, cm<sup>-1</sup>): 2919, 2850, 1849, 1720, 1599, 1509. HRMS (MALDI-TOF) Formula: calcd. 498.1831; found (M + 1) 499.1411.

#### Quantum Yield Determination for Solution.

Using both optically matched (3 experiments), and equimolar (3 experiments) solutions of the linked dimer, **4** – **6** relative quantum yield determinations were performed with valerophenone ( $\phi$  = 0.33) as an internal standard in a Rayonet photochemical reactor using either 312 nm lamps (BLE-8T312) or 365 nm lamps (BLE-8T365).<sup>92</sup> Quantitative conversion of **2**, and **4** – **6** produced the corresponding alkynes **13**, and **10** – **12** in 100% yield with no detection of secondary photoproducts.

#### Nanocrystalline Suspensions.

Samples to be used for actinometry experiments were prepared by injecting a solution in acetone of the compound to be studied (ca. 10  $\mu$ L of a ca. 1M) into 3 mL of vortexing water

(millipore). The resulting suspension (ca.  $1 \times 10^{-3}$  M) was sonicated three times at room temperature for 4 min, allowing for 2 min rest between runs.

### **Quantum Yield Determination for Nanocrystalline Suspension.**

Relative quantum yield determinations were performed with dicumyl ketone ( $\phi = 0.2$ ) as an internal standard in a Rayonet photochemical reactor using either 312 nm lamps (BLE-8T312) or 365 nm lamps (BLE-8T365). Quantum yields were determined with equimolar, optically dense suspensions. Two independent suspensions of actinometer and substrate were independently synthesized. The samples were then combined immediately prior to irradiation in a 50 mL quartz Erlenmeyer flask and irradiated for 2 min. Every 20 seconds, an aliquot was removed (approximately one-twentieth of the suspension). The aliquots were extracted with deuterated chloroform (2 mL), washed with brine ( $2 \times 2$  mL), and dried over magnesium sulfate.  $^1\text{H}$  NMR spectra were taken immediately to determine the extent of product formation. Immediately following, the same samples were then subjected to gas chromatography to determine the extent of dicumyl formation. The conversion of cyclopropenone derivatives (CPD) could not be monitored by gas chromatography due to partial thermal decarbonylation that occurred. Compounds **2**, **4 – 6**, and **10 – 12** were not thermally stable at elevated temperatures. Thermal decarbonylation was noted in all cases for the CPD when subjected to gas chromatography to give the acetylene exclusively. These experimental yields were reproduced at least in triplicate. High conversion data were not used to avoid potential problems caused by optical absorption of the products. Quantitative conversion of **2**, and **4 – 6** produced the corresponding alkynes **13**, and **10 – 12** in 100% yield with no detection of secondary photoproducts.

**4-(phenylethynyl)anisole (13).**<sup>93</sup>  $^1\text{H}$  NMR (300 MHz,  $\text{CDCl}_3$ )  $\delta$ 7.47 (2H, d,  $\text{OCCH}_2$ ), 7.42 (2H, d,  $\text{OCCH}_2\text{CH}_2$ ), 7.27 (3H, m,  $\text{CHCH}$ ), 6.82 (2H, d,  $\text{CHCH}$ ), 3.75 (3H, s,  $\text{CH}_3$ );  $^{13}\text{C}$  NMR (75

MHz, CDCl<sub>3</sub>)  $\delta$  159.57(OCCH), 133(CHCH), 131.40(CHCH), 128.25(CHCH), 127.86(CHCH), 123.54(CHCH), 115.30(CHCH), 113.97(CHCH), 89.32(CCC), 88.03(CCC), 55.19(CH<sub>3</sub>).

**1,2 di(4-phenoxy-(phenylethynyl)) ethane (10).** <sup>1</sup>H NMR (300 MHz, CDCl<sub>3</sub>)  $\delta$  7.29 (m, 4H, CHCH), 7.16 (m, 10H, CHCH), 7.58 (m, 3H, CHCH), 6.71 (d,  $J$  = 5 Hz, 4H, CHCH), 4.46 (s, 4H, CH<sub>2</sub>CH<sub>2</sub>); <sup>13</sup>C NMR (75 MHz, CDCl<sub>3</sub>)  $\delta$  157.51(OCCH), 132.75(CHCH), 131.03(CHCH), 127.99(CHCH), 127.72(CHCH), 123.08(CHCH), 116.05(CHCH), 113.33(CHCH), 88.86(CCC), 87.99(CCC), 72.47(CH<sub>2</sub>CH<sub>2</sub>). FTIR (solid, HATR, cm<sup>-1</sup>): 2917, 2849, 2218, 1723, 1595, 1515. HRMS (MALDI-TOF) Formula: calcd. (M) 424.1620; found (M) 424.1691.

**1,3 di(4-phenoxy-(phenylethynyl)) propane (11).** <sup>1</sup>H NMR (300 MHz, CDCl<sub>3</sub>)  $\delta$  7.46 (d,  $J$  = 4.4 Hz, 4H, CHCH), 7.42 (d,  $J$  = 8.7 Hz, 4H, CHCH), 7.32 (m, 6H, CHCH), 6.89 (d,  $J$  = 8.7 Hz, 2H, CHCH), 4.188 (t,  $J$  = 5.8 Hz, 4H, OCH<sub>2</sub>), 2.29 (t,  $J$  = 5.8 Hz, 2 H, CH<sub>2</sub>CH<sub>2</sub>); <sup>13</sup>C NMR (75 MHz, CDCl<sub>3</sub>)  $\delta$  158.93(OCCH), 133.11(CHCH), 131.52(CHCH), 128.31(CHCH), 127.94(CHCH), 123.62(CHCH), 115.56(CHCH), 114.55(CHCH), 87.46(CCC), 87.36(CCC), 65.50(OCH<sub>2</sub>), 32.00(CH<sub>2</sub>CH<sub>2</sub>). FTIR (solid, HATR, cm<sup>-1</sup>): 2918, 2850, 2214, 1723, 1595, 1505. HRMS (MALDI-TOF) Formula: calcd. 428.1776; found (M + 1) 428.1783.

**1,4 di(4-phenoxy-(phenylethynyl)) butane (12).** <sup>1</sup>H NMR (300 MHz, CDCl<sub>3</sub>)  $\delta$  7.42 (d,  $J$  = 8.4 Hz, 4H, CHCH), 7.321 (m, 10H, CHCH), 6.84 (d,  $J$  = 8.4 Hz, 4H, CHCH), 4.15 (t,  $J$  = 6, 4H, OCH<sub>2</sub>), 2.09 (t,  $J$  = 6, 4H, CH<sub>2</sub>CH<sub>2</sub>); <sup>13</sup>C NMR (75 MHz, CDCl<sub>3</sub>)  $\delta$  158.9(OCCH), 132.9(CHCH), 131.5(CHCH), 128.2(CHCH), 127.8(CHCH), 123.6(CHCH), 115.1(CHCH), 114.4(CHCH), 89.3(CCC), 87.9(CCC), 68.1(OCH<sub>2</sub>), 26.0(CH<sub>2</sub>CH<sub>2</sub>). FTIR (solid, HATR, cm<sup>-1</sup>): 2918, 2218, 1724, 1594, 1510, 1444. HRMS (MALDI-TOF) Formula: calcd. 442.1933; found (M + Na<sup>+</sup>) 465.1833.

### Isolation of Monodecarboxylated Intermediates 7-9.

Samples of **4 – 6** (ca. 20 mgs) dissolved in ca. 2 mL dichloromethane were irradiated at 365 nm. Samples were monitored by TLC (2:1) hexane:acetone, until the consumption of the starting material was complete ( $R_f = 0.15$ ). Preparative TLC purification was performed to separate the monodecarbonylated products **7 – 9** ( $R_f = 0.45$ ), from the didecarbonylated products **4 – 6** ( $R_f = 0.85$ ). This isolation produced a ca. 3:1 ratio of the di:mono decarbonylated products.

**1-(4-phenoxy (phenylcyclopropenone)), 2-(4-phenoxy-(phenylethynyl)) ethane (7).**  $^1\text{H}$  NMR (300 MHz,  $\text{CDCl}_3$ )  $\delta$  7.94 (m, 4H, CHCH), 7.88 (d,  $J = 4.8$  Hz, 2H, CHCH), 7.55 (m, 8H, CHCH), 7.02 (d,  $J = 5.1$  Hz, 2H, CHCH) 6.95 (d,  $J = 5.1$  Hz, 2H, CHCH), 4.704 (m, 2H,  $\text{OCH}_2$ ), 4.65 (m, 2H,  $\text{CH}_2\text{CH}_2$ );  $^{13}\text{C}$  NMR (75 MHz,  $\text{CDCl}_3$ )  $\delta$  160.8 (CO), 157.5 (CCO), 155.3(CCO), 147.3(OCCH), 145.2(OCCH), 133.7(CHCH), 132.8(CHCH), 132.3(CHCH), 131.1(CHCH), 131.0(CHCH), 129.2(CHCH), 128.0(CHCH), 127.7(CHCH), 124.0(CHCH), 123.1(CHCH), 117.7(CHCH), 116.0(CHCH), 115.2(CHCH), 114.3(CHCH), 88.6(CCC), 88.0(CCC), 72.6( $\text{OCH}_2$ ), 72.4( $\text{CH}_2\text{CH}_2$ ). FTIR (solid, HATR,  $\text{cm}^{-1}$ ): 2956, 2920, 2214, 1848, 1601, 1515. HRMS (MALDI-TOF) Formula: calcd. 442.1569; found ( $\text{M} + \text{Na}^+$ ) 414.1691.

**1-(4-phenoxy (phenylcyclopropenone)), 3-(4-phenoxy-(phenylethynyl)) propane (8).**  $^1\text{H}$  NMR (300 MHz,  $\text{CDCl}_3$ )  $\delta$  7.96 (d,  $J = 5.4$  Hz, 4H, CHCH), 7.57 (m, 4H, CHCH), 7.47 (m, 4H, CHCH), 7.08 (d,  $J = 5.4$  Hz, 2H, CHCH), 6.89 (d,  $J = 5.4$  Hz, 4H, CHCH), 4.28 (t,  $J = 3.6$  Hz, 2H,  $\text{OCH}_2$ ), 4.19 (t,  $J = 3.6$  Hz, 2H,  $\text{CH}_2\text{CH}_2$ ), 2.33 (t,  $J = 3.6$  Hz, 2H,  $\text{CH}_2\text{CH}_2$ );  $^{13}\text{C}$  NMR (75 MHz,  $\text{CDCl}_3$ )  $\delta$  162.58(CO), 158.90(CCO), 158.78(CCO), 148.44(OCCH), 143.49(OCCH), 134.20(CHCH), 133.15(CHCH), 132.42(CHCH), 131.48(CHCH), 129.41(CHCH), 128.33(CHCH), 128.00(CHCH), 127.85(CHCH), 123.61(CHCH), 123.56(CHCH), 115.70(CHCH), 115.41(CHCH), 114.57(CHCH), 89.36 (CCC), 88.16(CCC), 64.45( $\text{OCH}_2$ ), 64.25( $\text{OCH}_2$ ),



29.14(CH<sub>2</sub>CH<sub>2</sub>). FTIR (solid, HATR, cm<sup>-1</sup>): 2916, 2214, 1847, 1601, 1509. HRMS (MALDI-TOF) Formula: calcd. 428.1776; found (M + 1) 429.1792.

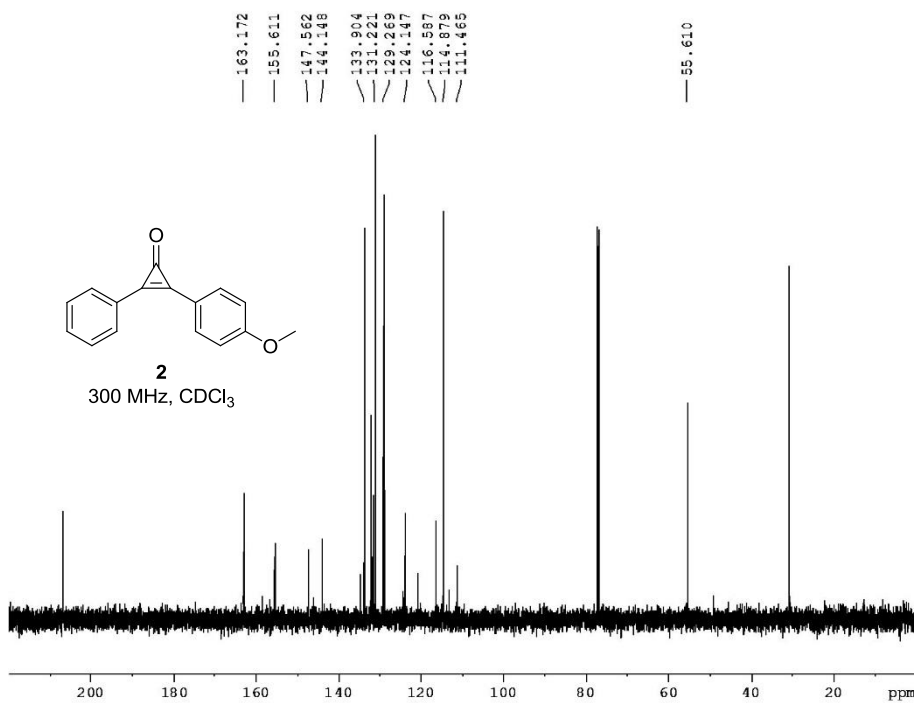
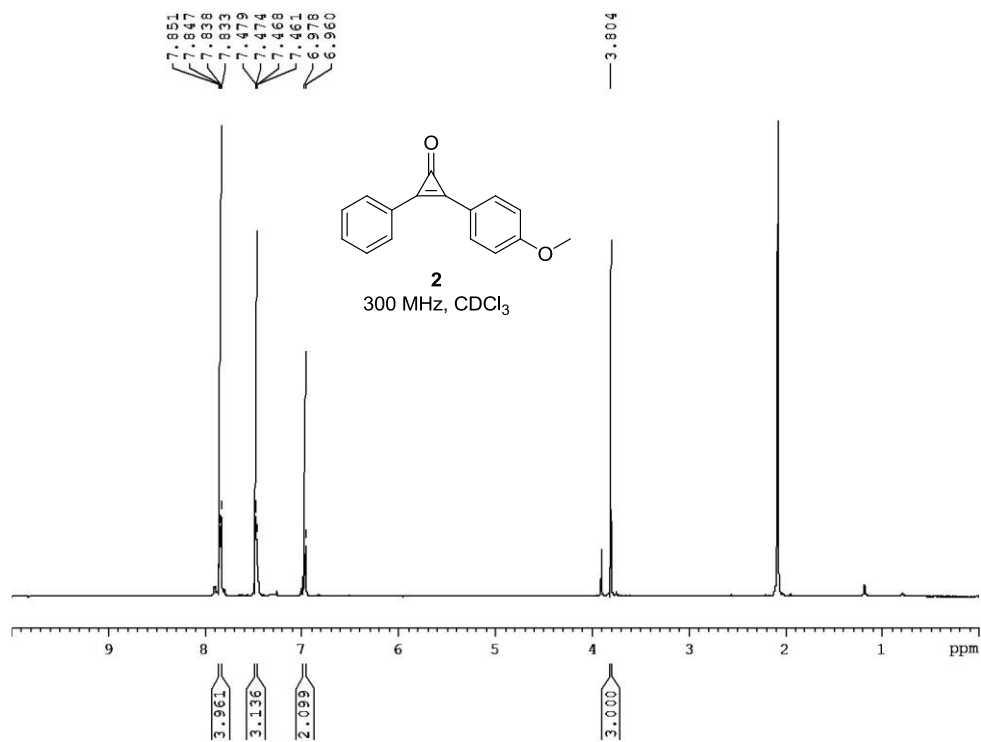
**1-(4-phenoxy (phenylcyclopropenone)), 4-(4-phenoxy-(phenylethynyl)) butane (9).** <sup>1</sup>H NMR (300 MHz, CDCl<sub>3</sub>) δ 7.95 (d, *J* = 5.4 Hz, 4H, CHCH), 7.57 (m, 4H, CHCH), 7.47 (m, 4H, CHCH), 7.05 (d, *J* = 5.4 Hz, 2H, CHCH), 6.87 (d, *J* = 5.4 Hz, 4H, CHCH), 4.16 (t, *J* = 3.6 Hz, 2H, OCH<sub>2</sub>), 4.08 (t, *J* = 3.6 Hz, 2H, OCH<sub>2</sub>), 2.03 (m, 4H, CH<sub>2</sub>CH<sub>2</sub>) ; <sup>13</sup>C NMR (75 MHz, CDCl<sub>3</sub>) δ 164.46(CO), 158.89(CCO), 155.72(CCO), 147.64(OCCH), 144.28(OCCH), 133.82(CHCH), 132.98(CHCH), 132.14(CHCH), 131.36(CHCH), 131.16(CHCH), 129.23(CHCH), 128.21(CHCH), 127.87(CHCH), 123.45(CHCH), 115.13(CCC), 113.41(CCC), 67.84(OCH<sub>2</sub>), 67.32(OCH<sub>2</sub>), 29.60(CH<sub>2</sub>CH<sub>2</sub>), 25.80(CH<sub>2</sub>CH<sub>2</sub>). FTIR (solid, HATR, cm<sup>-1</sup>): 2918, 2214, 1848, 1600, 1509. Formula: calcd. 470.1882; found (M - CO + Na<sup>+</sup>) 465.1833.

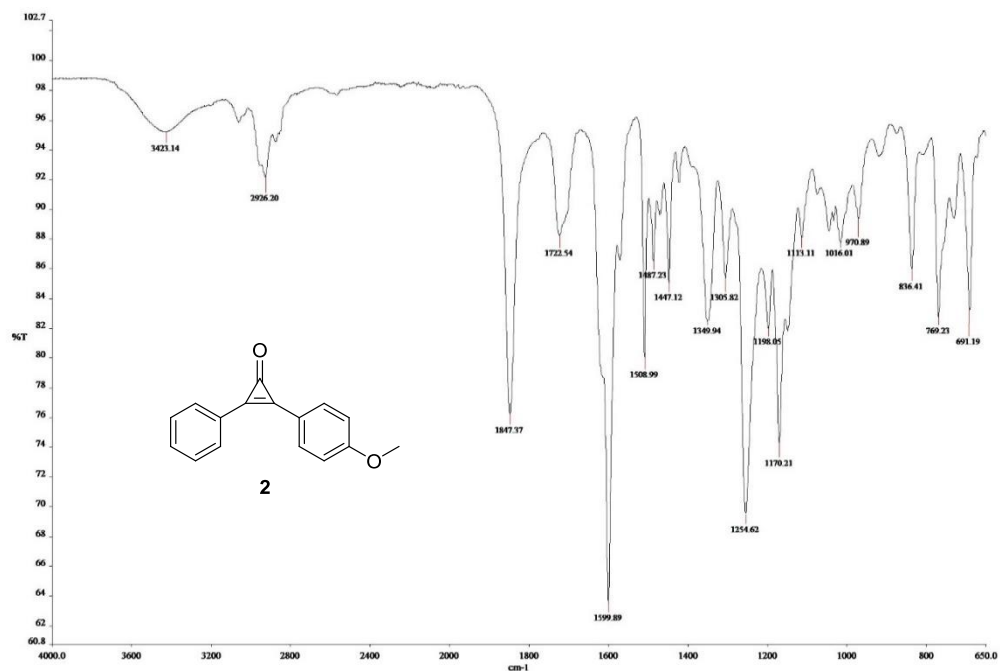
### 3. 5. Appendix

#### Characterization for Chapter 3

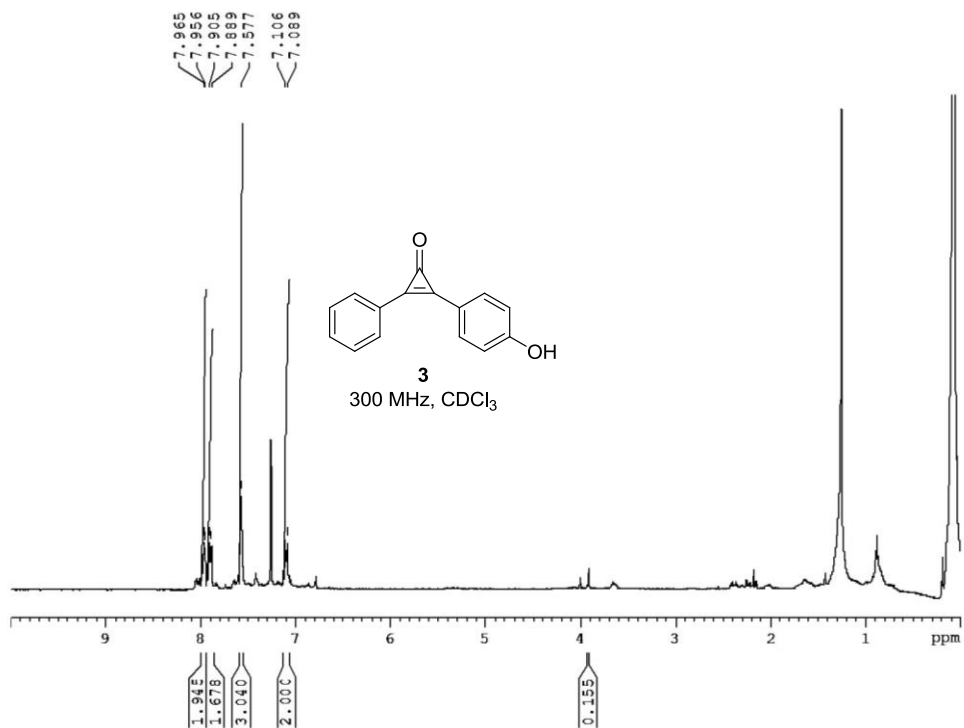
Full <sup>1</sup> H NMR, <sup>13</sup> C NMR, and IR spectra for <b>2</b> – <b>12</b> .....	64
UV Absorption spectra of cyclopropenone <b>3</b> (black) and tethered dimers <b>4</b> (red), <b>5</b> (blue), and <b>6</b> (green) measured in benzene.....	82
Thermal Analysis data.....	83
PXRD Studies of reaction progress.....	86
Relative energy and intrachromophore distances for all conformers of <b>4</b> - <b>6</b> predicted at B3LYP/6-31G*.....	89
Computational data including geometries and frequencies for all conformations of <b>4</b> – <b>6</b> (B3LYP/6-31G*).....	91

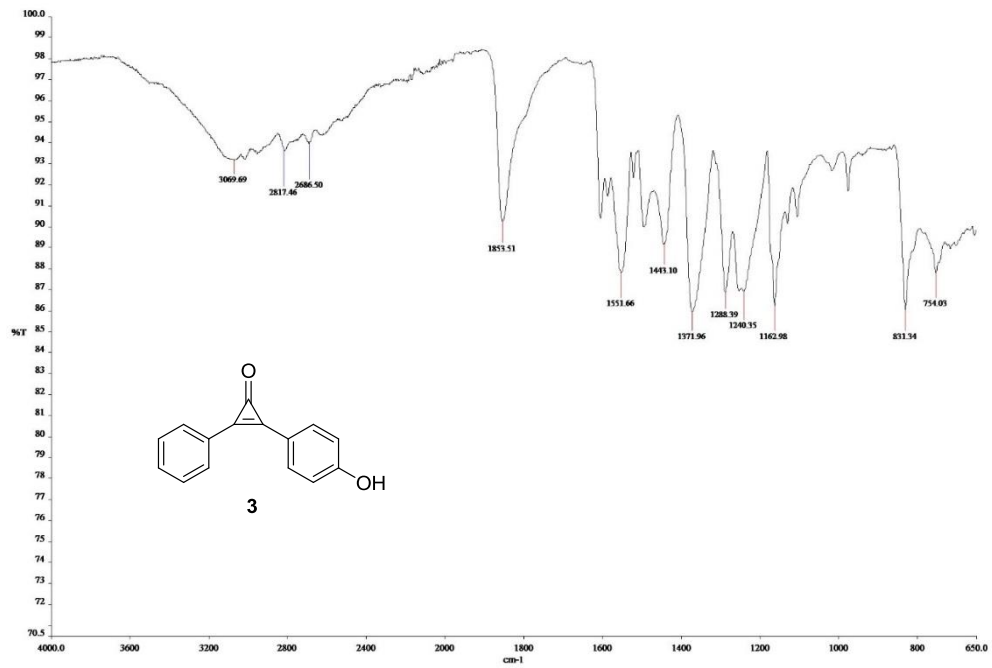
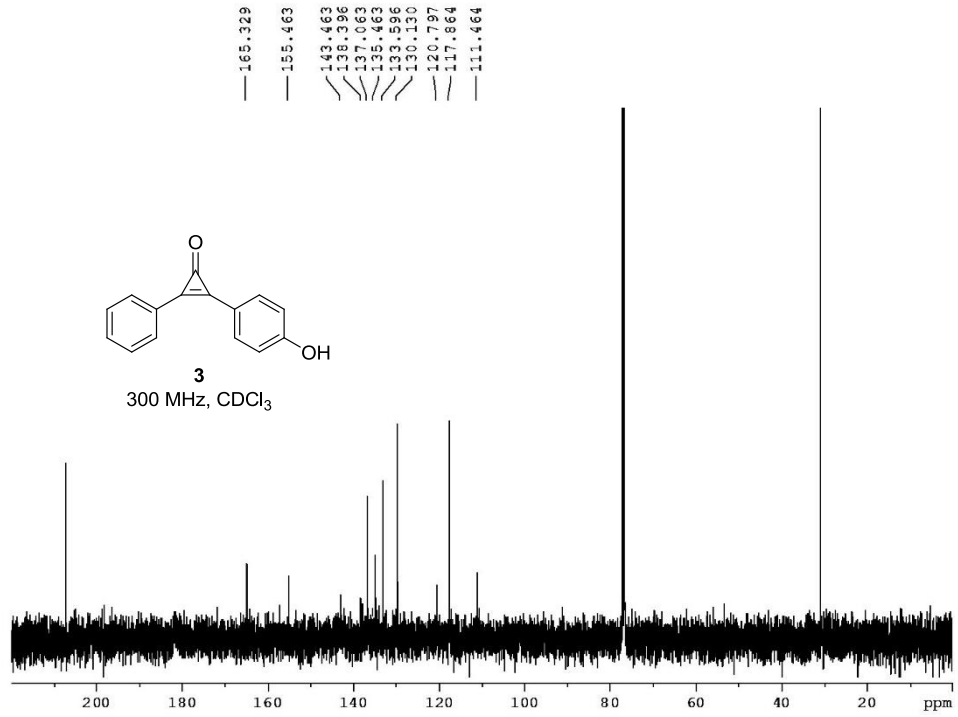
**(4-methoxyphenyl)-phenylcyclopropanone (2).**



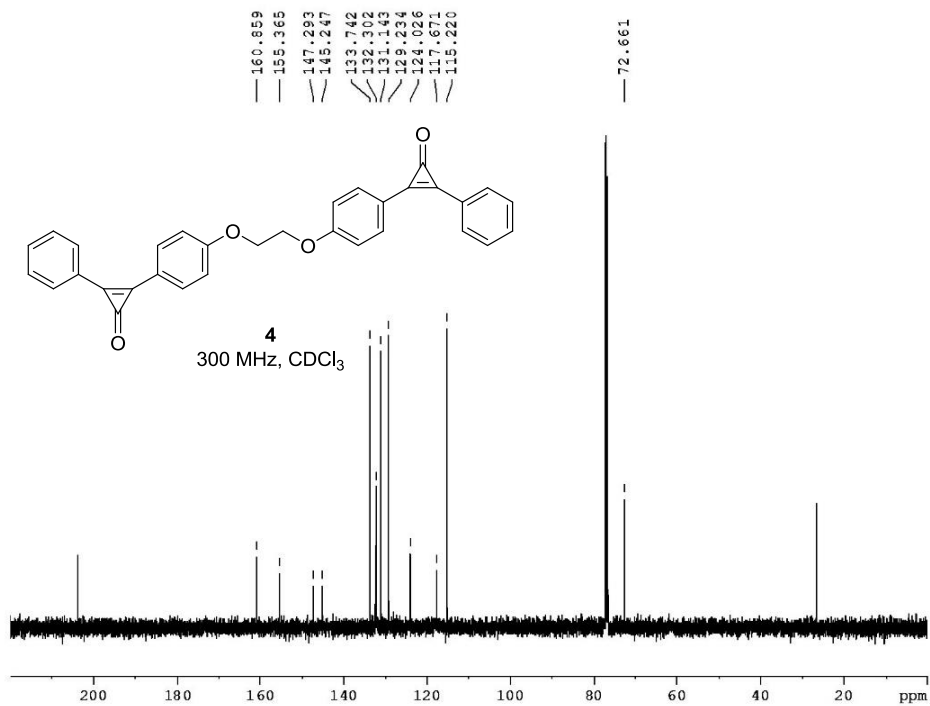
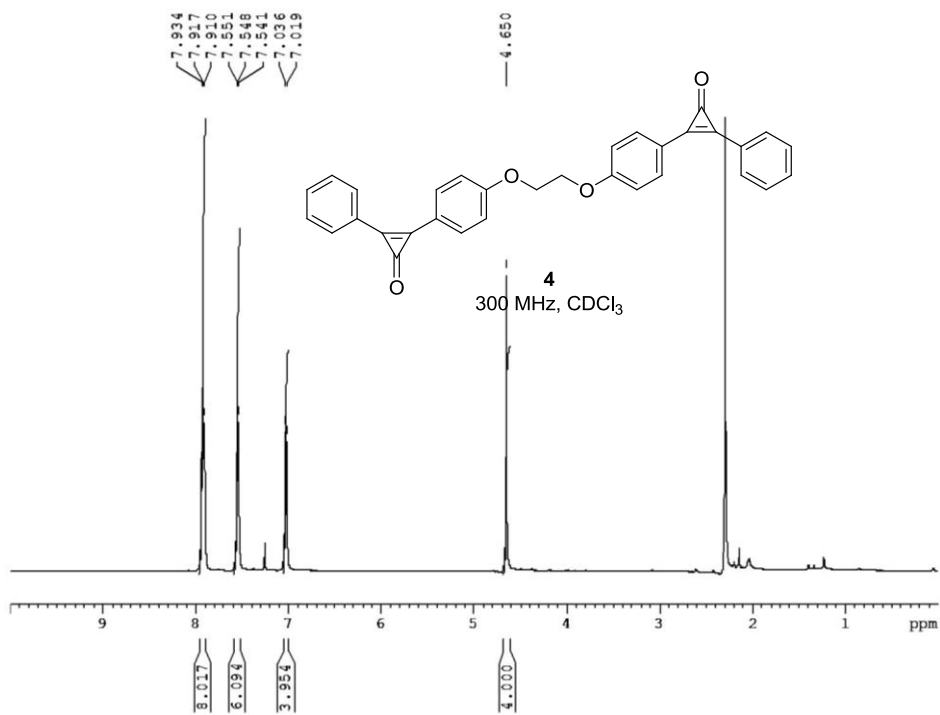


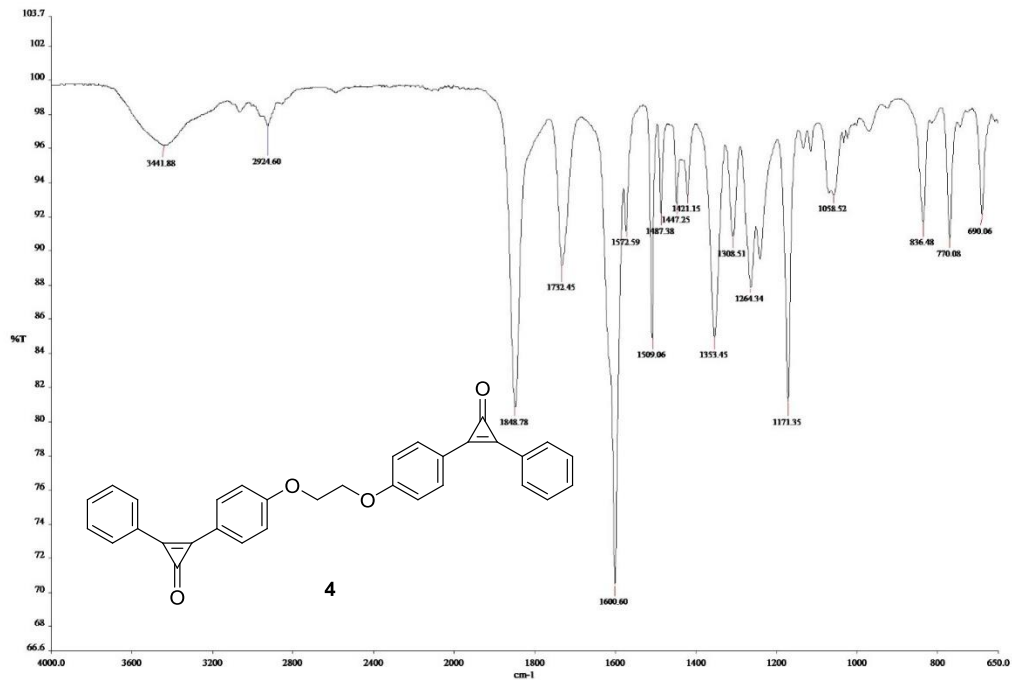
**(4-hydroxyphenyl)-phenylcyclopropenone (3).**



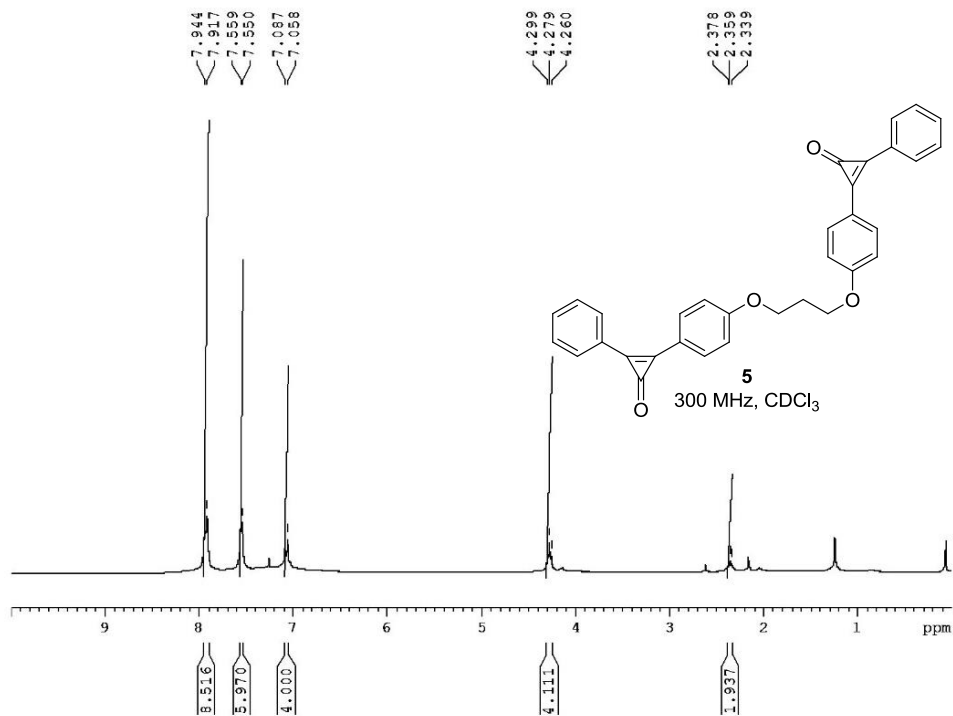


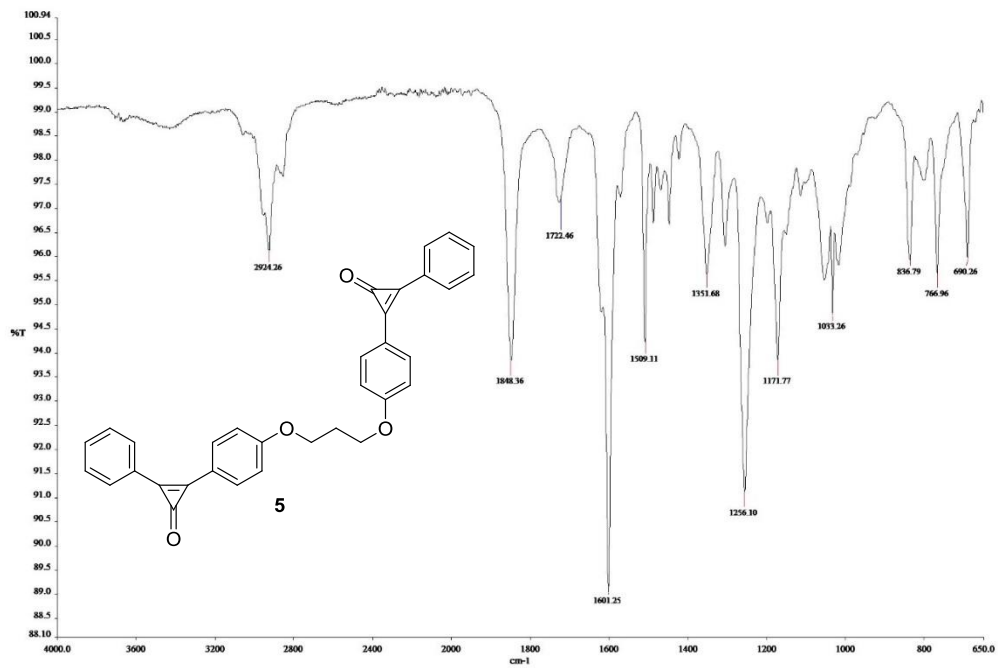
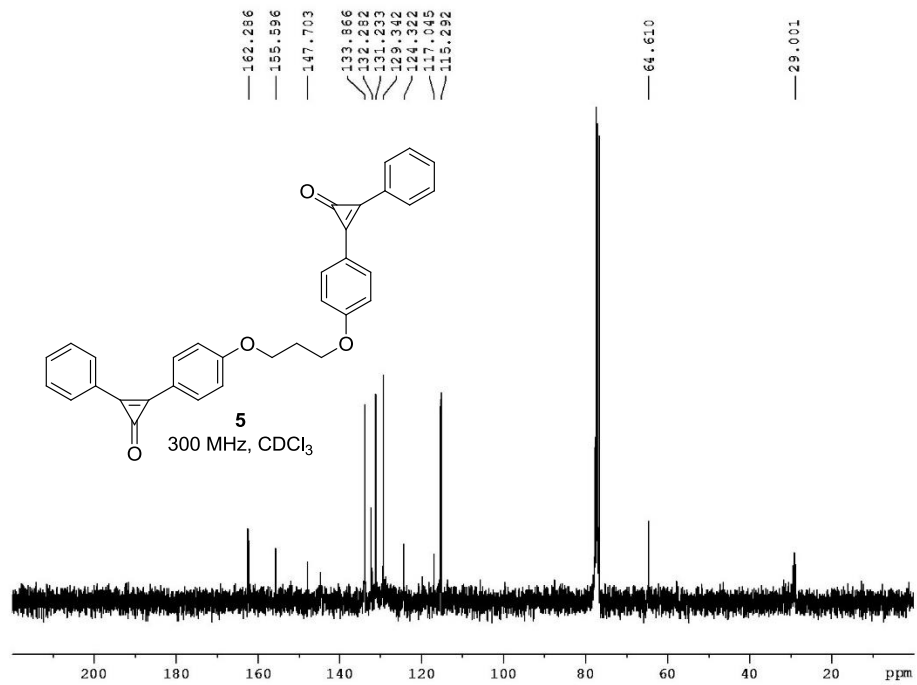
1,2 di(4-phenoxy (phenylcyclopropenone) ethane (4).





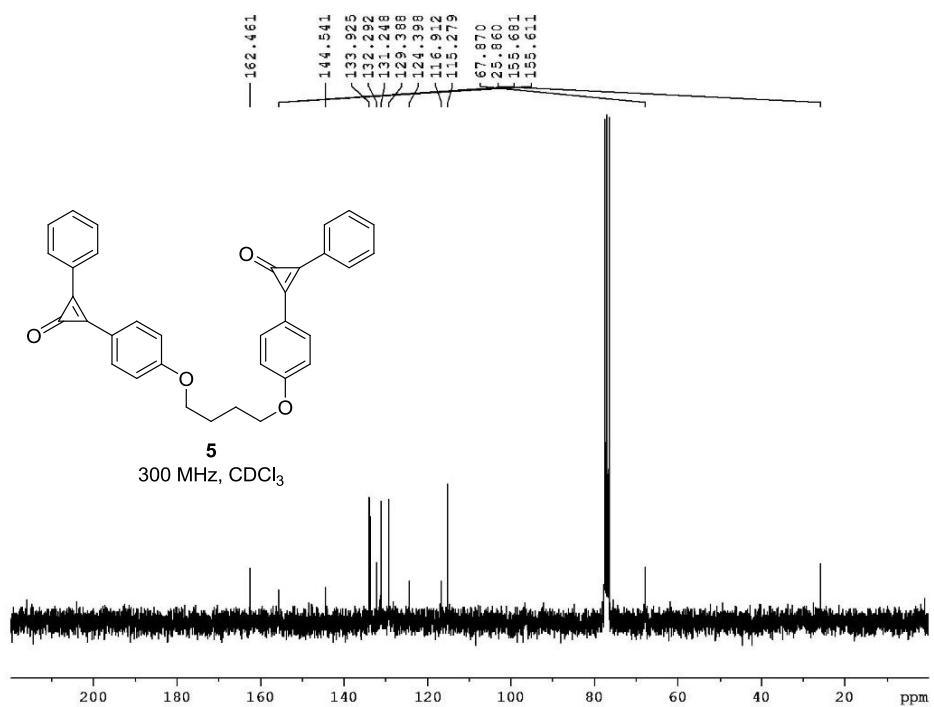
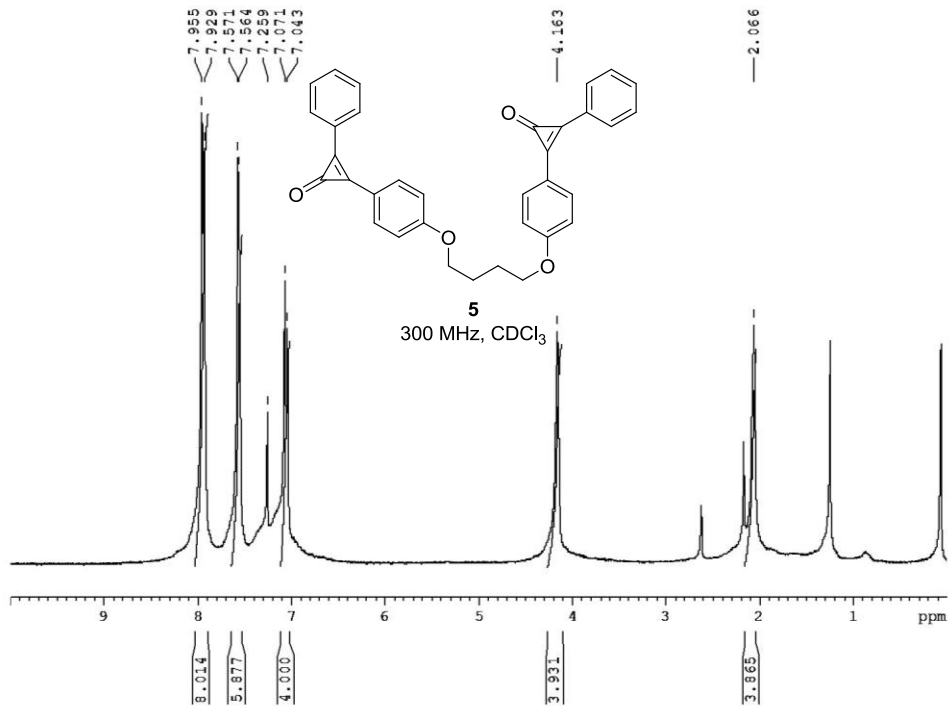
**1,3 di(4-phenoxy (phenylcyclopropenone) propane (5).**

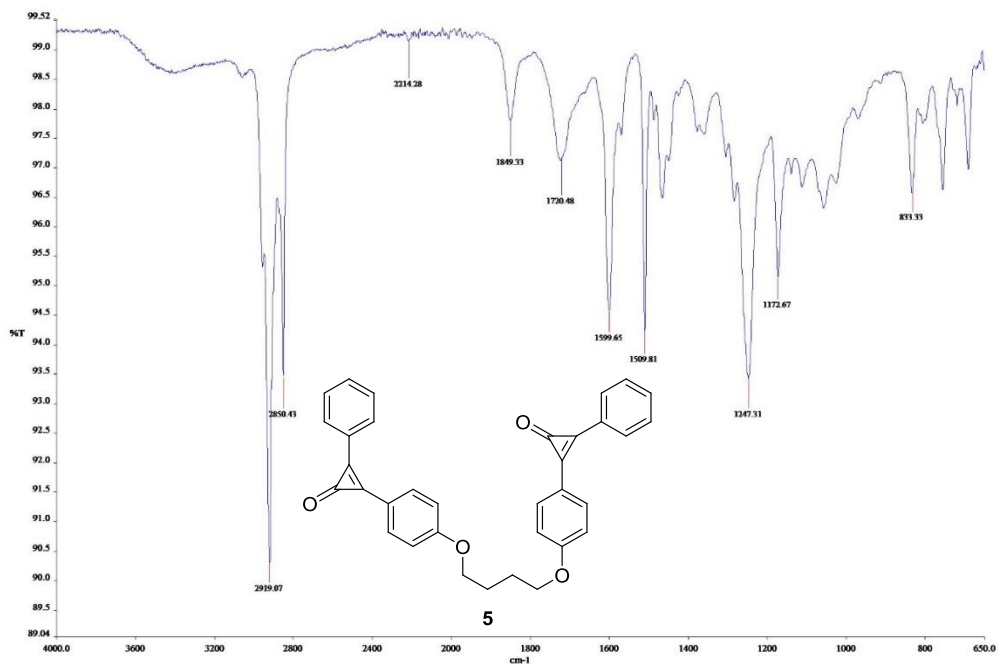




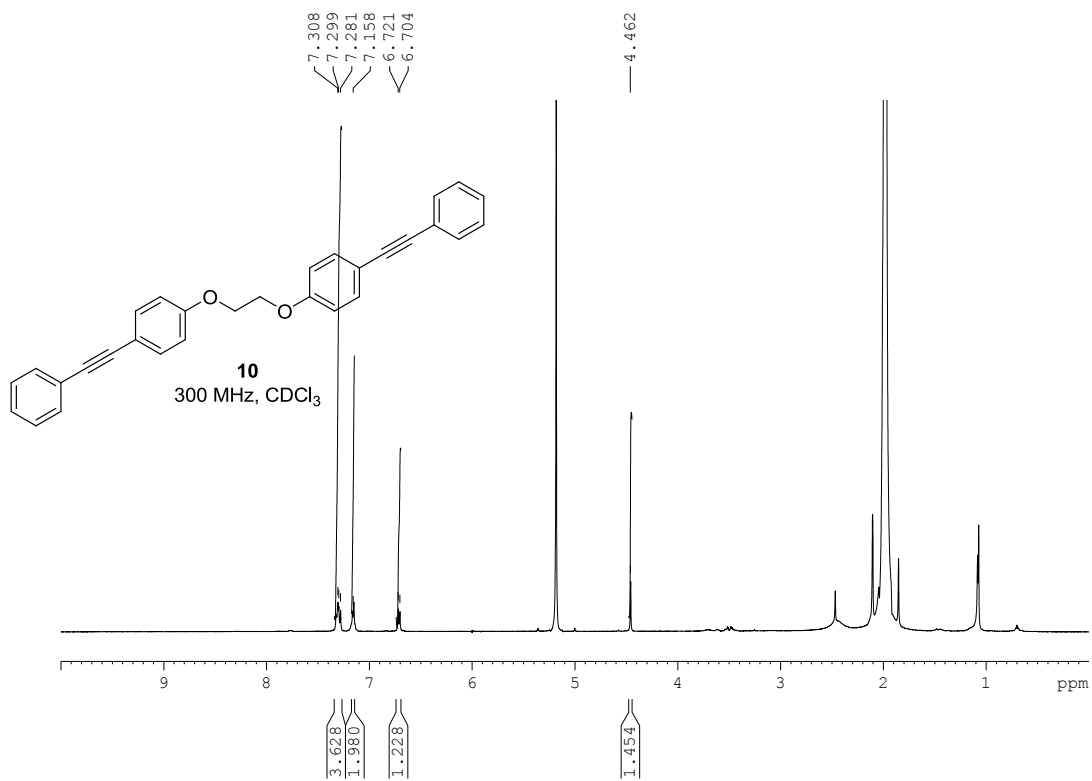


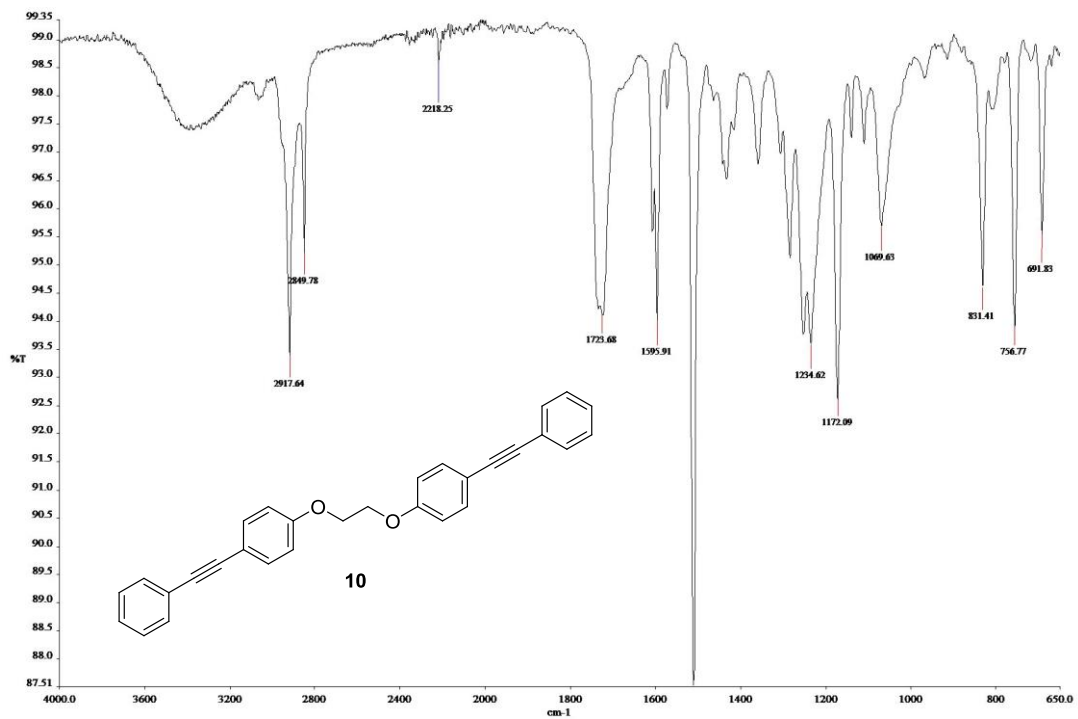
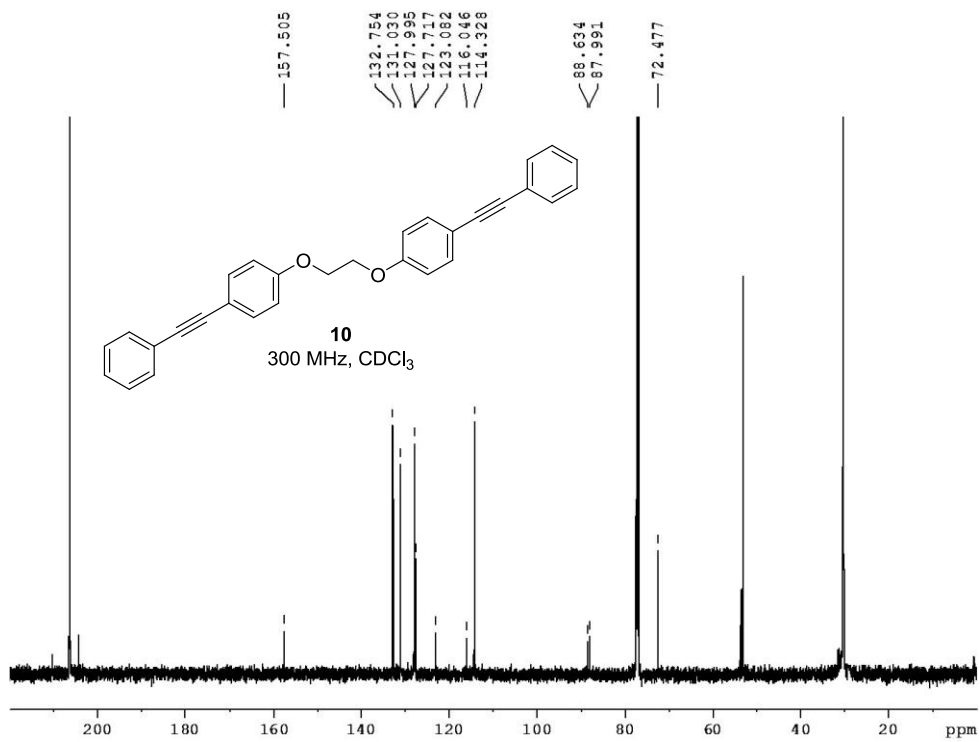
1,4 di(4-phenoxy (phenylcyclopropenone) butane (6).



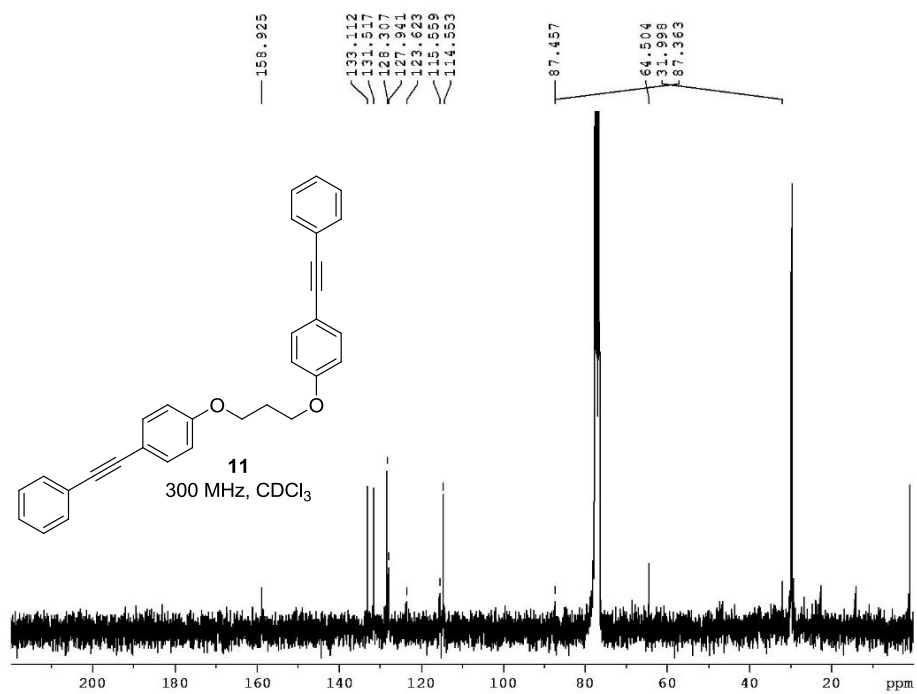
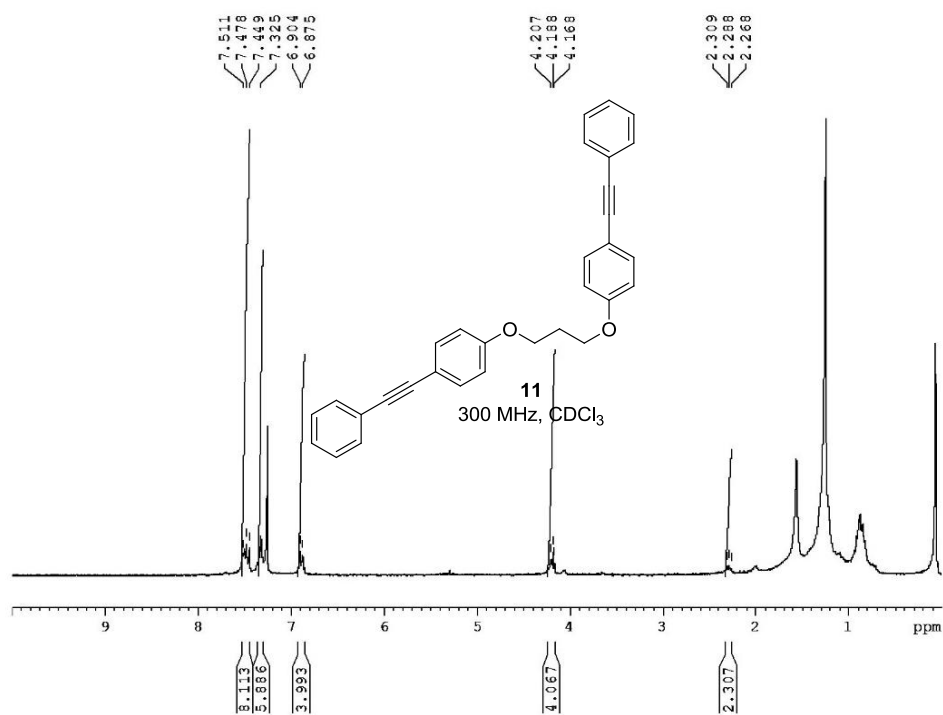


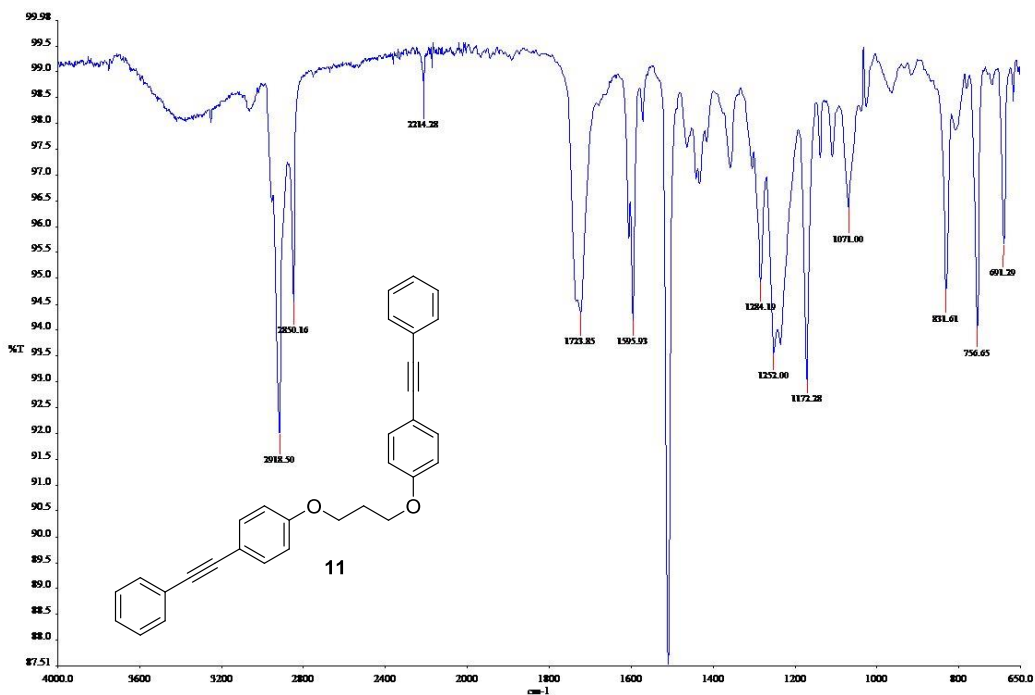
**1,4 di(4-phenoxy-(phenylethynyl)) ethane (10).**



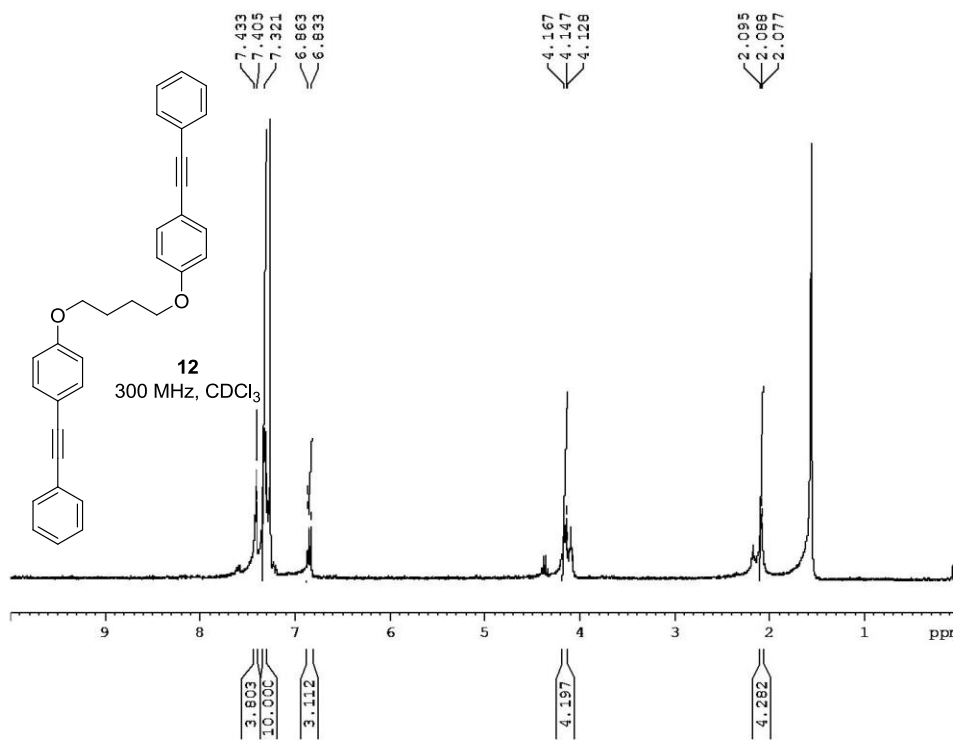


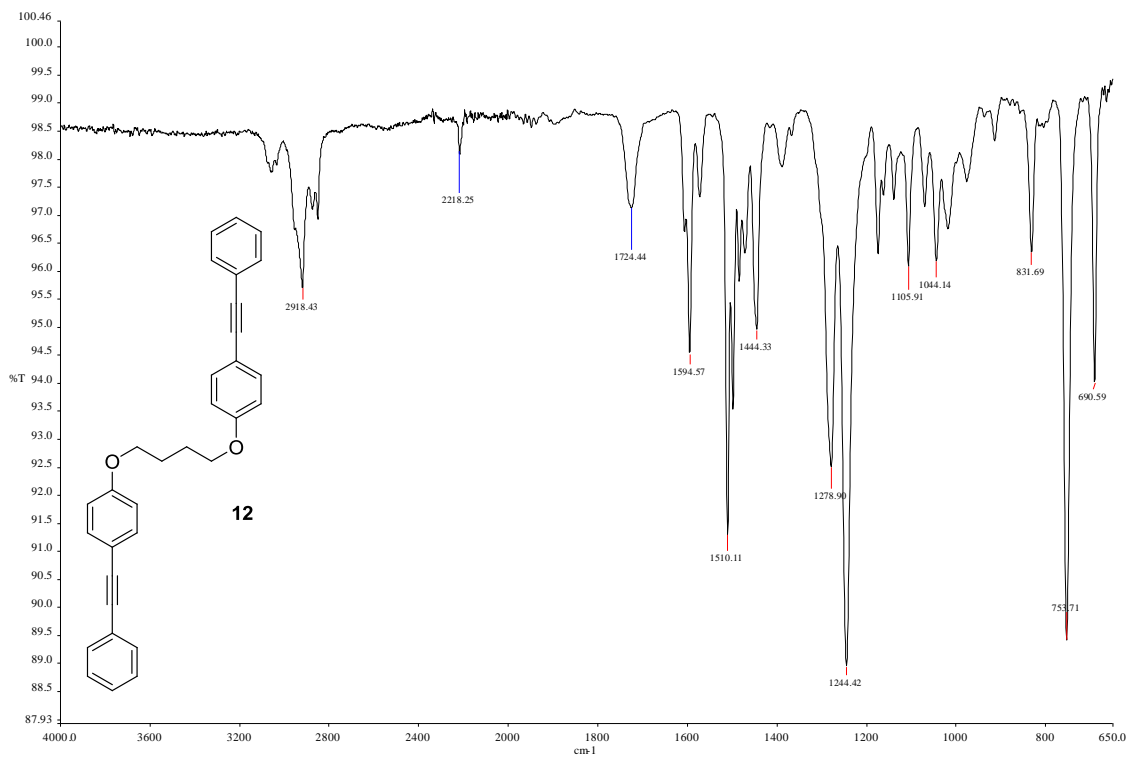
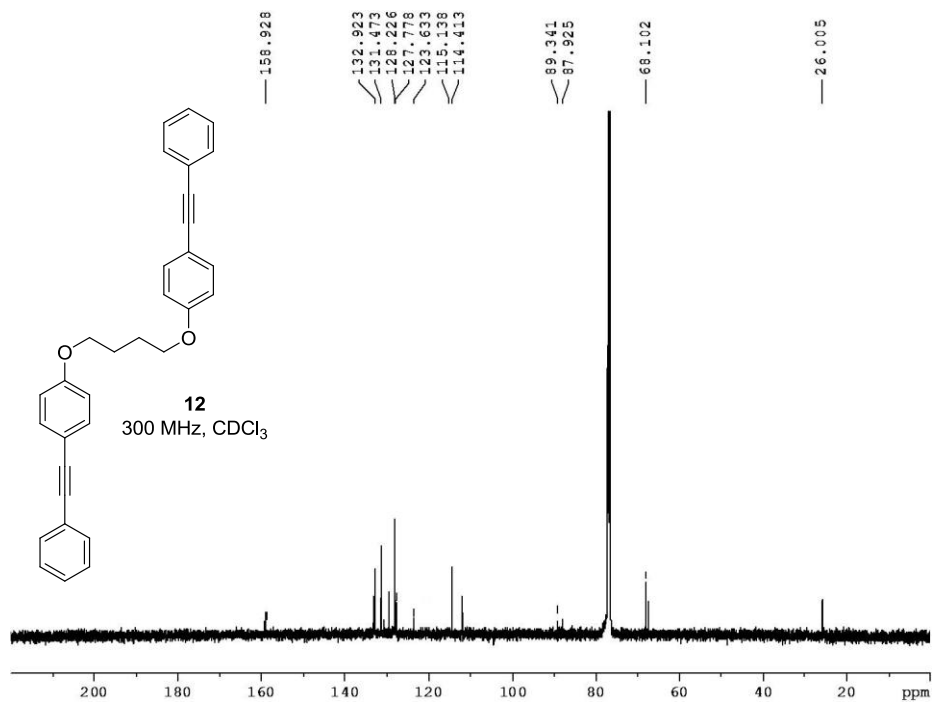
**1,3 di(4-phenoxy-(phenylethynyl)) propane (11).**



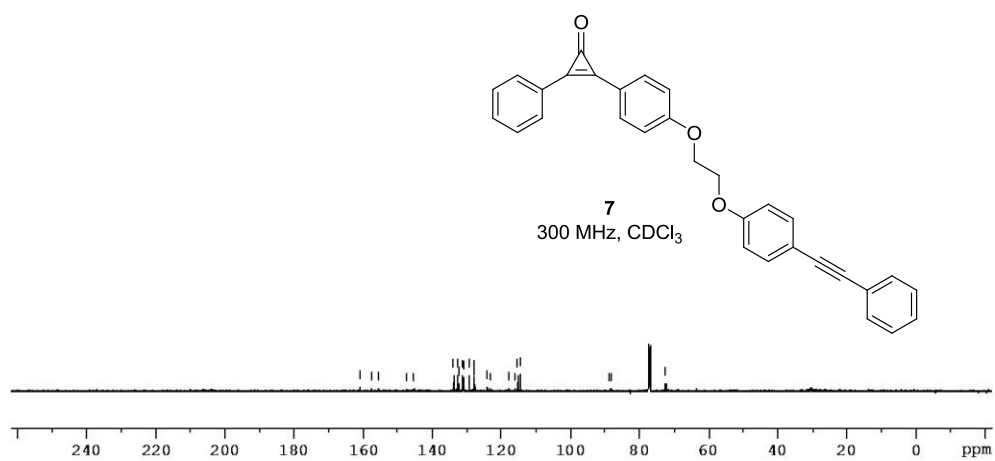
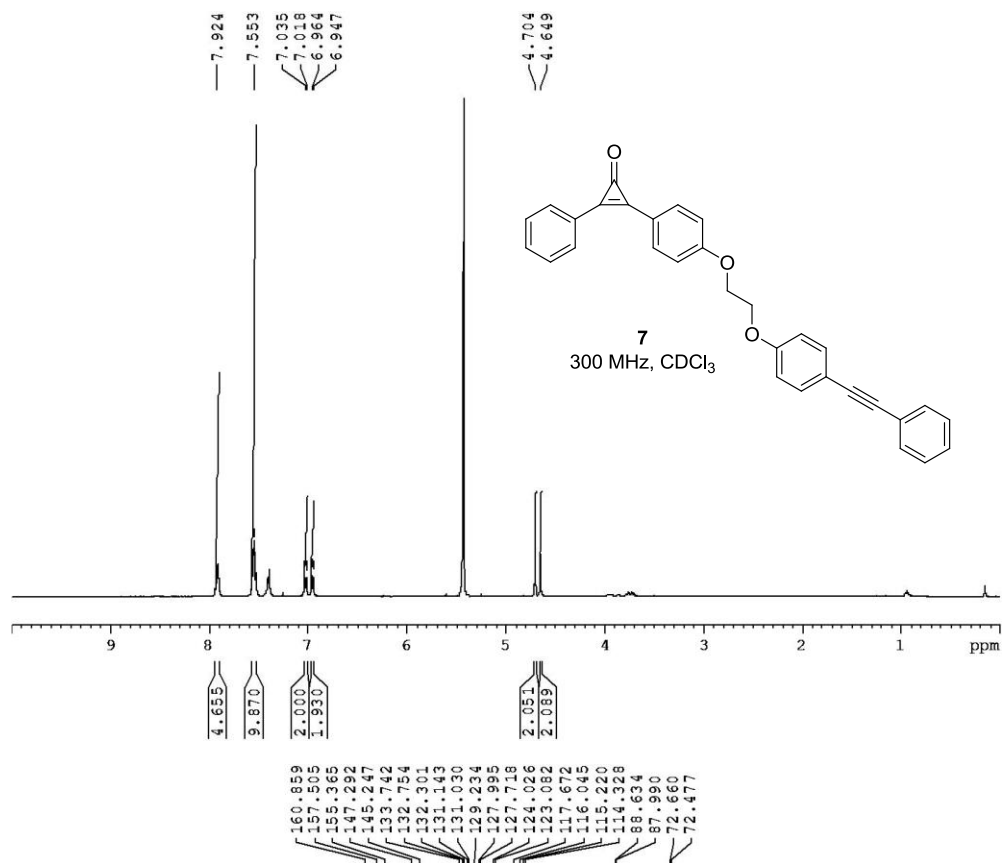


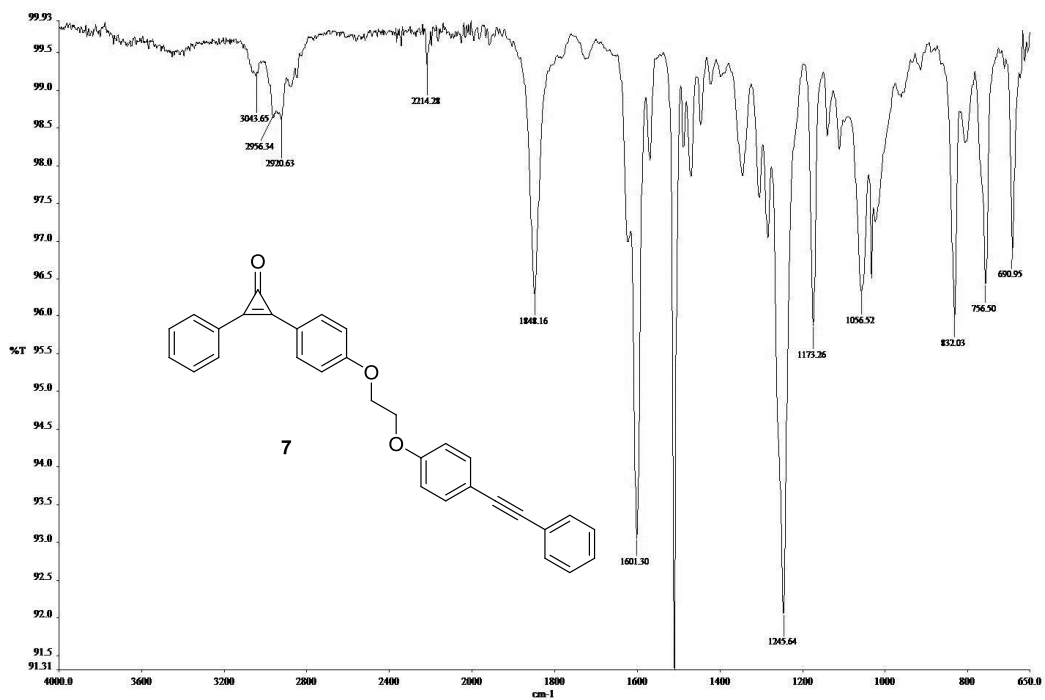
**1,4 di(4-phenoxy-(phenylethynyl)) butane (12).**



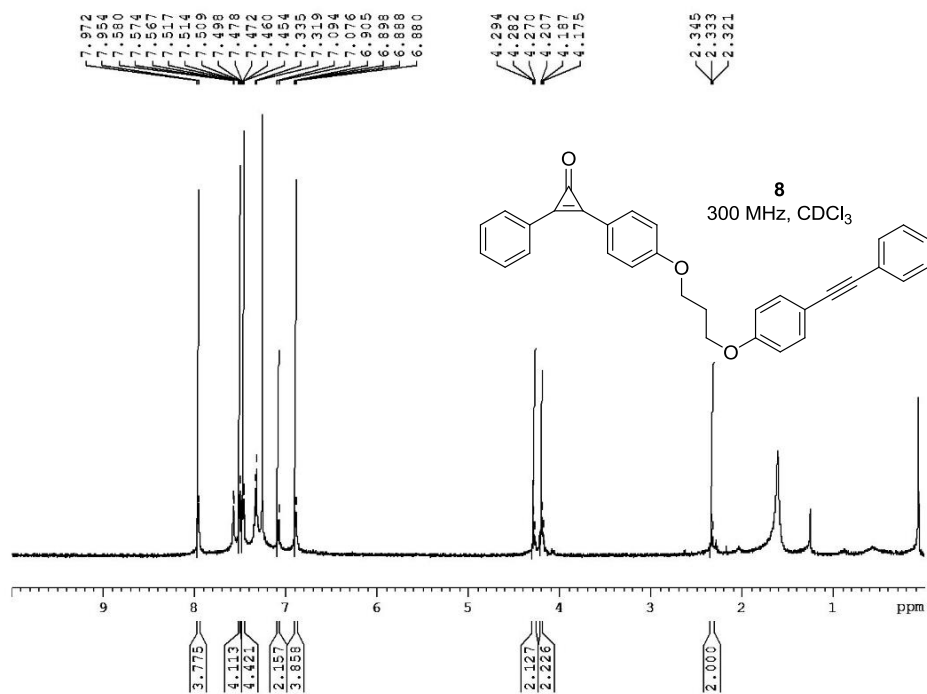


**1-(4-phenoxy (phenylcyclopropenone)), 2-(4-phenoxy-(phenylethynyl)) ethane (7)**

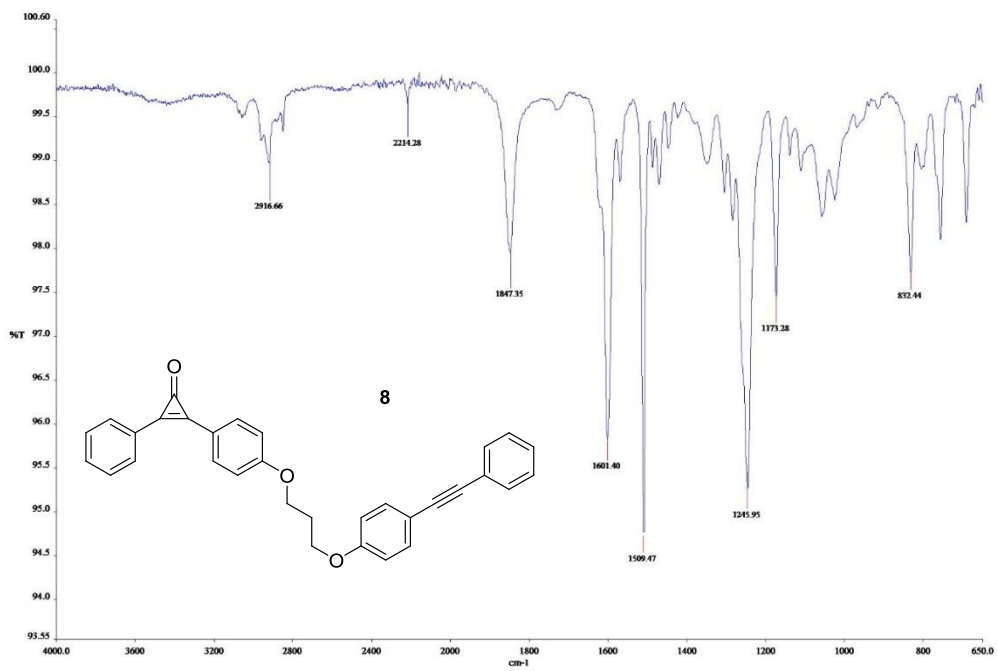
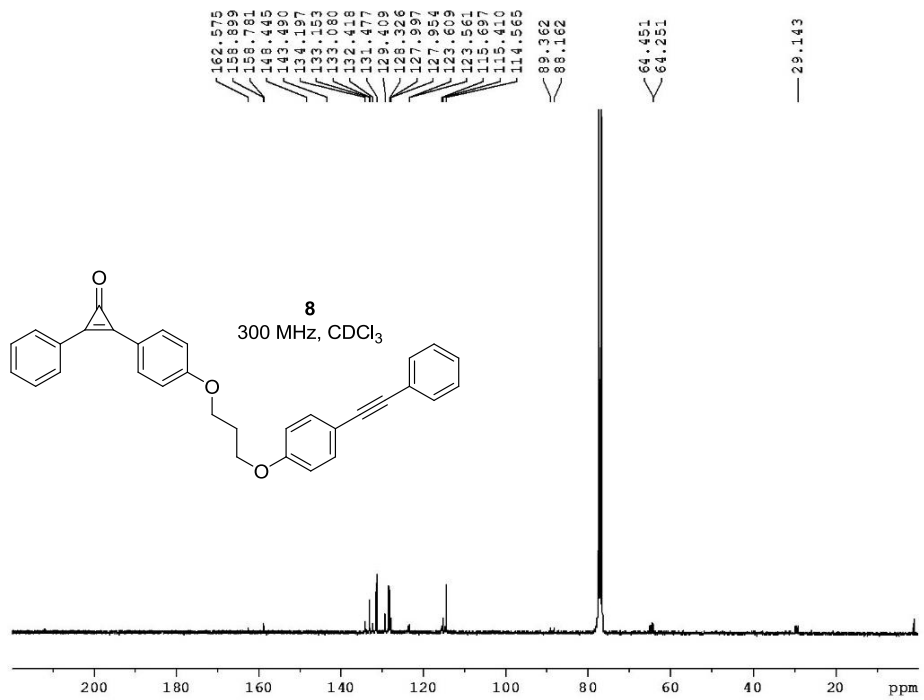




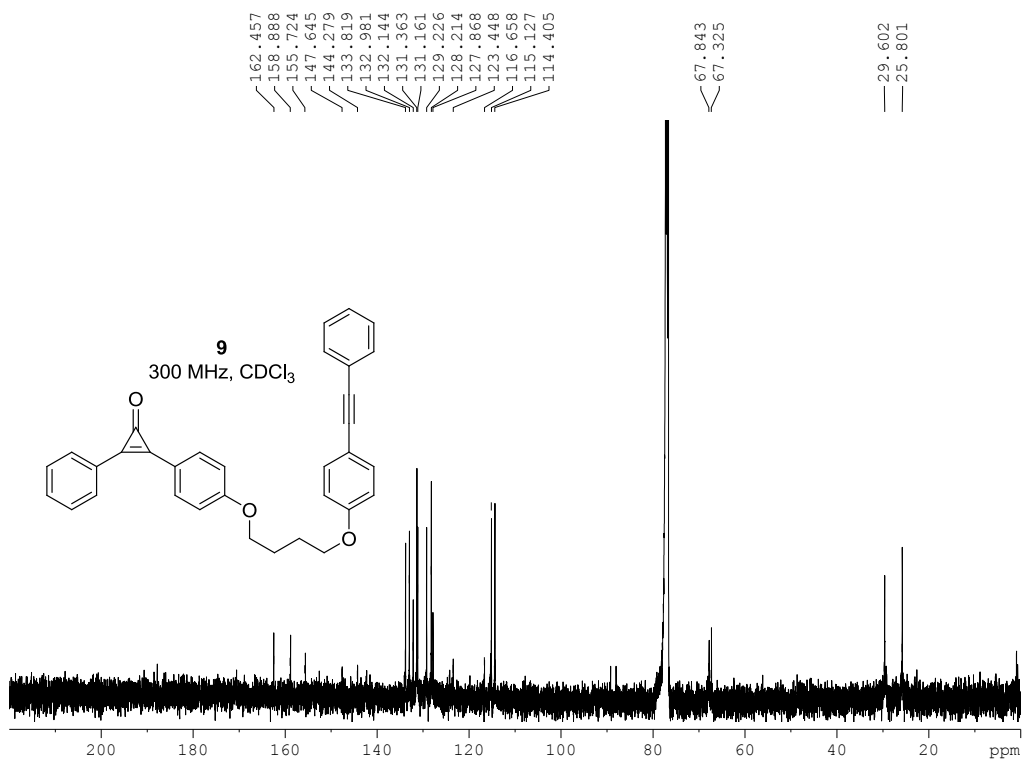
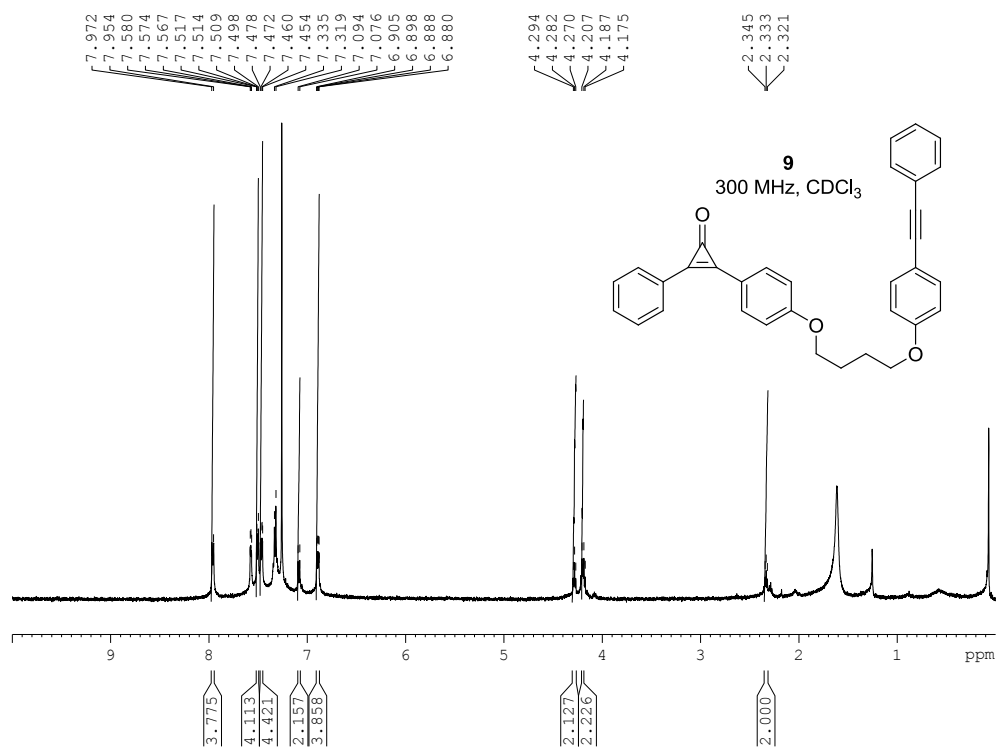
1-(4-phenoxy (phenylcyclopropenone)), 3-(4-phenoxy-(phenylethynyl)) propane (8).

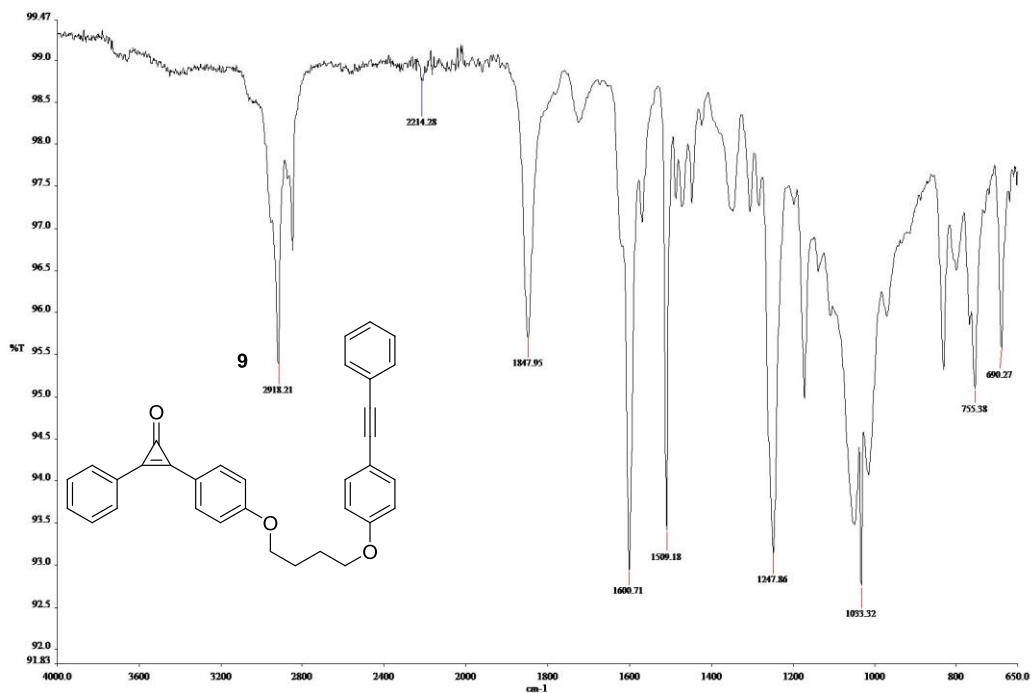




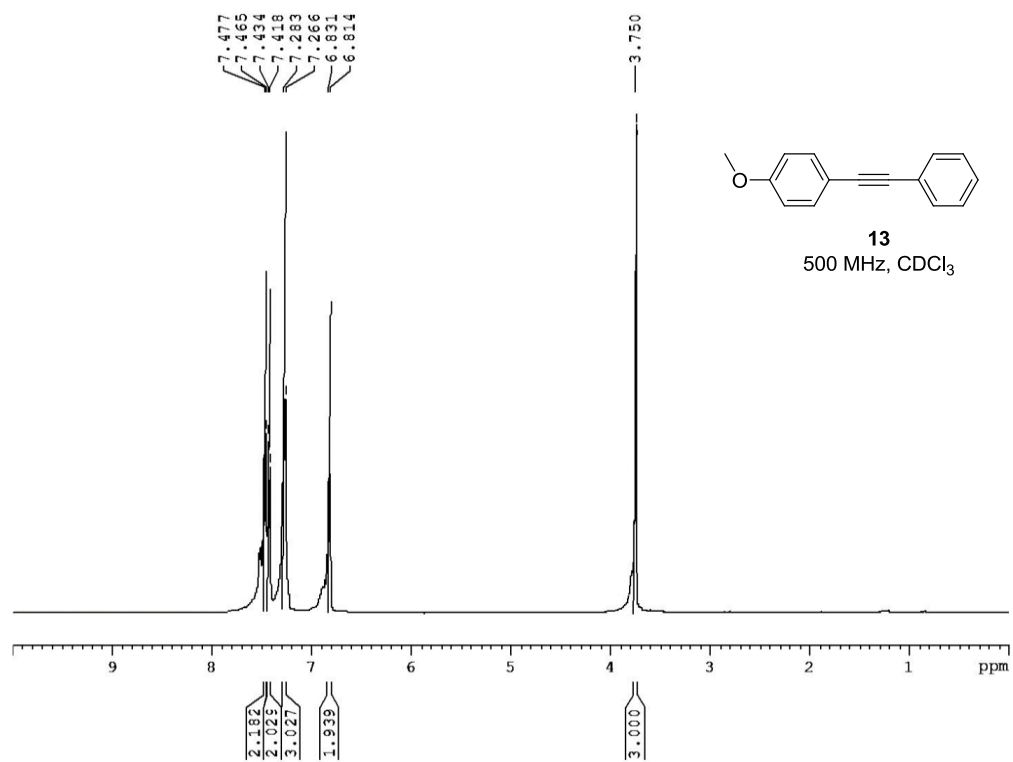


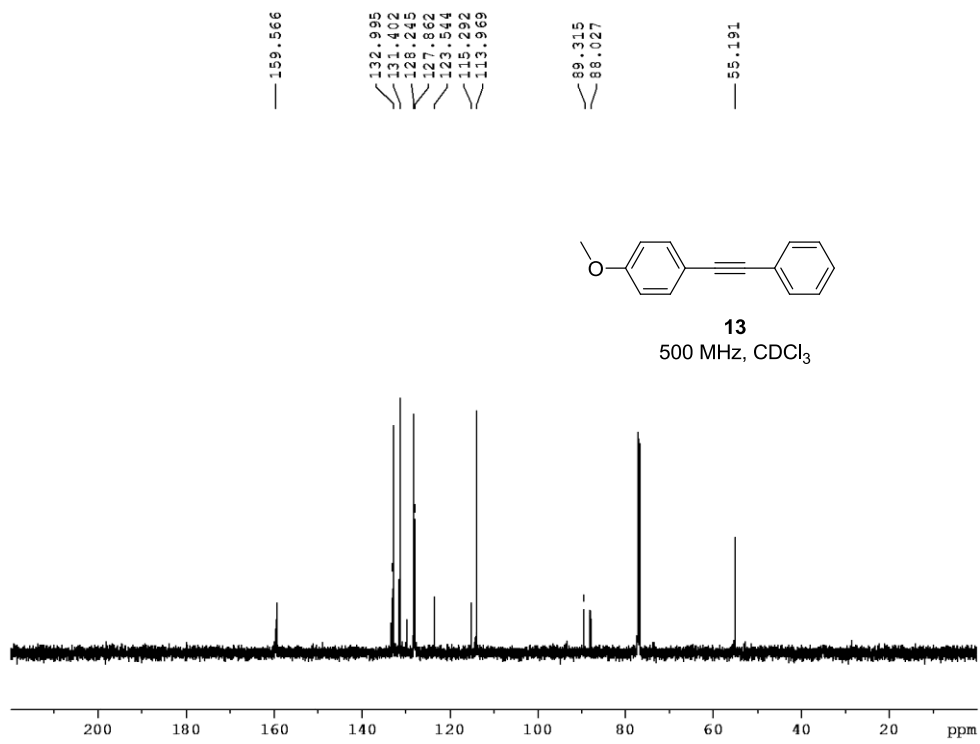
**1-(4-phenoxy (phenylcyclopropenone)), 4-(4-phenoxy-(phenylethynyl)) butane (9).**





### 4-(phenylethynyl)anisole (13)<sup>93</sup>





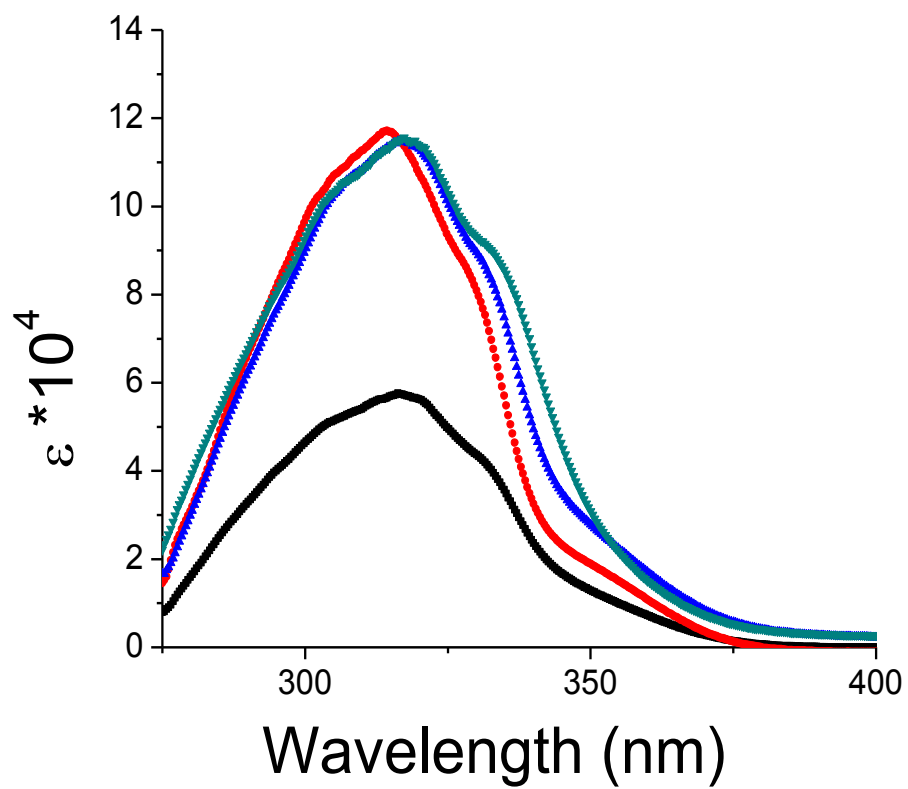


**Figure S1.** UV Absorption spectra of cyclopropenone **3** (black) and linked dimers **4** (red), **5** (blue), and **6** (green) measured in benzene.

## Thermal Analysis Data

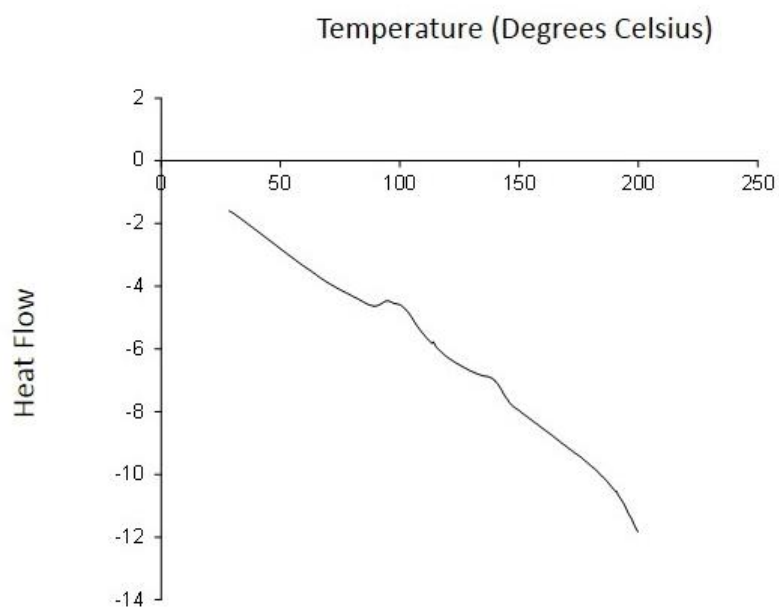


**Figure S2.** DSC of compound **4**

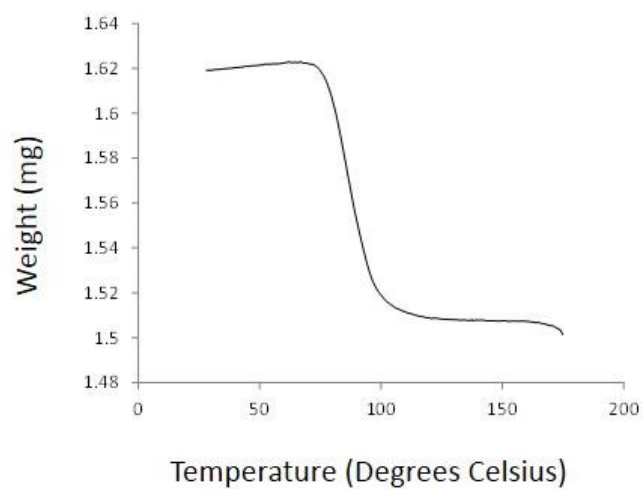


**Figure S6.** TGA of Compound **4**

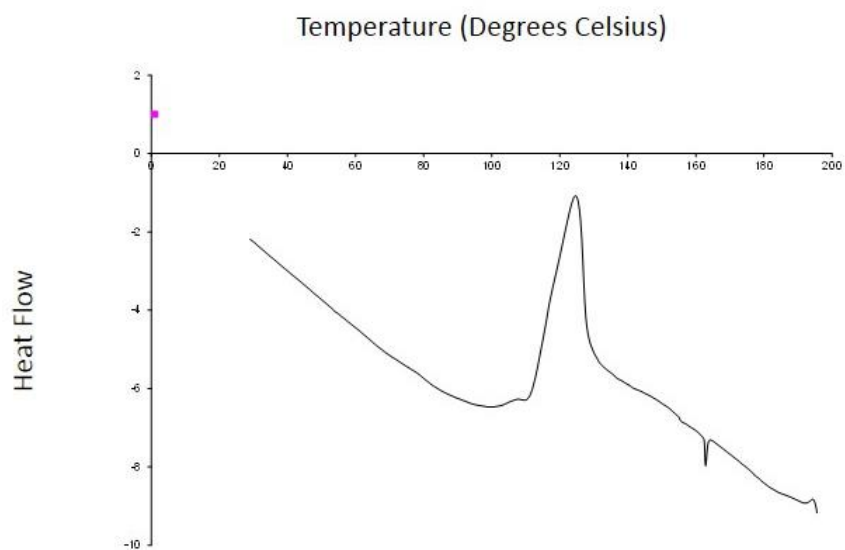


**Figure S7.** DSC of Compound 5

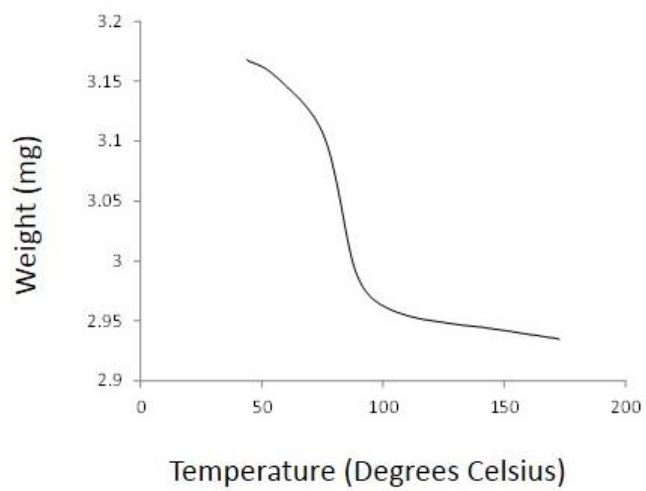


**Figure S8.** TGA of Compound 5

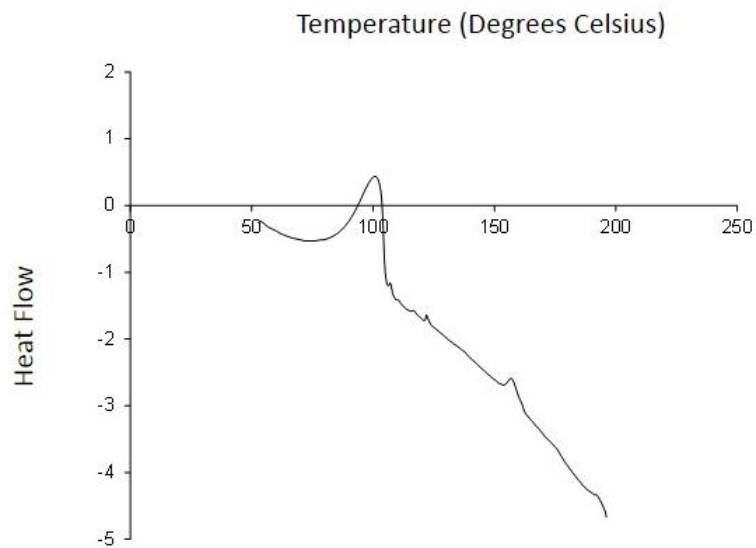


**Figure S9.** DSC of Compound 6

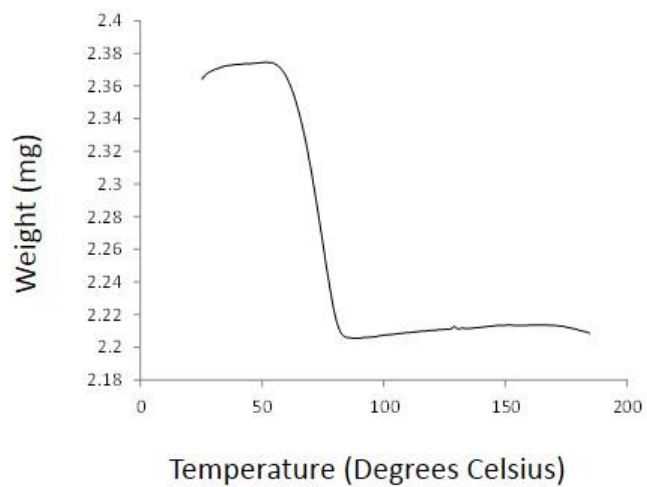


**Figure S10.** TGA of Compound 6



## PXRD Studies

PXRD analyses were carried out using  $\text{Cu-K}\alpha 1 = 1.5406\text{\AA}$  radiation. Data were collected at room temperature in the range of  $2\theta = 4\text{-}45^\circ$  (steps of 0.008, step time 120 s).

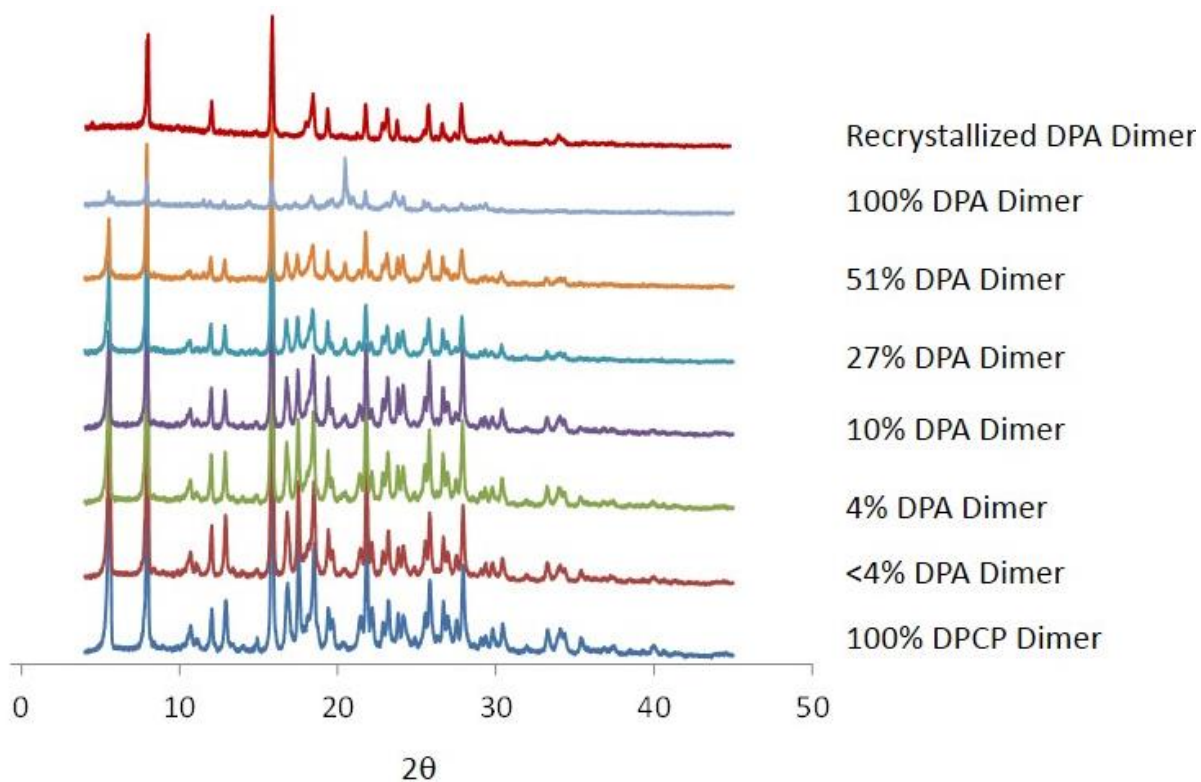


**Figure S11.** PXRD of Compound **4** at various conversions to Compound **10**.

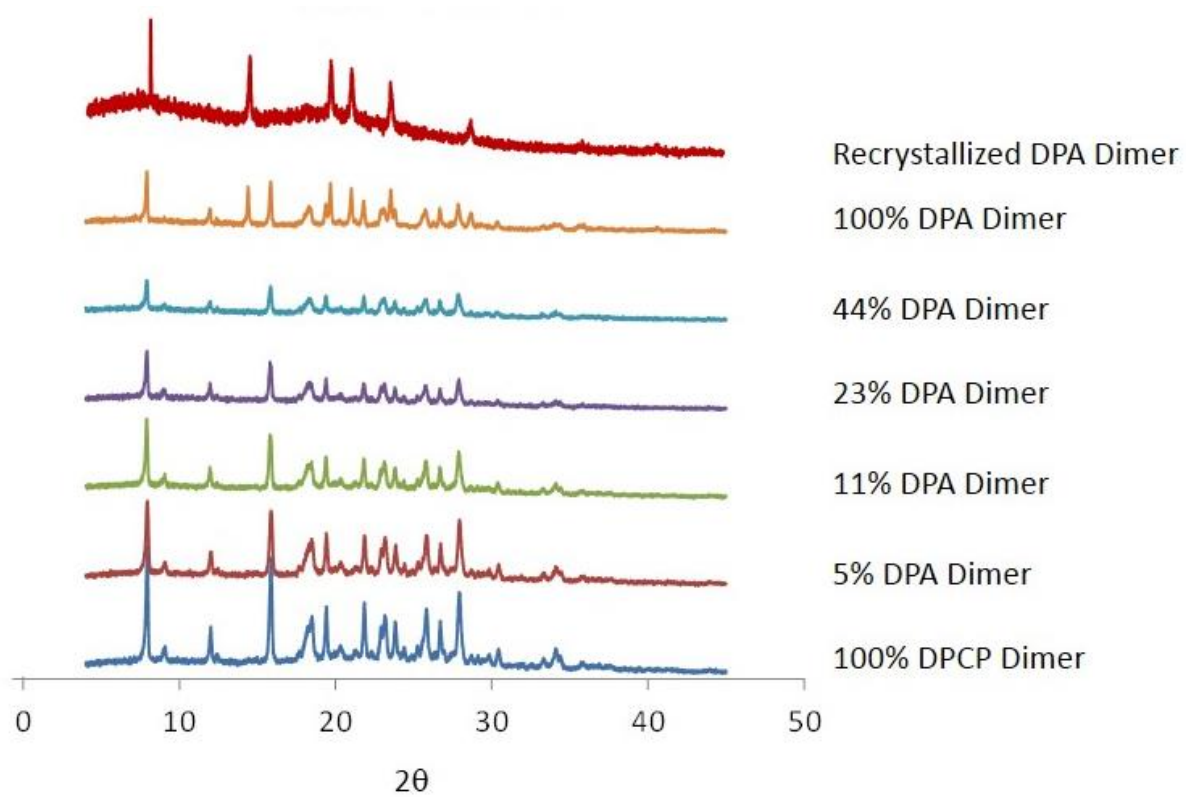


**Figure S12.** PXRD of Compound **5** at various conversions to Compound **11**.

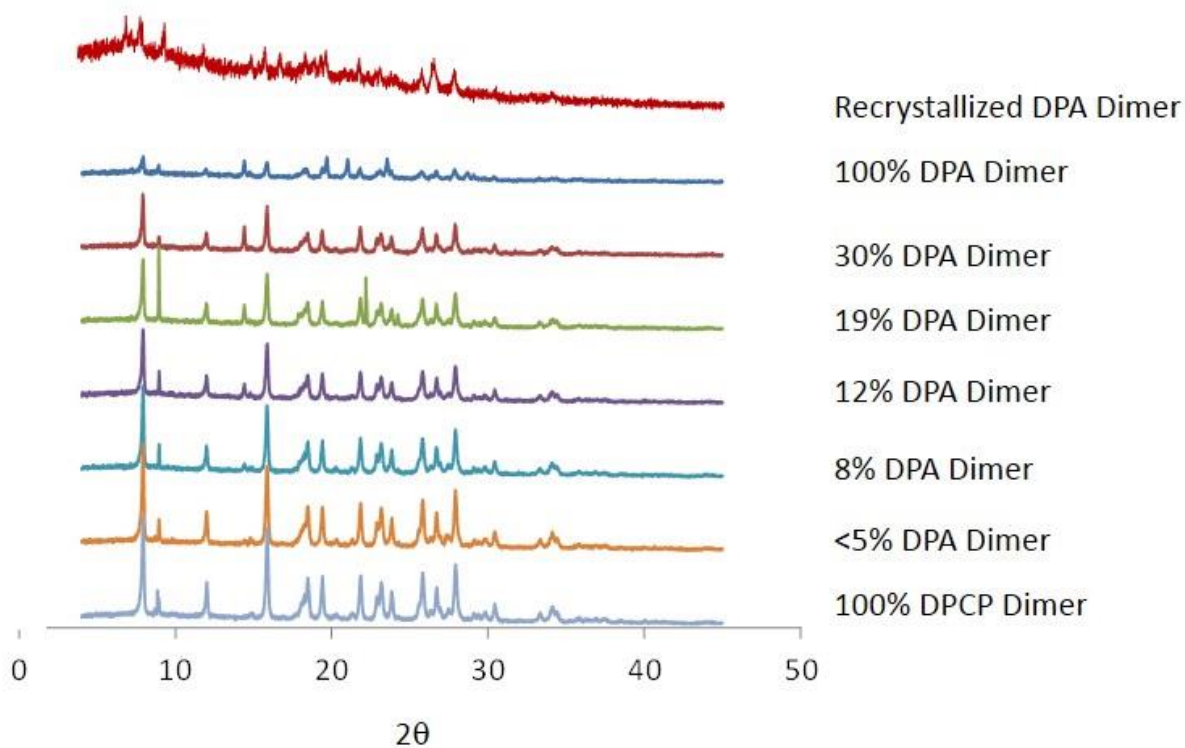


**Figure S13.** PXRD of Compound **6** at various conversions to Compound **12**.

**Table S1.** Relative energy, Boltzmann populations, and intramolecular chromophore to chromophore distance for conformations of ethyl linked dimer **4** with Boltzmann populations > 1%.

Conformation	Relative Energy (kcal/mol)	Boltzmann Population	Distance (Å)
<b>4_1</b>	0.000000000	0.36	5.52
<b>4_2</b>	0.000000000	0.36	5.52
<b>4_3</b>	0.471291385	0.16	6.04
<b>4_4</b>	1.842457211	0.03	4.98
<b>4_5</b>	1.849410022	0.03	4.98
<b>4_6</b>	2.023983304	0.02	5.46
<b>4_7</b>	2.143618086	0.02	4.43
<b>4_8</b>	2.217070641	0.02	5.46

**Table S2.** Relative energy, Boltzmann populations, and intramolecular chromophore to chromophore distance for conformations of propyl linked dimer **5** with Boltzmann populations > 1%.

Conformation	Relative Energy (kcal/mol)	Boltzmann Population	Distance (Å)
<b>5_1</b>	0	0.36	5.71
<b>5_2</b>	0.01	0.36	5.71
<b>5_3</b>	0.787054418	0.08	6.54
<b>5_4</b>	0.787468574	0.08	6.54
<b>5_5</b>	1.633797586	0.02	7.32
<b>5_6</b>	1.750696424	0.02	5.89
<b>5_7</b>	1.923443652	0.02	6.1
<b>5_8</b>	1.925614837	0.02	6.08
<b>5_9</b>	1.958226531	0.02	5.9
<b>5_10</b>	2.174184098	0.01	6.61
<b>5_11</b>	2.403940609	0.01	5.95
<b>5_12</b>	2.510253353	0.01	5.97

**Table S3.** Relative energy, Boltzmann populations, and intramolecular chromophore to chromophore distance for conformations of butyl linked dimer **6** with Boltzmann populations > 1%.

Conformation	Relative Energy (kcal/mol)	Boltzmann Population	Distance (Å)
<b>6_1</b>	0.00	0.10	8.6
<b>6_2</b>	0.08	0.17	7.72
<b>6_3</b>	0.12	0.16	7.83
<b>6_4</b>	0.22	0.13	7.84
<b>6_5</b>	0.32	0.11	7.25
<b>6_6</b>	0.39	0.10	6.71
<b>6_7</b>	0.39	0.10	7.41
<b>6_8</b>	1.33	0.02	7.19
<b>6_9</b>	1.48	0.02	7.97
<b>6_10</b>	1.54	0.01	7.21
<b>6_11</b>	1.55	0.01	6.73
<b>6_12</b>	1.70	0.01	6.14

Conformation: 4\_1

```
# b3lyp/6-31+g scrf=(cpcm, solvent=benzene) guess=read geom=connectivity\\Title Card Required\\0, 1\C, 0,
2.760155, -1.322078, -0.10335\C, 0, 3.496339, -2.135468, 0.794482\C, 0, 4.858643, -1.873252, 1.041201\C, 0,
5.500408, -0.796776, 0.396212\C, 0, 4.775853, 0.015795, -0.496919\C, 0, 3.414494, -0.249789, -0.742309\C, 0,
1.428274, -1.505217, -0.405378\C, 0, 6.918171, -0.539991, 0.666465\C, 0, 8.016876, 0.149124, 0.486267\C, 0,
7.997275, -0.855957, 1.281109\C, 0, 8.58719, -1.591105, 2.066631\C, 0, 10.222021, 3.345602, -1.326453\C, 0,
8.860628, 3.168361, -1.641453\C, 0, 8.12889, 2.119628, -1.050279\C, 0, 8.761169, 1.246676, -1.40644\C, 0,
10.123888, 1.423503, 0.17462\C, 0, 10.853983, 2.473262, -0.418053\C, 0, 0.728429, -2.563799, 0.237496\C, 0, -
0.728906, -2.563702, -0.237902\C, 0, -1.428165, -1.503375, 0.40295\C, 0, -5.500455, -0.796778, -0.395944\C, 0, -
4.858753, -1.873934, -1.039233\C, 0, -3.496685, -2.136425, -0.793144\C, 0, -2.759667, -1.320693, 0.101388\C, 0, -
3.413385, -0.247204, 0.738664\C, 0, -4.77576, 0.018198, 0.494905\C, 0, -6.918467, -0.539839, -0.665213\C, 0, -
8.017507, 0.148253, -0.484001\C, 0, -7.998324, -0.857472, -1.278399\C, 0, -8.588905, -1.594704, -2.061599\C, 0, -
10.221376, 3.346926, 1.324797\C, 0, -8.859178, 3.171672, 1.639148\C, 0, -8.128066, 2.121731, 1.04788\C, 0, -
8.760831, 1.245905, 0.141318\C, 0, -10.124669, 1.422951, -0.173343\C, 0, -10.853442, 2.473441, 0.418406\C, 0,
3.041061, -2.969274, 1.307621\C, 0, 5.407629, -2.500616, 1.727862\C, 0, 5.251639, 0.843062, -0.998327\C, 0,
2.862826, 0.377005, -1.427753\C, 0, 10.782561, 4.150214, -0.78152\C, 0, 8.376625, 3.837754, -2.33859\C, 0,
7.087534, 1.995062, -1.299229\C, 0, 10.613609, 0.757571, 0.87119\C, 0, 11.898527, 2.60848, -0.175984\C, 0, -
5.409425, -2.503727, -1.725248\C, 0, -3.042425, -2.970338, -1.305852\C, 0, -2.861394, 0.380641, 1.422565\C, 0, -
5.251367, 0.846113, 0.995558\C, 0, 1.18997, -3.514083, -0.031869\C, 0, 0.767015, -2.463838, 1.324032\C, 0, -
0.767111, -2.466925, -1.32429\C, 0, -1.190686, -3.51382, 0.033894\C, 0, -10.781355, 4.152578, 1.778633\C, 0, -
8.374679, 3.841853, 2.334646\C, 0, -7.08615, 1.996787, 1.296222\C, 0, -10.613804, 0.755371, -0.86798\C, 0, -
11.898267, 2.608124, 0.177253\\Version=AM64L-G09RevA.02\State=1-A\HF=-1532.9718701\RMSD=6.020e-
09\Dipole=0.0016058, 2.1807294, -0.003423\Quadrupole=-35.788023, 31.3882033, 4.3998197, -.0493739, -
56.3295132, 0.0007296\PG=C01 [X(C32H22O4)]\@\
```

Conformation: 4\_2

```
# b3lyp/6-31+g scrf=(cpcm, solvent=benzene) guess=read geom=connectivity\\Title Card Required\\0, 1\C, 0, -
2.75983, -1.319678, -0.101237\C, 0, -3.414999, -0.247524, -0.740293\C, 0, -4.776839, 0.017044, -0.495858\C, 0, -
5.500461, -0.795889, 0.397537\C, 0, -4.85867, -1.871839, 1.042647\C, 0, -3.496006, -2.134285, 0.795416\C, 0, -
1.428068, -1.502228, -0.403164\C, 0, -6.919001, -0.540045, 0.667644\C, 0, -8.017668, 0.14793, 0.485834\C, 0, -
7.998582, -0.856296, 1.282295\C, 0, -8.588092, -1.592078, 2.066317\C, 0, -10.225269, 3.343057, -1.327516\C, 0, -
8.862318, 3.167153, -1.642749\C, 0, -8.130582, 2.118339, -1.049972\C, 0, -8.762485, 1.244839, -0.141538\C, 0, -
10.125813, 1.421531, 0.174182\C, 0, -10.856484, 2.470147, -0.419504\C, 0, -0.728198, -2.5614, 0.239235\C, 0,
0.728213, -2.560732, -0.238142\C, 0, 1.427973, -1.501016, 0.402612\C, 0, 5.50089, -0.79617, -0.397814\C, 0,
4.857735, -1.872101, -1.042421\C, 0, 3.495989, -2.133006, -0.795673\C, 0, 2.759343, -1.31851, 0.101048\C, 0,
3.414698, -0.246463, 0.738794\C, 0, 4.776864, 0.017833, 0.495099\C, 0, 6.919019, -0.539647, -0.667752\C, 0, 8
.018043, 0.148053, -0.485829\C, 0, 7.99826, -0.857563, -1.281132\C, 0, 8.587714, -1.592587, -2.065101\C, 0,
10.224831, 3.342827, 1.327984\C, 0, 8.862832, 3.167394, 1.641625\C, 0, 8.130637, 2.119264, 1.049449\C, 0,
8.763327, 1.244596, 0.14084\C, 0, 10.126014, 1.420619, -0.173223\C, 0, 10.856766, 2.469735, 0.420349\C, 0, -
2.863217, 0.378996, -1.425929\C, 0, -5.252584, 0.84427, -0.997892\C, 0, -5.407769, -2.499695, 1.728418\C, 0, -
3.04065, -2.966875, 1.30883\C, 0, -10.78501, 4.147845, -1.782271\C, 0, -8.378938, 3.837157, -2.33879\C, 0, -
7.088737, 1.994385, -1.299508\C, 0, -10.614935, 0.754989, 0.870442\C, 0, -11.900669, 2.605129, -0.17731\C, 0,
5.408158, -2.499848, -1.728277\C, 0, 3.040625, -2.966406, .309384\C, 0, 2.862967, 0.380869, 1.424308\C, 0,
```

5.252503, 0.845788, 0.996349 \H, 0, -0.76617, -2.461816, 1.324721\H, 0, -1.190309, -3.511239, -0.031541\H, 0, 1.190817, -3.510683, 0.033225 \H, 0, 0.765827, -2.463578, -1.32398\H, 0, 10.785736, 4.14793, 1.782306\H, 0, 8.378645, 3.838519, 2.337335\ H, 0, 7.088314, 1.99524, 1.297414\H, 0, 10.615811, 0.753297, -0.868688\H, 0, 11.901858, 2.603713, 0.178961 \\Version=AM64L-G09RevA.02\State=1-A\HF=-1532.9717349\RMSD=9.114e-09\Dipole=0.0004287, 2.1745414, -0.0010306\Quadrupole=-35.6654167, 31.3063298, 4.3590869, -0.0078805, 56.2646115, -0065255\PG=C01 [X(C32H22O4)]\@\

Conformation: **4\_3**

# b3lyp/6-31+g scrf=(cpcm, solvent=benzene) guess=read geom=connectivity\\Title Card Required\\0, 1\C, 0, -3.022344, -0.098871, 0.017259\C, 0, -3.374013, 1.275583, 0.020913\C, 0, -4.728276, 1.664305, 0.015314\C, 0, -5.74536, 0.688789, 0.006884\C, 0, -5.40498, -0.678045, 0.003941\C, 0, -4.050551, -1.063838, 0.008909\O, 0, -1.727891, -0.570174, 0.021788\C, 0, -7.14838, 1.114829, 0.001623\C, 0, -8.431365, 0.849557, -0.005749\C, 0, -8.012944, 2.060685, 0.001061\O, 0, -8.261663, 3.262058, 0.003492\C, 0, -11.726712, -1.890337, -0.03072\C, 0, -10.40676, -2.384146, -0.025697\C, 0, -9.318192, -1.489198, -0.017414\C, 0, -9.549782, -0.098004, -0.013998\C, 0, -10.871418, 0.395639, -0.018648\C, 0, -11.959356, -0.500066, -0.027108\C, 0, -0.666226, 0.376168, 0.02538\C, 0, 0.666588, -0.378193, 0.026018\O, 0, 1.72732, 0.568333, 0.025476\C, 0, 5.745618, -0.689428, 0.009771\C, 0, 4.728702, -1.664213, 0.015848\C, 0, 3.373932, -1.275824, 0.021231\C, 0, 3.02259, 0.097302, 0.0204\C, 0, 4.049999, 1.062294, 0.014419\C, 0, 5.404934, 0.676833, 0.008403\C, 0, 7.149515, -1.114644, 0.003261\C, 0, 8.430761, -0.848528, -0.0049\C, 0, 8.013457, -2.060376, 0.001067\O, 0, 8.262108, -3.26167, 0.003734\C, 0, 11.726215, 1.891879, -0.032897\C, 0, 10.406386, 2.384599, -0.027113\C, 0, 9.318238, 1.489766, -0.017347\C, 0, 9.550071, 0.09859, -0.014286\C, 0, 10.871583, -0.393964, -0.020443\C, 0, 11.958472, 0.502382, -0.029858\H, 0, -2.625252, 2.052005, 0.027329\H, 0, -4.982753, 2.714095, 0.018077\H, 0, -6.171101, -1.435798, -0.002801\H, 0, -3.793708, -2.113031, 0.006363\H, 0, -12.561498, -2.577162, -0.036932\H, 0, -10.229888, -3.449494, -0.029051\H, 0, -8.313126, -1.878559, -0.014277\H, 0, -11.054963, 1.460876, -0.01597\H, 0, -12.970643, -0.121052, -0.030754\H, 0, 4.98343, -714618, 0.016628\H, 0, 2.625977, -2.052905, 0.026213\H, 0, 3.793587, 2.112533, 0.014011\H, 0, 6.170931, 1.435676, 0.004338\H, 0, -0.72386, 1.014652, -0.857486\H, 0, -0.726304, 1.01082, 0.91188\H, 0, 0.725328, -1.014567, 0.909454\H, 0, 0.72424, -1.013996, -0.858535\H, 0, 12.560203, 2.578729, -0.041016\H, 0, 10.228641, 3.450684, -0.03006\H, 0, 8.312785, 1.879901, -0.013831\H, 0, 11.05569, -1.459877, -0.018199\H, 0, 12.970887, 0.123577, -0.034439\\Version=AM64L-G09RevA.02\State=1-A\HF=-1532.9711191\RMSD=9.440e-09\Dipole=0.0101131, -0.0033557, -0.013301\Quadrupole=10.6514698, -12.4837168, 1.832247, 89.2489959, -0.0189049, 0.005005\PG=C01 [X(C32H22O4)]\@\

Conformation: **4\_4**

# b3lyp/6-31+g scrf=(cpcm, solvent=benzene) guess=read geom=connectivity\\Title Card Required\\0, 1\C, 0, -2.616857, 2.409096, -0.991742\C, 0, -2.976892, 2.632752, 0.360748\C, 0, -4.016095, 1.889288, 0.955237\C, 0, -4.708464, 0.916186, 0.207181\C, 0, -4.360004, 0.690428, -1.138411\C, 0, -3.321093, 1.434838, -1.728898\O, 0, -1.618893, 3.085182, -1.6635\C, 0, -5.786853, 0.153464, 0.843842\C, 0, -6.72695, -0.758082, 0.808715\C, 0, -6.497564, -0.093653, 1.881333\O, 0, -6.765888, 0.138973, 3.055001\C, 0, -8.999522, -3.771001, -1.219944\C, 0, -9.269303, -3.466727, 0.128808\C, 0, -8.519259, -2.474426, 0.791331\C, 0, -7.497405, -1.787026, 0.104399\C, 0, -7.227843, -2.091739, -1.246015\C, 0, -7.979347, -3.083907, -1.907176\C, 0, -0.780975, 3.997438, -0.957632\C, 0, 0.273266, 3.267369, -0.107749\O, 0, 1.270963, 2.731255, -0.968954\C, 0, 4.516788, 0.53817, 0.572265\C, 0, 4.360267, 0.740914, -0.811893\C, 0, 3.26164, 1.480162, -1.292899\C, 0, 2.310135, 2.022316, -0.406263\C, 0,

2.475153, 1.81395, 0.986092\C, 0, 3.573107, 1.074782, 1.470778\C, 0, 5.652004, -0.228666, 1.096701\C, 0, 6.751321, -0.918913, 0.924023\C, 0, 6.287594, -0.708905, 2.100517\O, 0, 6.382506, -0.860221, 3.313594\C, 0, 9.768218, -2.666567, -1.567426\C, 0, 9.833109, -2.811028, -0.16677\C, 0, 8.838176, -2.234582, 0.647866\C, 0, 7.777595, -1.511821, 0.060852\C, 0, 7.713434, -1.367427, -1.340485\C, 0, 8.710072, -1.945355, -2.153146\H, 0, -2.474916, 3.366946, 0.970777\H, 0, -4.279845, 2.068604, 1.987688\H, 0, -4.880498, -0.050108, -1.725055\H, 0, -3.057151, 1.25775, -2.761362\H, 0, -9.575779, -4.531389, -1.727756\H, 0, -10.052443, -3.992991, 0.656126\H, 0, -8.729883, -2.245368, 1.825887\H, 0, -6.449538, -1.572742, -1.78221\H, 0, -7.773194, -3.317965, -2.941626\H, 0, 5.072801, 0.337207, -1.512869\H, 0, 3.144889, 1.633809, -2.356208\H, 0, 1.775589, 2.209469, 1.706193\H, 0, 3.687643, 0.923123, 2.534454\H, 0, -0.275916, 4.628181, -1.689137\H, 0, -1.374107, 4.682941, -0.351839\H, 0, 0.736762, 3.984649, 0.571434\H, 0, -0.184939, 2.482782, 0.495171\H, 0, 10.531702, -3.108772, -2.190859\H, 0, 10.644929, -3.364112, 0.282227\H, 0, 8.891543, -2.348132, 1.721545\H, 0, 6.907333, -0.818494, -1.800575\H, 0, 8.660787, -1.834848, -3.226557\\Version=AM64L-G09RevA.02\State=1-A\HF=-1532.968934\RMSD=5.870e-09\Dipole=0.2907466, 0.4345395, -4.3396222\Quadrupole=1.4458267, 21.41802, -22.8638468, 10.7370527, -3.3575494, 12.777802\PG=C01 [X(C32H22O4)]\@

Conformation: 4\_5

# b3lyp/6-31+g scrf=(cpcm, solvent=benzene) guess=read geom=connectivity\\Title Card Required\\0, 1\C, 0, 2.615341, 2.410253, -0.988279\C, 0, 3.323005, 1.440421, -1.727821\C, 0, 4.361078, 0.693547, -1.137892\C, 0, 4.705347, 0.91419, 0.208915\C, 0, 4.01033, 1.882573, 0.960246\C, 0, 2.972433, 2.628114, 0.366825\O, 0, 1.618061, 3.088123, -1.659205\C, 0, 5.782094, 0.148663, 0.845152\C, 0, 6.721986, -0.762212, 0.809394\C, 0, 6.490128, -0.102428, 1.883814\O, 0, 6.755391, 0.124245, 3.059935\C, 0, 9.00201, -3.76504, -1.227619\C, 0, 9.268553, -3.466947, 0.123781\C, 0, 8.515161, -2.479076, 0.788539\C, 0, 7.495709, -1.787045, 0.101063\C, 0, 7.230125, -2.086452, -1.250932\C, 0, 7.983733, -3.074766, -1.914365\C, 0, 0.781492, 4.001584, -0.952189\C, 0, -0.274808, 3.273064, -0.103844\O, 0, -1.276669, 2.745752, -0.964646\C, 0, -4.516341, 0.541003, 0.573145\C, 0, -4.362074, 0.749566, -0.811855\C, 0, -3.266105, 1.492204, -1.291552\C, 0, -2.314439, 2.033735, -0.403487\C, 0, -2.478327, 1.82042, 0.988284\C, 0, -3.572754, 1.077375, 1.471365\C, 0, -5.648843, -0.229998, 1.095337\C, 0, -6.745852, -0.923608, 0.922455\C, 0, -6.281619, -0.716408, 2.098874\O, 0, -6.374479, -0.872051, 3.311251\C, 0, -9.762664, -2.671493, -1.570229\C, 0, -9.824591, -2.820217, -0.17048\C, 0, -8.829923, -2.244289, 0.643614\C, 0, -7.772282, -1.516924, 0.058694\C, 0, -7.710571, -1.367757, -1.342381\C, 0, -8.706134, -1.944606, -2.155882\H, 0, 3.060929, 1.267811, -2.761176\H, 0, 4.882513, -0.042773, -1.726835\H, 0, 4.271036, 2.05783, 1.993953\H, 0, 2.467791, 3.359511, 0.978544\H, 0, 9.580104, -4.522678, -1.737111\H, 0, 10.048861, -3.996391, 0.650318\H, 0, 8.722688, -2.254313, 1.825575\H, 0, 6.453239, -1.564507, -1.787321\H, 0, 7.781168, -3.303865, -2.95064\H, 0, -5.07431, 0.345625, -1.51268\H, 0, -3.150277, 1.649216, -2.354077\H, 0, -1.778391, 2.215047, 1.70837\H, 0, -3.685814, 0.921334, 2.534518\H, 0, 1.37688, 4.68421, -0.345922\H, 0, 0.279588, 4.634811, -1.683299\H, 0, 0.181197, 2.484349, 0.495297\H, 0, -0.733671, 3.989558, 0.579172\H, 0, -10.525556, -3.114075, -2.19499\H, 0, -10.634304, -3.377624, 0.27843\H, 0, -8.882065, -2.3615, 1.717355\H, 0, -6.907019, -0.814092, -1.801343\H, 0, -8.660207, -1.830703, -3.228961\\Version=AM64L-G09RevA.02\State=1-A\HF=-1532.9689229\RMSD=5.504e-09\Dipole=-0.2832723, 0.4540751, -4.3429615\Quadrupole=1.5468005, 21.3315849, -22.8783854, -10.6686965, 3.2206777, 12.892137\PG=C01 [X(C32H22O4)]\@

Conformation: 4\_6



b3lyp/6-31+g scrf=(cpcm, solvent=benzene) guess=read geom=connectivity\\Title Card Required\\0, 1\C, 0, 2.548513, 1.68028, -0.128509\C, 0, 2.412435, 0.523153, -0.936195\C, 0, 3.507692, -0.341558, -1.131444\C, 0, 4.748515, -0.062567, -0.524989\C, 0, 4.8919, 1.08546, 0.278598\C, 0, 3.795728, 1.94769, 0.472113\O, 0, 1.53471, 2.580546, 0.117642\C, 0, 5.874791, -0.975524, -0.740812\C, 0, 7.121722, -1.329762, -0.54985\C, 0, 6.343682, -2.039612, -1.279933\O, 0, 6.171405, -3.026405, -1.986985\C, 0, 11.003089, -0.731773, 1.16431\C, 0, 9.974834, 0.196468, 1.421887\C, 0, 8.695525, 0.005815, 0.862741\C, 0, 8.445211, -1.114844, 0.042962\C, 0, 9.475767, -2.042951, -0.215444\C, 0, 10.753771, -1.850809, 0.345144\C, 0, 0.261321, 2.337169, -0.464916\C, 0, -0.693903, 3.467058, -0.050552\O, 0, -1.963653, 3.334222, -0.68367\C, 0, -4.835317, 0.525639, 0.584027\C, 0, -3.666689, 0.692531, 1.353309\C, 0, -2.685703, 1.623921, 0.958152\C, 0, -2.862849, 2.398196, -0.216596\C, 0, -4.038692, 2.223608, -0.973359\C, 0, -5.021602, 1.293642, -0.582109\C, 0, -5.844592, -0.448839, 1.011959\C, 0, -6.989467, -1.063834, 0.852032\C, 0, -6.233078, -1.336853, 1.850281\O, 0, -6.028442, -1.981605, 2.872394\C, 0, -10.631929, -1.78182, -1.288372\C, 0, -10.350072, -2.496848, -0.107765\C, 0, -9.150783, -2.257129, 0.591838\C, 0, -8.231777, -1.300807, 0.110634\C, 0, -8.514926, -0.584614, -1.070959\C, 0, -9.715144, -0.82649, -1.769868\H, 0, 1.480099, 0.27418, -1.418489\H, 0, 3.39106, -1.220909, -1.749964\H, 0, 5.834571, 1.312532, 0.749868\H, 0, 3.911216, 2.826813, 1.089834\H, 0, 11.984045, -0.585145, 1.593807\H, 0, 10.16696, 1.054256, 2.049884\H, 0, 7.916626, 0.722356, 1.066756\H, 0, 9.289105, -2.902984, -0.84311\H, 0, 11.542602, -2.561969, 0.146644\H, 0, -3.518795, 0.108064, 2.249268\H, 0, -1.808766, 1.720488, 1.578266\H, 0, -4.187541, 2.81177, -1.867757\H, 0, -5.910503, 1.180097, -1.180255\H, 0, 0.343884, 2.315012, -1.552136\H, 0, -0.123782, 1.37056, -0.135459\H, 0, -0.782574, 3.552545, 1.032304\H, 0, -0.272184, 4.416587, -0.381232\H, 0, -11.551814, -1.96584, -1.825804\H, 0, -11.052609, -3.229308, 0.261169\H, 0, -8.939021, -2.807781, 1.496822\H, 0, -7.820745, 0.149246, -1.4496\H, 0, -9.931844, -0.278633, -2.675742\\Version=AM64L-G09RevA.02\State=1-A\HF=-1532.9686447\RMSD=5.450e-09\Dipole=-0.0641551, 3.3007638, -0.6381085\Quadrupole=44.1704391, -22.3103596, -21.8600795, 14.3052237, 51.6087901, 1.6736092\PG=C01 [X(C32H22O4)]\\@

Conformation: 4\_7

b3lyp/6-31+g scrf=(cpcm, solvent=benzene) guess=read geom=connectivity\\Title Card Required\\0, 1\C, 0, -2.594184, 3.274146, -0.161687\C, 0, -3.553274, 2.737915, 0.721851\C, 0, -4.126331, 1.472274, 0.488849\C, 0, -3.744816, 0.726628, -0.643249\C, 0, -2.791508, 1.252132, -1.53686\C, 0, -2.221647, 2.518315, -1.30131\O, 0, -2.100227, 4.522408, 0.152403\C, 0, -4.326526, -0.592852, -0.905875\C, 0, -5.129028, -1.579318, -0.593197\C, 0, -4.401293, -1.636504, -1.646617\O, 0, -4.037565, -2.24862, -2.645751\C, 0, -8.046276, -3.421733, 1.948657\C, 0, -7.596584, -4.08327, 0.789212\C, 0, -6.637105, -3.473106, -0.042842\C, 0, -6.126459, -2.199182, 0.283975\C, 0, -6.577429, -1.537654, 1.444958\C, 0, -7.536059, -2.149202, 2.27641\C, 0, -0.998868, 5.058267, -0.577745\C, 0, 0.347429, 4.515376, -0.067725\O, 0, 0.647316, 3.273115, -0.691945\C, 0, 4.075716, 1.079024, 0.377903\C, 0, 3.880556, 2.354225, 0.946336\C, 0, 2.742014, 3.112797, 0.609029\C, 0, 1.78521, 2.602066, -0.302634\C, 0, 1.993589, 1.32596, -0.865284\C, 0, 3.12914, 0.56463, -0.529179\C, 0, 5.266471, 0.304884, 0.741621\C, 0, 6.014876, -0.765759, 0.651274\C, 0, 6.356649, 0.209524, 1.409417\O, 0, 7.154097, 0.698481, 2.202769\C, 0, 6.866978, -4.662603, -0.916015\C, 0, 7.750856, -4.056049, -0.001987\C, 0, 7.46614, -2.775234, 0.510231\C, 0, 6.294991, -2.099298, 0.107606\C, 0, 5.410047, -2.70612, -0.80731\C, 0, 5.697107, -3.987787, -1.317584\H, 0, -3.851057, 3.306242, 1.590882\H, 0, -4.855994, 1.087076, 1.182993\H, 0, -2.492868, 0.686591, -2.407763\H, 0, -1.494383, 2.881169, -2.010586\H, 0, -8.781677, -3.889417, 2.586818\H, 0, -7.987394, -5.058479, 0.537799\H, 0, -6.294866, -3.984513, -0.931794\H, 0, -6.194719, -0.563893, 1.706533\H, 0, -7.882357, -1.64195, 3.165863\H, 0, 4.603372, 2.754772, 1.643299\H, 0, 2.630815, 4.085271, 1.063389\H, 0, 1.268434, 0.928176, -1.560274\H, 0, 3.263794, -0.408806, -0.973149\H, 0, -1.105472, 4.967255, -1.657878\H, 0, -1.019356, 6.13074, -0.382894\H, 0, 1.131904, 5.229615, -0.32159\H, 0, 0.319328, 4.41968, 1.018944\H, 0, 7.085208, -5.64604, -1.308768\H, 0, 8.648333, -4.573702, 0.306706\H, 0, 8.147297, -2.313607, 1.210639\H, 0, 4.511903, -2.200069, -1.121828\H, 0,

5.018498, -4.45413, -2.018503\\Version=AM64L-G09RevA.02\\State=1-A\\HF=-1532.968454\\RMSD=5.792e-09\\Dipole=-1.92901, 1.0667805, 0.3655435\\Quadrupole=-17.3651555, 30.4438897, -13.0787341, -16.4539333, -43.7679497, -10.8600526\\PG=C01 [X(C32H22O4)]\\@

Conformation: **4\_8**

# b3lyp/6-31+g scrf=(cpcm, solvent=benzene) guess=read geom=connectivity\\Title Card Required\\0, 1\\C, 0, -2.547624, 1.691677, -0.127792\\C, 0, -2.415369, 0.547108, -0.954492\\C, 0, -3.51021, -0.316966, -1.156051\\C, 0, -4.746488, -0.049733, -0.536373\\C, 0, -4.886793, 1.085405, 0.286294\\C, 0, -3.790916, 1.947302, 0.485172\\O, 0, -1.533678, 2.589224, 0.125731\\C, 0, -5.873791, -0.961253, -0.758577\\C, 0, -7.116669, -1.321475, -0.563347\\C, 0, -6.343413, -2.01726, -1.312019\\O, 0, -6.174225, -2.993198, -2.036451\\C, 0, -10.98693, -0.760555, 1.19009\\C, 0, -9.958474, 0.164321, 1.456125\\C, 0, -8.683212, -0.013933, 0.883331\\C, 0, -8.437779, -1.118896, 0.042101\\C, 0, -9.468084, -2.045028, -0.224002\\C, 0, -10.742219, -1.865287, 0.349513\\C, 0, -0.261238, 2.352298, -0.463176\\C, 0, 0.695964, 3.475143, -0.033315\\O, 0, 1.967284, 3.345633, -0.664371\\C, 0, 4.8284, 0.51707, 0.584056\\C, 0, 3.655804, 0.676397, 1.348789\\C, 0, 2.678032, 1.613384, 0.960187\\C, 0, 2.862883, 2.402302, -0.203531\\C, 0, 4.042889, 2.235383, -0.955877\\C, 0, 5.022584, 1.299704, -0.570206\\C, 0, 5.834398, -0.464031, 1.005585\\C, 0, 6.978541, -1.078184, 0.845724\\C, 0, 6.215926, -1.363227, 1.835429\\O, 0, 6.003545, -2.021471, 2.847712\\C, 0, 10.634987, -1.77175, -1.279139\\C, 0, 10.344015, -2.502654, -0.110663\\C, 0, 9.140084, -2.271191, 0.584877\\C, 0, 8.225918, -1.30694, 0.109946\\C, 0, 8.518494, -0.575125, -1.060142\\C, 0, 9.722348, -0.808985, -1.753393\\H, 0, -1.485932, 0.307541, -1.448151\\H, 0, -3.395495, -1.185828, -1.788552\\H, 0, -5.82656, 1.30427, 0.766661\\H, 0, -3.903625, 2.816447, 1.116727\\H, 0, -11.964777, -0.623572, 1.629723\\H, 0, -10.14724, 1.010973, 2.100422\\H, 0, -7.90343, 0.701126, 1.094198\\H, 0, -9.28486, -2.893103, -0.867793\\H, 0, -11.530735, -2.574213, 0.14521\\H, 0, 3.501754, 0.079898, 2.236871\\H, 0, 1.797891, 1.703754, 1.576141\\H, 0, 4.197346, 2.833598, -1.842585\\H, 0, 5.914241, 1.192087, -1.16584\\H, 0, 0.122593, 1.381115, -0.148784\\H, 0, -0.345548, 2.346214, -1.550516\\H, 0, 0.278205, 4.429769, -0.354835\\H, 0, 0.781935, 3.54742, 1.050901\\H, 0, 11.558288, -1.950025, -1.811883\\H, 0, 11.04392, -3.241109, 0.253286\\H, 0, 8.921503, -2.834407, 1.480302\\H, 0, 7.827728, 0.164682, -1.432848\\H, 0, 9.947028, -0.248293, -2.650379\\Version=AM64L-G09RevA.02\\State=1-A\\HF=-1532.968337\\RMSD=5.454e-09\\Dipole=0.0877852, 3.3040126, -0.5818911\\Quadrupole=44.2666501, -22.341985, -21.9246652, -13.6058557, -51.8155631, 1.57133\\PG=C01 [X(C32H22O4)]\\@

Conformation: **4\_9**

b3lyp/6-31+g scrf=(cpcm, solvent=benzene) guess=read geom=connectivity\\Title Card Required\\0, 1\\C, 0, -3.077727, -3.419416, 0.047985\\C, 0, -2.905883, -2.327458, -0.839415\\C, 0, -3.426285, -1.05726, -0.520955\\C, 0, -4.128408, -0.863518, 0.684617\\C, 0, -4.312134, -1.944215, 1.568415\\C, 0, -3.789481, -3.211822, 1.246185\\O, 0, -2.611603, -4.697907, -0.177576\\C, 0, -4.674901, 0.452141, 1.032784\\C, 0, -4.877829, 1.718803, 0.771972\\C, 0, -5.321306, 1.193668, 1.853443\\O, 0, -5.927569, 1.315872, 2.912498\\C, 0, -4.468958, 5.179569, -1.722936\\C, 0, -3.912078, 3.951368, -2.13317\\C, 0, -4.042786, 2.809322, -1.31847\\C, 0, -4.731718, 2.895772, -0.090688\\C, 0, -5.288034, 4.124781, 0.319377\\C, 0, -5.156023, 5.265631, -0.496692\\C, 0, -1.706517, -4.947648, -1.250844\\C, 0, -0.259579, -4.579003, -0.879628\\O, 0, -0.026086, -3.196781, -1.118436\\C, 0, 3.640144, -1.405026, -0.085181\\C, 0, 2.560234, -0.641159, -0.567182\\C, 0, 1.347425, -1.272477, -0.903482\\C, 0, 1.194773, -2.667455, -0.763598\\C, 0, 2.287295, -3.42983, -0.279671\\C, 0, 3.50215, -2.801068, 0.057155\\C, 0, 4.912646, -0.769167, 0.27105\\C, 0, 5.675554, 0.287504, 0.392535\\C, 0, 6.114271, -0.876115, 0.702891\\O, 0, 7.027049, -1.581958, 1.117008\\C, 0, 6.380118, 4.502033, 0.062494\\C, 0, 7.396702, 3.647401, 0.532107\\C, 0, 7.160322, 2.26179, 0.638245\\C, 0,

5.904966, 1.731292, 0.274999\C, 0, 4.88712, 2.588021, -0.194722\C, 0, 5.125851, 3.97225, -0.29961\H, 0, -  
2.372143, -2.431856, -1.771221\H, 0, -3.27835, -0.239762, -1.20836\H, 0, -4.851339, -1.806178, 2.494876\H, 0, -  
3.933117, -4.036986, 1.929034\H, 0, -4.367185, 6.054516, -2.348845\H, 0, -3.384944, 3.885408, -3.074867\H, 0, -  
3.613102, 1.875767, -1.643864\H, 0, -5.816563, 4.196549, 1.260519\H, 0, -5.582951, 6.207458, -0.181738\H, 0,  
2.649288, 0.427293, -0.681896\H, 0, 0.520417, -0.682378, -1.270854\H, 0, 2.221951, -4.49989, -0.158535\H, 0,  
4.327465, -3.393592, 0.425033\H, 0, -1.742499, -6.024294, -1.412919\H, 0, -2.020711, -4.508696, -2.197644\H, 0,  
-0.06589, -4.842332, 0.161487\H, 0, 0.4215, -5.1578, -1.504142\H, 0, 6.562377, 5.564452, -0.018216\H, 0,  
8.358726, 4.053138, 0.810056\H, 0, 7.943738, 1.610232, 0.998096\H, 0, 3.923128, 2.194342, -0.474843\H, 0,  
4.346346, 4.628564, -0.659162\\Version=AM64L-G09RevA.02\State=1-A\HF=-1532.9668191\RMSD=3.990e-  
09\Dipole=-0.0607072, 0.5792754, -3.7437801\Quadrupole=-53.9849714, 51.9864743, 1.9984971, 24.4368717,  
16.5785976, -1.6286696\PG=C01 [X(C32H22O4)]\\@

Conformation: **5\_1**

# b3lyp/6-31+g scrf=(cpcm, solvent=benzene) guess=read geom=connectivity\\Title Card Required\\0, 1\C, 0,  
2.852913, 2.325326, -0.106786\C, 0, 3.210344, 2.106796, -1.460812\C, 0, 4.262481, 1.228492, -7.87516\C, 0,  
4.968144, 0.558652, -0.767583\C, 0, 4.619622, 0.771492, 0.580339\C, 0, 3.568153, 1.649931, 0.9029 76\O, 0,  
1.840522, 3.164836, 0.304091\C, 0, 6.058864, -0.352869, -1.127421\C, 0, 7.010989, -1.191698, -0.805001\C, 0,  
6.776022, -0.909533, -2.032797\O, 0, 7.044506, -1.061649, -3.219447\C, 0, 9.319149, -3.36404, 2.079107\C, 0,  
9.588424, -3.504422, 0.703619\C, 0, 8.826724, -2.787233, -0.240078\C, 0, 7.794358, -1.929405, 0.191739\C, 0,  
7.525063, -1.789305, 1.568935\C, 0, 8.287391, -2.506924, 2.511984\O, 0, -1.838235, 3.163469, -0.304686\C, 0, -  
4.967917, 0.558193, 0.767778\C, 0, -4.617132, 0.768904, -0.58084\C, 0, -3.565198, 1.64728, -0.90361\C, 0, -  
2.851238, 2.323743, 0.105701\C, 0, -3.210862, 2.107366, 1.460301\C, 0, -4.262836, 1.228424, 1.786489\C, 0, -  
6.05887, -0.352438, 1.128061\C, 0, -7.011925, -1.190643, 0.804926\C, 0, -6.777402, -0.907429, 2.032639\O, 0, -  
7.047626, -1.058488, 3.219429\C, 0, -9.320529, -3.363409, -2.078389\C, 0, -9.590611, -3.501541, -0.702767\C, 0, -  
8.828842, -2.785254, 0.241712\C, 0, -7.794508, -1.928861, -0.191417\C, 0, -7.524405, -1.790447, -1.568748\C, 0, -  
8.287894, -2.508533, -2.510619\C, 0, 1.08168, 3.84383, -0.688616\C, 0, 0.000456, 4.68758, -0.000441\C, 0, -  
1.080105, 3.843286, 0.688143\H, 0, 2.694861, 2.600466, -2.269472\H, 0, 4.524764, 1.070395, -2.823651\H, 0,  
5.150045, 0.266913, 1.372153\H, 0, 3.303398, 1.810312, 1.93829\H, 0, 9.904087, -3.913435, 2.803865\H, 0,  
10.379885, -4.161148, 0.372481\H, 0, 9.037582, -2.898417, -1.29539\H, 0, 6.738107, -1.136641, 1.911744\H, 0,  
8.081497, -2.400023, 3.56723\H, 0, -5.146772, 0.26353, -1.372397\H, 0, -3.300039, 1.806265, -1.938741\H, 0, -  
2.695106, 2.601995, 2.268645\H, 0, -4.526026, 1.072163, 2.823264\H, 0, -9.904623, -3.91379, -2.801952\H, 0, -  
10.38303, -4.157943, -0.371233\H, 0, -9.04068, -2.89463, 1.295628\H, 0, -6.735979, -1.138964, -1.911678\H, 0, -  
8.080333, -2.402685, -3.566339\H, 0, 1.734674, 4.498363, -1.267898\H, 0, 0.617993, 3.13505, -1.377283\H, 0,  
0.473634, 5.341792, 0.731979\H, 0, -0.473435, 5.341287, -0.732968\H, 0, -616431, 3.134524, 1.376324\H, 0, -  
1.734419, 4.497385, 1.266258\\Version=AM64L-G09RevA.02\State=1-A\HF=-1572.2809246\RMSD=8.597e-  
09\Dipole=0.0015066, 1.3728329, -0.003026\Quadrupole=-12.0527549, 24.5701551, -12.5174002, 0.0488122,  
74.1574007, -0.0027154\PG=C01 [X(C33H24O4)]\\@

Conformation: **5\_2**

# b3lyp/6-31+g scrf=(cpcm, solvent=benzene) guess=read geom=connectivity\\Title Card Required\\0, 1\C, 0,  
2.855672, 2.302887, 0.108525\C, 0, 3.213247, 2.083945, 1.462722\C, 0, 4.270181, 1.211777, 1.790026\C, 0,  
4.9823, 0.54959, 0.769906\C, 0, 4.633548, 0.761223, -0.578398\C, 0, 3.576974, 1.6338, -0.902\O, 0, 1.839342,

3.136975, -0.30253\C, 0, 6.07943, -0.35428, 1.130575\C, 0, 7.040397, -1.183568, 0.806835\C, 0, 6.799899, -  
0.907042, 2.034996\O, 0, 7.066926, -1.06007, 3.222681\C, 0, 9.375593, -3.326174, -2.077038\C, 0, 9.642681, -  
3.46763, -0.701\C, 0, 8.871691, -2.761427, 0.242446\C, 0, 7.832602, -1.911151, -0.189798\C, 0, 7.565563, -  
1.770268, -1.567128\C, 0, 8.337725, -2.477619, -2.51002\O, 0, -1.839554, 3.136825, 0.301392\C, 0, -4.982163,  
0.549263, -0.770175\C, 0, -4.634934, 0.761732, 0.578136\C, 0, -3.57774, 1.634029, 0.901429\C, 0, -2.856254,  
2.303198, -0.108722\C, 0, -3.212741, 2.083425, -1.463429\C, 0, -4.269628, 1.210879, -1.789696\C, 0, -6.079937, -  
0.355183, -1.130274\C, 0, -7.039484, -1.184393, -0.806515\C, 0, -6.799373, -0.907979, -2.035243\O, 0, -7.066162,  
-1.062122, -3.221416\C, 0, -9.376022, -3.325263, 2.07846\C, 0, -9.642857, -3.468525, 0.70172\C, 0, -8.871546, -  
2.761355, -0.242915\C, 0, -7.832019, -1.911174, 0.189354\C, 0, -7.565442, -1.768236, 1.567776\C, 0, -8.338086, -  
2.475727, 2.510955\C, 0, 1.079155, 3.814906, 0.689455\C, 0, 0.000095, 4.659646, -0.000328\C, 0, -1.078834,  
3.814866, -0.69032\H, 0, 2.692094, 2.573018, 2.271896\H, 0, 4.531948, 1.05409, 2.825567\H, 0, 5.168885,  
0.261637, -1.37077\H, 0, 3.312604, 1.793461, -1.936966\H, 0, 9.967403, -3.868135, -2.800519\H, 0, 10.438918, -  
4.119525, -0.368925\H, 0, 9.080102, -2.873586, 1.29759\H, 0, 6.773404, -1.122975, -1.910167\H, 0, 8.133594, -  
2.369891, -3.565361\H, 0, -5.169241, 0.262723, 1.369754\H, 0, -3.313592, 1.794359, 1.936167\H, 0, -2.691239,  
2.572199, -2.272662\H, 0, -4.531716, 1.052415, -2.826732\H, 0, -9.967967, -3.867215, 2.801815\H, 0, -10.438628,  
-4.118881, 0.370361\H, 0, -9.079852, -2.873898, -1.296736\H, 0, -6.773947, -1.12185, 1.910795\H, 0, -8.13426, -  
2.367323, 3.565669\H, 0, 0.614428, 3.106102, 1.377016\H, 0, 1.731228, 4.469792, 1.269571\H, 0, -0.474526,  
5.31376, 0.731244\H, 0, 0.474536, 5.31325, -0.732708\H, 0, -1.731593, 4.469009, -1.27107\H, 0, -0.61517,  
3.105564, -1.377718\\Version=AM64L-G09RevA.02\State=1-A\HF=-1572.2807547\RMSE=3.098e-09\Dipole=-  
0.0037504, 1.3831115, -0.0058715\Quadrupole=-11.528307, 24.0960083, -12.5677013, 0.0077448, -74.5093829,  
0.0100706\PG=C01 [X(C33H24O4)]\\@

Conformation: 5\_3

# b3lyp/6-31+g scrf=(cpcm, solvent=benzene) geom=connectivity\\Title Card Required\\0, 1\C, 0, -3.247318, -  
1.728833, -0.326537\C, 0, -4.063714, -2.50526, 0.534287\C, 0, -5.381777, -2.10104, 0.822126\C, 0, -5.900644, -  
0.920365, 0.255714\C, 0, -5.096275, -0.142951, -0.601592\C, 0, -3.778699, -0.550267, -0.887954\O, 0, -1.94921, -  
2.046416, -0.662841\C, 0, -7.27521, -0.515301, 0.567316\C, 0, -8.287077, 0.305224, 0.448618\C, 0, -8.376971, -  
0.740542, 1.183662\O, 0, -9.039113, -1.448401, 1.934352\C, 0, -10.12335, 3.842219, -1.128587\C, 0, -10.842559,  
2.996063, -0.261314\C, 0, -10.233986, 1.83406, 0.254639\C, 0, -8.905448, 1.518448, -0.097292\C, 0, -8.185996,  
2.366153, -0.965302\C, 0, -8.79621, 3.526825, -1.480524\O, 0, 2.301624, -2.47618, -0.583738\C, 0, 5.453534,  
0.164566, 0.318669\C, 0, 5.665063, -0.990598, -0.459041\C, 0, 4.586915, -1.852485, -0.742605\C, 0, 3.292339, -  
1.577116, -0.25648\C, 0, 3.089489, -0.412029, 0.525944\C, 0, 4.165106, 0.452012, 0.810482\C, 0, 6.560105,  
1.076455, 0.627091\C, 0, 7.818676, 1.427269, 0.543038\C, 0, 6.982109, 2.144499, 1.196881\O, 0, 6.749982,  
3.136971, 1.878503\C, 0, 11.834988, 0.807569, -0.817916\C, 0, 10.829922, -0.119733, -1.159019\C, 0, 9.507639,  
0.077523, -0.715842\C, 0, 9.189306, 1.20419, 0.071141\C, 0, 10.195901, 2.132135, 0.412743\C, 0, 11.517789,  
1.932299, -0.031913\C, 0, -1.374029, -3.219461, -0.102468\C, 0, 0.069456, -3.356782, -0.603481\C, 0, 0.985131, -  
2.231574, -0.107058\H, 0, -3.703552, -3.416488, 0.987379\H, 0, -5.993274, -2.702033, 1.480335\H, 0, -5.478029,  
0.763172, -1.044065\H, 0, -3.166049, 0.048961, -1.54542\H, 0, -10.590793, 4.732396, -1.524401\H, 0, -11.860261,  
3.237489, 0.009221\H, 0, -10.789459, 1.188587, 0.92072\H, 0, -7.169401, 2.135825, -1.242736\H, 0, -8.245819,  
4.176435, -2.14638\H, 0, 6.644252, -1.225087, -0.842986\H, 0, 4.753204, -2.736818, -1.339702\H, 0, 2.11699, -  
0.15727, 0.919393\H, 0, 3.996022, 1.33678, 1.407566\H, 0, 12.848868, 0.654687, -1.15876\H, 0, 11.074738, -  
0.982449, -1.762062\H, 0, 8.746904, -0.638713, -0.983299\H, 0, 9.95705, 2.99639, 1.015565\H, 0, 12.287741,  
2.643229, 0.230168\H, 0, -1.384271, -3.172709, 0.987347\H, 0, -1.946928, -4.095601, -0.408877\H, 0, 0.472393, -  
4.313701, -0.268744\H, 0, 0.077643, -3.384539, -1.69343\H, 0, 0.621563, -1.270891, -0.47511\H, 0, 0.978983, -  
2.204486, 0.983514\\Version=AM64L-9RevA.02\State=1-A\HF=-1572.2796703\RMSE=5.773e-

09\Dipole=1.4775927, -1.1028435, -2.6177251\Quadrupole=-0.6857722, 6.4570505, -5.7712783, -54.2631495, 5.4646605, -8.9672198\PG=C01 [X(C33H24O4)]\ \@

Conformation: 5\_4

```
# b3lyp/6-31+g scrf=(cpcm, solvent=benzene) geom=connectivity\Title Card Required\0, 1\C, 0, 3.247753, -1.723956, -0.324687\C, 0, 3.781044, -0.544891, -0.885\C, 0, 5.099124, -0.140689, -0.599843\C, 0, 5.902631, -0.919346, 0.256078\C, 0, 5.382571, -2.100326, 0.822331\C, 0, 4.063682, -2.502323, 0.535307\O, 0, 1.948919, -2.038836, -0.659444\C, 0, 7.278314, -0.517379, 0.567768\C, 0, 8.291834, 0.302047, 0.448306\C, 0, 8.379831, -0.744237, 1.181541\O, 0, 9.042279, -1.454148, 1.932234\C, 0, 10.132116, 3.837209, -1.128029\C, 0, 10.850664, 2.988448, -0.261361\C, 0, 10.240278, 1.827776, 0.253872\C, 0, 8.910736, 1.514675, -0.097096\C, 0, 8.192796, 2.364624, -0.964231\C, 0, 8.803966, 3.5243, -1.478838\O, 0, -2.301947, -2.47049, -0.586208\C, 0, -5.45709, 0.167034, 0.318321\C, 0, -5.666311, -0.988616, -0.460179\C, 0, -4.588039, -1.849266, -0.744165\C, 0, -3.293451, -1.57229, -0.25847\C, 0, -3.091726, -0.407121, 0.523799\C, 0, -4.168278, 0.455656, 0.809018\C, 0, -6.564264, 1.076927, 0.625819\C, 0, -7.823464, 1.425907, 0.542505\C, 0, -6.987047, 2.144427, 1.196078\O, 0, -6.757204, 3.137906, 1.877556\C, 0, -11.839441, 0.800107, -0.81711\C, 0, -11.523574, 1.926131, -0.03082\C, 0, -10.202116, 2.126662, 0.41298\C, 0, -9.19435, 1.200364, 0.071277\C, 0, -9.510825, 0.073152, -0.714547\C, 0, -10.833979, -0.125617, -1.158211\C, 0, 1.372831, -3.212935, -0.101533\C, 0, -0.069819, -3.350796, -0.603676\C, 0, -0.985562, -2.225906, -0.107484\H, 0, 3.168244, 0.055176, -1.542122\H, 0, 5.481819, 0.765678, -1.041576\H, 0, 5.994282, -2.702539, 1.478996\H, 0, 3.702642, -3.413076, 0.987664\H, 0, 10.600736, 4.727293, -1.522798\H, 0, 11.869253, 3.22888, 0.007113\H, 0, 10.795511, 1.180845, 0.918052\H, 0, 7.175608, 2.135753, -1.240011\H, 0, 8.253973, 4.175161, -2.143321\H, 0, -6.645717, -1.223805, -0.844369\H, 0, -4.752767, -2.733806, -1.341796\H, 0, -2.119871, -0.150975, 0.917253\H, 0, -4.000766, 1.340581, 1.406969\H, 0, -12.853717, 0.646034, -1.157927\H, 0, -12.294767, 2.636257, 0.231278\H, 0, -9.964906, 2.992046, 1.015551\H, 0, -8.749775, -0.641727, -0.982689\H, 0, -11.077213, -0.988838, -1.760978\H, 0, 1.945857, -4.089263, -0.408803\H, 0, 1.382506, -3.167186, 0.988764\H, 0, -0.077189, -3.376729, -1.694066\H, 0, -0.472594, -4.307218, -0.27072\H, 0, -0.980648, -2.198423, 0.983657\H, 0, -0.621878, -1.264094, -0.475538\Version=AM64L-G09RevA.02\State=1-A\HF=-1572.2796697\RMSE=6.878e-09\Dipole=-1.4787389, -1.0994003, -2.6220335\Quadrupole=-0.8076275, 6.502455, -5.6948275, 54.5166276, -5.5404227, -8.9276199\PG=C01 [X(C33H24O4)]\ \@
```

Conformation: 5\_5

```
# b3lyp/6-31+g scrf=(cpcm, solvent=benzene) geom=connectivity\Title Card Required\0, 1\C, 0, -3.515825, -0.783189, 0.014812\C, 0, -3.572872, 0.633255, 0.022453\C, 0, -4.815356, 1.297795, 0.0195\C, 0, -6.013709, 0.556964, 0.009635\C, 0, -5.967252, -0.850763, 0.002915\C, 0, -4.722774, -1.511288, 0.004919\O, 0, -2.348831, -1.515198, 0.016249\C, 0, -7.296617, 1.266469, 0.006592\C, 0, -8.606142, 1.275291, 0.00004\C, 0, -7.944321, 2.373308, 0.008933\O, 0, -7.935165, 3.599919, 0.015365\C, 0, -12.402256, -0.712388, -0.02975\C, 0, -12.338327, 0.695256, -0.023229\C, 0, -11.088162, 1.343359, -0.013337\C, 0, -9.898927, 0.5838, -0.010062\C, 0, -9.963862, -0.824837, -0.01658\C, 0, -11.216019, -1.471929, -0.026379\O, 0, 2.399787, -2.204188, 0.011063\C, 0, 6.502187, -1.260526, -0.001146\C, 0, 6.056306, -2.596331, -0.002731\C, 0, 4.676382, -2.876462, 0.001721\C, 0, 3.726595, -1.835033, 0.008188\C, 0, 4.183859, -0.492641, 0.009931\C, 0, 5.56412, -0.208827, 0.004906\C, 0, 7.942748, -0.983439, -0.006958\C, 0, 8.953822, -0.152619, -0.008878\C, 0, 9.148301, -1.419393, -0.012299\O, 0, 9.926284, -2.366326, -0.016904\C, 0, 10.597578, 3.805426, -0.00699\C, 0, 11.449205, 2.683268, -0.012291\C, 0, 10.903838, 1.383811, -0.013323\C, 0, 9.504534, 1.20684, -0.008303\C, 0, 8.651921, 2.331003, -0.002912\C, 0, 9.200249,
```

3.629472, -0.003005\C, 0, -1.112273, -0.814093, 0.018417\C, 0, 0.028482, -1.838576, 0.014998\C, 0, 1.41311, -1.180762, 0.014526\H, 0, -2.67723, 1.235822, 0.030378\H, 0, -4.844432, 2.377947, 0.025636\H, 0, -6.874466, -1.432555, -0.005713\H, 0, -4.691667, -2.591481, -0.000283\H, 0, -13.362311, -1.210471, -0.037629\H, 0, -13.249088, 1.27746, -0.02514\H, 0, -11.043897, 2.423704, -0.008208\H, 0, -9.062474, -1.416668, -0.013977\H, 0, -11.265964, -2.551555, -0.031973\H, 0, 6.768012, -3.409722, -0.008402\H, 0, 4.339716, -3.903207, -0.000191\H, 0, 3.49658, 0.339284, 0.014683\H, 0, 5.891791, 0.817971, 0.007108\H, 0, 11.017027, 4.801663, -0.007598\H, 0, 12.521817, 2.818737, -0.015383\H, 0, 11.561303, 0.52673, -0.017507\H, 0, 7.580715, 2.209206, -0.000141\H, 0, 8.546808, 4.490527, 0.001164\H, 0, -1.038151, -0.175963, -0.863862\H, 0, -1.037608, -0.182857, 0.906219\H, 0, -0.064059, -2.487279, 0.886554\H, 0, -0.066181, -2.481715, -0.859825\H, 0, 1.521515, -0.549176, -0.868704\H, 0, 1.524386, -0.553399, 0.900711\\Version=AM64L-G09RevA.02\State=1-A\HF=-1552.7691121\RMSD=5.722e-09\Dipole=-0.8683594, 0.024727, 0.0009983\Quadrupole=-16.5167031, 5.7314356, 10.7852675, 48.4864769, 0.283795, -0.0412035\PG=C01 [X(C33H24O4)]\ \@

Conformation: 5\_6

# b3lyp/6-31+g scrf=(cpcm, solvent=benzene) guess=read geom=connectivity\\Title Card Required\\0, 1\C, 0, 2.862982, -1.586563, -0.81955\C, 0, 3.681117, -2.542203, -0.165513\C, 0, 5.016427, -2.233868, 0.16151\C, 0, 5.550839, -0.97162, -0.160508\C, 0, 4.74654, -0.017135, -0.813439\C, 0, 3.412898, -0.32861, -1.139295\O, 0, 1.547584, -1.793252, -1.180948\C, 0, 6.943011, -0.66963, 0.188137\C, 0, 7.972768, 0.138697, 0.213797\C, 0, 8.052875, -1.040334, 0.710807\O, 0, 8.714739, -1.903029, 1.279542\C, 0, 9.861069, 3.888017, -0.645135\C, 0, 10.578366, 2.865208, 0.004904\C, 0, 9.953026, 1.634173, 0.2855\C, 0, 8.607922, 1.425913, -0.085647\C, 0, 7.890148, 2.450606, -0.736793\C, 0, 8.517783, 3.680727, -1.015416\O, 0, -1.813422, -2.247617, 0.338859\C, 0, -5.198205, 0.236269, 0.650263\C, 0, -5.229598, -0.955181, -0.1007\C, 0, -4.078968, -1.762746, -0.182742\C, 0, -2.887803, -1.396912, 0.476821\C, 0, -2.865441, -0.196316, 1.23188\C, 0, -4.015162, 0.613806, 1.316075\C, 0, -6.383946, 1.09341, 0.750484\C, 0, -7.631465, 1.368008, 0.466012\C, 0, -6.941253, 2.153565, 1.20731\O, 0, -6.866945, 3.181004, 1.872994\C, 0, -11.358356, 0.474299, -1.451233\C, 0, -10.267772, -0.404538, -1.599779\C, 0, -9.039041, -0.116854, -0.971941\C, 0, -8.901631, 1.052202, -0.19454\C, 0, -9.994402, 1.931336, -0.046353\C, 0, -11.222765, 1.642385, -0.674699\C, 0, 0.888117, -2.999589, -0.805667\C, 0, 0.457967, -2.978693, 0.673864\C, 0, -0.591787, -1.903869, 0.981136\H, 0, 3.311334, -3.520468, 0.099017\H, 0, 5.627848, -2.971709, 0.661775\H, 0, 5.1409, 0.953797, -1.069415\H, 0, 2.799313, 0.406366, -1.639889\H, 0, 10.340769, 4.832748, -0.860497\H, 0, 11.608635, 3.023904, 0.289126\H, 0, 10.508011, 0.852269, 0.783887\H, 0, 6.861132, 2.303267, -1.024814\H, 0, 7.967864, 4.465826, -1.514162\H, 0, -6.126456, -1.258712, -0.615705\H, 0, -4.106449, -2.675472, -0.760123\H, 0, -1.979025, 0.127139, 1.75457\H, 0, -3.984672, 1.526246, 1.894383\H, 0, -12.300987, 0.25393, -1.933288\H, 0, -10.372622, -1.299966, -2.195702\H, 0, -8.210743, -0.796478, -1.093106\H, 0, -9.895118, 2.828615, 0.548793\H, 0, -12.059355, 2.316188, -0.560771\H, 0, 0.002068, -3.097614, -1.433685\H, 0, 1.495893, -3.874414, -1.034799\H, 0, 0.054688, -3.954907, 0.946381\H, 0, 1.32605, -2.821555, 1.312644\H, 0, -0.746973, -1.850692, 2.060105\H, 0, -0.2353, -0.928919, 0.64441\\Version=AM64L-G09RevA.02\State=1-A\HF=-1572.2781347\RMSD=6.773e-09\Dipole=-1.2813271, -0.8155234, -2.105598\Quadrupole=-5.8628646, 6.1226507, -0.2597861, 62.1065086, 7.7064372, -6.7756692\PG=C01 [X(C33H24O4)]\ \@

Conformation: 5\_7

# b3lyp/6-31+g scrf=(cpcm, solvent=benzene) guess=read geom=connectivity\\Title Card Required\\0, 1\C, 0, 2.784419, -1.662952, -0.284591\C, 0, 3.19078, -0.3586, 0.064824\C, 0, 4.55014, 0.008411, 0.033894\C, 0,

5.522795, -0.933742, -0.349532\C, 0, 5.131379, -2.240911, -0.701124\C, 0, 3.770873, -2.606014, -0.670419\O, 0, 1.434272, -1.931327, -0.224336\C, 0, 6.943972, -0.574261, -0.390105\C, 0, 7.916404, 0.287797, -0.23212\C, 0, 8.159514, -0.910198, -0.617272\O, 0, 8.971456, -1.764437, -0.95722\C, 0, 9.393954, 4.180506, 0.781161\C, 0, 8.010927, 3.918823, 0.847754\C, 0, 7.518056, 2.641582, 0.51525\C, 0, 8.410122, 1.624127, 0.11702\C, 0, 9.794489, 1.886791, 0.051925\C, 0, 10.28564, 3.164969, 0.383351\O, 0, -2.416801, -3.22885, 1.148847\C, 0, -4.962096, -0.010577, 0.192717\C, 0, -3.569558, 0.181858, 0.112884\C, 0, -2.689503, -0.873522, 0.425308\C, 0, -3.195433, -2.137456, 0.820922\C, 0, -4.592187, -2.314428, 0.89774\C, 0, -5.474473, -1.261825, 0.58646\C, 0, -5.861511, 1.099891, -0.136457\C, 0, -7.060897, 1.606519, -0.274571\C, 0, -6.019967, 2.316739, -0.509119\O, 0, -5.527804, 3.387909, -0.846308\C, 0, -11.333267, 1.308386, -0.119761\C, 0, -10.719947, 2.517761, -0.502276\C, 0, -9.314376, 2.611068, -0.550888\C, 0, -8.521556, 1.492123, -0.217616\C, 0, -9.136831, 0.281485, 0.164137\C, 0, -10.541592, 0.191349, 0.213287\C, 0, 0.990424, -3.241547, -0.557068\C, 0, -0.534124, -3.299778, -0.409622\C, 0, -0.9992, -3.137184, 1.047144\H, 0, 2.447239, 0.367846, 0.359823\H, 0, 4.832534, 1.013192, 0.305788\H, 0, 5.87377, -2.969297, -0.997831\H, 0, 3.512316, -3.615413, -0.94726\H, 0, 9.77095, 5.160898, 1.035803\H, 0, 7.327633, 4.698857, 1.152582\H, 0, 6.457779, 2.452765, 0.569885\H, 0, 10.481969, 1.110798, -0.253285\H, 0, 11.34574, 3.366286, 0.333375\H, 0, -3.168286, 1.13969, -0.188958\H, 0, -1.629331, -0.684167, 0.349046\H, 0, -4.989744, -3.27262, 1.199832\H, 0, -6.537755, -1.425813, 0.653566\H, 0, -4.11093, 1.237599, -0.081982\H, 0, -11.326529, 3.375004, -0.757341\H, 0, -8.848569, 3.540396, -0.845061\H, 0, -8.540951, -0.57934, 0.421106\H, 0, -11.013026, -0.735723, 0.506341\H, 0, 1.262563, -3.474082, -1.587754\H, 0, 1.456924, -3.984483, 0.092347\H, 0, -0.983909, -2.539572, -1.046572\H, 0, -0.891918, -4.258937, -0.786826\H, 0, -0.582959, -3.95021, 1.642527\H, 0, -0.618561, -2.223148, 1.50357\Version=AM64L-G09RevA.02\State=1-A\HF=-1572.2778594\RMSD=6.897e-09\Dipole=-2.2151639, -1.0433257, 1.1661326\Quadrupole=-0.8479164, 4.4741346, -3.6262181, 52.2414892, 8.1642371, 5.8555107\PG=C01 [X(C33H24O4)]\@\@

Conformation: 5\_8

# b3lyp/6-31+g scrf=(cpcm, solvent=benzene) geom=connectivity\Title Card Required\0, 1\C, 0, -2.77363, -1.680873, -0.29198\C, 0, -3.170981, -0.372809, 0.056087\C, 0, -4.528163, 0.002402, 0.029014\C, 0, -5.507523, -0.934998, -0.350911\C, 0, -5.125296, -2.24581, -0.701935\C, 0, -3.76689, -2.618316, -0.672817\O, 0, -1.4256, -1.956258, -0.235497\C, 0, -6.926708, -0.566911, -0.386693\C, 0, -7.894136, 0.300524, -0.227859\C, 0, -8.145861, -0.896812, -0.609588\O, 0, -8.963211, -1.747032, -0.945117\C, 0, -9.345319, 4.203769, 0.785016\C, 0, -10.245014, 3.192395, 0.394129\C, 0, -9.761523, 1.910469, 0.062112\C, 0, -8.379229, 1.639985, 0.121426\C, 0, -7.479203, 2.653546, 0.512645\C, 0, -7.963976, 3.934316, 0.844514\O, 0, 2.415623, -3.251504, 1.147784\C, 0, 4.942737, -0.019002, 0.18944\C, 0, 3.547976, 0.162371, 0.102906\C, 0, 2.674775, -0.896669, 0.41688\C, 0, 3.188057, -2.15673, 0.819485\C, 0, 4.585524, -2.323336, 0.902469\C, 0, 5.461519, -1.26584, 0.58984\C, 0, 5.835356, 1.096832, -0.141364\C, 0, 7.031525, 1.611104, -0.277686\C, 0, 5.985699, 2.312389, -0.518113\O, 0, 5.487722, 3.37896, -0.860719\C, 0, 11.304702, 1.343558, -0.108566\C, 0, 10.683701, 2.547227, -0.496285\C, 0, 9.27882, 2.629999, -0.549994\C, 0, 8.492824, 1.507052, -0.215426\C, 0, 9.114776, 0.302352, 0.17211\C, 0, 10.520433, 0.221439, 0.22485\C, 0, -0.990321, -3.271308, -0.560355\C, 0, 0.533817, -3.337674, -0.411493\C, 0, 0.996919, -3.167084, 1.045896\H, 0, -2.422412, 0.349122, 0.34725\H, 0, -4.803277, 1.00919, 0.299516\H, 0, -5.87241, -2.970063, -0.994321\H, 0, -3.514431, -3.630296, -0.949781\H, 0, -9.716123, 5.187138, 1.040122\H, 0, -11.305017, 3.398732, 0.348473\H, 0, -10.455417, 1.137629, -0.237471\H, 0, -6.419835, 2.459565, 0.561895\H, 0, -7.275224, 4.711088, 1.14442\H, 0, 3.142384, 1.116613, -0.203628\H, 0, 1.613845, -0.715789, 0.335043\H, 0, 4.987991, -3.277635, 1.209483\H, 0, 6.526304, -1.422076, 0.662198\H, 0, 12.383523, 1.280459, -0.067086\H, 0, 11.285328, 3.407543, -0.752019\H, 0, 8.806868, 3.555523, -0.848245\H, 0, 8.524657, -0.563121, 0.429243\H, 0, 10.997627, -0.701976, 0.522064\H, 0, -1.461064, -4.007157, 0.093908\H, 0, -1.263946, -3.50828, -1.589602\H, 0, 0.886861, -4.29945, -0.781834\H, 0, 0.988459, -2.582331, -1.051587\H, 0, 0.612433, -253031, 1.499657\H, 0, 0.584271, -

3.980057, 1.644178\\Version=AM64L-G09RevA.02\State=1-A\HF=-1572.2778559\RMSD=6.838e-09\Dipole=2.2369988, -1.0573096, 1.1734335\Quadrupole=-1.1995022, 4.8947023, -3.6952002, -51.4900614, -7.8666204, 5.9610499\PG=C01 [X(C33H24O4)]\\@

Conformation: 5\_9

# b3lyp/6-31+g scrf=(cpcm, solvent=benzene) guess=read geom=connectivity\\Title Card Required\\0, 1\C, 0, 2.88829, -1.391718, 0.477587\C, 0, 2.867246, -0.192088, 1.232338\C, 0, 4.017998, 0.616891, 1.317135\C, 0, 5.20077, 0.237723, 0.651266\C, 0, 5.230319, -0.952151, -0.101616\C, 0, 4.078048, -1.758618, -0.183518\O, 0, 1.812892, -2.242715, 0.339261\C, 0, 6.387356, 1.093056, 0.751597\C, 0, 7.635412, 1.367081, 0.466053\C, 0, 6.947352, 2.152656, 1.207706\O, 0, 6.874796, 3.178728, 1.875345\C, 0, 11.360677, 0.468817, -1.454972\C, 0, 11.226353, 1.636069, -0.675948\C, 0, 9.999289, 1.926255, -0.046596\C, 0, 8.905471, 1.048401, -0.195804\C, 0, 9.039613, -0.119833, -0.974762\C, 0, 10.267445, -0.408071, -1.60333\O, 0, -1.547296, -1.78708, -1.178479\C, 0, -5.552853, -0.970989, -0.160357\C, 0, -4.748821, -0.014923, -0.812285\C, 0, -3.413828, -0.324305, -1.136492\C, 0, -2.862744, -1.581841, -0.817514\C, 0, -3.680282, -2.539444, -0.165123\C, 0, -5.015912, -2.232841, 0.161508\C, 0, -6.944988, -0.670804, 0.187792\C, 0, -7.97616, 0.135062, 0.212104\C, 0, -8.0549, -1.04354, 0.709284\O, 0, -8.716419, -1.907404, 1.275813\C, 0, -9.868037, 3.884201, -0.645518\C, 0, -10.58534, 2.85887, 0.004274\C, 0, -9.957989, 1.628352, 0.283511\C, 0, -8.612216, 1.421977, -0.086462\C, 0, -7.895627, 2.448482, -0.73592\C, 0, -8.524058, 3.678212, -1.014694\C, 0, 0.593158, -1.897848, 0.983723\C, 0, -0.456707, -2.973813, 0.675448\C, 0, -0.886505, -2.992983, -0.803211\H, 0, 1.982411, 0.131535, 1.757319\H, 0, 3.988665, 1.529167, 1.896194\H, 0, 6.126915, -1.255937, -0.617262\H, 0, 4.104288, -2.6703, -0.762298\H, 0, 12.301769, 0.246609, -1.937587\H, 0, 12.064261, 2.308444, -0.561446\H, 0, 9.90154, 2.822802, 0.54925\H, 0, 8.210527, -0.798406, -1.096528\H, 0, 10.371525, -1.302847, -2.200845\H, 0, -5.144105, 0.954888, -1.067791\H, 0, -2.801974, 0.411472, -1.637234\H, 0, -3.310191, -3.517167, 0.100267\H, 0, -5.627327, -2.971918, 0.659818\H, 0, -10.348647, 4.827779, -0.859463\H, 0, -11.615196, 3.017106, 0.287846\H, 0, -10.511756, 0.845953, 0.781975\H, 0, -6.866496, 2.302283, -1.02445\H, 0, -7.975034, 4.464549, -1.513192\H, 0, 0.748518, -1.847047, 2.062494\H, 0, 0.236777, -0.923275, 0.647764\H, 0, -0.054181, -3.948979, 0.94735\H, 0, -1.325721, -2.816817, 1.314355\H, 0, -0.001398, -3.091136, -1.431897\H, 0, -1.493941, -3.868757, -1.033367\\Version=AM64L-G09RevA.02\State=1-A\HF=-1572.277804\RMSD=6.794e-09\Dipole=1.2835617, -0.8124596, -2.1031695\Quadrupole=-5.9118475, 6.1094012, -0.1975537, -62.1983182, -7.8133243, -6.7751906\PG=C01 [X(C33H24O4)]\\@

Conformation: 5\_10

# b3lyp/6-31+g scrf=(cpcm, solvent=benzene) geom=connectivity\\Title Card Required\\0, 1\C, 0, 3.215837, -0.121315, 0.606987\C, 0, 3.575085, 1.24704, 0.69646\C, 0, 4.920574, 1.640368, 0.555823\C, 0, 5.920546, 0.675247, 0.323631\C, 0, 5.571441, -0.685891, 0.234053\C, 0, 4.226281, -1.0769, 0.375405\O, 0, 1.928161, -0.59682, 0.731693\C, 0, 7.315433, 1.105232, 0.17983\C, 0, 8.58328, 0.847317, -0.018003\C, 0, 8.179781, 2.051533, 0.158764\O, 0, 8.436222, 3.247465, 0.245062\C, 0, 11.826178, -1.861617, -0.73037\C, 0, 12.068835, -0.477508, -0.621628\C, 0, 10.998576, 0.408113, -0.387331\C, 0, 9.684811, -0.089871, -0.261622\C, 0, 9.442767, -1.47511, -0.369777\C, 0, 10.514583, -2.360014, -0.60432\O, 0, -2.087113, -1.789463, -0.149892\C, 0, -5.801562, 0.192232, -0.325289\C, 0, -4.625336, 0.937773, -0.539042\C, 0, -3.366489, 0.306433, -0.487928\C, 0, -3.2699, -1.082242, -0.217794\C, 0, -4.455283, -1.816218, -0.007971\C, 0, -5.715166, -1.18842, -0.05971\C, 0, -7.10162, 0.86739, -0.383517\C, 0, -8.408836, 0.85409, -0.307251\C, 0, -7.778173, 1.942573, -0.556101\O, 0, -7.803364, 3.14511, -0.790908\C, 0, -12.142298, -1.159929, 0.300457\C, 0, -10.936195, -1.885147, 0.374061\C, 0, -9.70473, -



1.229495, 0.174755\C, 0, -9.679888, 0.154198, -0.097283\C, 0, -10.887311, 0.879326, -0.171384\C, 0, -12.117548, 0.222072, 0.026961\C, 0, 0.87975, 0.339423, 0.946985\C, 0, -0.453326, -0.41175, 1.041408\C, 0, -0.844921, -1.104312, -0.276446\H, 0, 2.839337, 2.015701, 0.873905\H, 0, 5.182094, 2.687186, 0.625631\H, 0, 6.324548, -1.437506, 0.057665\H, 0, 3.962682, -2.121611, 0.306713\H, 0, 12.647263, -2.54144, -0.909369\H, 0, 13.075111, -0.09643, -0.717647\H, 0, 11.189431, 1.468937, -0.305306\H, 0, 8.443388, -1.867714, -0.275903\H, 0, 10.329392, -3.420915, -0.6873\H, 0, -4.684144, 1.997338, -0.744954\H, 0, -2.492755, 0.915235, -0.657511\H, 0, -4.394066, -2.874912, 0.195404\H, 0, -6.605188, -1.7741, 0.106693\H, 0, -13.085526, -1.664256, 0.452591\H, 0, -10.956249, -2.945516, 0.582469\H, 0, -8.788916, -1.794958, 0.234204\H, 0, -10.874006, 1.940307, -0.380077\H, 0, -13.042044, 0.778023, -0.029811\H, 0, 1.053266, 0.882216, 1.877784\H, 0, 0.838779, 1.067534, 0.134392\H, 0, -0.398886, -1.152091, 1.838541\H, 0, -1.230829, 0.292339, 1.335562\H, 0, -0.843701, -0.416158, -1.121449\H, 0, -0.091282, -1.85526, -0.516742\\Version=AM64L-G09RevA.02\State=1-A\HF=-1572.2774598\RMSD=8.163e-09\Dipole=-0.3279139, -4.3553024, 0.4377774\Quadrupole=17.9655514, -17.7844728, -0.1810786, -6.6092268, -16.2003933, 3.3025338\PG=C01 [X(C33H24O4)]\@\@

Conformation: 5\_11

# b3lyp/6-31+g scrf=(cpcm, solvent=benzene) guess=read geom=connectivity\\Title Card Required\\0, 1\C, 0, 3.200268, 2.57102, -0.670015\C, 0, 3.734324, 1.519049, -1.442227\C, 0, 4.734142, 0.673332, -0.923566\C, 0, 5.215915, 0.876636, 0.384654\C, 0, 4.694517, 1.926718, 1.166363\C, 0, 3.694219, 2.769827, 0.644243\C, 0, 2.225755, 3.341277, -1.269418\C, 0, 6.255704, 0.009927, 0.946842\C, 0, 7.086094, -0.998171, 0.854063\C, 0, 7.021347, -0.299546, 1.926472\C, 0, 7.410653, -0.082679, 3.069917\C, 0, 8.844357, -4.267104, -1.287712\C, 0, 9.257851, -3.976127, 0.027758\C, 0, 8.676911, -2.899513, 0.726897\C, 0, 7.680394, -2.11433, 0.111777\C, 0, 7.266754, -2.405873, -1.204981\C, 0, 7.8492, -3.482952, -1.902534\C, 0, -1.562075, 2.555576, 0.628382\C, 0, -4.937033, 0.349905, -5.87456\C, 0, -4.707992, 0.652954, 0.769048\C, 0, -3.567864, 1.392355, 1.141041\C, 0, -2.646911, 1.839342, 0.171714\C, 0, -2.884758, 1.530526, -1.191363\C, 0, -4.023725, 0.790791, -1.566444\C, 0, -6.115283, -0.419011, -0.998109\C, 0, -7.221274, -1.063384, -0.723245\C, 0, -6.810659, -0.954898, -1.932335\C, 0, -6.9684, -1.191909, -3.124775\C, 0, -10.156642, -2.533753, 2.031887\C, 0, -9.051821, -1.80306, 2.511017\C, 0, -8.082384, -1.316322, 1.611955\C, 0, -8.219562, -1.560943, 0.229599\C, 0, -9.325978, -2.292997, -0.250308\C, 0, -10.29372, -2.778721, 0.651224\C, 0, 1.561612, 4.354222, -0.518262\C, 0, 0.500121, 3.763863, 0.425718\C, 0, -0.610724, 3.017122, -0.322024\H, 0, 3.368119, 1.358627, -2.446139\H, 0, 5.122946, -0.123992, -1.53578\H, 0, 5.060183, 2.089307, 2.170161\H, 0, 3.322794, 3.560999, 1.276609\H, 0, 9.29062, -5.092756, -1.824097\H, 0, 10.021831, -4.577997, 0.499333\H, 0, 8.997886, -2.679959, 1.735569\H, 0, 6.505507, -1.813091, -1.686849\H, 0, 7.532114, -3.707074, -2.911191\H, 0, -5.395826, 0.32323, 1.530364\H, 0, -3.395832, 1.622666, 2.181903\H, 0, -2.209258, 1.848378, -1.970925\H, 0, -4.193, 0.561506, -2.609618\H, 0, -10.899637, -2.906286, 2.722701\H, 0, -8.94743, -1.61583, 3.570608\H, 0, -7.240798, -0.758402, 1.990731\H, 0, -9.434912, -2.484092, -1.309246\H, 0, -11.141153, -3.339397, 0.282852\H, 0, 2.271122, 4.986249, 0.017488\H, 0, 1.072653, 5.017865, -1.231775\H, 0, 0.960041, 3.092167, 1.149904\H, 0, 0.052776, 4.572965, 1.003635\H, 0, -1.088897, 3.685993, -1.039817\H, 0, -0.183705, 2.175488, -0.86942\\Version=AM64L-G09RevA.02\State=1-A\HF=-1572.2770937\RMSD=6.694e-09\Dipole=-0.3092624, 0.7597572, 0.0982804\Quadrupole=-11.5061408, 27.4009339, -15.8947931, -12.6137388, -70.6380774, -2.8604752\PG=C01 [X(C33H24O4)]\@\@

Conformation: 5\_12

```
# b3lyp/6-31+g scrf=(cpcm, solvent=benzene) guess=read geom=connectivity\\Title Card Required\\0, 1\C, 0, -
3.199875, 2.540624, -0.677469\C, 0, -3.689371, 2.749633, 0.636292\C, 0, -4.699195, 1.919485, 1.162868\C, 0, -
5.234388, 0.874398, 0.384221\C, 0, -4.756837, 0.66158, -0.922997\C, 0, -3.746904, 1.49255, -1.445534\O, 0, -
2.21737, 3.298523, -1.280711\C, 0, -6.285153, 0.022639, 0.949719\C, 0, -7.128711, -0.974186, 0.860789\C, 0, -
7.052125, -0.274512, 1.931993\O, 0, -7.436278, -0.050332, 3.075194\C, 0, -8.937477, -4.220731, -1.273244\C, 0, -
7.932619, -3.450223, -1.892526\C, 0, -7.333723, -2.381993, -1.196556\C, 0, -7.740715, -2.08268, 0.119886\C, 0, -
8.746204, -2.854425, 0.739437\C, 0, -9.344206, -3.921908, 0.041557\O, 0, 1.573857, 2.518288, 0.618254\C, 0,
4.962559, 0.331327, -0.590065\C, 0, 4.044369, 0.756826, -1.569945\C, 0, 2.899994, 1.49019, -1.197874\C, 0,
2.663063, 1.807225, 0.163641\C, 0, 3.589706, 1.374464, 1.133631\C, 0, 4.734321, 0.640979, 0.765291\C, 0,
6.1467, -0.431604, -0.99754\C, 0, 7.259986, -1.063718, -0.719646\C, 0, 6.844694, -0.968372, -1.928283\O, 0,
7.001671, -1.215063, -3.119994\C, 0, 10.216435, -2.484079, 2.038621\C, 0, 10.350154, -2.740993, 0.659708\C, 0,
9.37597, -2.271023, -0.243049\C, 0, 8.264381, -1.543765, 0.233625\C, 0, 8.130532, -1.287303, 1.613873\C, 0,
9.106374, -1.757626, 2.515172\C, 0, -1.549187, 4.313401, -0.537604\C, 0, -0.487629, 3.725425, 0.410112\C, 0,
0.622527, 2.97473, -0.334109\H, 0, -3.308143, 3.537923, 1.267073\H, 0, -5.061372, 2.090151, 2.167075\H, 0, -
5.155261, -0.132786, -1.532768\H, 0, -3.384362, 1.325006, -2.449396\H, 0, -9.396896, -5.040553, -1.808359\H, 0,
-7.622096, -3.679664, -2.901459\H, 0, -6.565995, -1.799185, -1.680658\H, 0, -9.061408, -2.628969, 1.748811\H, 0,
-10.114277, -4.512741, 0.516709\H, 0, 4.213427, 0.522172, -2.610922\H, 0, 2.220878, 1.79702, -1.97727\H, 0,
3.418486, 1.61008, 2.173974\H, 0, 5.426891, 0.322667, 1.527105\H, 0, 10.963817, -2.84396, 2.73018\H, 0,
11.201198, -3.296905, 0.293779\H, 0, 9.482824, -2.471003, -1.300066\H, 0, 7.286058, -0.73309, 1.991113\H, 0,
9.004107, -1.561459, 3.572842\H, 0, -1.057668, 4.970725, -1.255784\H, 0, -2.255179, 4.951185, -0.005291\H, 0, -
0.040381, 4.535859, 0.985098\H, 0, -0.949793, 3.058051, 1.135989\H, 0, 0.195258, 2.130276, -0.877449\H, 0,
1.100182, 3.639878, -1.056234\\Version=AM64L-G09RevA.02\State=1-A\HF=-1572.2769243\RMSD=7.929e-
09\Dipole=0.2973835, 0.7617045, 0.098004\Quadrupole=-10.7234301, 26.6686247, -15.9451946, 13.3847121,
71.0776206, -3.1322626\PG=C01 [X(C33H24O4)]\\@
```

Conformation: 6\_1

```
# b3lyp/6-31+g scrf=(cpcm, solvent=benzene) guess=read geom=connectivity\\Title Card Required\\0, 1\C, 0,
4.295038, 0.143719, 0.057281\C, 0, 5.32735, 1.104149, 0.03747\C, 0, 6.680106, 0.712512, 0.021901\C, 0,
7.014291, -0.655769, 0.025008\C, 0, 5.993005, -1.625853, 0.046615\C, 0, 4.640893, -1.231186, 0.062823\O, 0,
3.002512, 0.621321, 0.07102\C, 0, 8.416437, -1.087603, 0.0063\C, 0, 9.698397, -0.827212, -0.016574\C, 0,
9.276436, -2.037718, 0.001464\O, 0, 9.520105, -3.239353, 0.00834\C, 0, 13.005295, 1.897789, -0.100439\C, 0,
11.687274, 2.396985, -0.08359\C, 0, 10.595868, 1.506963, -0.056388\C, 0, 10.822301, 0.114929, -0.045018\C, 0,
12.141201, -0.384537, -0.061473\C, 0, 13.232259, 0.507028, -0.089381\O, 0, -3.00313, -0.627837, 0.046267\C, 0, -
7.014053, 0.654617, 0.012853\C, 0, -6.681195, -0.713572, 0.001221\C, 0, -5.329064, -1.107614, 0.013308\C, 0, -
4.29517, -0.149951, 0.036285\C, 0, -4.638707, 1.226347, 0.046826\C, 0, -5.990195, 1.623419, 0.035379\C, 0, -
8.414737, 1.08789, 0.001382\C, 0, -9.697818, 0.83048, -0.016877\C, 0, -9.273718, 2.039857, 0.002677\O, 0, -
9.515139, 3.241825, 0.013852\C, 0, -13.008724, -1.889051, -0.087786\C, 0, -11.692667, -2.390595, -0.079029\C,
0, -10.598256, -1.502007, -0.055557\C, 0, -10.822956, -0.110583, -0.040762\C, 0, -12.141245, 0.391105, -
0.04952\C, 0, -13.233481, -0.498505, -0.073466\C, 0, 1.937503, -0.318286, 0.06887\C, 0, 0.614436, 0.456346,
0.069856\C, 0, -0.613896, -0.465589, 0.060743\C, 0, -1.936949, 0.309226, 0.059287\H, 0, 5.075212, 2.153955,
0.034338\H, 0, 7.449542, 1.467796, 0.006151\H, 0, 6.243204, -2.677936, 0.049975\H, 0, 3.887778, -2.00437,
0.078144\H, 0, 13.842736, 2.581904, -0.121131\H, 0, 11.514683, 3.464094, -0.092351\H, 0, 9.592356, 1.900696, -
0.044027\H, 0, 12.320138, -1.450536, -0.053412\H, 0, 14.24229, 0.124034, -0.101312\H, 0, -7.451444, -1.467966,
-0.016128\H, 0, -5.077918, -2.159053, 0.004849\H, 0, -3.884836, 1.997765, 0.064129\H, 0, -6.239052, 2.675592,
0.044315\H, 0, -13.846477, -2.571516, -0.105864\H, 0, -11.521433, -3.458124, -0.090368\H, 0, -9.595789, -
```

1.897809, -0.049247\H, 0, -12.318352, 1.457919, -0.038268\H, 0, -14.242942, -0.113836, -0.07942\H, 0, 1.993965, -0.953129, -0.81633\H, 0, 1.992898, -0.955405, 0.952899\H, 0, 0.579933, 1.104948, 0.945974\H, 0, 0.585399, 1.113163, -0.801089\H, 0, -0.578918, -1.113796, -0.816161\H, 0, -0.584915, -1.123284, 0.931213\H, 0, -1.987487, 0.952203, -0.821411\H, 0, -1.9969, 0.938667, 0.948567\\Version=AM64L-G09RevA.02\State=1-A\HF=-1611.58529\RMSD=9.342e-09\Dipole=0.0011948, -0.0021394, -0.0392472\Quadrupole=1.1205213, -7.973018, 6.8524967, 99.2873329, -0.0108443, -0.03796\PG=C01 [X(C34H26O4)]\\@

Conformation: 6\_2

# b3lyp/6-31+g scrf=(cpcm, solvent=benzene) guess=read geom=connectivity\\Title Card Required\\0, 1\C, 0, 3.733057, -1.078719, 0.218049\C, 0, 4.364659, 0.079447, 0.713848\C, 0, 5.737525, 0.304335, 0.494653\C, 0, 6.497998, -0.639082, -0.224118\C, 0, 5.880124, -1.804694, -0.719605\C, 0, 4.50586, -2.025792, -0.502331\C, 0, 2.386382, -1.21148, 0.477005\C, 0, 7.927922, -0.422774, -0.46635\C, 0, 9.016845, 0.295158, -0.355186\C, 0, 9.035656, -0.833955, -0.96192\C, 0, 9.662144, -1.69074, -1.57687\C, 0, 11.130138, 3.783682, 0.962411\C, 0, 11.807985, 2.763286, 0.26647\C, 0, 11.107988, 1.617955, -0.163638\C, 0, 9.728759, 1.493162, 0.102446\C, 0, 9.050356, 2.514167, 0.798952\C, 0, 9.752223, 3.659388, 1.227481\C, 0, -2.645334, -2.047971, -0.50386\C, 0, -6.605479, -0.829003, 0.238301\C, 0, -5.720774, -0.031139, -0.513157\C, 0, -4.403523, -0.47123, -0.744595\C, 0, -3.951011, -1.702409, -0.229908\C, 0, -4.848646, -2.501765, 0.52281\C, 0, -6.16858, -2.064786, 0.753189\C, 0, -7.981274, -0.388949, 0.493522\C, 0, -8.950248, 0.483928, 0.376694\C, 0, -9.12897, -609647, 1.020307\C, 0, -9.866663, -1.341557, 1.672034\C, 0, -10.534143, 4.213188, -1.021782\C, 0, -3.42476, 3.334958, -0.273049\C, 0, -10.816815, 2.10969, 0.183429\C, 0, -9.481437, 1.762509, -0.109077\C, 0, -8.673175, 2.641382, -858573\C, 0, -9.201048, 3.866329, -1.315114\C, 0, 1.698122, -2.322214, -0.07973\C, 0, 0.216048, -2.204547, 0.292685\C, 0, -0.6371, -3.346644, -0.282944\C, 0, -2.119732, -3.228368, 0.090035\H, 0, 3.785221, 0.805155, 1.265125\H, 0, 6.195096, 1.199965, 0.882561\H, 0, 6.457707, -2.533047, -1.271626\H, 0, 4.068597, -2.929134, -0.897319\H, 0, 11.666978, 4.661833, 1.291499\H, 0, 12.865145, 2.858504, 0.061893\H, 0, 11.632789, 0.838665, -0.698584\H, 0, 7.995765, 2.431861, 1.0063\H, 0, 9.232731, 4.442786, 1.76146\H, 0, -6.04012, 0.917089, -0.915508\H, 0, -3.727032, 0.143789, -1.319975\H, 0, -4.550937, -3.45494, 0.932189\H, 0, -6.843188, -2.683559, 1.329163\H, 0, -10.937412, 5.153105, -1.372182\H, 0, -12.365741, 3.600924, -0.049235\H, 0, -11.441463, 1.439783, 0.75755\H, 0, -7.650508, 2.386958, -1.088339\H, 0, -8.581052, 4.54028, -1.889328\H, 0, 1.806268, -2.328737, -1.166219\H, 0, 2.105953, -3.254956, 0.311679\H, 0, 0.117936, -2.182799, 1.377955\H, 0, -0.165769, -1.248352, -0.06829\H, 0, -0.53946, -3.371183, -1.36921\H, 0, -0.254671, -4.301334, 0.080552\H, 0, -2.227704, -3.197923, 1.175685\H, 0, -2.65835, -4.101823, -0.279497\\Version=AM64L-G09RevA.02\State=1-A\HF=-1611.5851577\RMSD=2.145e-09\Dipole=0.0807662, 2.3025515, -0.0682564\Quadrupole=-60.425974, 47.2739554, 13.1520186, 4.949269, 47.9978124, -1.511302\PG=C01 [X(C34H26O4)]\\@

Conformation: 6\_3

# b3lyp/6-31+g scrf=(cpcm, solvent=benzene) guess=read geom=connectivity\\Title Card Required\\0, 1\C, 0, -3.838812, -0.639683, -0.16986\C, 0, -4.597843, 0.547422, -0.133194\C, 0, -6.005479, 0.507347, -0.106016\C, 0, -6.671105, -0.734169, -0.114179\C, 0, -5.925765, -1.928995, -0.145376\C, 0, -4.517046, -1.884765, -0.1733\C, 0, -2.468475, -0.500788, -0.19934\C, 0, -8.136484, -0.801058, -0.090963\C, 0, -9.312709, -0.229323, -0.070392\C, 0, -9.206375, -1.506832, -0.080843\C, 0, -9.742411, -2.609801, -0.082207\C, 0, -11.833249, 3.237368, -0.02309\C, 0, -12.400094, 1.947338, -0.025431\C, 0, -11.566462, 0.811167, -0.038742\C, 0, -10.164992, 0.96431, -0.052261\C, 0, -9.597512, 2.255599, -0.050027\C, 0, -10.432275, 3.390869, -0.035335\C, 0, 2.592193, -1.300968, 0.66338\C, 0,

6.749416, -0.94328, 0.098074\C, 0, 5.992813, 0.222369, 0.326843\C, 0, 4.599999, 0.135791, 0.521125\C, 0, 3.947546, -1.122533, 0.486734\C, 0, 4.717446, -2.281891, 0.261372\C, 0, 6.109486, -2.19819, 0.06603\C, 0, 8.199183, -0.869677, -0.107252\C, 0, 9.313446, -0.188639, -0.201392\C, 0, 9.313116, -1.46306, -0.331901\O, 0, 9.931393, -2.503142, -0.529818\C, 0, 11.514727, 3.488685, -0.146008\C, 0, 10.121783, 3.504381, 0.06418\C, 0, 9.390713, 2.299133, 0.047793\C, 0, 10.054658, 1.076265, -0.179788\C, 0, 11.450377, 1.060713, -0.390504\C, 0, 12.178741, 2.266626, -0.373005\C, 0, -1.673001, -1.674702, -0.294555\C, 0, -0.197375, -1.262753, -0.37393\C, 0, 0.309296, -0.591007, 0.913107\C, 0, 1.774691, -0.148498, 0.81488\H, 0, -4.089997, 1.501367, -0.127576\H, 0, -6.560388, 1.430189, -0.0803\H, 0, -6.431216, -2.884883, -0.150298\H, 0, -3.981298, -2.820829, -0.197268\H, 0, -12.472059, 4.10826, -0.013084\H, 0, -13.473563, 1.829299, -0.017223\H, 0, -12.007183, -0.176396, -0.041717\H, 0, -8.527165, 2.386194, -0.059843\H, 0, -9.997872, 4.380629, -0.034653\H, 0, 6.46984, 1.188251, 0.355542\H, 0, 4.055204, 1.050297, 0.695889\H, 0, 4.230023, -3.246282, 0.235267\H, 0, 6.681099, -3.098343, -0.107819\H, 0, 12.073706, 4.413467, -0.133461\H, 0, 9.613233, 4.441893, 0.238744\H, 0, 8.32544, 2.325047, 0.21012\H, 0, 11.964428, 0.126745, -0.565492\H, 0, 13.246836, 2.254346, -0.535713\H, 0, -1.834437, -2.322202, 0.56828\H, 0, -1.939143, -2.234619, -1.193054\H, 0, 0.406056, -2.148091, -0.577208\H, 0, -0.05536, -0.594798, -1.223407\H, 0, -0.308483, 0.280644, 1.131903\H, 0, 0.191524, -1.269156, 1.758417\H, 0, 2.053812, 0.388962, 1.722394\H, 0, 1.900221, 0.529634, -0.031327\\Version=AM64L-G09RevA.02\State=1-A\HF=-1611.5851015\RMSD=9.957e-09\Dipole=-0.195992, 4.7843106, 0.4535335\Quadrupole=-41.9967897, 24.0763671, 17.9204225, 3.4726366, 5.7686456, -0.4580808\PG=C01 [X(C34H26O4)] \\@

Conformation: 6\_4

# b3lyp/6-31+g scrf=(cpcm, solvent=benzene) geom=connectivity\\Title Card Required\\0, 1\C, 0, -3.821102, -0.758944, 0.002092\C, 0, -4.50928, -1.671537, -0.837576\C, 0, -5.896399, -1.538955, -1.049462\C, 0, -6.612276, -0.497803, -0.425926\C, 0, -5.93598, 0.41574, 0.406538\C, 0, -4.548945, 0.281785, 0.61394\O, 0, -2.470773, -0.814675, 0.267171\C, 0, -8.055921, -0.3838, -0.653356\C, 0, -9.209898, 0.20049, -0.452283\C, 0, -9.118649, -0.820316, -1.220387\O, 0, -9.660151, -1.633071, -1.963167\C, 0, -11.66086, 3.21484, 1.358449\C, 0, -12.232972, 2.258352, 0.495478\C, 0, -11.422276, 1.270233, -0.097699\C, 0, -10.03721, 1.237885, 0.172718\C, 0, -9.465933, 2.194814, 1.036016\C, 0, -10.278598, 3.182497, 1.627802\O, 0, 2.666746, -1.675173, -0.35158\C, 0, 6.695555, -0.735046, 0.430353\C, 0, 6.119062, -1.846219, 1.077452\C, 0, 4.773345, -2.1858, 0.83686\C, 0, 3.98733, -1.414726, -0.056379\C, 0, 4.575455, -0.303899, -0.69467\C, 0, 5.921018, 0.037872, -0.457422\C, 0, 8.099441, -0.40171, 0.690497\C, 0, 9.160404, 0.340968, 0.497569\C, 0, 9.197599, -0.658066, 1.299915\O, 0, 9.828753, -1.357392, 2.085765\C, 0, 11.190014, 3.626895, -1.3583\C, 0, 11.87161, 2.795181, -0.448526\C, 0, 11.199309, 1.71695, 0.159951\C, 0, 9.843481, 1.469451, -0.1419\C, 0, 9.161808, 2.30226, -1.053345\C, 0, 9.836078, 3.380926, -1.660432\C, 0, -1.722336, -1.895, -0.272268\C, 0, -0.274959, -1.777014, 0.218088\C, 0, 0.615945, -2.92704, -0.279033\C, 0, 2.060221, -2.824433, 0.224123\H, 0, -3.997313, -2.482567, -1.332201\H, 0, -6.407671, -2.242355, -1.690948\H, 0, -6.468615, 1.219351, 0.888884\H, 0, -4.034328, 0.983422, 1.254119\H, 0, -12.283467, 3.972916, 1.81273\H, 0, -13.2927, 2.28238, 0.288391\H, 0, -11.864999, 0.538663, -0.758383\H, 0, -8.409315, 2.179896, 1.250405\H, 0, -9.841439, 3.915998, 2.290006\H, 0, 6.706738, -2.442743, 1.760358\H, 0, 4.368413, -3.043309, 1.351476\H, 0, 3.985127, 0.290441, -1.375296\H, 0, 6.346651, 0.891621, -0.959902\H, 0, 11.706208, 4.453629, -1.825213\H, 0, 12.910183, 2.983406, -0.217546\H, 0, 11.726347, 1.080514, 0.857791\H, 0, 8.126346, 2.12372, -1.292482\H, 0, 9.313699, 4.019435, -2.358326\H, 0, -2.144719, -2.846959, 0.055734\H, 0, -1.747592, -1.865017, -1.362643\H, 0, 0.139266, -0.823176, -0.111897\H, 0, -0.265926, -1.753642, 1.308253\H, 0, 0.192772, -3.876637, 0.052944\H, 0, 0.614224, -2.954319, -1.369699\H, 0, 2.609258, -3.720841, -0.06974\H, 0, 2.071773, -2.762324, 1.314412\\Version=AM64L-G09RevA.02\State=1-A\HF=-1611.5849351\RMSD=4.887e-09\Dipole=-0.0436911, 2.131116, -0.0745874\Quadrupole=-46.8342291, 36.99079, 9.8434391, -3.3935508, -62.255436, -1.3935942\PG=C01 [X(C34H26O4)] \\@

Conformation: 6\_5

```
# b3lyp/6-31+g scrf=(cpcm, solvent=benzene) guess=read geom=connectivity\\Title Card Required\\0, 1\C, 0, -
3.627211, 0.047849, -0.036042\C, 0, -4.009612, 1.301502, -0.554341\C, 0, -5.368698, 1.64444, -0.685568\C, 0, -
6.366452, 0.727802, -0.297521\C, 0, -5.998169, -0.528957, 0.220896\C, 0, -4.636591, -0.869409, 0.351344\O, 0, -
2.275925, -0.199239, 0.057824\C, 0, -7.776412, 1.100267, -0.442052\C, 0, -9.053814, 0.839674, -0.321838\C, 0, -
8.657771, 1.961781, -0.796676\O, 0, -8.927094, 3.065801, -1.257543\C, 0, -12.301093, -1.729456, 0.783891\C, 0, -
10.972891, -2.165388, 0.958518\C, 0, -9.900195, -1.327302, 0.596705\C, 0, -10.156928, -0.049024, 0.059674\C, 0,
-11.486618, 0.388847, -0.114804\C, 0, -12.557759, -0.452137, 0.246582\O, 0, 2.278014, -0.194038, -0.12484\C, 0,
6.363001, 0.732772, 0.291836\C, 0, 6.002653, -0.521453, -0.237838\C, 0, 4.643625, -0.862478, -0.388994\C, 0,
3.628247, 0.0519, -0.011356\C, 0, 4.002322, 1.302674, 0.519125\C, 0, 5.359795, 1.646597, 0.670708\C, 0,
7.771319, 1.106718, 0.452871\C, 0, 9.05006, 0.842831, 0.349624\C, 0, 8.648661, 1.969535, 0.812022\O, 0,
8.912937, 3.07624, 1.269522\C, 0, 12.306444, -1.736027, -0.701864\C, 0, 12.559136, -0.45307, -0.178409\C, 0,
11.485165, 0.39156, 0.166563\C, 0, 10.156323, -0.048234, -0.014584\C, 0, 9.904161, -1.332704, -0.539891\C, 0,
10.979832, -2.175654, -0.88305\C, 0, -1.849721, -1.436898, 0.610685\C, 0, -0.315922, -1.455035, 0.653364\C, 0,
0.324902, -1.444353, -0.745097\C, 0, 1.857731, -1.424801, -0.699474\H, 0, -3.248461, 2.007628, -0.852623\H, 0, -
5.641488, 2.611101, -1.083775\H, 0, -6.751324, -1.23946, 0.521803\H, 0, -4.394319, -1.841147, 0.752531\H, 0, -
13.122871, -2.373275, 1.06143\H, 0, -10.776957, -3.144665, 1.370969\H, 0, -8.887581, -1.671627, 0.735786\H, 0,
-11.687886, 1.367601, -0.526733\H, 0, -13.575933, -0.116124, 0.113245\H, 0, 6.760154, -1.230771, -0.531742\H,
0, 4.406278, -1.832158, -0.797945\H, 0, 3.235758, 2.006748, 0.810942\H, 0, 5.625718, 2.611544, 1.077662\H, 0,
13.131183, -2.383745, -0.965312\H, 0, 13.576419, -0.115429, -0.040176\H, 0, 11.682781, 1.375123, 0.568463\H,
0, 8.893823, -1.680174, -0.682145\H, 0, 10.787617, -3.159652, -1.285749\H, 0, -2.238626, -1.545957, 1.624299\H,
0, -2.218177, -2.273661, 0.01402\H, 0, 0.03493, -0.597662, 1.22869\H, 0, 0.015248, -2.341958, 1.193736\H, 0, -
0.005504, -2.324299, -1.298826\H, 0, -0.026531, -0.579505, -1.307787\H, 0, 2.250717, -1.51463, -1.713549\H, 0,
2.22644, -2.27019, -0.116963\\Version=AM64L-G09RevA.02\State=1-A\HF=-1611.5847752\RMSD=4.640e-
09\Dipole=0.0191481, -6.2841148, -0.0044756\Quadrupole=2.1496032, -4.6958959, 2.5462927, -0.1294114, -
39.789448, -0.0286761\PG=C01 [X(C34H26O4)]\\@
```

Conformation: 6\_6

```
# b3lyp/6-31+g scrf=(cpcm, solvent=benzene) guess=read geom=connectivity\\Title Card Required\\0, 1\C, 0, -
3.292987, 1.713779, -0.549514\C, 0, -3.163343, 0.567742, -1.373801\C, 0, -4.21665, -0.362709, -1.471079\C, 0, -
5.410368, -0.159232, -0.74931\C, 0, -5.545883, 0.975623, 0.073758\C, 0, -4.489251, 1.902081, 0.171143\O, 0, -
2.31771, 2.675188, -0.396507\C, 0, -6.497973, -1.135835, -0.867556\C, 0, -7.70207, -1.556379, -0.573258\C, 0, -
6.949689, -2.226649, -1.365692\O, 0, -6.783142, -3.20612, -2.084342\C, 0, -11.461026, -1.152519, 1.445818\C, 0, -
10.464856, -0.171883, 1.62043\C, 0, -9.2259, -0.298949, 0.960991\C, 0, -8.983381, -1.408687, 0.124752\C, 0, -
9.980818, -2.390592, -0.048524\C, 0, -11.219524, -2.262298, 0.61157\O, 0, 2.347336, 2.783159, 0.257359\C, 0,
5.461896, 0.013196, 0.847352\C, 0, 4.323321, -0.058971, 1.673911\C, 0, 3.263271, 0.853236, 1.501848\C, 0,
3.333769, 1.85131, 0.497405\C, 0, 4.478967, 1.913403, -0.321965\C, 0, 5.538914, 1.00203, -0.15295\C, 0,
6.553509, -0.946055, 1.040574\C, 0, 7.724834, -1.434967, 0.718771\C, 0, 7.044369, -1.943695, 1.678677\O, 0,
6.938546, -2.781905, 2.567968\C, 0, 11.279882, -1.471631, -1.675462\C, 0, 10.275061, -0.516112, -1.928419\C, 0,
9.104443, -0.497402, -1.145458\C, 0, 8.938266, -1.436693, -0.106269\C, 0, 9.942855, -2.392632, 0.147565\C, 0,
11.113387, -2.409701, -0.636913\C, 0, -1.127677, 2.559313, -1.165044\C, 0, -0.225753, 3.76564, -0.866133\C, 0,
0.229671, 3.869652, 0.602235\C, 0, 1.170921, 2.744037, 1.05324\H, 0, -2.266351, 0.378299, -1.94289\H, 0, -
```

4.106565, -1.231587, -2.103769\H, 0, -6.451403, 1.145694, 0.633575\H, 0, -4.59807, 2.772229, 0.802497\H, 0, -12.411127, -1.054814, 1.952262\H, 0, -10.651257, 0.678488, 2.260494\H, 0, -8.472612, 0.459509, 1.101469\H, 0, -9.800792, -3.242772, -0.688867\H, 0, -11.982991, -3.014543, 0.477073\H, 0, 4.25751, -0.815239, 2.443204\H, 0, 2.408331, 0.765585, 2.154454\H, 0, 4.54241, 2.670002, -1.089447\H, 0, 6.404309, 1.071921, -0.793056\H, 0, 12.176994, -1.485245, -2.276505\H, 0, 10.403778, 0.202876, -2.725136\H, 0, 8.342982, 0.237491, -1.349597\H, 0, 9.820063, -3.115523, 0.941701\H, 0, 11.883349, -3.143062, -0.443468\H, 0, -0.60784, 1.628059, -0.940129\H, 0, -1.373996, 2.551607, -2.228437\H, 0, 0.649255, 3.731308, -1.516044\H, 0, -0.762482, 4.675883, -1.135253\H, 0, 0.734724, 4.824566, 0.747151\H, 0, -0.64578, 3.892122, 1.253181\H, 0, 0.676953, 1.775963, 0.96995\H, 0, 1.429233, 2.893882, 2.103599\\Version=AM64L-G09RevA.02\State=1-A\HF=-1611.5846715\RMSD=8.605e-09\Dipole=-0.1345192, 3.9885362, -0.3826453\Quadrupole=36.4370632, -23.5952923, -12.841771, -4.8364452, -57.7295492, 1.2727909\PG=C01 [X(C34H26O4)]\\@

Conformation: 6\_7

# b3lyp/6-31+g scrf=(cpcm, solvent=benzene) guess=read geom=connectivity\\Title Card Required\\0, 1\C, 0, -3.677178, -1.145237, -0.480365\C, 0, -4.225282, 0.030023, 0.07042\C, 0, -5.615348, 0.260663, 0.046462\C, 0, -6.475024, -0.692145, -0.534616\C, 0, -5.940235, -1.871732, -1.089141\C, 0, -4.550214, -2.098981, -1.063602\O, 0, -2.307567, -1.285401, -0.412569\C, 0, -7.924633, -0.474231, -0.572775\C, 0, -8.987698, 0.242411, -0.30812\C, 0, -9.090312, -0.883476, -0.911332\O, 0, -9.79633, -1.739269, -1.435643\C, 0, -10.902386, 3.713421, 1.31698\C, 0, -11.667463, 2.706323, 0.697465\C, 0, -11.032594, 1.566856, 0.164021\C, 0, -9.630438, 1.43496, 0.251039\C, 0, -8.864946, 2.444187, 0.871693\C, 0, -9.502925, 3.582789, 1.404375\O, 0, 2.30586, -1.280553, 0.409305\C, 0, 6.472702, -0.689199, 0.530672\C, 0, 5.614548, 0.261591, -0.054259\C, 0, 4.224012, 0.032999, -0.077429\C, 0, 3.674368, -1.140225, 0.478238\C, 0, 4.546774, -2.09213, 1.065323\C, 0, 5.936376, -1.8659, 1.089738\C, 0, 7.923216, -0.474521, 0.567634\C, 0, 8.988543, 0.239574, 0.303882\C, 0, 9.08861, -0.887831, 0.903847\O, 0, 9.793461, -1.745709, 1.426299\C, 0, 10.910659, 3.711277, -1.313393\C, 0, 11.674415, 2.697335, -0.700612\C, 0, 11.036565, 1.558447, -0.171698\C, 0, 9.633567, 1.432401, -0.253877\C, 0, 8.870712, 2.446737, -0.866843\C, 0, 9.509463, 3.586017, -1.395942\C, 0, -1.72534, -2.47075, -0.937607\C, 0, -0.205687, -2.417167, -0.733454\C, 0, 0.200292, -2.401179, 0.750287\C, 0, 1.71936, -2.455171, 0.955557\H, 0, -3.569834, 0.763527, 0.515961\H, 0, -6.008855, 1.168986, 0.475128\H, 0, -6.593371, -2.60666, -1.537256\H, 0, -4.179326, -3.014698, -1.499172\H, 0, -11.390638, 4.587847, 1.725914\H, 0, -12.741843, 2.80631, 0.630394\H, 0, -11.623261, 0.796287, -0.309656\H, 0, -7.79345, 2.354143, 0.945822\H, 0, -8.917264, 4.356047, 1.881002\H, 0, 6.008562, 1.168127, -0.485596\H, 0, 3.569192, 0.765142, -0.526148\H, 0, 4.175309, -3.005455, 1.50552\H, 0, 6.590236, -2.599931, 1.540582\H, 0, 11.399643, 4.584964, -1.719716\H, 0, 12.748213, 2.792715, -0.637669\H, 0, 11.626759, 0.782971, 0.297337\H, 0, 7.797548, 2.362381, -0.935706\H, 0, 8.925574, 4.364243, -1.866274\H, 0, -2.134238, -3.353226, -0.441267\H, 0, -1.942911, -2.551235, -2.003879\H, 0, 0.245549, -3.282124, -1.221288\H, 0, 0.197587, -1.537611, -1.23634\H, 0, -0.199283, -1.507359, 1.232037\H, 0, -0.254543, -3.25199, 1.257771\H, 0, 2.125154, -3.347261, 0.47533\H, 0, 1.937215, -2.517492, 2.022631\\Version=AM64L-G09RevA.02\State=1-A\HF=-1611.5846639\RMSD=7.391e-09\Dipole=0.0066147, 2.5442294, 0.0195397\Quadrupole=-60.6807022, 42.2525449, 18.4281573, 0.113541, -45.7617905, -0.0473478\PG=C01 [X(C34H26O4)]\\@

Conformation: 6\_8

# b3lyp/6-31+g scrf=(cpcm, solvent=benzene) geom=connectivity scf=maxcycle=1000\\Title Card Required\\0, 1\C, 0, 3.241148, 0.906218, -0.691863\C, 0, 3.297254, -0.410982, -1.210991\C, 0, 4.495749, -1.148486, -1.156335\C, 0,

5.651605, -0.579663, -0.584881\C, 0, 5.603934, 0.727865, -0.062865\C, 0, 4.403298, 1.460852, -0.117394\O, 0, 2.114562, 1.700466, -0.70519\C, 0, 6.892568, -1.359622, -0.545027\C, 0, 8.158712, -1.492908, -0.237227\C, 0, 7.520014, -2.445603, -0.809033\O, 0, 7.514548, -3.579842, -1.275622\C, 0, 11.829081, -0.006591, 1.403219\C, 0, 10.677539, 0.805112, 1.416994\C, 0, 9.467207, 0.322842, 0.879993\C, 0, 9.408283, -0.974403, 0.328693\C, 0, 10.560679, -1.786502, 0.315257\C, 0, 11.770486, -1.302191, 0.853007\O, 0, -2.842027, 3.341308, -0.58004\C, 0, -5.750792, 0.604274, 0.757558\C, 0, -5.798753, 1.155061, -0.537295\C, 0, -4.807787, 2.067396, -0.948552\C, 0, -3.759892, 2.440347, -0.083081\C, 0, -3.72174, 1.88338, 1.22041\C, 0, -4.711298, 0.97028, 1.636075\C, 0, -6.773514, -0.345719, 1.207807\C, 0, -7.860194, -1.046385, 1.00424\C, 0, -7.243472, -1.105944, 2.126737\O, 0, -7.161829, -1.561597, 3.261974\C, 0, -11.141043, -2.31159, -1.446967\C, 0, -10.195385, -1.401416, -1.958914\C, 0, -9.114611, -0.980791, -1.158958\C, 0, -8.978417, -1.472749, 0.156266\C, 0, -9.924044, -2.385372, 0.668232\C, 0, -11.005373, -2.803568, -0.133394\C, 0, 0.952762, 1.211744, -1.362926\C, 0, -0.134203, 2.291615, -1.305546\C, 0, -0.623414, 2.57013, 0.125283\C, 0, -1.689391, 3.678465, 0.186572\H, 0, 2.433264, -0.881691, -1.656949\H, 0, 4.526021, -2.151936, -1.557653\H, 0, 6.478951, 1.177028, 0.377421\H, 0, 4.371154, 2.46427, 0.282701\H, 0, 12.756505, 0.363792, 1.814464\H, 0, 10.723149, 1.799042, 1.837347\H, 0, 8.591965, 0.953873, 0.896014\H, 0, 10.522167, -2.781167, -0.106128\H, 0, 12.653124, -1.925743, 0.84182\H, 0, -6.587598, 0.887594, -1.221505\H, 0, -4.848145, 2.487497, -1.943217\H, 0, -2.944364, 2.13779, 1.924164\H, 0, -4.669098, 0.552662, 2.631944\H, 0, -11.970764, -2.6321, -2.060639\H, 0, -10.300081, -1.024677, -2.965968\H, 0, -8.398645, -0.283731, -1.562183\H, 0, -9.824544, -2.765852, 1.675161\H, 0, -11.730562, -3.50164, 0.259444\H, 0, 1.182807, 0.98567, -2.404972\H, 0, 0.595241, 0.296778, -0.8892\H, 0, 0.243113, 3.210679, -1.756526\H, 0, -0.980353, 1.975408, -1.917082\H, 0, -1.008276, 1.649653, 0.564136\H, 0, 0.225077, 2.86682, 0.743574\H, 0, -1.274218, 4.592483, -0.238808\H, 0, -1.949888, 3.934252, 1.21311\Version=AM64L-G09RevA.02\State=1-A\HF=-1611.5831647\RMSD=6.113e-09\Dipole=-0.1221842, 3.3725864, -1.4006708\Quadrupole=27.1062516, -14.7742787, -12.331973, 32.0322293, 56.9514139, 5.8581156\PG=C01 [X(C34H26O4)]\@\

Conformation: 6\_9

# b3lyp/6-31+g scrf=(cpcm, solvent=benzene) guess=read geom=connectivity\Title Card Required\0, 1\C, 0, 3.274795, -1.308976, -0.408998\C, 0, 4.429865, -1.236357, -1.213942\C, 0, 5.593953, -0.593097, -0.750988\C, 0, 5.611968, -0.011126, 0.531075\C, 0, 4.463429, -0.075605, 1.345972\C, 0, 3.301292, -0.720563, 0.880314\O, 0, 2.184212, -1.958821, -0.945346\C, 0, 6.812708, 0.663269, 1.034933\C, 0, 8.05183, 1.063075, 0.894644\C, 0, 7.403528, 1.305992, 1.973792\O, 0, 7.371342, 1.797725, 3.096963\C, 0, 11.683907, 1.408985, -1.353044\C, 0, 10.575397, 0.744278, -1.913697\C, 0, 9.3772, 0.627001, -1.180966\C, 0, 9.289016, 1.175113, 0.115293\C, 0, 10.399095, 1.84131, 0.676511\C, 0, 11.59582, 1.958178, -0.058134\O, 0, -3.579631, -4.048259, -0.2359\C, 0, -6.490457, -1.062689, 0.364786\C, 0, -6.594711, -2.326575, 0.976934\C, 0, -5.601928, -3.300525, 0.752601\C, 0, -4.496069, -3.029886, -0.078708\C, 0, -4.401408, -1.754824, -0.6937\C, 0, -5.392559, -0.778576, -0.471113\C, 0, -7.53054, -0.057465, 0.607845\C, 0, -8.042208, 1.134726, 0.430799\C, 0, -8.630909, 0.274266, 1.17682\O, 0, -9.569985, -0.02106, 1.907616\C, 0, -7.973306, 5.06331, -1.279223\C, 0, -6.931486, 4.159411, -1.562482\C, 0, -6.946599, 2.865732, -1.004161\C, 0, -8.007819, 2.475551, -0.160243\C, 0, -9.051525, 3.381957, 0.123408\C, 0, -9.03363, 4.675091, -0.435892\C, 0, 1.014176, -2.082784, -0.149273\C, 0, -0.036357, -2.852076, -0.957816\C, 0, -1.348483, -3.055453, -0.184392\C, 0, -2.399273, -3.826925, -1.000628\H, 0, 4.420538, -1.68139, -2.198164\H, 0, 6.464203, -0.552722, -1.386453\H, 0, 4.470581, 0.368955, 2.330401\H, 0, 2.442184, -0.749674, 1.533012\H, 0, 12.602086, 1.499571, -1.915951\H, 0, 10.643791, 0.324796, -2.906726\H, 0, 8.536466, 0.115628, -1.620381\H, 0, 10.336621, 2.263228, 1.669691\H, 0, 12.446245, 2.467501, 0.372177\H, 0, -7.43408, -2.554902, 1.618851\H, 0, -5.6869, -4.267989, 1.225017\H, 0, -3.577638, -1.49656, -1.339414\H, 0, -5.300167, 0.18502, -0.946841\H, 0, -7.9603, 6.055191, -1.708305\H, 0, -6.117999, 4.458316, -2.208965\H, 0, -6.143011, 2.183243, -1.227756\H, 0, -9.866642, 3.088268, 0.769508\H, 0, -9.833342, 5.368677, -0.21869\H, 0, 1.239299, -2.619881, 0.773159\H, 0,

0.628885, -1.09572, 0.113348\H, 0, -0.237455, -2.315948, -1.885979\H, 0, 0.373221, -3.821579, -1.243905\H, 0, -1.146878, -3.600667, 0.738009\H, 0, -1.743725, -2.085661, 0.117772\H, 0, -1.99843, -4.807955, -1.255081\H, 0, -2.617326, -3.346909, -1.954963\\Version=AM64L-G09RevA.02\State=1-A\HF=-1611.5829289\RMSE=9.598e-09\Dipole=2.2402909, -0.2631767, -4.0814026\Quadrupole=-33.0790711, 28.8909001, 4.188171, -27.7878767, -8.3928726, -10.1552205\PG=C01 [X(C34H26O4)]\\@

Conformation: 6\_10

```
# b3lyp/6-31+g scrf=(cpcm, solvent=benzene) guess=read geom=connectivity\\Title Card Required\\0, 1\C, 0, 3.753365, 2.377188, 0.008471\C, 0, 4.838735, 2.088884, -0.8437\C, 0, 5.830954, 1.163457, -0.467246\C, 0, 5.745861, 0.511283, 0.778395\C, 0, 4.667138, 0.788933, 1.640973\C, 0, 3.676433, 1.717124, 1.261193\O, 0, 2.83908, 3.302047, -0.450808\C, 0, 6.768484, -0.453335, 1.192648\C, 0, 7.876838, -1.117419, 0.98026\C, 0, 7.21783, -1.275264, 2.067742\O, 0, 7.101784, -1.819801, 3.160851\C, 0, 11.273295, -2.134947, -1.427204\C, 0, 11.09426, -2.732443, -0.164182\C, 0, 9.975121, -2.394557, 0.622719\C, 0, 9.035119, -1.457795, 0.146887\C, 0, 9.214488, -0.859915, -1.11807\C, 0, 10.333359, -1.199373, -1.904294\O, 0, -2.153316, 1.772511, -0.713959\C, 0, -5.69795, -0.499594, -0.698786\C, 0, -4.573685, -0.999531, -1.385625\C, 0, -3.37219, -0.262799, -1.408565\C, 0, -3.283979, 0.985648, -0.742505\C, 0, -4.415633, 1.472941, -0.058415\C, 0, -5.617737, 0.739541, -0.033884\C, 0, -6.94003, -1.279059, -0.689255\C, 0, -8.189277, -1.447408, -0.335393\C, 0, -7.585405, -2.326585, -1.045582\O, 0, -7.608469, -3.39937, -1.639715\C, 0, -11.760006, -0.16756, 1.65872\C, 0, -11.737561, -1.390221, 0.958964\C, 0, -10.560755, -1.806967, 0.305962\C, 0, -9.404568, -0.999436, 0.351283\C, 0, -9.428302, 0.224752, 1.051118\C, 0, -10.606122, 0.63931, 1.704546\C, 0, 1.684716, 3.605466, 0.326281\C, 0, 0.599419, 2.525474, 0.174018\C, 0, 0.100876, 2.385026, -1.273687\C, 0, -1.004513, 1.332607, -1.426017\H, 0, 4.909026, 2.587574, -1.799734\H, 0, 6.649428, 0.962539, -1.139277\H, 0, 4.595492, 0.292959, 2.598346\H, 0, 2.869174, 1.900362, 1.951298\H, 0, 12.131383, -2.395037, -2.031756\H, 0, 11.81456, -3.449413, 0.201523\H, 0, 9.842114, -2.855209, 1.592018\H, 0, 8.502231, -0.142185, -1.49361\H, 0, 10.471726, -0.742068, -2.873332\H, 0, -4.627889, -1.949671, -1.897736\H, 0, -2.533711, -0.679249, -1.945146\H, 0, -4.358314, 2.423172, 0.452184\H, 0, -6.468696, 1.136654, 0.495674\H, 0, -12.663767, 0.151116, 2.159476\H, 0, -12.622265, -2.009633, 0.92335\H, 0, -10.547695, -2.746232, -0.229609\H, 0, -8.551857, 0.851219, 1.093945\H, 0, -10.624702, 1.576442, 2.241844\H, 0, 1.938469, 3.779101, 1.372301\H, 0, 1.292272, 4.556994, -0.032495\H, 0, 0.96762, 1.562872, 0.528482\H, 0, -0.241441, 2.782258, 0.819143\H, 0, -0.263245, 3.346301, -1.637016\H, 0, 0.939619, 2.111909, -1.916214\H, 0, -0.658694, 0.369494, -1.047599\H, 0, -1.244945, 1.214056, -2.48363\\Version=AM64L-G09RevA.02\State=1-A\HF=-1611.582837\RMSE=8.339e-09\Dipole=0.2570087, 3.4451847, -1.0429377\Quadrupole=27.1972661, -15.3481023, -11.8491638, -26.6157527, -60.9775498, 4.9303526\PG=C01 [X(C34H26O4)]\\@
```

Conformation: 6\_11

```
# b3lyp/6-31+g scrf=(cpcm, solvent=benzene) guess=read geom=connectivity\\Title Card Required\\0, 1\C, 0, -3.632906, -2.94823, -0.232833\C, 0, -4.673519, -2.408313, -1.015414\C, 0, -5.266472, -1.175204, -0.682137\C, 0, -4.816525, -0.462835, 0.446875\C, 0, -3.773031, -0.987202, 1.234642\C, 0, -3.183568, -2.222432, 0.899058\O, 0, -3.12718, -4.167024, -0.636739\C, 0, -5.419817, 0.821911, 0.81637\C, 0, -6.280709, 1.788286, 0.619911\C, 0, -5.463737, 1.830769, 1.606301\O, 0, -5.032903, 2.415635, 2.594506\C, 0, -9.471341, 3.627589, -1.573356\C, 0, -8.930176, 4.2645, -0.438835\C, 0, -7.882926, 3.654618, 0.279701\C, 0, -7.373663, 2.406761, -0.137948\C, 0, -7.91527, 1.769669, -1.2738\C, 0, -8.964344, 2.380381, -1.99034\O, 0, 1.879543, -3.02512, 0.591108\C, 0, 5.374775, -0.801925, -0.165021\C, 0, 4.226591, -0.199836, 0.387101\C, 0, 3.074909, -0.973209, 0.629078\C, 0,
```



3.049926, -2.348581, 0.322308\C, 0, 4.209174, -2.947934, -0.23086\C, 0, 5.364073, -2.176348, -0.47216\C, 0, 6.585408, -0.016611, -0.425223\C, 0, 7.245434, 1.113557, -0.420143\C, 0, 7.796593, 0.03563, -0.841089\O, 0, 8.77652, -0.534307, -1.307837\C, 0, 7.539781, 5.319127, 0.351006\C, 0, 8.641655, 4.61532, -0.174098\C, 0, 8.539686, 3.232743, -0.424982\C, 0, 7.334559, 2.552732, -0.149415\C, 0, 6.233127, 3.25672, 0.377019\C, 0, 6.336379, 4.640538, 0.626555\C, 0, -2.1119, -4.799373, 0.136066\C, 0, -0.721706, -4.244216, -0.214062\C, 0, 0.400906, -4.92136, 0.589276\C, 0, 1.796103, -4.397696, 0.229758\H, 0, -5.022259, -2.951455, -1.881821\H, 0, -6.062912, -0.786882, -1.296808\H, 0, -3.41979, -0.444606, 2.100379\H, 0, -2.385552, -2.585782, 1.527832\H, 0, -10.274016, 4.096639, -2.124081\H, 0, -9.318861, 5.220779, -0.118437\H, 0, -7.470532, 4.14728, 1.14911\H, 0, -7.535603, 0.814399, -1.601856\H, 0, -9.381004, 1.892895, -2.859788\H, 0, 4.218369, 0.85153, 0.628884\H, 0, 2.197286, -0.508201, 1.053579\H, 0, 4.241004, -3.99709, -0.480043\H, 0, 6.241025, -2.64614, -0.894283\H, 0, 7.617863, 6.379818, 0.542532\H, 0, 9.565517, 5.135278, -384652\H, 0, 9.387457, 2.697311, -0.828449\H, 0, 5.306052, 2.748434, 0.590807\H, 0, 5.491954, 5.181038, 1.02897\H, 0, -2.320439, -4.745713, 1.205699\H, 0, -2.140334, -5.861847, -0.108544\H, 0, -0.543792, -4.381631, -1.280871\H, 0, -0.691319, -3.169462, -0.040903\H, 0, 0.228644, -4.780248, 1.656708\H, 0, 0.370988, -5.99671, 0.413789\H, 0, 1.980443, -4.528854, -0.837788\H, 0, 2.547162, -4.97153, 0.775872\\Version=AM64L-G09RevA.02\State=1-A\HF=-1611.5828246\RMSD=5.780e-09\Dipole=-2.4879824, -1.0370756, -0.9115598\Quadrupole=-.1482365, 38.1398269, -8.9915903, 18.4456608, 38.6586628, -11.9602038\PG=C01 [X(C34H26O4)]\\@@

Conformation: 6\_12

# b3lyp/6-31+g scrf=(cpcm, solvent=benzene) guess=read geom=connectivity\\Title Card Required\\0, 1\C, 0, 3.676324, -3.146659, 0.170321\C, 0, 4.32947, -2.371609, -0.808471\C, 0, 4.760651, -1.060022, -0.527477\C, 0, 4.543579, -0.509782, 0.750318\C, 0, 3.899002, -1.274951, 1.742031\C, 0, 3.469137, -2.586494, 1.456647\O, 0, 3.290613, -4.416142, -0.204378\C, 0, 4.978627, 0.85476, 1.066268\C, 0, 5.538525, 1.989581, 0.730443\C, 0, 5.075445, 1.812255, 1.912348\O, 0, 4.870716, 2.246615, 3.0414\C, 0, 7.486354, 4.554138, -2.09696\C, 0, 7.236793, 5.003834, -0.78481\C, 0, 6.595586, 4.157513, 0.14057\C, 0, 6.204558, 2.858142, -0.245594\C, 0, 6.455831, 2.407495, -1.558151\C, 0, 7.09636, 3.256292, -2.482343\O, 0, -1.156282, -2.991154, -0.425021\C, 0, -4.81715, -0.915974, -0.334472\C, 0, -4.828415, -2.300467, -0.595819\C, 0, -3.619393, -3.02396, -0.631902\C, 0, -2.383718, -2.366722, -0.406848\C, 0, -2.388078, -0.981346, -0.14448\C, 0, -3.594695, -0.256042, -0.10743\C, 0, -6.085732, -0.179867, -0.303127\C, 0, -6.768518, 0.92741, -0.155103\C, 0, -7.362624, -0.180247, -0.408604\O, 0, -8.403408, -0.796345, -0.608089\C, 0, -7.030367, 5.138292, 0.598086\C, 0, -8.198423, 4.3845, 0.367037\C, 0, -8.106747, 3.000601, 0.119464\C, 0, -6.845364, 2.368663, 0.104328\C, 0, -5.676791, 3.123218, 0.335767\C, 0, -5.769809, 4.50727, 0.582256\C, 0, 2.481674, -5.198044, 0.671149\C, 0, 1.01635, -4.725195, 0.667292\C, 0, 0.358492, -4.833105, -0.718607\C, 0, -1.106264, -4.379959, -0.723176\H, 0, 4.496836, -2.789174, -1.790217\H, 0, 5.25454, -0.488774, -1.297258\H, 0, 3.729657, -0.859753, 2.725894\H, 0, 2.978051, -3.136856, 2.243426\H, 0, 7.978868, 5.204107, -2.805987\H, 0, 7.536712, 5.999311, -0.489168\H, 0, 6.405634, 4.507711, 1.145394\H, 0, 6.16076, 1.417352, -1.865501\H, 0, 7.289015, 2.911662, -3.488807\H, 0, -5.763746, -2.813275, -0.770171\H, 0, -3.66859, -4.082987, -0.835494\H, 0, -1.451244, -0.471929, 0.029377\H, 0, -3.568442, 0.802551, 0.094065\H, 0, -7.100873, 6.200201, 0.787926\H, 0, -9.164, 4.868809, 0.378902\H, 0, -9.005034, 2.427341, -0.057608\H, 0, -4.706946, 2.652001, 0.325998\H, 0, -4.875047, 5.086547, 0.759927\H, 0, 2.523495, -6.228279, 0.316519\H, 0, 2.893758, -5.22758, 1.679677\H, 0, 0.450902, -5.32524, 1.380478\H, 0, 0.950152, -3.696559, 1.021435\H, 0, 0.919781, -4.23896, -1.440388\H, 0, 0.413617, -5.865989, -1.065176\H, 0, -1.67692, -4.953162, 0.008539\H, 0, -1.538068, -4.563981, -1.708786\\Version=AM64L-G09RevA.02\State=1-A\HF=-1611.5825806\RMSD=5.736e-09\Dipole=2.2702182, -0.7043843, -1.7210261\Quadrupole=-43.1666348, 47.1364663, -3.9698314, -19.8560154, -32.2428885, -14.7121316\PG=C01 [X(C34H26O4)]\\@@

## Computational References:

### OPLS (for Monte Carlo Conformational Search)

(a) Jorgensen, W. L.; Tirado-Rives, J. *J. Am. Chem. Soc.* **1988**, *110*, 1657. (b) Jorgensen, W. L.; Maxwell, D. S.; Tirado-Rives, J. *J. Am. Chem. Soc.* **1996**, *118*, 11225.

### MacroModel (for OPLS calculations)

Guimarães, C. R. W.; Cardozo, M. *J. Chem. Inf. Model* **2008**, *48*, 958.

### B3LYP (for single point energy calculations)

(a) Becke, A. D. *J. Chem. Phys.* **1993**, *98*, 5648-5652. (b) Becke, A. D. *J. Chem. Phys.* **1993**, *98*, 1372-1377. (c) Lee, C.; Yang, W.; Parr, R. G. *Phys. Rev. B* **1988**, *37*, 785-789.

### 6-31+G (for single point energy calculations)

(a) Clark, T.; Chandrasekhar, J.; Spitznagel, G. W.; Schleyer, P. v. R. *J. Comput. Chem.* **1983**, *4*, 294. (b) Frisch, M. J.; Pople, J. A.; Binkley, J. S. *J. Chem. Phys.* **1984**, *80*, 3265. (c) Latajka, Z.; Scheiner, S. *Chem. Phys. Lett.* **1984**, *105*, 435.

### Gaussian 03, revision C.02 (for B3LYP/6-31+G calculations) (Ref. 18)

Frisch, M. J.; Trucks, G. W.; Schlegel, H. B.; Scuseria, G. E.; Robb, M. A.; Cheeseman, J. R.; Montgomery, Jr., J. A.; Vreven, T.; Kudin, K. N.; Burant, J. C.; Millam, J. M.; Iyengar, S. S.; Tomasi, J.; Barone, V.; Mennucci, B.; Cossi, M.; Scalmani, G.; Rega, N.; Petersson, G. A.; Nakatsuji, H.; Hada, M.; Ehara, M.; Toyota, K.; Fukuda, R.; Hasegawa, J.; Ishida, M.; Nakajima, T.; Honda, Y.; Kitao, O.; Nakai, H.; Klene, M.; Li, X.; Knox, J. E.; Hratchian, H. P.; Cross, J. B.; Bakken, V.; Adamo, C.; Jaramillo, J.; Gomperts, R.; Stratmann, R. E.; Yazyev, O.; Austin, A. J.; Cammi, R.; Pomelli, C.; Ochterski, J. W.; Ayala, P. Y.; Morokuma, K.; Voth, G. A.; Salvador, P.; Dannenberg, J. J.; Zakrzewski, V. G.; Dapprich, S.; Daniels, A. D.; Strain, M. C.; Farkas, O.; Malick, D. K.; Rabuck, A. D.; Raghavachari, K.; Foresman, J. B.; Ortiz, J. V.; Cui, Q.; Baboul, A. G.; Clifford, S.; Cioslowski, J.; Stefanov, B. B.; Liu, G.; Liashenko, A.; Piskorz, P.; Komaromi, I.; Martin, R. L.; Fox, D. J.; Keith, T.; Al-Laham, M. A.; Peng, C. Y.; Nanayakkara, A.; Challacombe, M.; Gill, P. M. W.; Johnson, B.; Chen, W.; Wong, M. W.; Gonzalez, C.; and Pople, J. A.; Gaussian, Inc., Wallingford CT, 2004.

## **Chapter 4**

### **Photochemistry of Aryl-Tethered Diarylcyclopropenones in the Solid State and Application to Materials Development**

#### 4. 1. Introduction

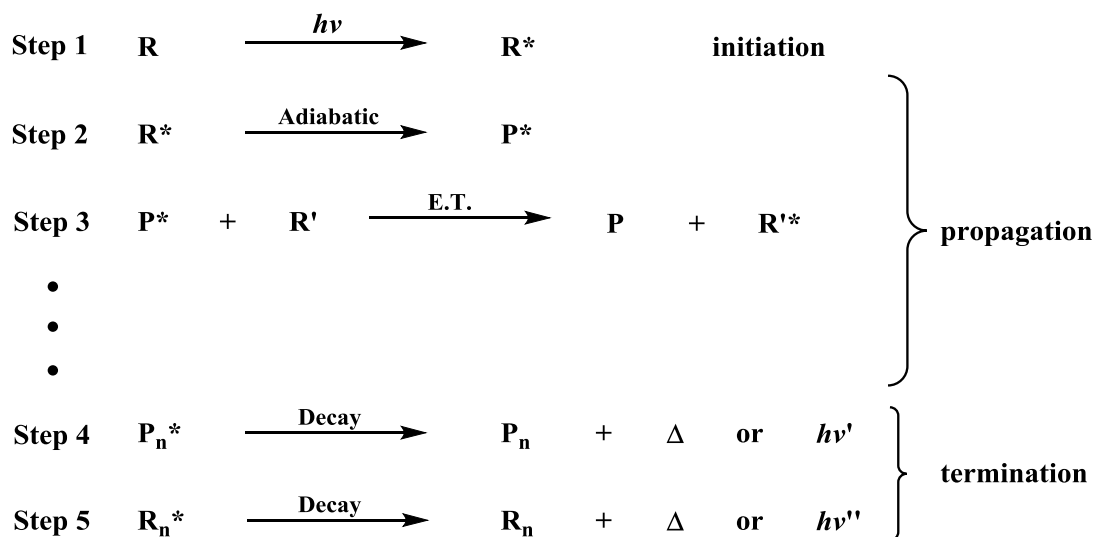
Optoelectronics, a sub-set of photonics, is a field of study that focuses on the efficient detection, capture, and control of photons for the generation of electricity, interaction with electric fields, or the generation of an electrical impulse for sensing applications.<sup>94, 95</sup> Materials utilized in this field require the ability to absorb photons and react to form a product molecule or cause a photochemical transformation that can be used to transmit a signal or information to a detector.<sup>96,97</sup> The majority of molecules that can absorb light to undergo photoreactions require more than a single incident photon of the appropriately energetic wavelength to elicit the reaction of a single ground state (non-energized) molecule to form the desired product(s).<sup>98</sup> The methods of photon utilization in optoelectronic technology, post-capture and/or absorption, are already well-developed, but advancement in methods of capture or absorption are lacking. Most photoreactive materials are inherently inefficient in photon utilization. Therefore, the bulk of research in the field of optoelectronics has concentrated on methods and mechanisms of capturing/absorbing the maximum number of incident photons.<sup>99</sup> As a result, the overall advancement of these types of devices that rely upon efficient photon absorption and energy transport will potentially depend largely upon the creation of materials that can inherently utilize incident photons with greater efficiency, i.e. undergo photonic amplification with a gain.<sup>100</sup> Such a material would not only be able to “harvest” more incident photons, but could do so with a minimal loss of their energy to the surrounding environment and could elicit a long range signal with a short range impulse. This ideally would take place in such a way that a single photon with appropriate energy would be able to elicit more than one reaction upon capture/absorption, via an energy transfer mechanism.

To date, there are a number of systems in which efficient energy transfer, via a quantum chain, is known to occur, including triplet reactions of Dewar benzene and super-high-spin

magnetic polycarbenes.<sup>101,102</sup> In order to make the practical use of such materials a reality, it will be crucial to develop a greater understanding of energy transfer in these systems and the various mechanisms it can take in both solution and the solid state. Toward this purpose, the exploration of quantum chain reactions, where energy can be transferred with high efficiency between neighboring molecules with minimal loss of energy,<sup>103</sup> could prove to be quite useful in determining the parameters necessary for the development of the next generation of optoelectronic devices. Energy transfer typically occurs between the lowest singlet ( $S_1$ ) or Triplet ( $T_1$ ) excited states. Energy transfer from upper excited states ( $S_n$ ,  $n>1$ ) is not typically considered for these applications, as internal conversion to  $S_1$  has been observed to be more expedient. To date, there are very few documented instances of energy transfer from upper excited states.<sup>104</sup> Previous work published by our lab has revealed that energy transfer takes place from upper excited states in crystalline diphenylcyclopropanone and synthesized derivatives of diphenylcyclopropanone.<sup>105</sup>

The majority of photoreactions require one or more photons of light to produce a single photoproduct molecule from a single ground state reactant molecule. Conversely, a quantum chain reaction, in essence, is a photochemical reaction that is characterized by the formation of more than one molecule of photoproduct per single photon of light absorbed.<sup>106</sup> Mechanistically, a quantum chain reaction is similar to a radical propagation mechanism, only the chain carriers in this case are in the excited state, as was first revealed by Hammond.<sup>107</sup>

**Scheme 4. 1. 1.** The mechanism of a quantum chain reaction.



A quantum chain process proceeds as follows: a molecule in the ground state  $\mathbf{R}$  (Step 1, **Scheme 4. 1. 1**) absorbs a photon of light and is promoted to an excited state  $\mathbf{R}^*$ , where it reacts to give the photoproduct  $\mathbf{P}^*$  (Step 2). This mechanism is unique compared to other photoreactions, however, as the photoproduct lingers in an excited state for a period of time long enough to transfer energy adiabatically (without loss of heat or light to the surrounding environment) to a ground state reactant  $\mathbf{R}'$  (Step 3). The energetic input is large enough to promote the ground state reactant to an excited state ( $\mathbf{R}'^*$ ), which then reacts to form  $\mathbf{P}^*$  and propagates the energy transfer (Step 3). This occurs until the chain of energy transfer is terminated by decay of either the excited state product ( $\mathbf{P}_n^*$ ) or the excited state reactant ( $\mathbf{R}_n^*$ ) back to the ground state with concomitant loss of energy as heat or light to the surrounding media (Step 4 and/or Step 5).

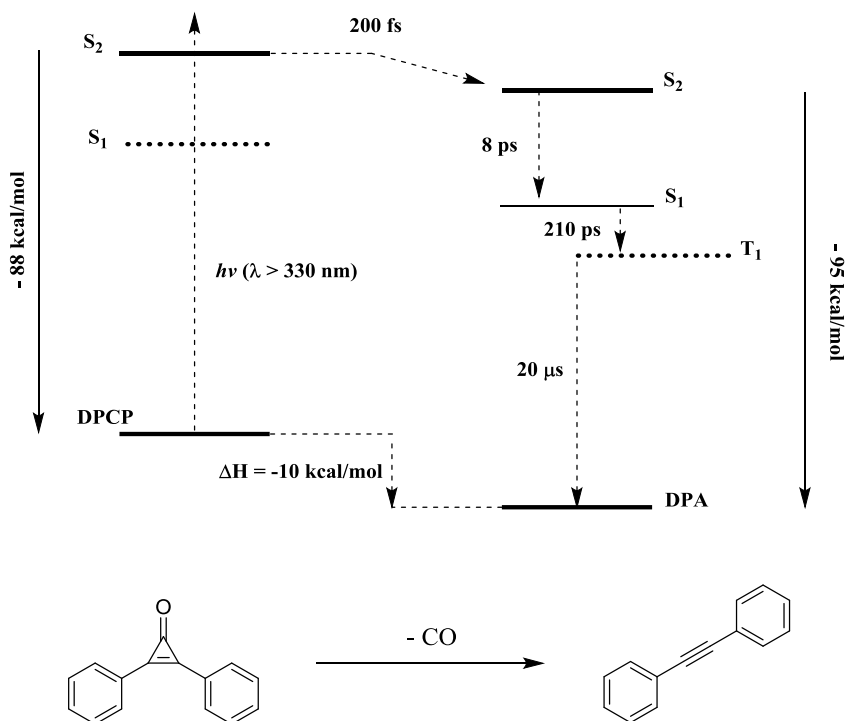
It is evident, then, that the utilization of such reactions, in particular, those with longer propagation lengths, could be quite valuable in technologies that rely upon the amplification of photonic signals, such as lithography or sensing applications.<sup>108</sup> Although the majority of

technology currently aimed at signal amplification is focused on more efficient photon capture and utilization, the use of materials capable of a quantum chain would be very desirable if good strategies could be developed to set them up and control them. The major limitation to the utilization of quantum chain reactions has two parts. In order to optimize such a process, the efficiency of the adiabatic reactions to form  $\mathbf{P}_n^*$  must be maximized (Step 2), and the adiabatic energy transfers (Step 3) should be highly efficient, in order to minimize the loss of energy to the surrounding environment. Work done by our lab has revealed that this is possible in the reactions of some crystalline solids.<sup>47</sup>

The photochemical decarbonylation of commercially available diphenylcyclopropanone (**DPCP**) has previously been revealed to be efficient in both solution phase and solid state experiments (**Scheme 4. 1. 2**).<sup>111</sup> The conversion of **DPCP** to product proceeds by a ring-opening mechanism where **DPCP** in the second excited state (**S<sub>2</sub>-DPCP**) reacts adiabatically to give diphenylacetylene (**DPA**) in the second excited state (**S<sub>2</sub>-DPA**), which then undergoes internal conversion after a period of 8 picoseconds to the ground state (**S<sub>1</sub>-DPA**).<sup>5</sup> In pioneering work by our group, we were able to show that the photochemical decarbonylation of **DPCP** (and synthesized derivatives) in aqueous nanocrystalline suspensions can proceed via a quantum chain reaction, where the excited state intermediate, presumed to be diphenylacetylene (or a derivative), exists transiently in an excited state, and can adiabatically transfer energy to a ground state diphenylcyclopropanone molecule to elicit a subsequent photoreaction without loss of energy as heat or light to the surrounding media. In some cases we were able to show absolute quantum yields as high as  $\Phi_{\text{NC}} = 3.3$  (3.3 reactions per photon of light) and quantum yield amplifications of up to 1100%.<sup>46</sup> In these reactions, nanocrystalline suspensions of **DACP** molecules were excited

at 312 nm to form DPA\*. Energy is transferred adiabatically from the excited state product to a ground state reactant (**Scheme 4. 1. 2**).

**Scheme 4. 1. 2.** Mechanism of quantum chain reaction in diphenylcyclopropane.

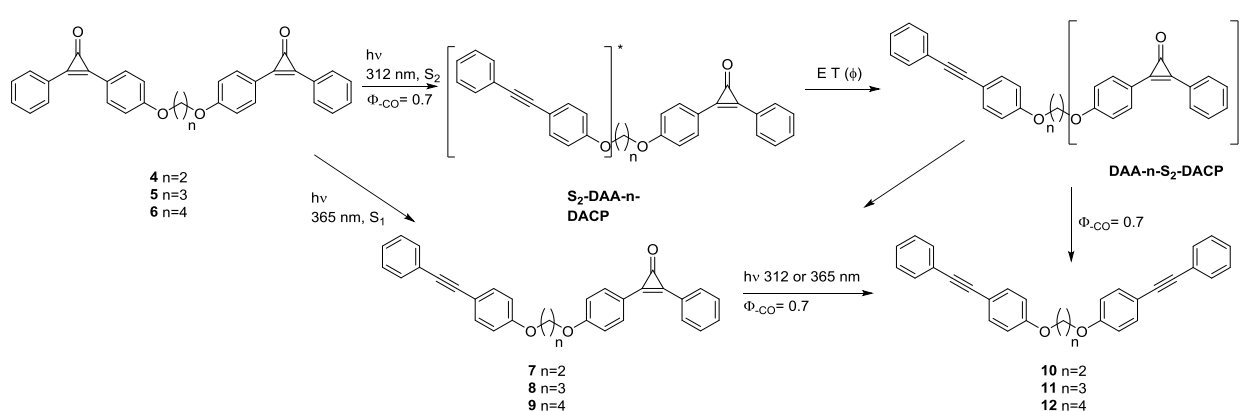


This set of experiments represented the first step toward our goal of synthesizing photoactive materials or polymers that could undergo adiabatic energy transfer over a longer range. Scrutinizing the photoreactions of the DPCP system gave us crucial information on the potential mechanisms of the energy transfer in the solid state, and made it possible to begin to formulate what might happen in a material containing a polymeric or dendritic system of DPCP-derived molecules. With this in mind, a series of DPCP derived dimers was synthesized, all tethered by alkyl chains of varying length through a *p*-ether linkage. This study revealed that energy transfer in the solid state alkyl-tethered system was effective over short distances and not in effect over longer ranges. This, aided by our optical data and computational modeling, led us to infer that



energy transfer, in this case, was likely operative via a Dexter mechanism (**Scheme 4. 1. 3**). A Dexter mechanism would require wave function overlap and is only operative at shorter distances compared to Förster resonance energy transfer (FRET) (15-20 angstroms).<sup>109</sup> DACP dimers tethered by an alkyl chain were able to sustain a quantum chain in both solution and in nanocrystalline suspensions, albeit with higher quantum yields in the solid state.

**Scheme 4. 1. 3.** Mechanism of energy transfer via a quantum chain in alkyl-tethered DPCP dimers.



This was an important discovery, but also had a significant drawback. The tether itself was a limitation to materials synthesis in two ways. Synthetic yields of the reactions to tether the DPCP derivatives were too low to consider using the same or similar methods to form a more extensive polymeric system. The tether also presented a limitation in that materials made via this method would be linear chains; this would prevent the creation of a more branched structure. Ideally, the tether would allow for both linear and branched structures to be synthesized with similar ease. A quick assessment of the options available led to the idea of using a benzene ring as a central core around which the DACP molecules could be arranged in varying substitution patterns, utilizing a benzylic linkage to maximize photonic amplification in multiple directions. Since the calculated intrachromophore distances in the aryl linked dimers was larger than that of the alkyl-tethered systems, we could not exclude that a through bond, rather than through space, process through the

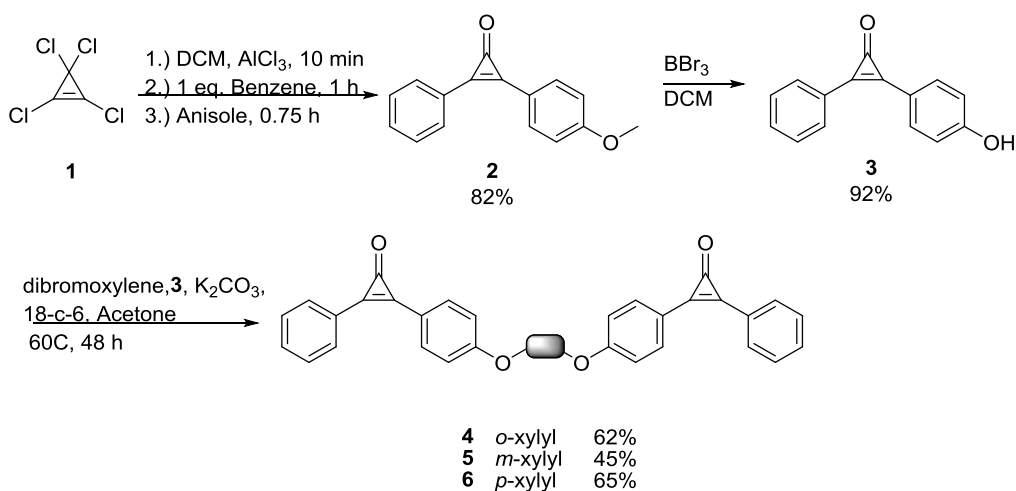
conjugated system and aromatic ring might be what would give us enhanced quantum yields, if they were observed.<sup>110</sup> With that in mind, four aryl-tethered DPCP derivatives were synthesized to test the electronic and spatial limitations of the energy transfer step observed previously in the monomeric and dimeric systems.

## 4. 2. Results and Discussion

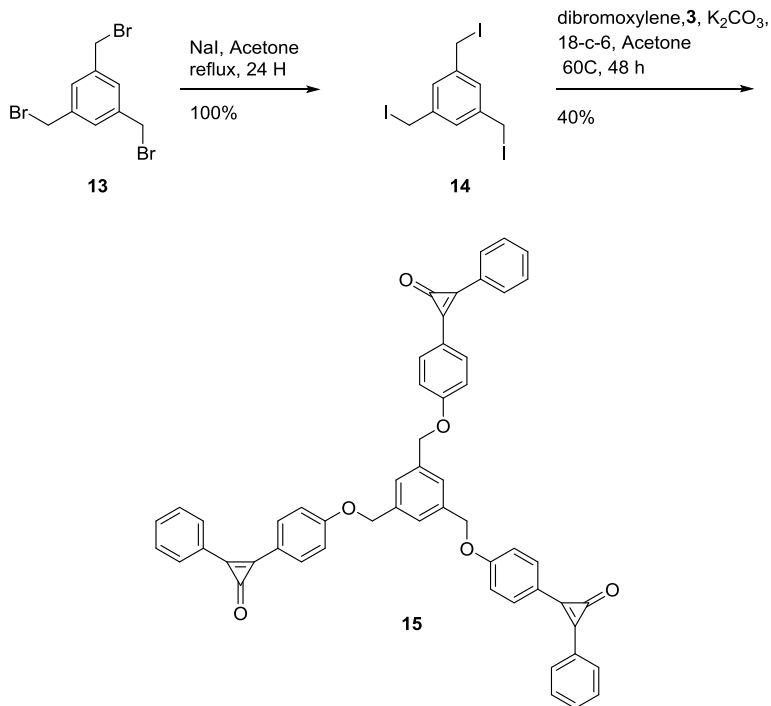
### Synthesis of Aryl-Tethered Diarylcyclopropenone Derivatives

The crystalline aryl-tethered dimers **4** – **6** and trimer **15** were synthesized (**Scheme 4. 2. 1**, **Scheme 4. 2. 2**) from commercially available tetrachlorocyclopropene (**1**) in three steps utilizing a Friedel-Crafts reaction in DCM at  $-78^{\circ}$ , with yields ranging from 40-65%. The dimeric and trimeric products were purified via column chromatography (silica gel, 3:1 hexane:acetone) and recrystallized from hexane with 10%DCM. The aryl-tethered dimers and trimer, and all intermediates, were characterized by  $^1\text{H}$  and  $^{13}\text{C}$  NMR, IR, UV-Vis, mass spectrometry, and differential scanning calorimetry.

#### Scheme 4. 2. 1. Synthesis of aryl-tethered DPCP dimers.



#### Scheme 4. 2. 2. Synthesis of aryl-tethered DPCP trimer.



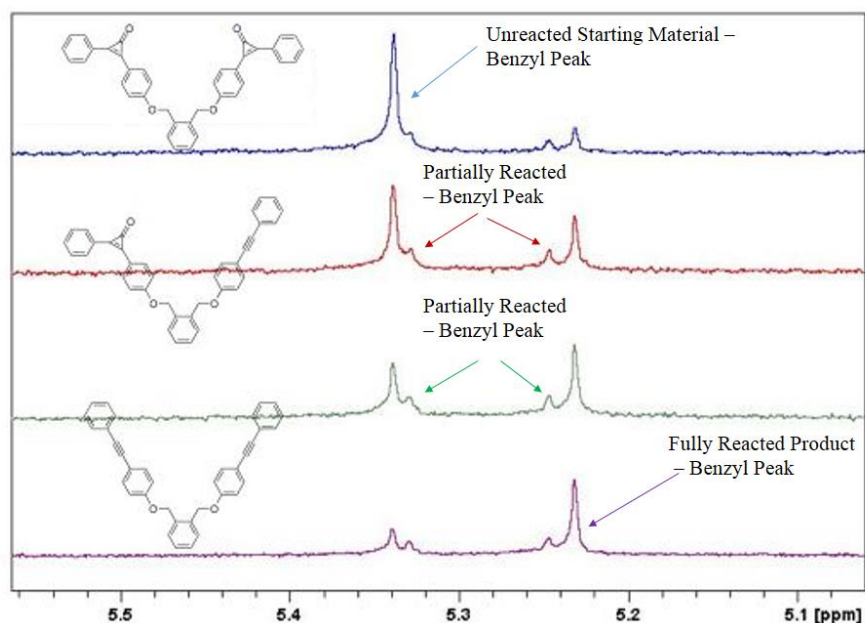
All four derivatives were characterized by the  $^1\text{H}$  NMR resonances corresponding to the protons *meta* to the cyclopropenone moiety at  $\delta > 8$  ppm and the  $^{13}\text{C}$  NMR resonance of the cyclopropenone carbonyl carbon at ca. 165 ppm. All four derivatives were crystalline powders with high melting points.

#### 4. 3. Photochemical Reactivity of Aryl-Tethered Diarylcyclopropenone Derivatives

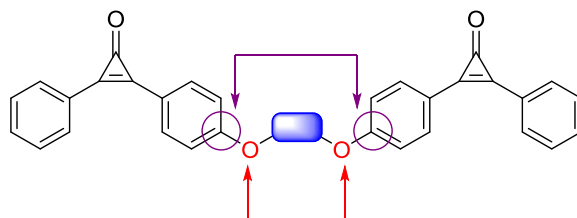
Solution phase experiments were carried out in benzene by excitation at 312 nm. The DACP monomer and dimers **4-6** and trimer **15** were all found to decarbonylate with a 100% chemical yield to give the corresponding acetylenes. There were no other photoproducts detected by  $^1\text{H}$  NMR analysis with extended irradiation times. Relative quantum yield measurements of the compounds were carried out using equimolar amounts of DACP dimer/trimer with monomer **2** as actinometer ( $\Phi = 0.7$ ) in  $d_6$ -benzene (repeated in triplicate). The extent of reaction upon irradiation was determined by the disappearance of starting material as monitored by  $^1\text{H}$  NMR. These

experiments revealed that a quantum chain was effective in solution, and all compounds reacted cleanly by  $^1\text{H}$  NMR analysis to give the product acetylenes without showing any presence of the partially reacted substrate. The one exception to this was the *ortho*-tethered dimer **4**, which reacted cleanly to give the product, but under these conditions the  $^1\text{H}$  NMR analysis showed the presence of the half-reacted dimer as well, which would indicate that a quantum chain was not as effective in that species (**Figure 4. 3. 1**).

**Figure 4. 3. 1.** Photolysis of *ortho*-tethered dimer, monitored via benzylic peak shift.



This result was curious, as the *ortho*-tethered dimer was the most similar in intrachromophore distance to the ethyl-tethered dimer which had previously shown to be the most effective for energy transfer in previous experiments. Other dimers showed a quantum chain that was more effective, despite a larger intrachromophore distance. This suggests that a through bond, rather than through space, energy transfer may be taking place through the conjugated system. Unfortunately, synthetic yields of the cyclopropanones in this study were too low to allow for solid state analysis of energy transfer efficiencies with nanocrystalline suspensions.

**Table 4. 3. 1.** Energy transfer efficiencies in solution and solid state studies.

Tether	C-C Dist.	O-O Dist.	ET Effic.	$\Phi$ (Soln)	$\Phi$ (NC)
n = 2	5.57	3.10	90	1.14	2.52
n = 3	5.87	-	65	1.02	2.39
n = 4	7.26	4.20	0	0.7	2.47
<i>ortho</i>	5.55	4.20	63	1.20	-
<i>meta</i>	7.96	6.18	92	1.39	-
<i>para</i>	8.99	7.22	72	1.26	-
trimer	7.96	6.18	92	2.01	-

(Note: Quantum yields reported for aryl-tethered dimers are relative quantum yields. Those reported for the alkyl-tethered dimers are absolute quantum yields.)

The efficiency of energy transfer in solution (ET effic. in **Table 4. 3. 1**) was calculated using the following method established in our previously published material.<sup>52</sup> It was assumed that, at 312 nm excitation, that S<sub>2</sub>-DACP\*-DACP would progress to S<sub>2</sub>-DAA\*-DACP with a quantum yield of  $\Phi = 0.7$ , as was observed in the monomer **2**. This half-reacted dimer can undergo an energy transfer with some efficiency  $\phi_{ET}$  to form DAA-S<sub>2</sub>-DACP\*, or it can decay to give the ground state half-reacted dimer DAA-DACP. If the energy transfer event takes place to give DAA-DAA with the same quantum yield as **2** ( $\Phi = 0.7$ ), then the efficiency at which the energy has been

transferred can be calculated as shown below, where  $\Phi_{\text{monomer}}$  refers to the methoxy-substituted DPCP monomer.

$$\Phi_{\text{dimer}} = \Phi_{\text{monomer}} + \varphi_{\text{ET}} (\Phi_{\text{monomer}})^2$$

The values for  $\varphi_{\text{ET}}$  can be found in **Table 4.3.1**. While energy transfer in the alkyl-tethered dimers showed a marked dependence on the intrachromophore distance, the aryl-tethered dimers show a different trend. The *meta*-tethered dimer was found to have the greatest efficiency of energy transfer over both *ortho* and *para*-tethered dimers. However, this is not as revealing as it may seem. As was stated previously,  $^1\text{H}$  NMR analysis of the solution phase photolysis of the *ortho*-tethered dimer showed the presence of the half-reacted dimer, an indication that an energy transfer event may not be taking place. With that in mind, it is difficult to ascertain a trend from the efficiency of energy transfer in the other aryl-tethered dimers in solution.

#### 4.4. Conclusions

The solid state decarbonylation of diarylcyclopropenones and derivatives continues to be of interest due to the quantum yield amplification previously observed in diphenylcyclopropenone. However, designing and synthesizing derivatives that have equal or better photophysical properties continues to be a challenge. The reactions to form the cyclopropenones tended to be low yielding and difficult to purify. As a result, the data gathered is minimal and few conclusions can be made about mechanistic details outside of that obtained from product analysis. Significant advances will need to be made to the synthetic procedure to not only have a full analysis of the compounds, but also to tailor any synthetic scheme to the creation of a photoactive polymer matrix. While the synthesis of highly branched systems of diarylcyclopropenones is attractive, it remains a synthetic challenge.

## 4. 5. Experimental

### General Methods.

All chemicals were purchased from Sigma-Aldrich Co. Inc. and Fisher Scientific Co. Inc. and used without further purification. Anhydrous DCM was acquired by distillation from sodium. Anhydrous acetone was obtained via distillation over calcium chloride or drying over Potassium Carbonate. Purification was carried out using Silica-P flash silica gel (40-62 angstrom) purchased from SiliCycle Inc.  $^1\text{H}$  and  $^{13}\text{C}$  spectra were obtained on a Bruker Advance AV300. IR spectra were collected using a Perkin-Elmer Spectrum instrument equipped with a universal attenuated total reflectance (ATR) accessory. Mass spectra were obtained using an Applied Biosystems Voyager DE-STR-MALDI-TOF. UV-Vis spectra were collected with an Ocean Optics USB2000.

### Computational Methods.

All reported geometries were from the OPLS optimized structures in the gas phase as implemented in Macromodel. Single point energies were calculated using B3LYP/6-31G\* in benzene using the CPCM solvent model as implemented in Gaussian 09.

### Synthesis of Cyclopropenones

#### Synthesis of (4-methoxyphenyl)-phenylcyclopropenone (2)

Following a modified procedure by Wadsworth,<sup>111</sup>  $\text{AlCl}_3$  (4 eq) was added to a clean, flame-dried flask under argon, suspended in dry DCM, and cooled to  $0^\circ\text{C}$  with stirring. To this, tetrachlorocyclopropene **1** (1 eq) was added dropwise over 30 minutes, creating a suspension yellow in color, and allowed to stir with cooling for an additional 10 minutes. Benzene (1 eq) was added dropwise, causing the slurry to turn reddish-brown in color, and the suspension was allowed to stir with cooling at  $0^\circ\text{C}$ . After 90 minutes, dropwise addition of anisole (1 eq) at  $0^\circ\text{C}$  resulted in a deep purple suspension, which was allowed to warm to room temperature until complete consumption of starting material was shown by TLC analysis, approximately 1 hour. The reaction

mixture was slowly quenched with saturated aqueous ammonium chloride solution, extracted with DCM, washed with brine, and dried over sodium sulfate. The solvent was removed under reduced pressure and the yellow solid subjected to column chromatography (1:2 acetone:hexane,  $R_f = 0.4$ ) to give a total yield of 90%. The resulting crystalline solid was recrystallized from a ca. 10:1 hexane: DCM solution.

**(4-methoxyphenyl)-phenylcyclopropenone (2).** Yield 85%; m.p. 128 °C;  $\lambda_{\max} = 330$  (log  $\epsilon = 4.70$ ), 315 (log  $\epsilon = 4.76$ ), 303 (log  $\epsilon = 4.63$ ) nm;  $^1\text{H NMR}$  (300 MHz,  $\text{CDCl}_3$ )  $\delta$  7.84 (d,  $J = 2.7$  Hz, 2H,  $\text{CCH}_2\text{CH}_2$ ), 7.84 (d,  $J = 5.4$  Hz, 2H,  $\text{CCH}_2\text{CH}_2$ ), 7.47 (m, 3H,  $\text{CHCH}$ ), 6.969 (d,  $J = 5.4$  Hz, 2H,  $\text{CHCH}$ ), 3.80 (s, 3H,  $\text{CH}_3$ );  $^{13}\text{C NMR}$  (75 MHz,  $\text{CDCl}_3$ )  $\delta$  163.17(CO), 155.61(CCO), 147.56(OCCH), 144.15(CHCH), 133.90(CHCH), 131.22(CHCH), 129.26(CHCH), 124.15(CHCH), 116.59(CHCH), 114.88(CHCH), 111.47(CHCH), 55.61( $\text{CH}_3$ ). FTIR (solid, HATR,  $\text{cm}^{-1}$ ): 2926, 1847, 1722, 1599, 1508, 1487, 1447. HRMS (MALDI-TOF) Formula:  $\text{C}_{16}\text{H}_{12}\text{O}_2$  calcd 236.0837; found ( $\text{M} + \text{Na}^+$ ) 259.1239.

### Synthesis of (4-hydroxyphenyl)-phenylcyclopropenone (3)

1 eq of **2** was added to a clean, flame-dried flask under argon at 0° C, and suspended in dry DCM with stirring. To this solution, 1M  $\text{BBr}_3$  in DCM (2.25 eq) was added, resulting in a color change from yellow to reddish or brown. This solution was stirred with cooling for 1 hour before allowing to warm to room temperature. After stirring overnight at room temperature, the solution was carefully quenched with saturated aqueous ammonium chloride and extracted with DCM. The mixture was washed with brine and dried over sodium sulfate prior to removal of solvent under reduced pressure. The resulting solid (90%) was used without purification.

**(4-hydroxyphenyl)-phenylcyclopropenone (3).** Yield 90%; m.p. 181 °C (decomp.);  $^1\text{H NMR}$  (300 MHz,  $\text{CDCl}_3$ )  $\delta$  7.96 (d,  $J = 2.7$  Hz, 2H,  $\text{CCH}_2\text{CH}_2$ ), 7.88 (d,  $J = 4.8$  Hz, 2H,  $\text{CCH}_2\text{CH}_2$ ),



7.58 (m, 3H, CHCH), 7.10 (d,  $J = 4.8$  Hz, 2H, CHCH);  $^{13}\text{C}$  NMR (75 MHz,  $\text{CDCl}_3$ )  $\delta$  165.32, 155.46, 143.46, 138.40, 137.06, 135.46, 133.60, 130.13, 120.80, 117.86, 111.46. FTIR (solid, HATR,  $\text{cm}^{-1}$ ): 3069, 2817, 2686, 1853, 1551, 1443. HRMS (MALDI-TOF) Formula: calcd. 222.0681; found ( $\text{M} + \text{Na}^+$ ) 244.0437.

### Synthesis of Aryl Tethered Dimers 4-6

2.5 eq of **3** was added to a clean, flame-dried, two-neck flask fitted to a reflux condenser under argon, and suspended in dry acetone with stirring. To this suspension potassium carbonate (3.5 eq), 18-crown-6 (0.3 eq), and the corresponding di-haloxylene (1 eq) were added. The reaction was covered with aluminum foil and heated to reflux for 48 hours. Upon completion, the solution was cooled to room temperature and solvent removed under reduced pressure. The resulting residue was re-dissolved in DCM and washed with water and brine prior to drying over sodium sulfate. Solvent was removed under reduced pressure, and the resulting solid subjected to column chromatography (1:2 acetone:hexane)  $R_f = 0.2$ . The resulting solid was recrystallized from a ca. 10:1 DCM:acetone solution.

***o*-di(4-phenoxy (phenylcyclopropenone) xylene (4)** Yield: 62%;  $^1\text{H}$  NMR (300 MHz,  $\text{CDCl}_3$ )  $\delta$  7.90, (m, 8H, CHCH), 7.55 (m, 8H, CHCH), 7.44 (m, 2H, CHCH), 7.13 (d,  $J = 8.8$  Hz, 4H, CCHCH), 5.29 (s, 4H,  $\text{OCH}_2$ );  $^{13}\text{C}$  NMR (75MHz,  $\text{CDCl}_3$ )  $\delta$  162.12(CO), 155.52(CCO), 147.67(OCCH), 144.82(CCH<sub>2</sub>O), 136.18(CHCH), 133.89(CHCH), 132.33(CHCH), 131.28(CHCH), 129.36(CHCH), 127.91(CHCH), 124.31(CHCH), 117.20(CHCH), 115.67(CHCH), 69.94(CH<sub>2</sub>). FTIR (solid, HATR,  $\text{cm}^{-1}$ ): 2925, 1845, 1617, 1571, 1508, 1446.

***m*-di(4-phenoxy (phenylcyclopropenone) xylene (5)** Yield: 45%;  $^1\text{H}$  NMR (300 MHz,  $\text{CDCl}_3$ )  $\delta$  7.95 (m, 8H, CHCH), 7.57 (m, 7H, CHCH), 7.49 (m, 3H, CHCH), 7.15 (d,  $J = 9.0$  Hz, 4H, CHCH), 5.20 (s, 4H,  $\text{CH}_2$ );  $^{13}\text{C}$  NMR (75MHz,  $\text{CDCl}_3$ )  $\delta$  162.12(CO), 155.52(CCO),

147.67(OCCH), 144.82(CCH<sub>2</sub>O), 136.18(CHCH), 133.89(CHCH), 132.33(CHCH), 131.28(CHCH), 129.36(CHCH), 127.91(CHCH), 124.31(CHCH), 117.20(CHCH), 115.67(CHCH), 69.94(CH<sub>2</sub>). FTIR (solid, HATR, cm<sup>-1</sup>): 2925, 1850, 1724, 1600, 1508, 1487, 1447.

***p*-di(4-phenoxy (phenylcyclopropenone) xylene (6)** Yield: 65%; <sup>1</sup>H NMR (300 MHz, CDCl<sub>3</sub>) δ 7.95 (m, 8H, CHCH), 7.58 (m, 6H, CHCH), 7.51 (s, 4H, CHCH), 7.15 (d, *J* = 8.7 Hz, 4H, OCCH), 5.20 (s, 4H, CH<sub>2</sub>); <sup>13</sup>C NMR (75MHz, CDCl<sub>3</sub>) δ 162.12(CO), 155.52(CCO), 147.67(OCCH), 144.82(CCH<sub>2</sub>O), 136.18(CHCH), 133.89(CHCH), 132.33(CHCH), 131.28(CHCH), 129.36(CHCH), 127.91(CHCH), 124.31(CHCH), 117.20(CHCH), 115.67(CHCH), 69.94(CH<sub>2</sub>). FTIR (solid, HATR, cm<sup>-1</sup>): 2926, 1846, 1709, 1598, 1508, 1486, 1446.

#### Synthesis of 14

1 eq of 1,3,5-trisbromomethyl benzene was added to a clean, flame-dried flask under argon attached a reflux condenser. To this was added 3.6 eq of Sodium Iodide, and the mixture was suspended in dry acetone and heated to reflux, covered in foil, for 24 hours. When complete, the flask was removed from heating and the solvent removed under reduced pressure. The resulting yellowish solid was dissolved in water, and extracted three times with DCM, which was then dried over sodium sulfate. Solvent was removed under reduced pressure to give 1,3,5-trisiodomethyl benzene in quantitative yield. The crystalline solid was used without further purification.

**1,3,5-trisiodomethyl benzene (14)** Yield: 100%; <sup>1</sup>H NMR (300 MHz, CDCl<sub>3</sub>) δ 6.96 (s, 3H, CCH), 4.42 (s, 6H, CH<sub>2</sub>); <sup>13</sup>C NMR (75MHz, CDCl<sub>3</sub>) δ 140.23(CCH<sub>2</sub>), 129.65(CHCCH<sub>2</sub>), 6.94 (CH<sub>2</sub>).

## Synthesis of 15

3.25 eq of **3** was added to a clean, flame-dried, flask under argon, and suspended in dry acetone with stirring. To this suspension potassium carbonate (5.25 eq), 18-crown-6 (0.3 eq), and 1, 3, 5-trisiodomethylbenzene (1 eq) were added. The reaction was covered with aluminum foil and allowed to stir at room temperature for 48 hours. Upon completion, the solvent was removed under reduced pressure. The residue was re-dissolved in DCM and washed with water and brine prior to drying over sodium sulfate. The solvent was removed under reduced pressure, and the resulting solid subjected to column chromatography (1:1 acetone:hexane)  $R_f = 0.1$ . The resulting crystalline solid was recrystallized from a ca. 10:1 DCM:acetone solution.

**1, 3, 5-tri(4-phenoxy (phenylcyclopropenone) mesitylene (15)** Yield: 40%;  $^1\text{H}$  NMR (300 MHz,  $\text{CDCl}_3$ )  $\delta$  7.95 (m, 12H, CHCH), 7.56 (m, 12H, CHCH), 7.15 (d,  $J = 9.0$  Hz, CHCH), 5.25 (s, 6H,  $\text{CH}_2$ );  $^{13}\text{C}$  NMR (75 MHz,  $\text{CDCl}_3$ )  $\delta$  161.83(CO), 155.52(CCO), 147.44(OCCH), 144.88(CCH<sub>2</sub>O), 137.22(CHCH), 133.81(CHCH), 132.28(CHCH), 131.20(CHCH), 129.26(CHCH), 126.23(CHCH), 124.14(CHCH), 117.26(CHCH), 115.51(CHCH), 69.69( $\text{CH}_2$ ). FTIR (solid, HATR,  $\text{cm}^{-1}$ ): 3404, 1849, 1597, 1508, 1346, 1255.

## Relative Quantum Yield Determination

### Solution Studies

Using equimolar solutions of the tethered dimers or trimer (**4 – 7**), relative quantum yield determinations were performed using (4-methoxyphenyl)-phenylcyclopropenone (**2**) ( $\Phi = 0.7$ ) as an internal standard in a Rayonet photochemical reactor using 312nm lamps (BLE-8T312). Quantitative conversion of **5 – 7** produced the corresponding alkynes **12 – 15** in 100% yield with no detection of secondary photoproducts. However, conversion of **4** showed the presence of the product alkyne, as well as the half reacted dimer.

## Nanocrystalline Suspensions

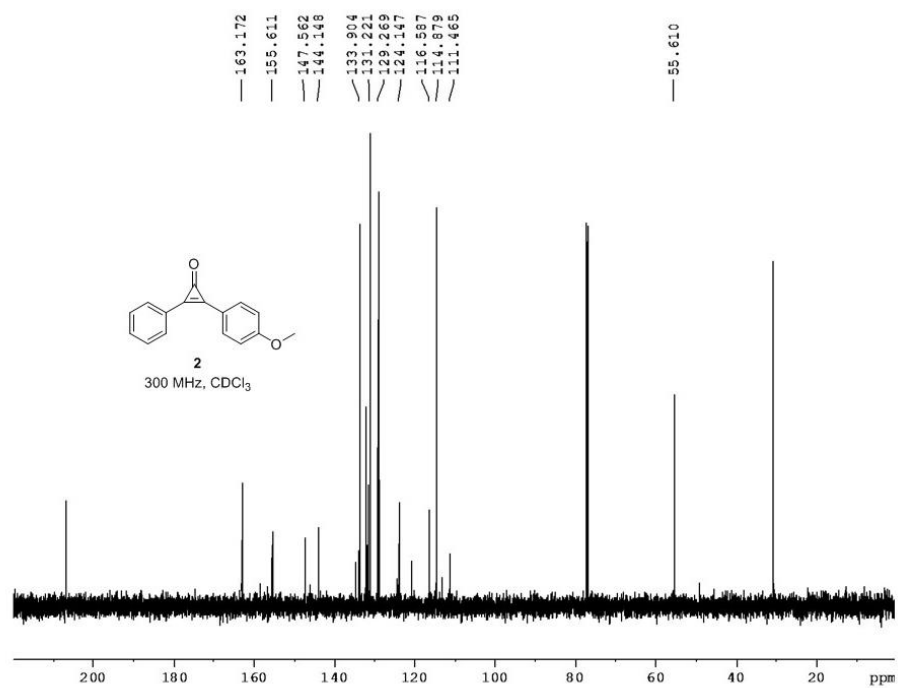
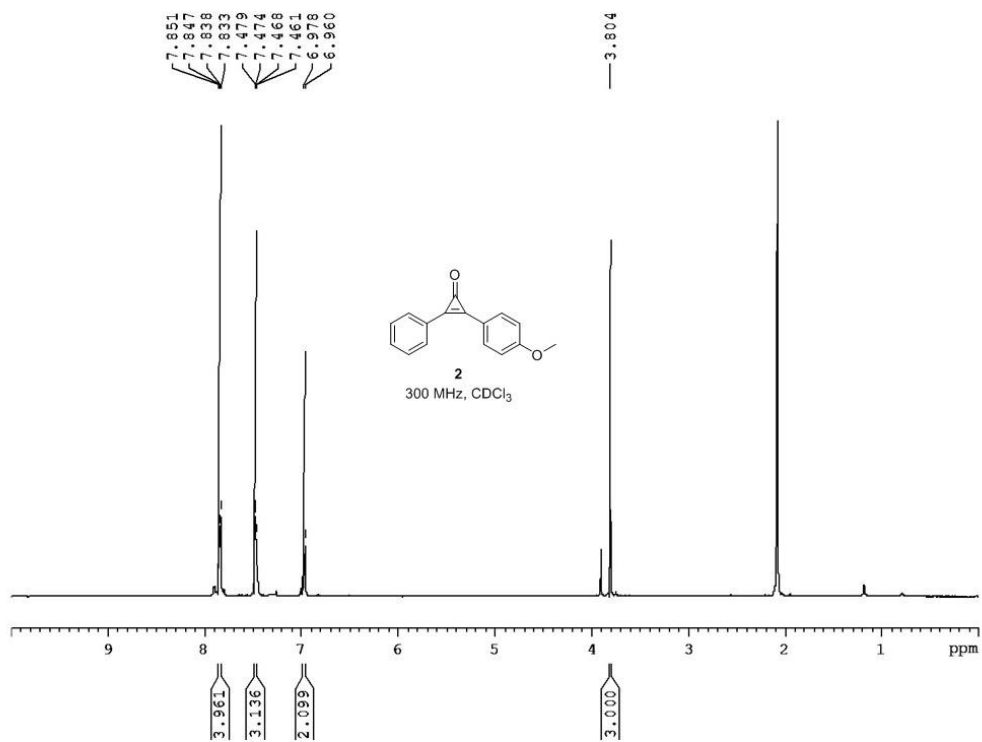
Relative quantum yield determinations were performed using dicumyl ketone ( $\phi = 0.2$ ) as an actinometer. Reactions were carried out in a Rayonet photochemical reactor using BLE-8T312 lamps (312 nm) or BLE-8T365 lamps (365 nm) with equimolar, optically dense solutions of actinometer and substrate. The solutions of each were prepared separately, and then combined immediately prior to photolysis in a quartz Erlenmeyer flask. Samples were irradiated for 2 minutes total, with aliquots being taken every 20 seconds. Each aliquot was extracted with chloroform-d, washed with brine, and dried over sodium sulfate. The extent of product formation was determined by  $^1\text{H}$  NMR. The extent of dicumyl formation was determined by gas chromatography. (The cyclopropanone derivatives could not be analyzed via gas chromatography, due to thermal decarbonylation taking place.)

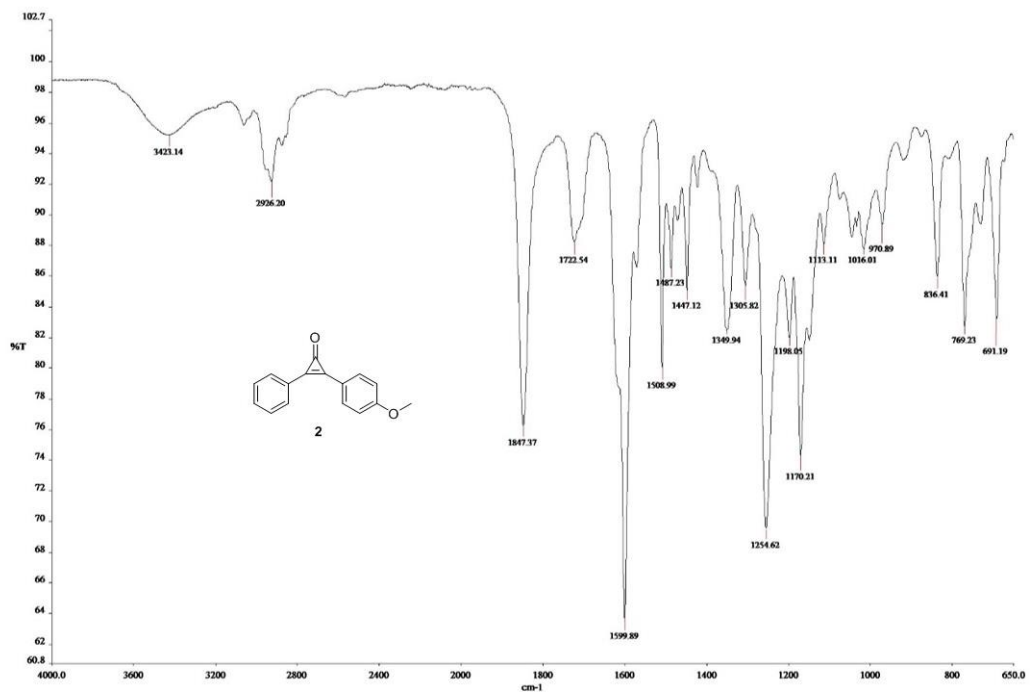
## 4. 6. Appendix

### Characterization for Chapter 4

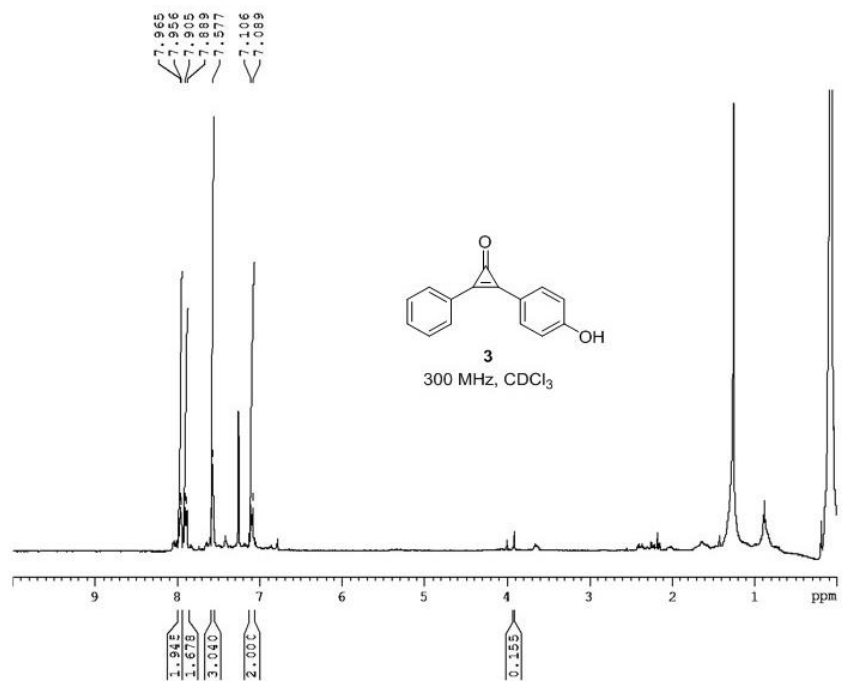
$^1\text{H}$ , $^{13}\text{C}$ , and IR for <b>2</b> .....	131
$^1\text{H}$ , $^{13}\text{C}$ , and IR for <b>3</b> .....	132
$^1\text{H}$ , $^{13}\text{C}$ , and IR for <b>4</b> .....	134
$^1\text{H}$ , $^{13}\text{C}$ , and IR for <b>5</b> .....	135
$^1\text{H}$ , $^{13}\text{C}$ , and IR for <b>6</b> .....	137
$^1\text{H}$ , $^{13}\text{C}$ , and IR for <b>15</b> .....	138

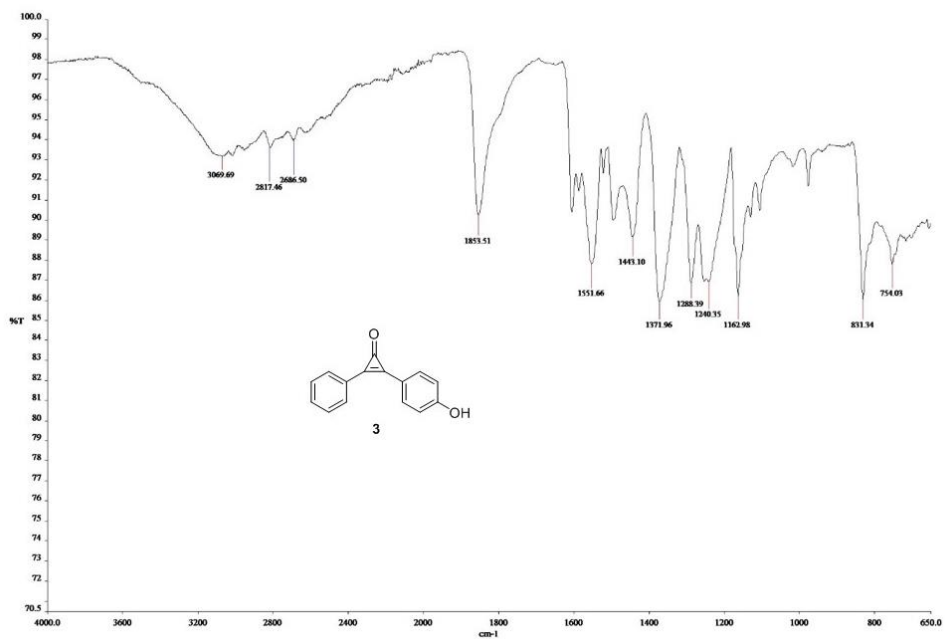
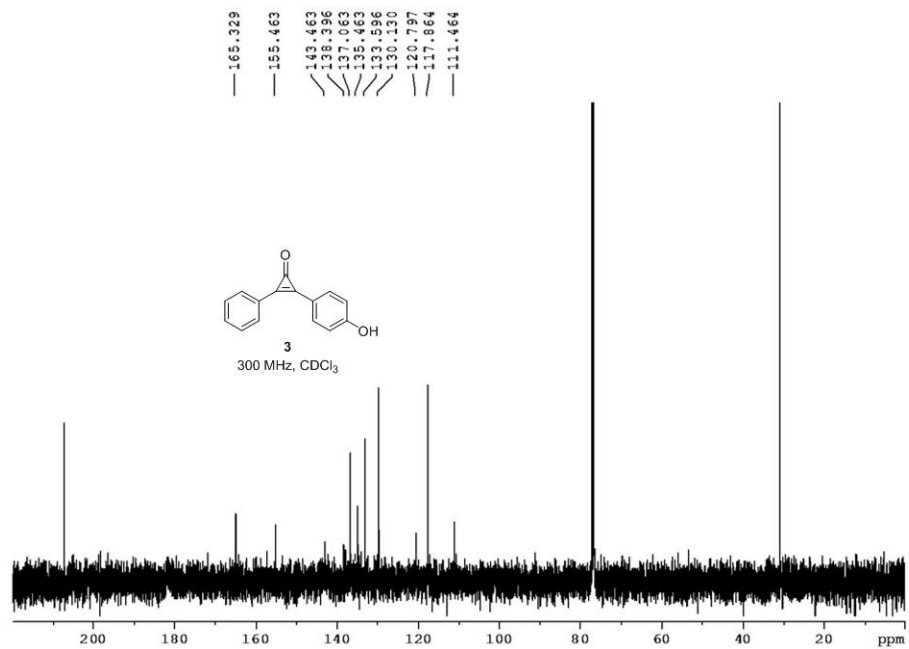
**(4-methoxyphenyl)-phenylcyclopropenone (2)**





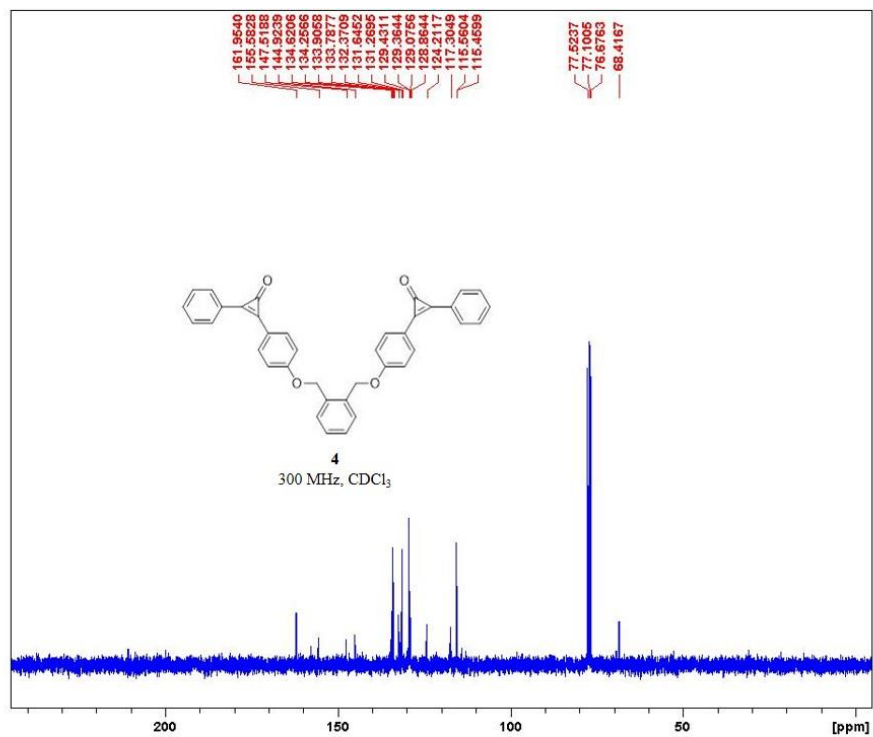
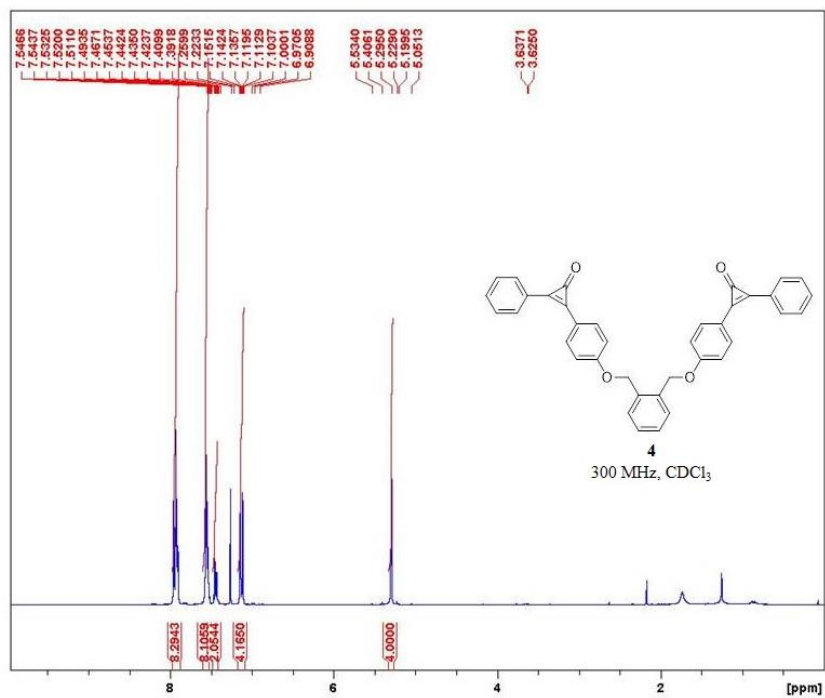
**(4-hydroxyphenyl)-phenylcyclopropenone (3)**

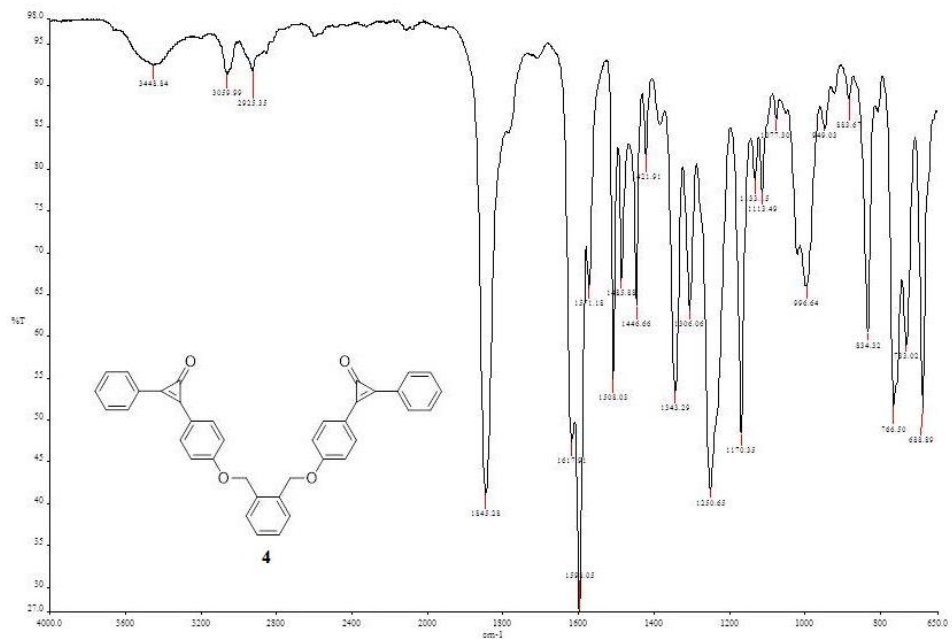




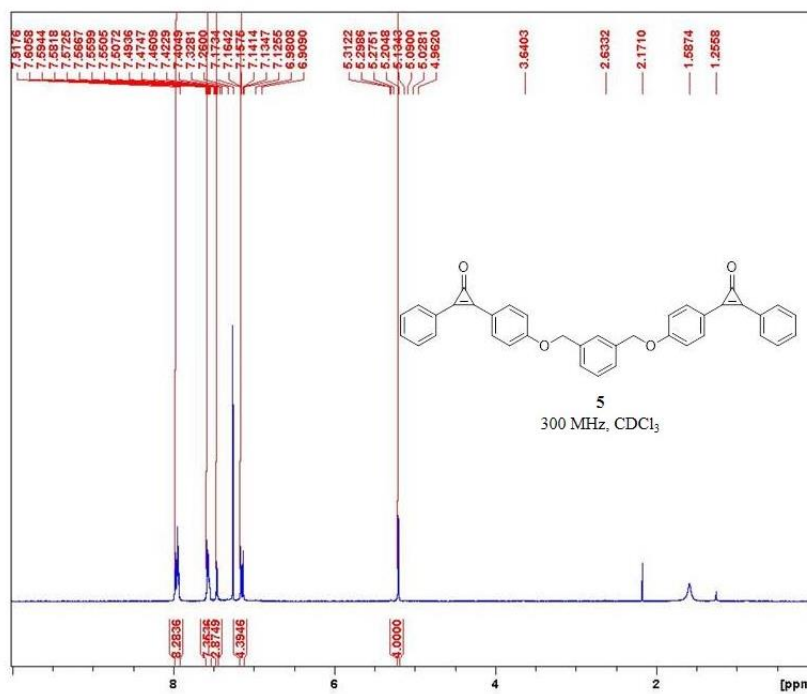


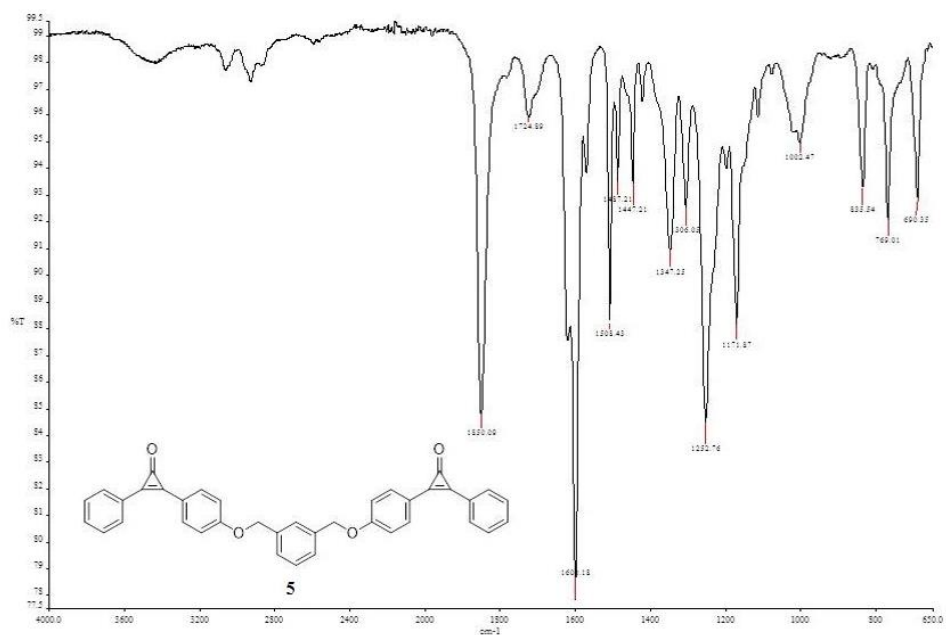
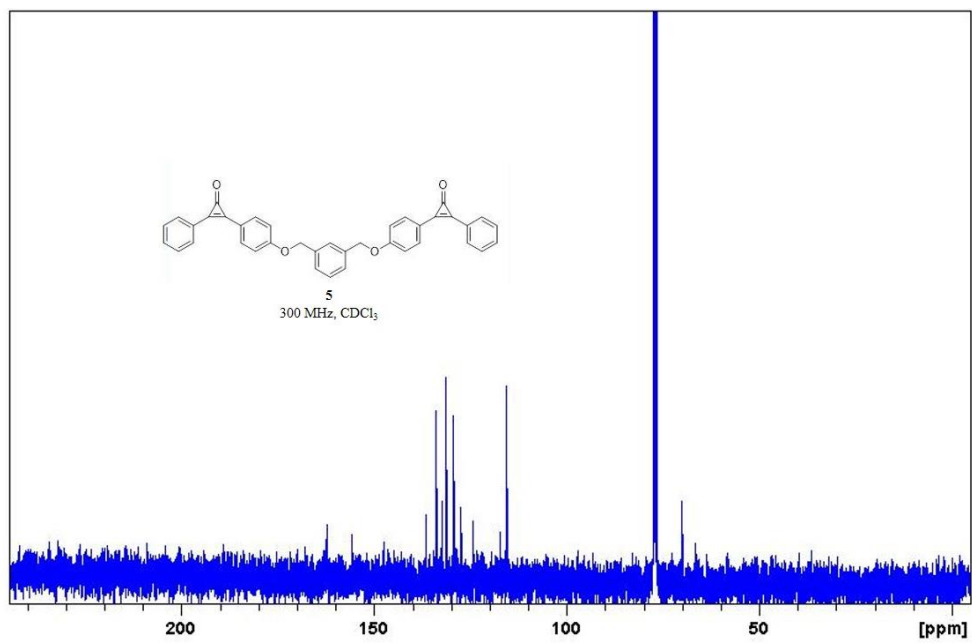
***o*-di(4-phenoxy (phenylcyclopropenone) xylene) (4)**



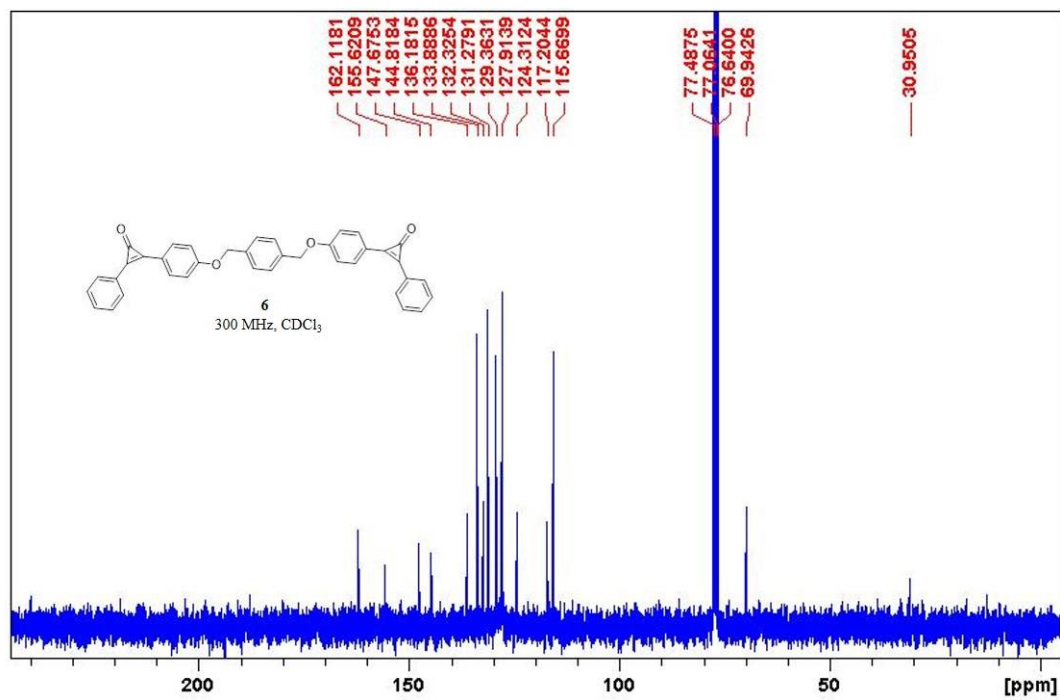
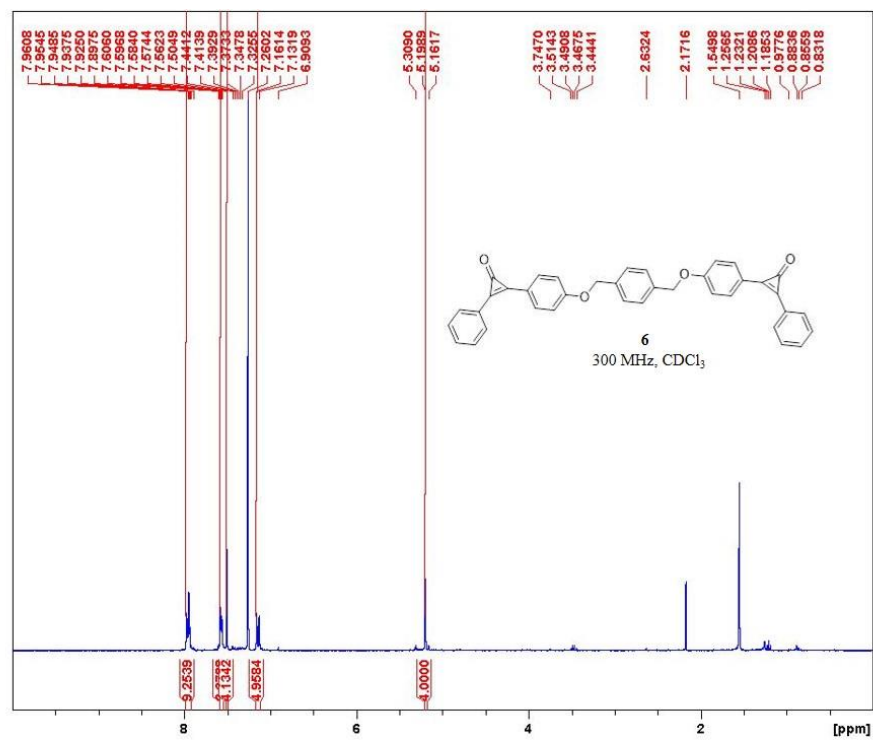


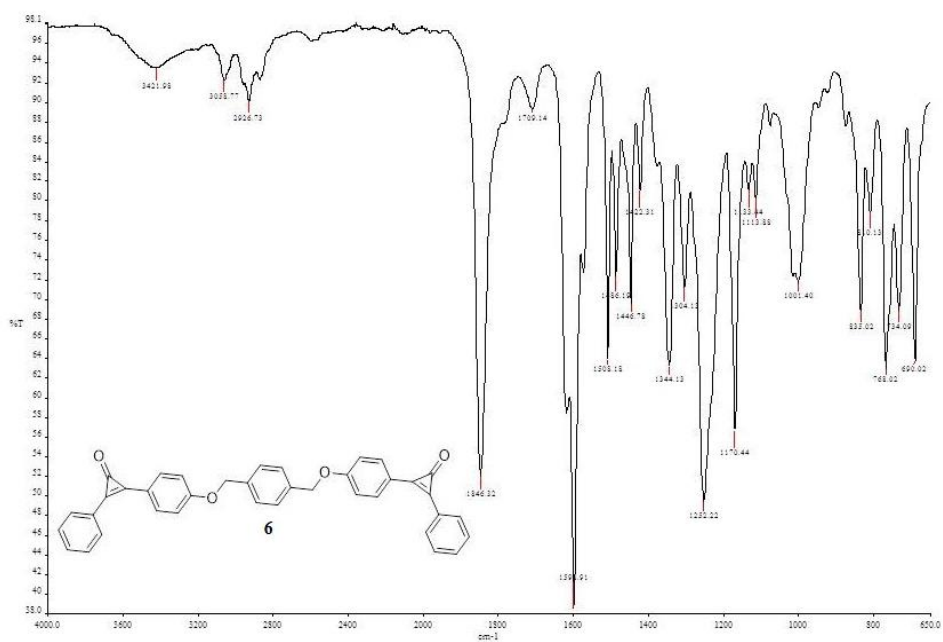
***m*-di(4-phenoxy (phenylcyclopropanone) xylene (5)**



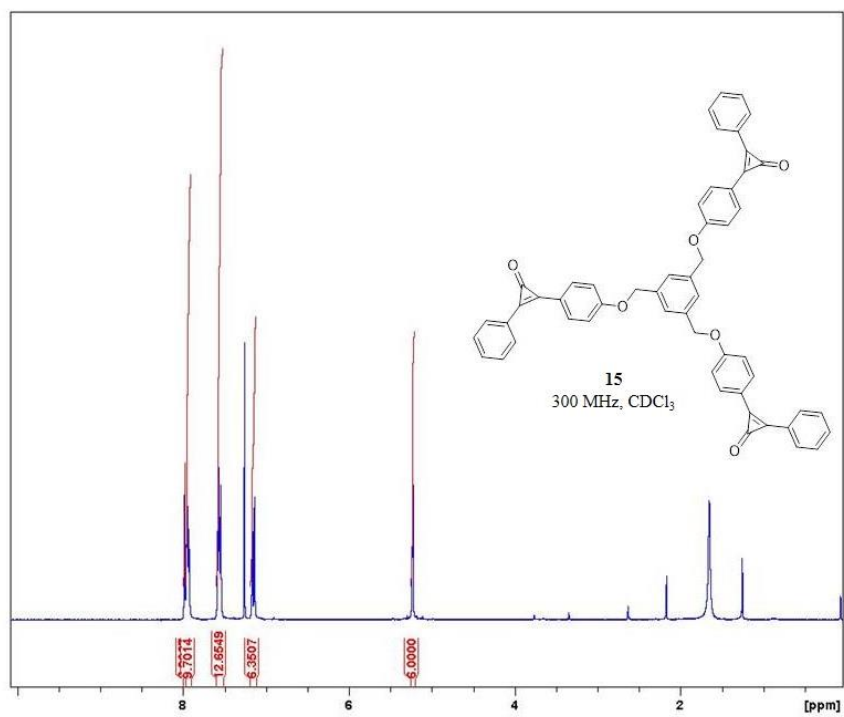


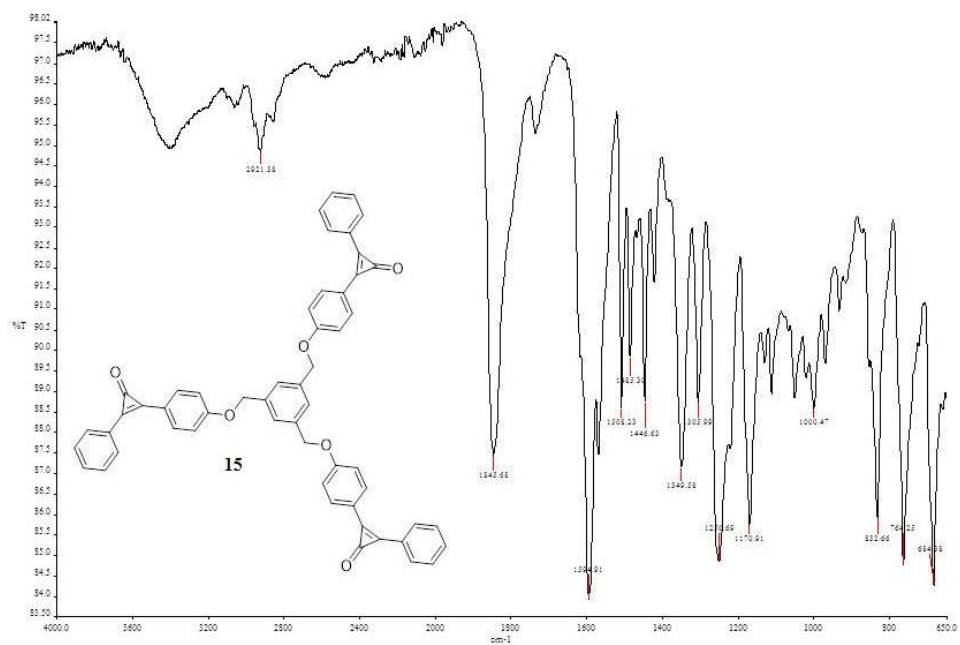
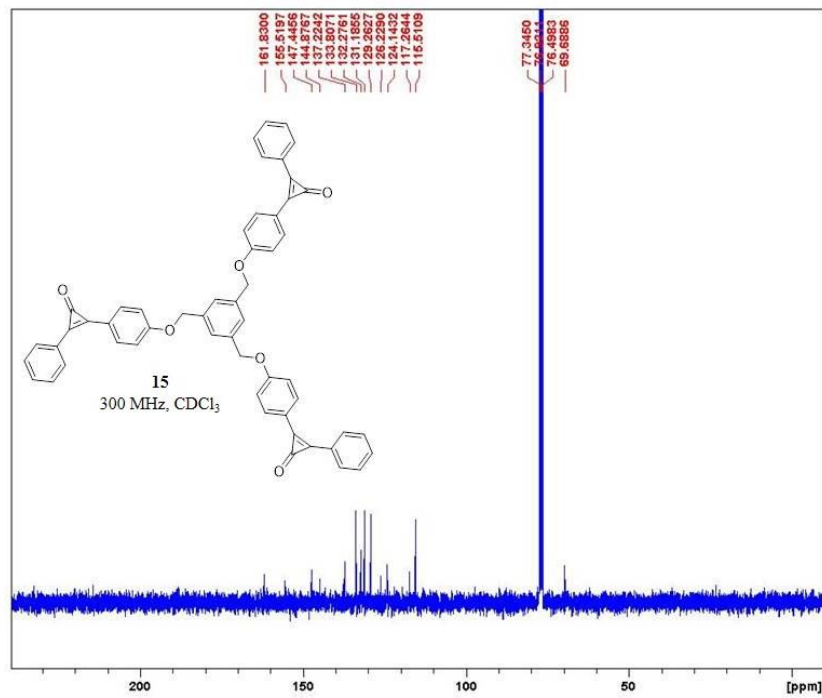
*p*-di(4-phenoxy (phenylcyclopropenone) xylene) (6)





**1, 3, 5-tri(4-phenoxy (phenylcyclopropenone) mesitylene (15)**





## **Chapter 5**

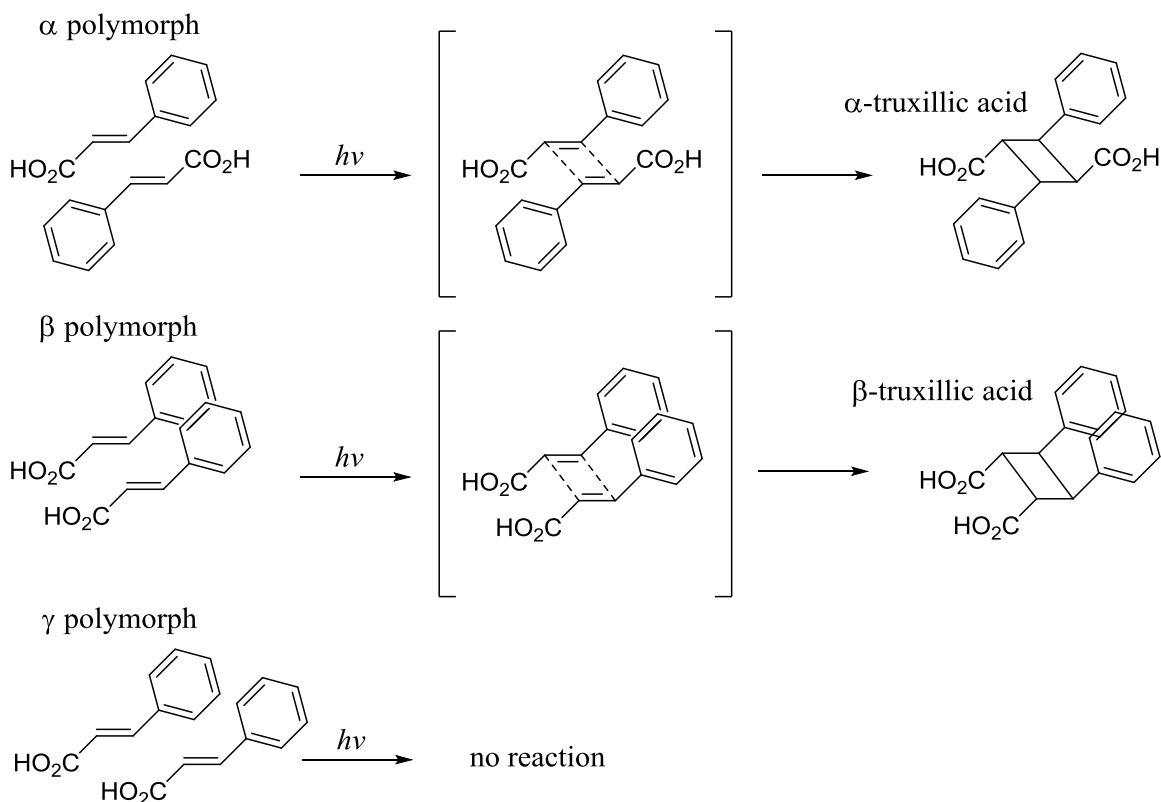
### **Photo-Induced Decarbonylation of Crystalline Biaryl Cyclopropanones with Bulky Substituents: Insights into Reactions that Challenge the Topochemical Postulate**

## 5. 1. Introduction

The topochemical postulate, a general set of rules formulated for reactions in crystals, was initially suggested by Kohlshutter<sup>112</sup> in 1918. The postulate stated that reactions in the solid state could only take place with a minimum amount of atomic and molecular motion, due to the physical constraints of the crystal lattice. This postulate was later supported and validated by the work of Schmidt and Cohen in 1964<sup>113</sup> while studying the solid state photo-induced dimerization of *trans*-cinnamic acid, when they observed that reaction outcomes in organic crystals seemed to be controlled by the relative orientations and geometries of the molecules in the crystal lattice.<sup>114</sup> *Trans*-cinnamic acid is known to exist in three separate crystal polymorphs:  $\alpha$ ,  $\beta$ , and  $\gamma$ .<sup>115</sup> Recognizing that product formation from their potential [2+2] dimerization reaction was different for all three polymorphs, they studied the impact of molecular orientation and distance on the photochemically induced dimerization in the solid state via single crystal x-ray crystallography analysis. As is illustrated in **Scheme 5. 1. 1**, the three crystal polymorphs of *trans*-cinnamic acid differ from each other in both their orientation and their spacing relative to their nearest neighbor. Schmidt and Cohen observed that both the  $\alpha$  and  $\beta$  polymorphs reacted under photochemical conditions in the solid-state to give the corresponding  $\alpha$  or  $\beta$  truxillic acid, but that the remaining polymorph,  $\gamma$ , failed to dimerize under identical conditions. It was deduced by Schmidt that, in the solid-state, the photochemical [2+2] reaction could only take place when the two-reacting double bonds were parallel and at a distance of less than 4.1 Å from each other.



**Scheme 5. 1. 1.** Solid-state dimerization of *trans*-cinnamic acid.

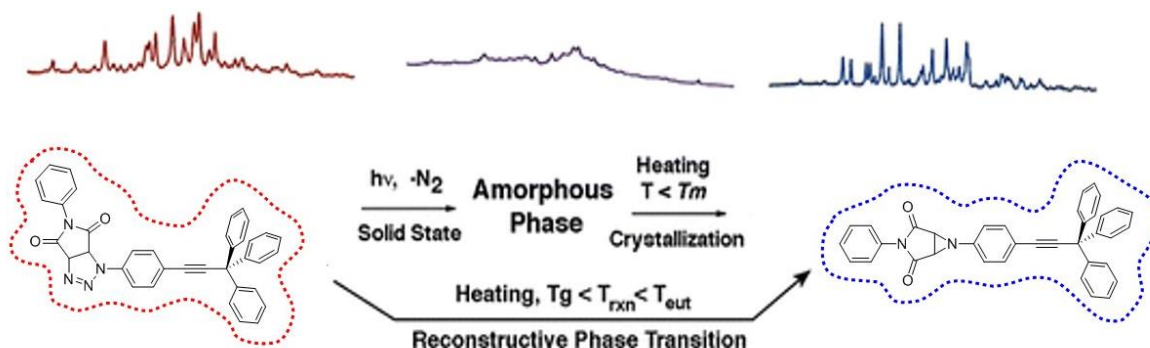


This study, in particular, led to the development and greater acceptance of the topochemical postulate. In very general terms, the postulate stated that: a) Reactions in crystals took place, but only with a minimum amount of atomic and molecular motion, and b) Due to the structural rigidity of the crystal lattice, the crystal packing and molecular geometry had a greater impact on reaction outcomes than intrinsic reactivity.

In research recently published by our lab,<sup>116</sup> it was shown that the solid state photo-induced de-nitrogenation of triazolines with bulky substituents to aziridines could take place via a solid-to-solid transformation, despite the large structural changes that were required for product formation, seemingly in violation of the topochemical postulate. Through this study, aided by powder x-ray diffraction (PXRD), thermogravimetric analysis (TGA), dynamic scanning calorimetry (DSC),

solid state FTIR Spectroscopy, and  $^{13}\text{C}$  CPMAS NMR, it was found that the solid state photoreactions could occur via metastable phases that were susceptible to amorphization or through reconstructive phase transitions (**Figure 5. 1. 2**).

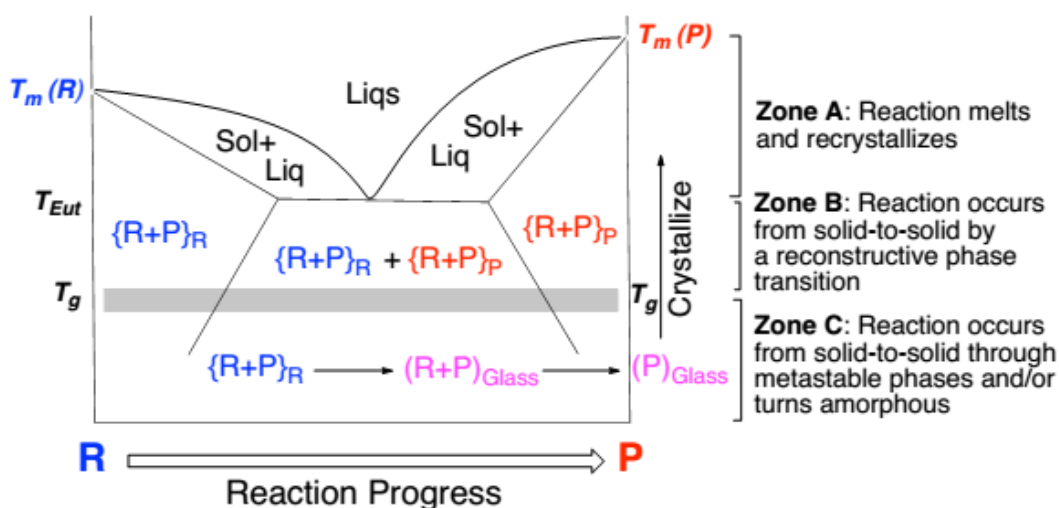
**Figure 5. 1. 2.** Solid-state de-nitrogenation of triazolines with bulky substituents.



This study was able to lend support to the proposal of an alternate definition of the topochemical postulate,<sup>117</sup> from an energetic viewpoint: Reactions in crystals typically require conditions where chemical reactions can take place even if the kinetic energy of the reacting molecules is minimal, which requires substrates that possess, or can acquire, large amounts of potential energy.

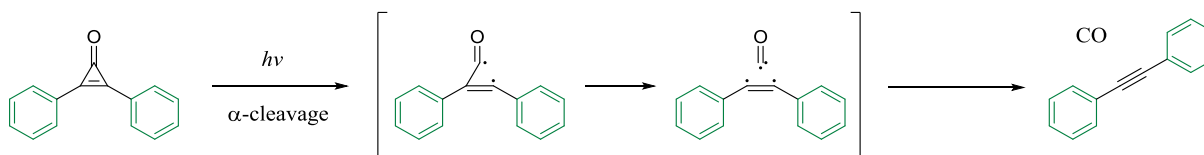
From a topochemical perspective, reactant-like transitions states are the most ideal, as they would require only minimal structural changes as they progressed to product formation. It has been suggested, via the Hammond Postulate,<sup>112</sup> that substrates high in potential energy tend to have early, reactant-like, transitions states which tend to have relatively low activation barriers (**Figure 5. 1. 3**).

**Figure 5. 1. 3.** Phase diagram of solid state triazoline denitrogenation reaction progress.



When studying solid state photoreactions in our group, the rational design of a substrate is crucial. Many of our studies focus on the use of materials that incorporate high ring strain, like that found in a cyclopropenone. These cyclopropenones, when reacted with a photon, are unable to react in the reverse reaction, which helps to drive the reaction forward. One such project in our group focused on the Norrish type I reaction of diphenylcyclopropenone. The cyclopropenone moiety is so highly strained that the reaction, once alpha cleavage commenced, the remainder of the reaction pathway was essentially irreversible (**Scheme 5. 1. 2**).

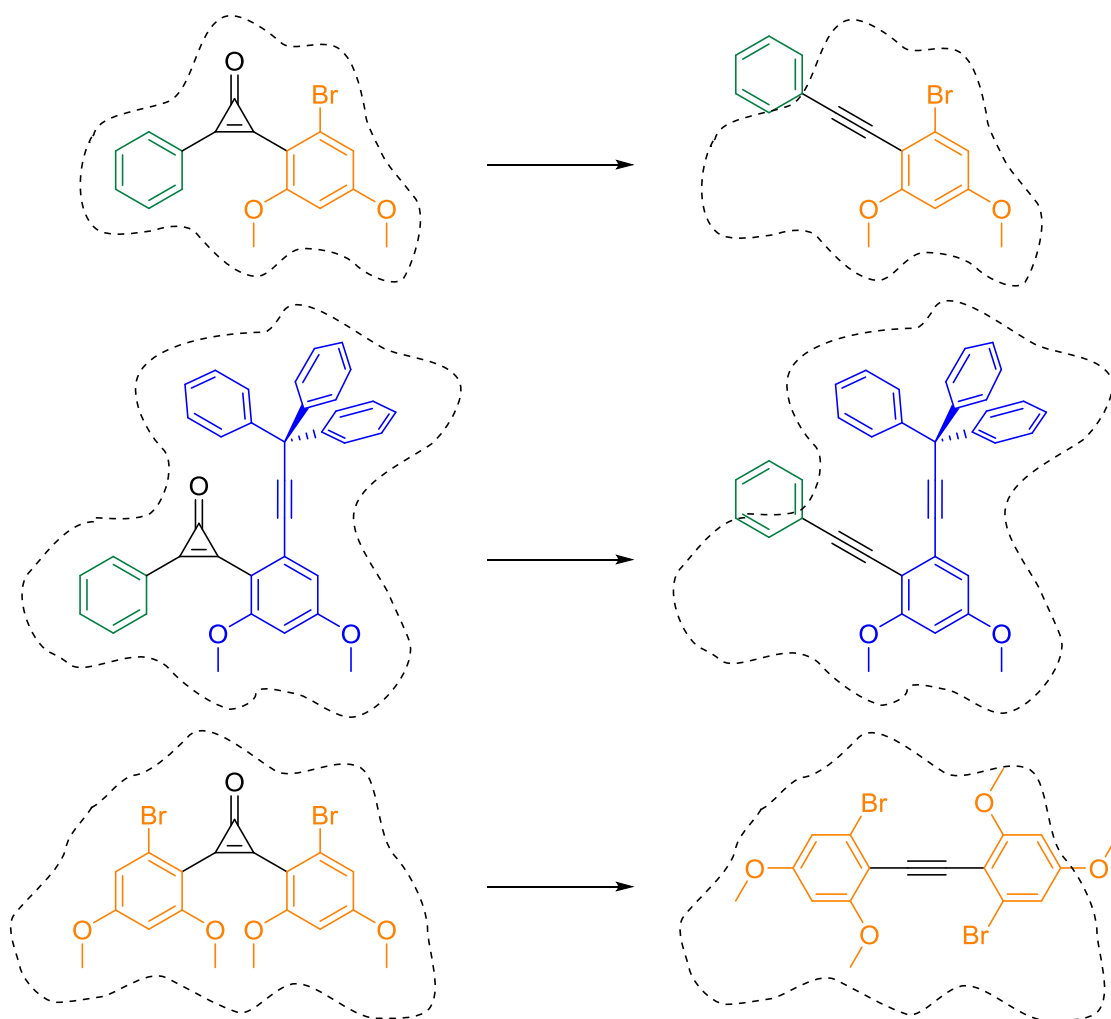
**Scheme 5. 1. 2.** Photoinduced decarbonylation of diphenylcyclopropenone.



Published research in our lab has previously revealed that the solid state photochemical reactions for diphenylcyclopropenone to diphenylacetylene in nanocrystalline suspensions takes

place with a photonic amplification of up to 1100% and absolute quantum yields of up to 3.3 reactions per photon.<sup>22</sup> However, phase changes that may take place in the solid state photolysis of cyclopropanones, and the impact that bulky substituents might have upon them, have not been previously studied. We decided to pursue the study of diphenylcyclopropanones with similarly bulky substituents as had been previously explored with triazolines to test the limits of the topochemical postulate. We thought the size and orientation of the cyclopropanone and its substituents might have an impact on the solid state photolysis (**Scheme 5. 1. 3**).

**Scheme 5. 1. 3.** Solid-state photolysis of cyclopropanones.

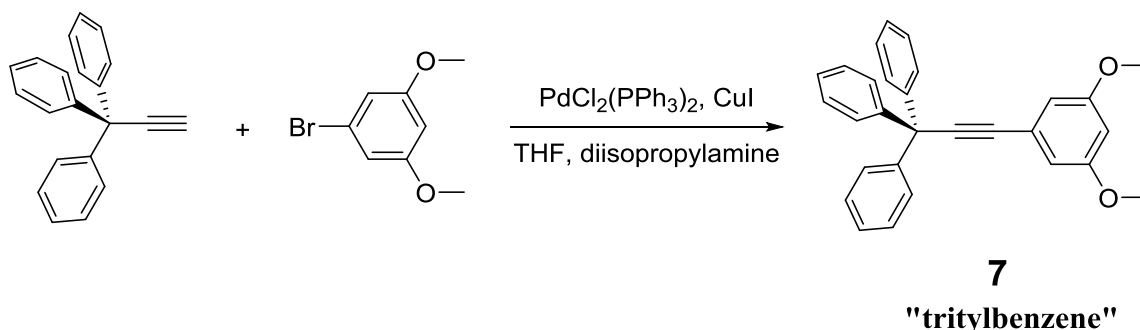


## 5. 2. Results and Discussion

### Synthesis and Design of Cyclopropenones with “Bulky” Substituents

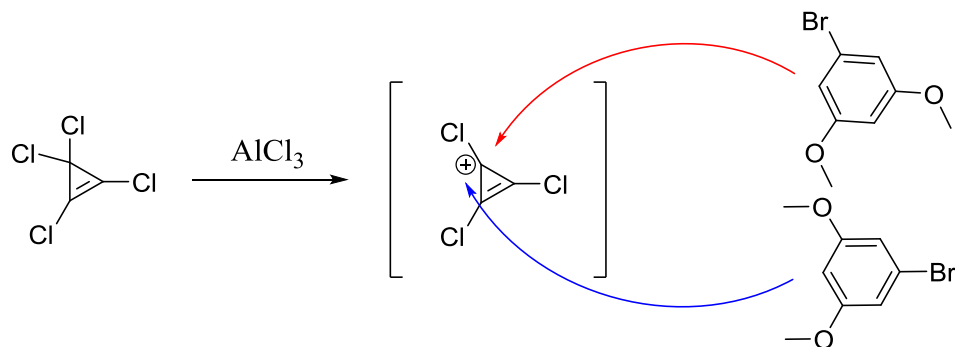
The set of compounds tested was designed around previously utilized methodology for the formation of symmetric and asymmetric aryl cyclopropenones via a Friedel-Crafts reaction on tetrachlorocyclopropene. We incorporated either benzene, 1,3-dimethoxy-4-bromobenzene, or a 1,3-dimethoxy-4-(3'3'3'-triphenylpropinyl benzene) (tritylbenzene) as the bulky aryl groups. The substituents ranged in size from “small” (benzene) to “medium” (3, 5-dimethoxy-bromobenzene) to “large” (tritylbenzene) (Scheme 5. 2. 1).

**Scheme 5. 2. 1.** Synthesis of tritylbenzene, the largest substituent utilized in this study.



The compounds were synthesized from commercially available tetrachlorocyclopropene (**1**) in three steps via utilization of a Friedel-Crafts reaction in DCM at -78°, with yields ranging from 40-65%. The products were purified via column chromatography (silica gel, 3:1 hexane:acetone) and recrystallized from methylcyclohexane with 10% DCM. All compounds were characterized by <sup>1</sup>H and <sup>13</sup>C NMR, IR, and UV-Vis. It was in this step that we noticed an interesting result in the substitution pattern on the “tritylbenzene”. Based upon previous synthetic experience with similar substrates, we had predicted that the cyclopropenium cation would be attacked by an aromatic ring with a position *ortho* to both methoxy groups and *para* to the alkyne (or bromide) (Scheme 5. 2. 2).

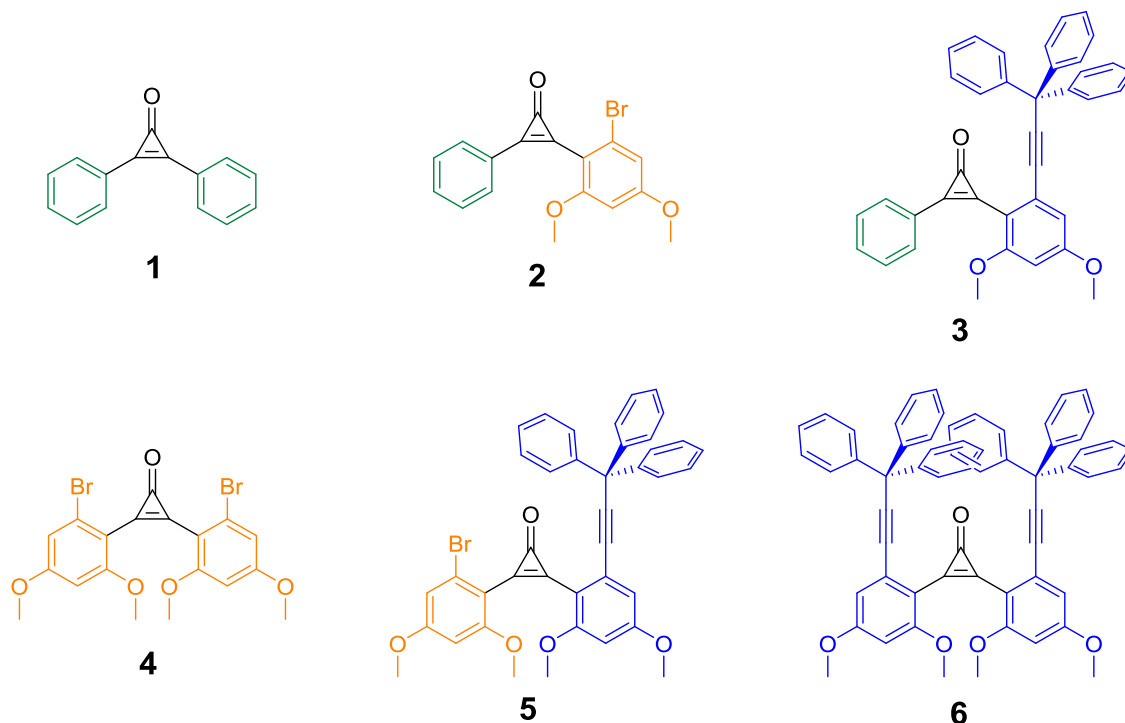
**Scheme 5. 2. 2.** Predicted attack on cyclopropenium cation.



However, during the process of characterization, we observed formation of the cyclopropenone in a position that was *ortho* to a methoxy group and the alkyne or the bromine, and *para* to the second methoxy group. In all cases this was the only product formed – we did not observe addition at the 4 position (between both methoxy groups). Our crystal structures corroborated our finding, and provided an additional explanation for our observations. While the precedent for substitution based upon electron donating substituents had been established, we had not previously explored the impact sterically bulky substituents and crowding would have on the asymmetric Friedel-Crafts reaction. The crystal structures revealed that, even though the tritylbenzene was much larger in size than the methoxy groups, the alkyne actually held the bulky trityl group farther away from the reaction center and created more space than what was present with the methoxy groups. From observation of our structure, it was also apparent that the methoxy hydrogen atoms created steric crowding around the reaction center. This was also observed in reactions with 3,5 *bis*-methoxy bromobenzene. It seems logical, then, to conclude that this trend, in both cases, was caused by steric crowding and not due to other electronic or steric effects. While these compounds were different than the ones originally intended and designed for the study, we quickly realized that these new compounds could potentially create some interesting results, as reaction to form the alkyne now would involve the movement of the trityl group or groups over

the reaction center (**Chart 5.2.1**). This could potentially be a greater steric test of the topochemical postulate than the compounds originally planned.

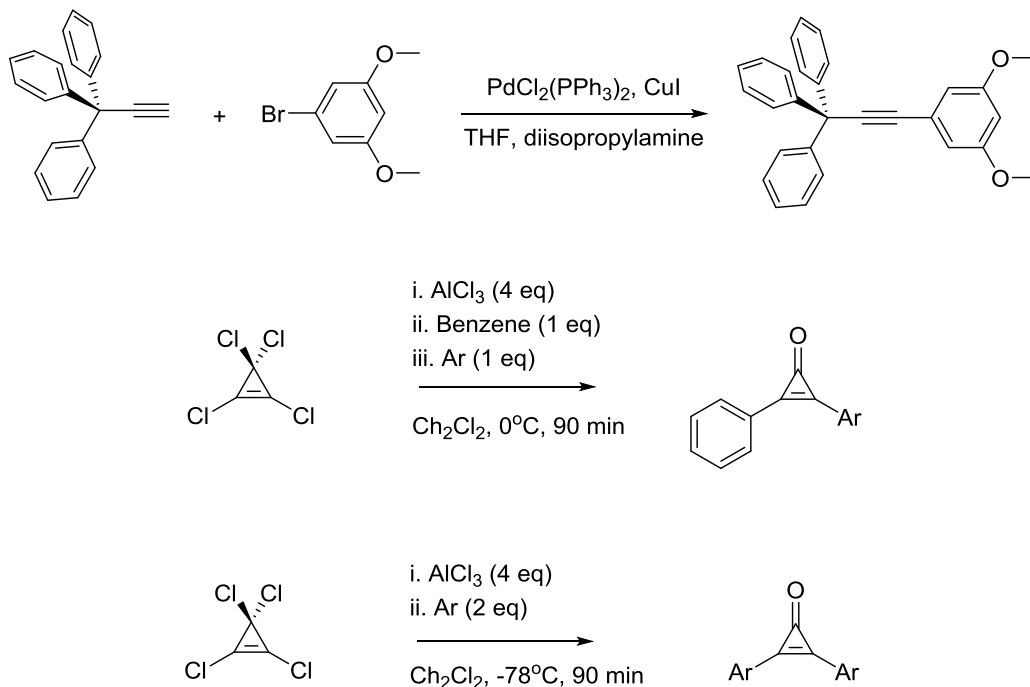
**Chart 5.2.1.** Set of cyclopropenones designed to test the limits of the topochemical postulate.



Unfortunately, synthesis of cyclopropenone **5** and cyclopropenone **6** proved to be synthetically challenging. Previous syntheses of asymmetric cyclopropenones had been successful when there was a large electronic difference between the two aromatic substituents. We had previously discovered that addition of the “less reactive” substituent to the reaction, usually benzene, first led to greater overall synthetic yields, especially when the second added substituent had an electron donating group, such as the methoxy in anisole. Though many variations and iterations of the modified Friedel-Crafts reaction were attempted, synthetic yields of **5** were too low to be included in this study. Synthesis of symmetrically substituted cyclopropenones was often low yielding, even with highly reactive substituents featuring electron donating groups.<sup>53</sup> Attempts to synthesize cyclopropenone **6** resulted in complex mixtures that were difficult to purify.

In contrast to this, synthetic yields of symmetric cyclopropenone **4** were quite good (**Scheme 5. 2. 3**).

**Scheme 5. 2. 3.** Synthetic route to cyclopropenones with bulky substituents.

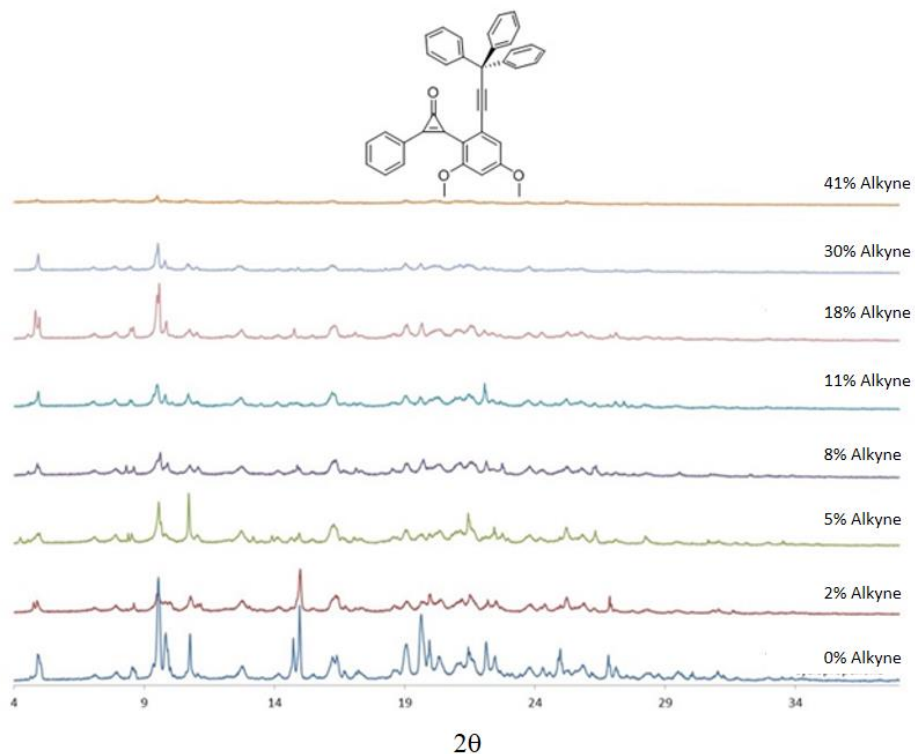


### Photochemical Reactions and PXRD Analysis as a Function of Reaction Progress

When crushed crystalline powders of **2**, **3**, and **4** were exposed to 312 nm light at room temperature, the photolysis formed the corresponding alkynes as the only products. Full conversion to products took place within 60 minutes, as monitored via  $^1\text{H}$  NMR at 10-15 minute intervals. The solid state photolysis was also monitored via PXRD of the samples, in the range of  $2\theta = 5 - 50^\circ$ . Prior to reaction, all three crystalline cyclopropenones showed Bragg reflections characteristic of crystalline materials, as did the corresponding recrystallized photoproducts. PXRD experiments were then conducted on the three cyclopropenones as a function of conversion, with samples taken from the photoreaction for characterization every 10-15 minutes.

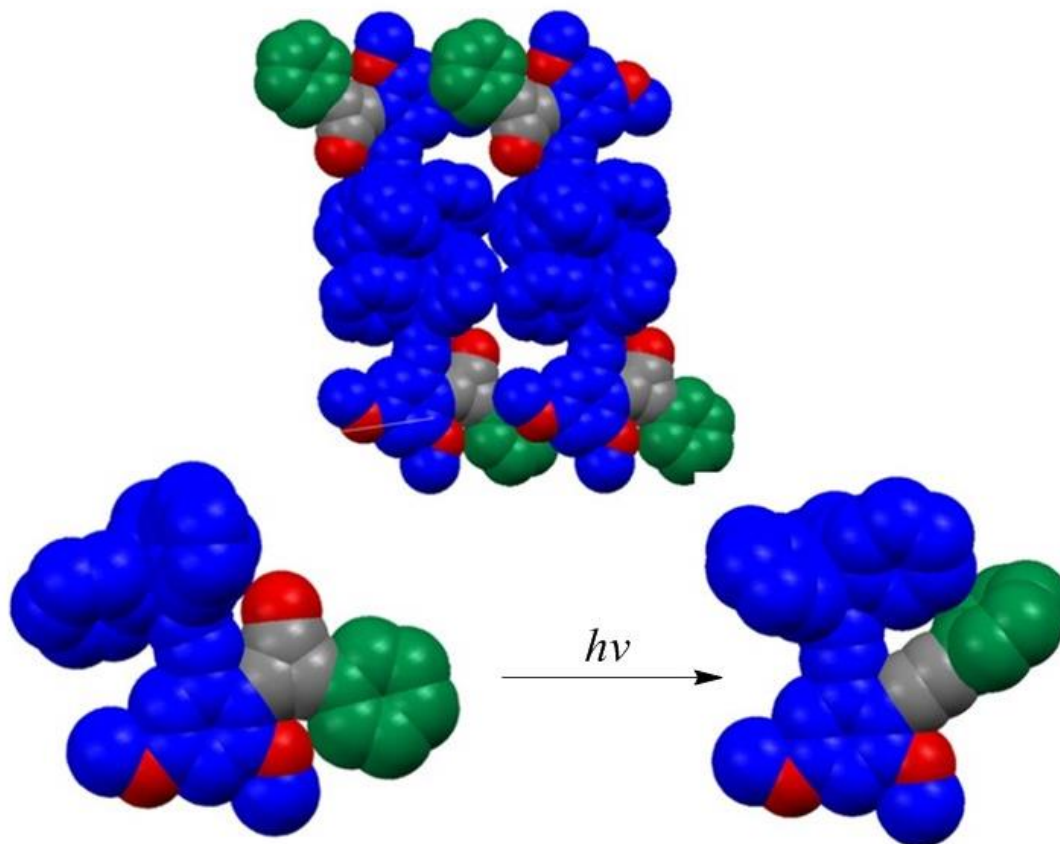


**Figure 5. 2. 1.** PXRD of cyclopropenone **3** as a function of conversion.



We began our study with cyclopropenone **3**, and observed that, while the material was initially quite crystalline, as indicated by the tall sharp peaks in the PXRD (**Figure 5. 2. 1**), at relatively low conversions (less than 20 % conversion to corresponding alkyne) the material became amorphous with extended reaction times and greater conversions. This was not a surprising result. The crystal structure obtained of the starting material shows a six-fold trityl embrace<sup>118</sup> (**Figure 5. 2. 2** Top, in blue) as part of the structure, which may be a key piece of evidence for the apparent amorphization observed with reaction progress.

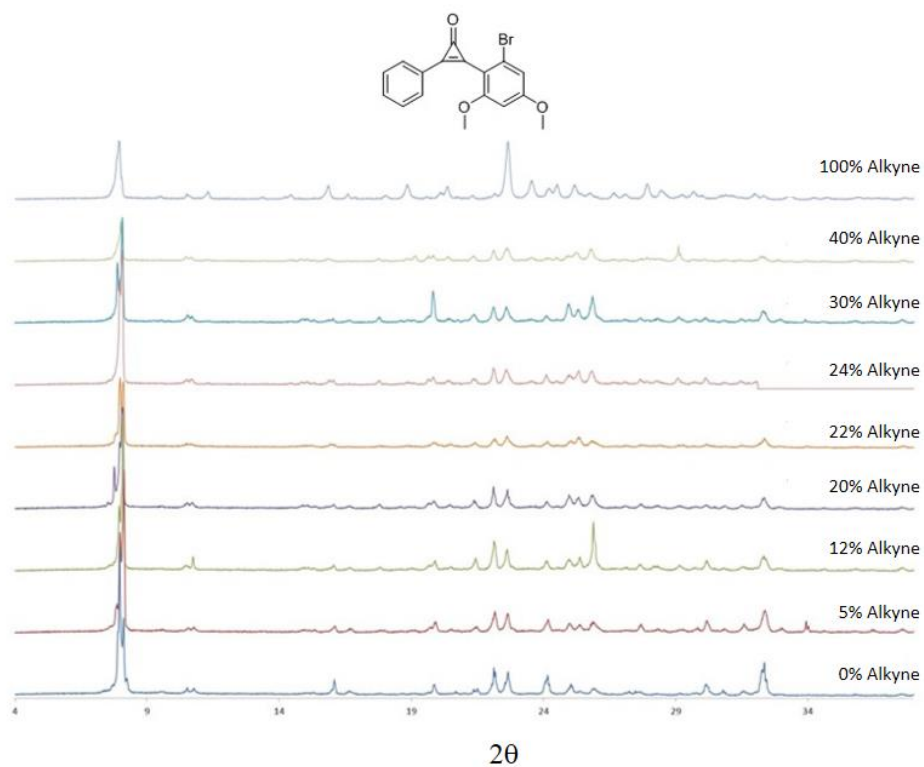
**Figure 5. 2. 2.** Crystal structure of cyclopropenone **3** and the corresponding alkyne.



While the six-fold trityl embrace might enhance the crystallinity of cyclopropenone **3**, it also would provide a great deal of structural rigidity to the crystal lattice, locking the layers together like the gears in a clock. It is possible that upon photolysis, this rigidity is weakened and the crystal lattice broken by the movement involved in the formation of the alkyne, as can be seen in the crystal structure. The smaller benzene substituent and the tritylbenzene, upon photolysis and formation of the alkyne, swing toward each other and simultaneously twist. (**Figure 5. 2. 2** Bottom) It is possible that this movement, even at low conversion rates, disrupts the electronic interactions supporting the crystal structure and causes the observed amorphization of the sample.

Very different, and potentially exciting, results were observed in cyclopropanones **2** and **4**. Cyclopropanone **2** was observed to be quite crystalline prior to photolysis as apparent in the tall and sharp peaks present in the PXRD of the compound. However, when subjected to identical reaction conditions as cyclopropanone **3**, cyclopropanone **2** showed no evidence of amorphization, and retained its crystallinity, even at extended reaction times (**Figure 5. 2. 3**).

**Figure 5. 2. 3.** PXRD of cyclopropanone **2** as a function of conversion.



Observing the obtained crystal structure of the compound (**Figure 5. 2. 4**), it is evident that the amount of molecular movement or rotation necessary for reaction to take place would be smaller than that required in the case of **3**, as both substituents on cyclopropanone **2** are smaller in size.

**Figure 5. 2. 4.** Crystal structure and packing of cyclopropeone **2**.

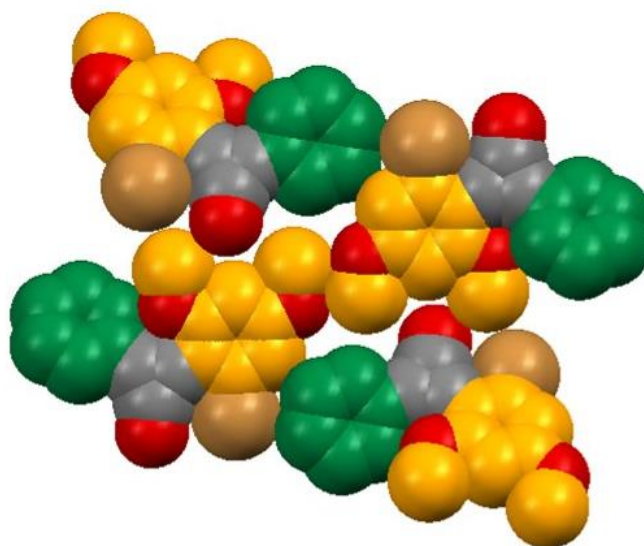
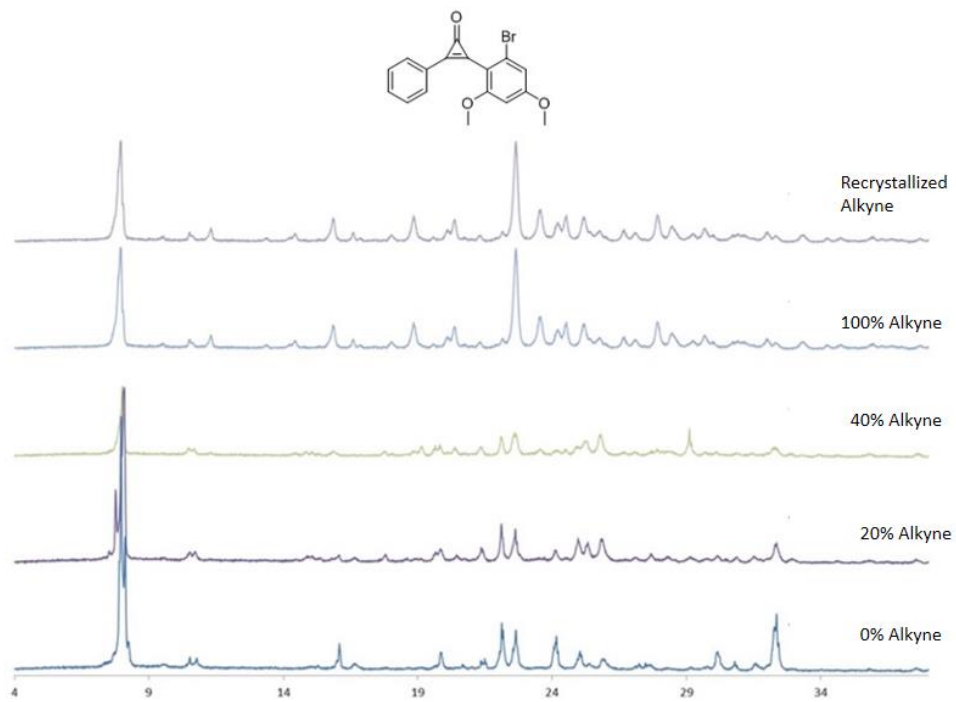


**Figure 5. 2. 5.** PXRD of cyclopropeone **2** illustrating a reconstructive phase transformation.

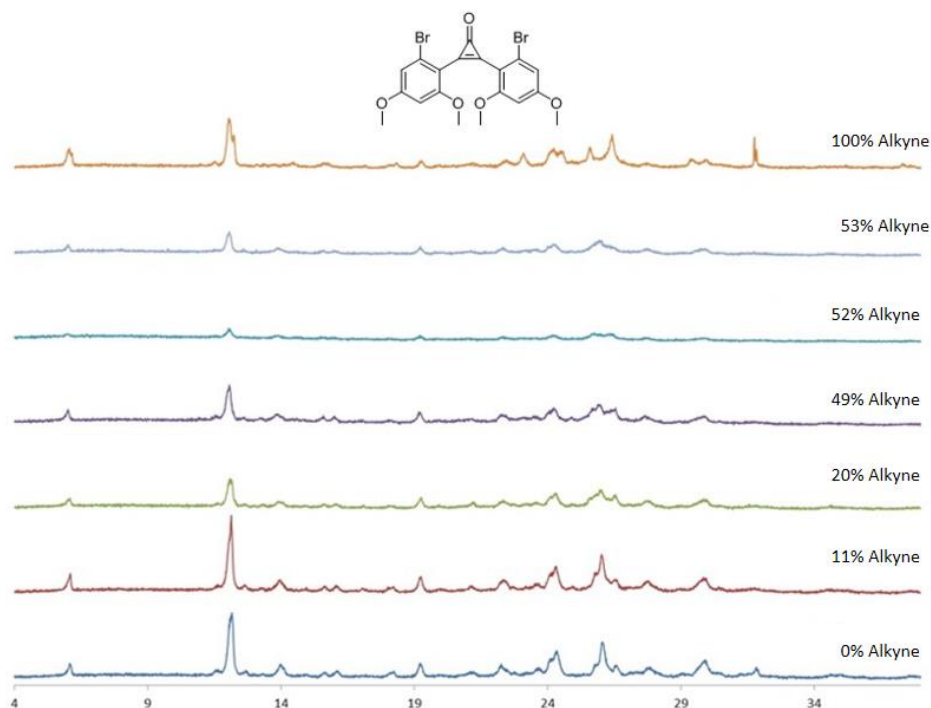


2θ

Closer inspection of the PXRD for cyclopropenone **2** and the recrystallized product revealed that an interesting transformation had taken place (**Figure 5. 2. 5**).

The PXRD of the solid state photolysis showed that the diffractogram evolved as a function of conversion, suggesting that the sample retained a high crystallinity, even at extended reaction times, which is an indication of a solid to solid reconstructive phase transition.<sup>119</sup> This was also supported by the finding that there are few changes or instances of broadening that took place in the PXRD as the reaction progressed. Additionally, the PXRD of the recrystallized product (**Figure 5. 2. 5 Top**) is very similar, if not the same, to the product obtained in the solid state photolysis prior to recrystallization (**Figure 5. 2. 5 Second from top**). This could indicate that the reaction progressed through a meta-stable phase prior to recrystallizing in the new product phase. This is evidence that cyclopropenone **2** underwent a solid to solid transformation, despite the steric bulk of the substituents.

**Figure 5. 2. 6.** PXRD of cyclopropenone **4** as a function of conversion.

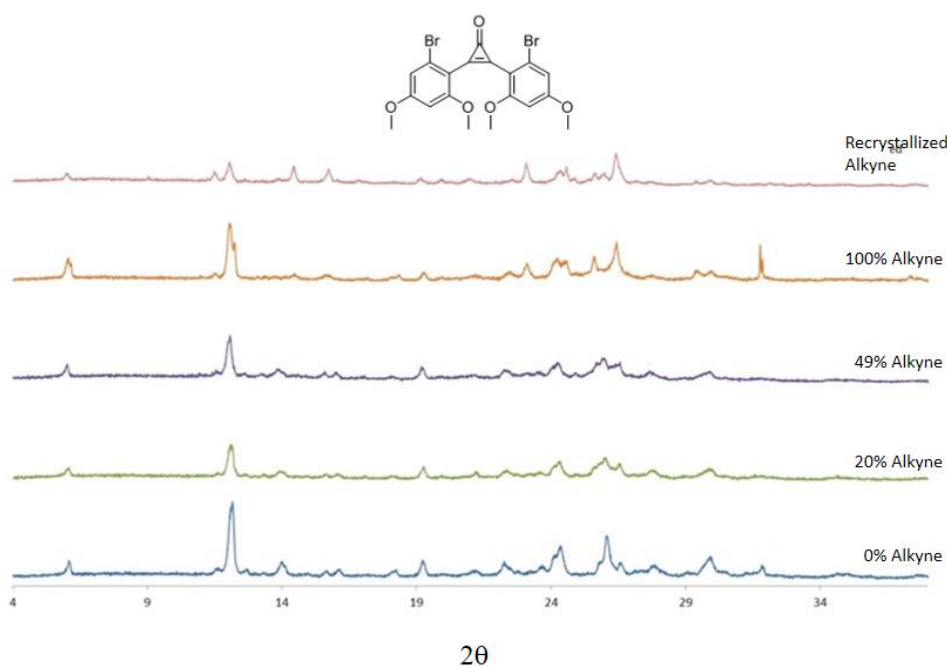


20

A similar observation was made during the solid state photolysis of compound **4**. While the peaks of compound **4** were not as sharp as those observed in compound **2**, compound **4** still appeared to retain crystallinity through the reaction, though with significant peak broadening in the PXRD (**Figure 5. 2. 6**).

Similar to the example above, closer inspection of the PXRD and the recrystallized endpoint indicated that the photoreaction progressed through a reconstructive phase transition (**Figure 5. 2. 7**).

**Figure 5. 2. 7.** PXRD of cyclopropenone **4**, illustrating a reconstructive phase transformation.

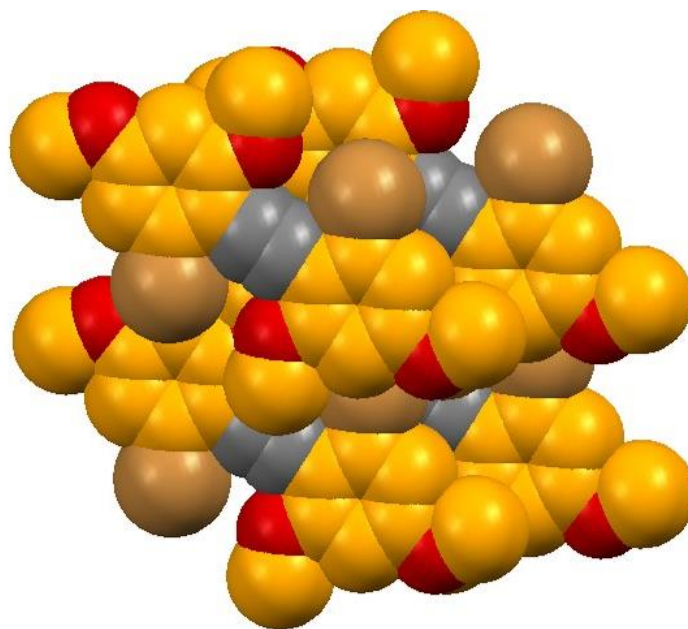


Though the PXRD did display some peak broadening, the recrystallized product is a good match for the photolyzed product (prior to recrystallization) (**Figure 5. 2. 7**), and also shows some great similarity to the crystalline starting material (**Figure 5. 2. 7** Bottom). While the PXRD showed evidence of peak broadening, it was difficult to determine if this was due to amorphization or as a result of the small sample size. Regardless of this, there was good evidence that the reaction

may have progressed through a reconstructive phase transition. Unfortunately, in this case, a crystal structure of the cyclopropanone **4** was not able to be obtained, as single crystals of x-ray quality could not be obtained.

From analysis of the crystal structure of the product (**Figure 5. 2. 8**), one can see that the bromine atoms on either side of the cyclopropanone adopt opposite sides in the plane of the molecule. However, conclusions regarding the nature of the transformation are difficult to make without the crystal structure of the starting material. This particular cyclopropanone was the only symmetric compound studied via this method. Perhaps this symmetry, paired with the “medium” sized bulky groups provided enough space in the crystal structure for reaction to take place with a minimal amount of rotational change or movement.

**Figure 5. 2. 8.** Crystal structure and packing for the photoproducts of cyclopropanone **4**.



### 5. 3. Conclusions

As advances continue for the analysis of solid state reactions and crystal engineering, chemists will close-in on a greater understanding of the mechanisms and reaction pathways in crystals, and will come closer to an understanding of the balance struck between innate reactivity and environmental constraints. In this study, a small set of compounds capable of acquiring a large amount of potential energy, in the form of excitation energy and ring strain, was examined under solid state photochemical conditions. One of the compounds was found to test the physical limits of the crystal lattice and showed signs of amorphization as the reaction progressed to product. However, the other two compounds tested were found to react smoothly in the solid state with some evidence of a reconstructive phase transition,<sup>120</sup> though their substituents were composed of moderate bulk. Though this particular study was hindered by synthetic difficulties, continued studies, featuring the solid state photoreactions of highly strained systems that can acquire large amounts of potential energy while undergoing a significant geometric change, will test the limits outlined by the topochemical postulate, and open new doorways to advances in crystal engineering.



## 5. 4. Experimental

### General Methods

All commercial chemicals were used without further purification. THF was distilled over sodium and benzophenone.  $^1\text{H}$  and  $^{13}\text{C}$  NMR spectra were acquired in  $\text{CDCl}_3$  respectively at 300 MHz and 125 MHz on a Bruker spectrometer. NMR chemical shifts are reported in parts per million (ppm) relative to the residual peak of the solvent ( $\text{CDCl}_3$ :  $^1\text{H}$   $\delta = 7.26$  ppm;  $^{13}\text{C}$   $\delta = 77.16$  ppm). Multiplicity is abbreviated to s (singlet), d (doublet), m (multiplet), br (broad) and app (apparent).  $^2\text{H}$  NMR were acquired in natural abundance solvents at 77 MHz. IR spectra were recorded on a Perkin-Elmer ATR-FTIR instrument. Decomposition temperatures were determined using a standard melting point apparatus. Mass spectra were acquired on an Agilent 6210 LCMS system. X-Ray crystal structure was acquired at 100 K on a Bruker Smart 1000K diffractometer. Scanning Electron Microscopy pictures were obtained using a JEOL JSM-6700F FE-SEM microscope.

### Synthesis of Crystalline Cyclopropenones

Cyclopropenones **2** and **3** were synthesized via a modified procedure from Wadsworth.  $\text{AlCl}_3$  (4 eq) was added to a clean, flame-dried flask under argon, suspended in dry DCM, and cooled to  $0^\circ\text{C}$  with stirring. To this, tetrachlorocyclopropene **1** (1 eq) was added dropwise over 30 minutes, creating a suspension yellow in color, and allowed to stir with cooling for an additional 10 minutes. Benzene (1 eq) was added dropwise, causing the slurry to turn reddish-brown in color, and the suspension was allowed to stir with cooling at  $0^\circ\text{C}$ . After 90 minutes, dropwise addition of Ar (1 eq) at  $0^\circ\text{C}$  resulted in a deep purple or red color, which was allowed to warm to room temperature until complete consumption of starting material was shown by TLC analysis, approximately 1 hour. The reaction mixture was slowly quenched with saturated aqueous ammonium chloride solution, extracted with DCM, washed with brine, and dried over sodium

sulfate. The solvent was removed under reduced pressure and the yellow solid subjected to column chromatography (1:2 acetone:hexane,  $R_f = 0.4$ ) to give a total yields ranging from 50-70%. The resulting crystalline solid was recrystallized from a ca. 10:1 methylcyclohexane: DCM solution.

**2-bromo-4,6-methoxy-phenylcyclopropenone (2).**

$^1\text{H}$  NMR (300 MHz,  $\text{CDCl}_3$ ):  $\delta$  7.79 (m, 2H, **CHCH**), 7.44 (m, 3H, **CHCH**), 6.78 (d, 1H,  $J = 2.1$  Hz, **BrCCH**), 6.41 (d, 1H,  $J = 2.0$  Hz, **OCCH**), 3.81 (s, 3H, **OCH<sub>3</sub>**), 3.80 (s, 3H, **OCH<sub>3</sub>**);  $^{13}\text{C}$  NMR (125 MHz,  $\text{CDCl}_3$ ):  $\delta$  163.51(**CO**), 161.17(**CCO**), 129.17(**CHCH**), 129.07(**CHCH**), 127.94(**CHCH**), 127.08(**CHCH**), 126.71(**CHCH**), 109.59(**BrCCH**), 97.39(**OCCH**), 56.16 (**OCH<sub>3</sub>**), 55.82(**OCH<sub>3</sub>**), 31.60, 22.66, 14.11; FTIR (solid HATR,  $\text{cm}^{-1}$ ): 3056, 1840, 1589, 1567, 1596, 1490, 1445, 1320, 1206, 1164.

**Tetrakis-1,3,5,7-(4'-(3'',3'',3''-triphenylpropynyl)-phenylene)adamantane phenylcyclopropenone(3).**

$^1\text{H}$  NMR (300 MHz,  $\text{CDCl}_3$ ):  $\delta$  7.58 (m, 2H, **CHCH**), 7.37 (m, 1H, **CHCH**), 7.28 (m, 20H, **CHCH**), 6.76 (d, 1H,  $J = 2.3$  Hz, **CHCH**), 6.50 (d, 1H,  $J = 2.3$  Hz, **CHCH**), 3.88 (s, 3H, **OCH<sub>3</sub>**), 3.87 (s, 3H, **OCH<sub>3</sub>**);  $^{13}\text{C}$  NMR (125 MHz,  $\text{CDCl}_3$ ):  $\delta$  163.25(**CO**), 160.11(**CCO**), 156.02(**CCO**), 148.24(**COCH<sub>3</sub>**), 144.82(**COCH<sub>3</sub>**), 132.12(**CHCH**), 129.29(**CHCH**), 128.72(**CHCH**), 127.95(**CHCH**), 126.82(**CHCH**), 124.90(**CHCH**), 110.15(**CCCC**), 103.06(**CCC**), 98.86(**CCC**), 83.13(**CPh<sub>3</sub>**), 56.64(**COCH<sub>3</sub>**), 55.96(**COCH<sub>3</sub>**); FTIR (solid HATR,  $\text{cm}^{-1}$ ): 3057, 2036, 1851, 1613, 1590, 1567, 1490, 1446, 1350, 1207, 1164, 1131.

Cyclopropenone **4** was synthesized via a modified procedure from Wadsworth also.  $\text{AlCl}_3$  (4 eq) was added to a clean, flame-dried flask under argon, suspended in dry DCM, and cooled to  $78^\circ\text{C}$  with stirring. To this, tetrachlorocyclopropene **1** (1 eq) was added dropwise over 30 minutes, creating a suspension yellow in color, and allowed to stir with cooling for an additional 10 minutes. Ar (2 eq) was added dropwise over 30 minutes, causing the slurry to turn orange in color, and the

suspension was allowed to stir with cooling at  $-78^{\circ}\text{C}$  until complete by TLC analysis, usually after 30-60 minutes. The reaction mixture was slowly quenched with saturated aqueous ammonium chloride solution, extracted with DCM, washed with brine, and dried over sodium sulfate. The solvent was removed under reduced pressure and the yellow solid subjected to column chromatography (1:2 acetone:hexane,  $R_f = 0.4$ ) to give a total yields ranging from 45-70%. The resulting crystalline solid was recrystallized from a ca. 10:1 methylcyclohexane: DCM solution.

**Bis-2-bromo-4,6-methoxy phenylcyclopropenone(4).**

$^1\text{H}$  NMR (300 MHz,  $\text{CDCl}_3$ ):  $\delta$  6.84 (d, 1H,  $J = 2.2$  Hz, CHCH), 6.44 (d, 1H,  $J = 2.2$  Hz, CHCH), 3.88 (s, 3H,  $\text{OCH}_3$ ), 3.74 (s, 3H,  $\text{OCH}_3$ );  $^{13}\text{C}$  NMR (125 MHz,  $\text{CDCl}_3$ ):  $\delta$  163.51(CO), 161.78(CCO), 146.65( $\text{COCH}_3$ ), 127.00(CHCH), 111.13(CHCH), 109.59(CHCH), 107.46(CHCH), 97.39(CBr), 56.19( $\text{OCH}_3$ ), 55.96( $\text{OCH}_3$ ); FTIR (solid HATR,  $\text{cm}^{-1}$ ): 2987, 1850, 1590, 1551, 1404, 1210, 1150, 1031.

**Tetrakis-1,3,5,7-(4'-(3'',3'',3''-triphenylpropynyl)-phenylene)adamantane (1).**

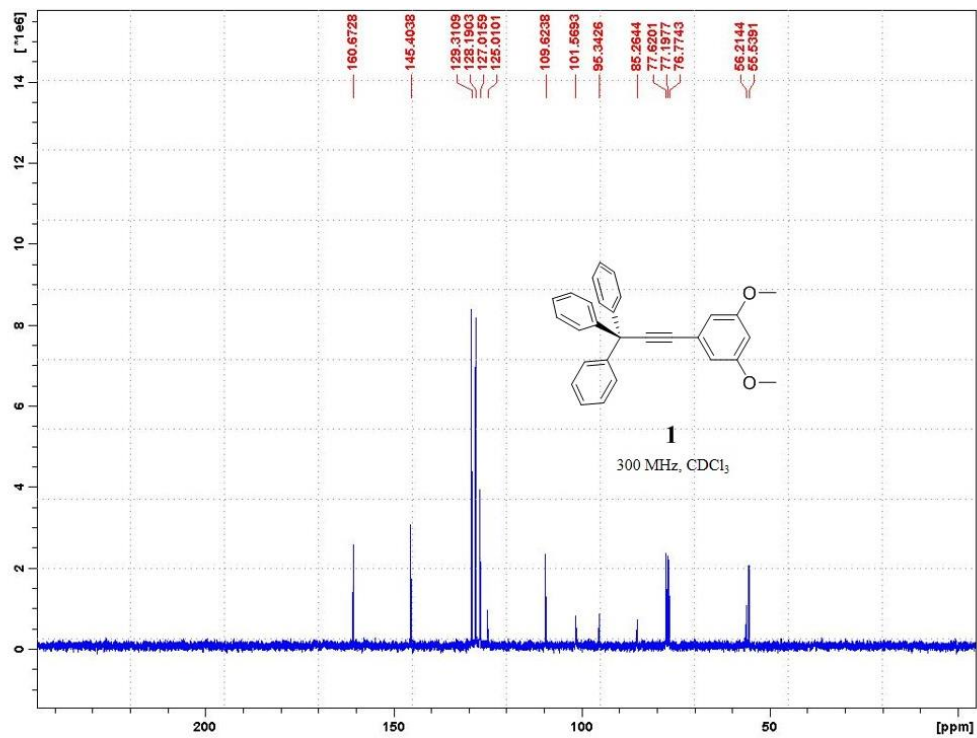
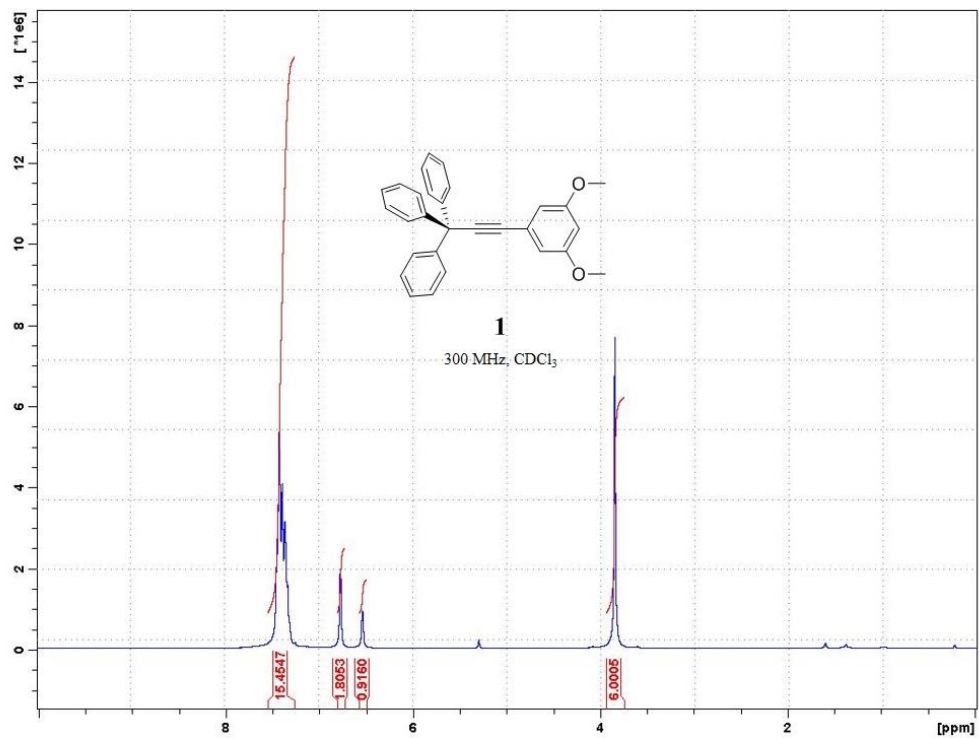
$^1\text{H}$  NMR (500 MHz,  $\text{CDCl}_3$ ):  $\delta$  7.50 (app d, 8H,  $J = 8.3$  Hz, CHCH), 7.41 (app d, 8H,  $J = 8.3$  Hz, CHCH), 7.34-7.24 (m, 6H, CHCH), 2.12 (br s, 12H, CHCH);  $^{13}\text{C}$  NMR (125 MHz,  $\text{CDCl}_3$ ):  $\delta$  149.13(CHCH), 145.52(CHCH), 131.88(CHCH), 129.34(CHCH), 128.15(CHCH), 126.96(CHCH), 125.10(CHCH), 121.71(CHCH), 95.68(CCC), 85.07(CCC), 56.26( $\text{CPh}_3$ ), 47.02( $\text{COCH}_3$ ), 39.43( $\text{COCH}_3$ ); FTIR (solid HATR,  $\text{cm}^{-1}$ ): 3058, 3024, 2922, 2852, 1596, 1504, 1490, 1446, 1031, 1026, 842, 834, 758, 740, 726, 695; HRMS  $\text{C}_{118}\text{H}_{89}$  [ $\text{M} + \text{H}^+$ ] calcd 1505.6959; found 1505.6900

## 5. 5. Appendix

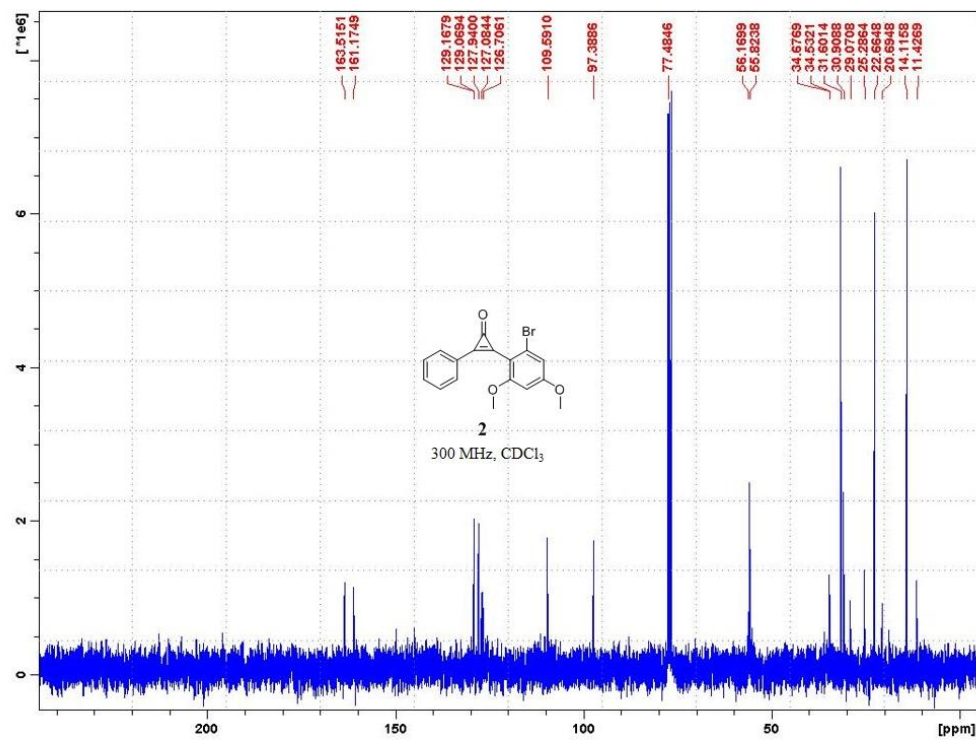
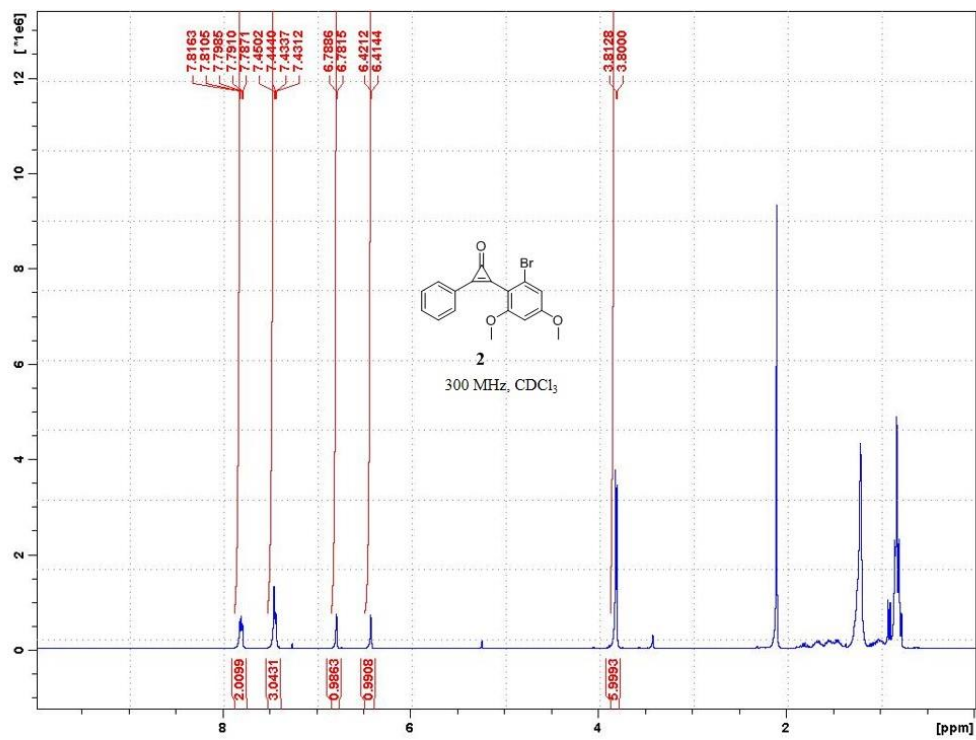
### Characterization for Chapter 5

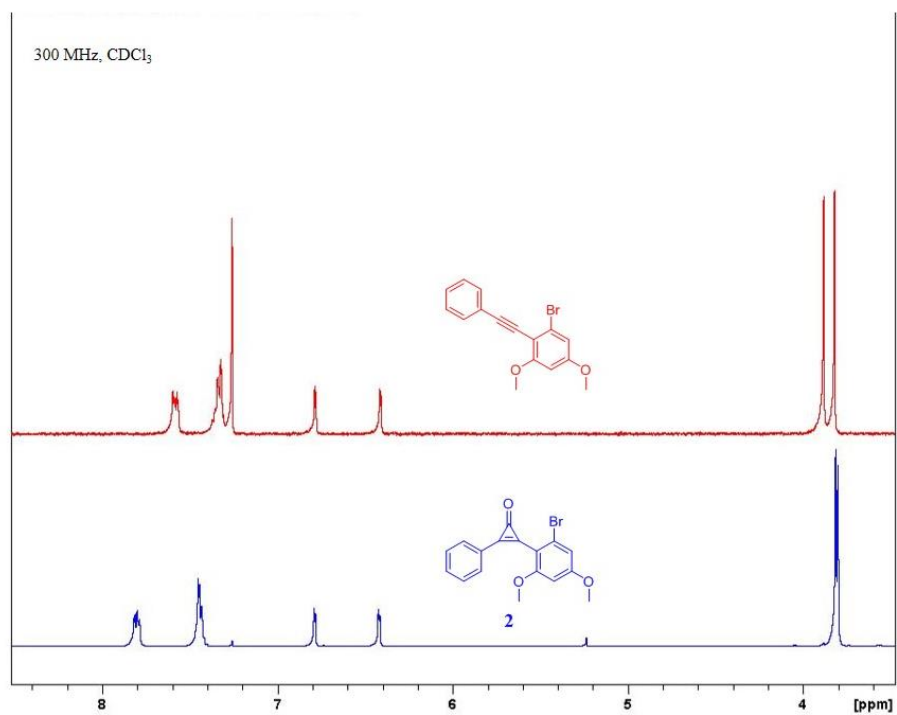
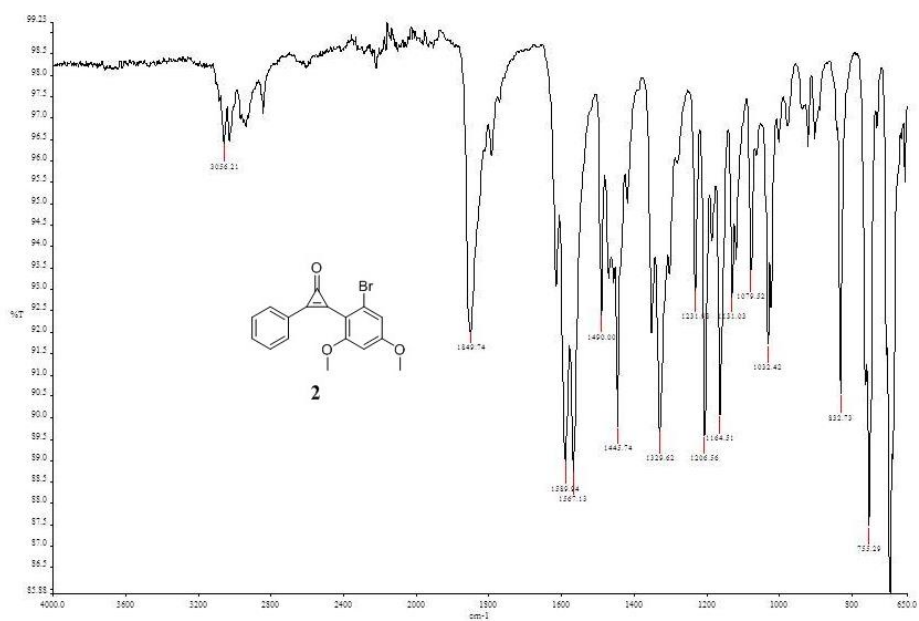
$^1\text{H}$ and $^{13}\text{C}$ for <b>1</b> .....	162
$^1\text{H}$ , $^{13}\text{C}$ , and IR for <b>2</b> .....	163
$^1\text{H}$ , $^{13}\text{C}$ , and IR for <b>3</b> .....	165
$^1\text{H}$ , $^{13}\text{C}$ , and IR for <b>4</b> .....	168
DSC Data for <b>2</b> , <b>3</b> , and <b>4</b> .....	171
References.....	173

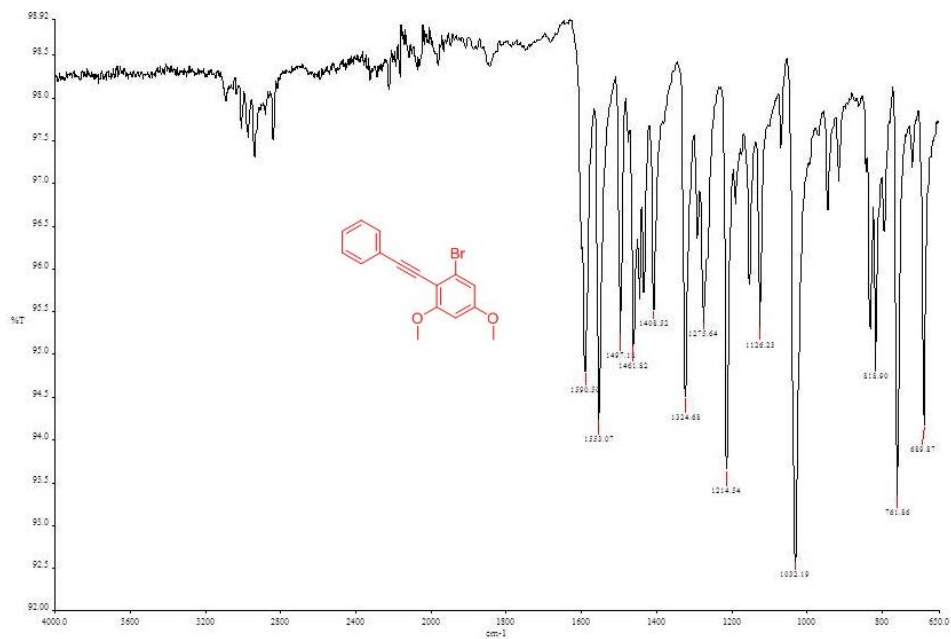
Tetrakis-1,3,5,7-(4'-(3'',3'',3''-triphenylpropynyl)-phenylene)adamantane (1).



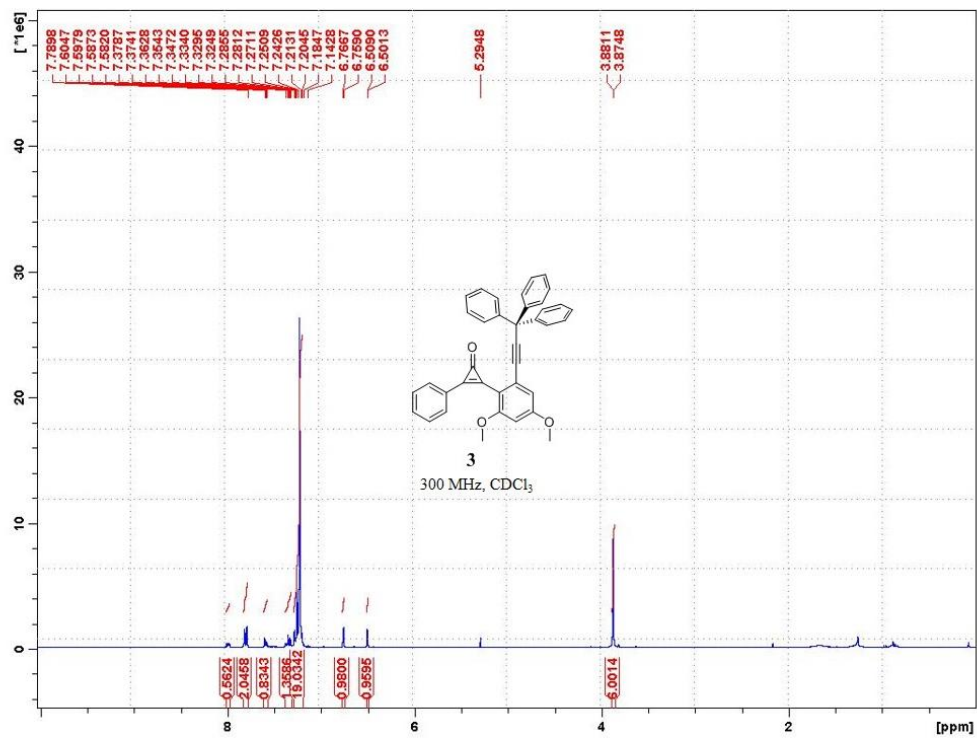
## 2-bromo-4,6-methoxy-phenylcyclopropenone (2).



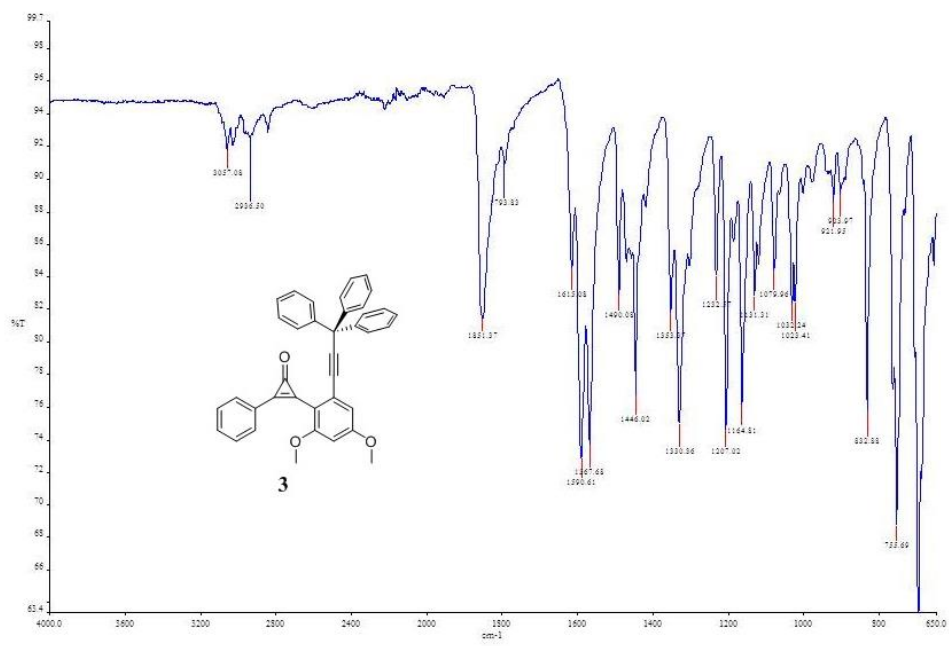
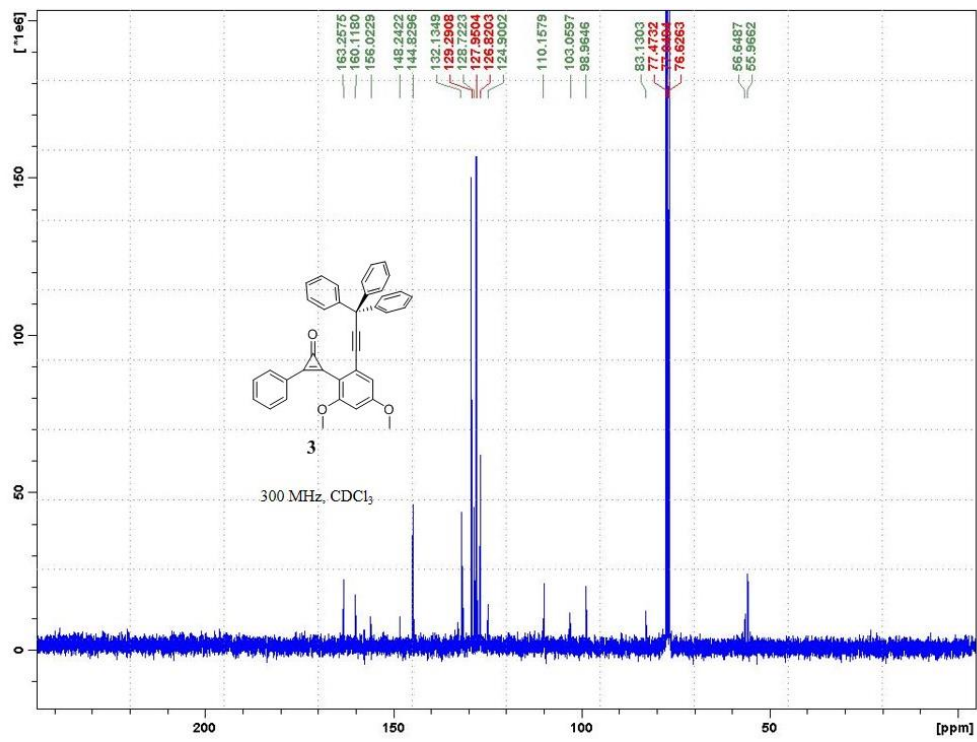


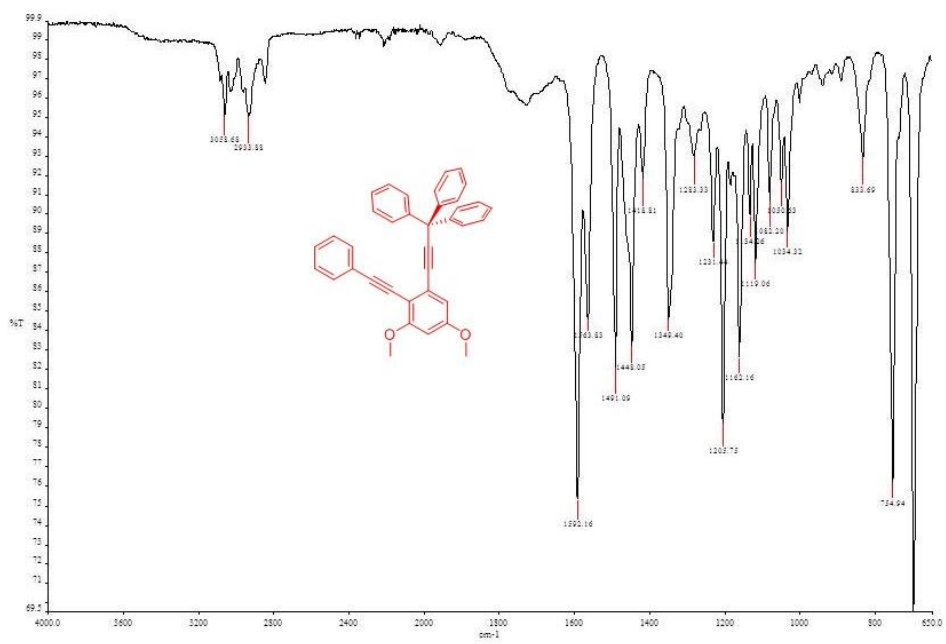
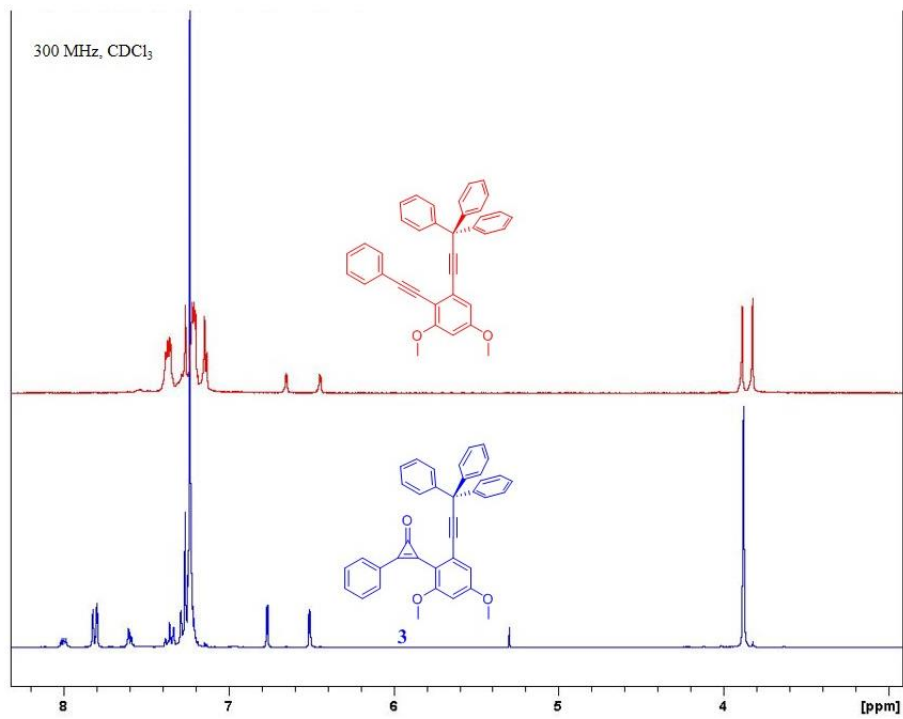


**Tetrakis-1,3,5,7-(4'-(3'',3'',3''-triphenylpropynyl)-phenylene)adamantane phenylcyclopropanone(3).**

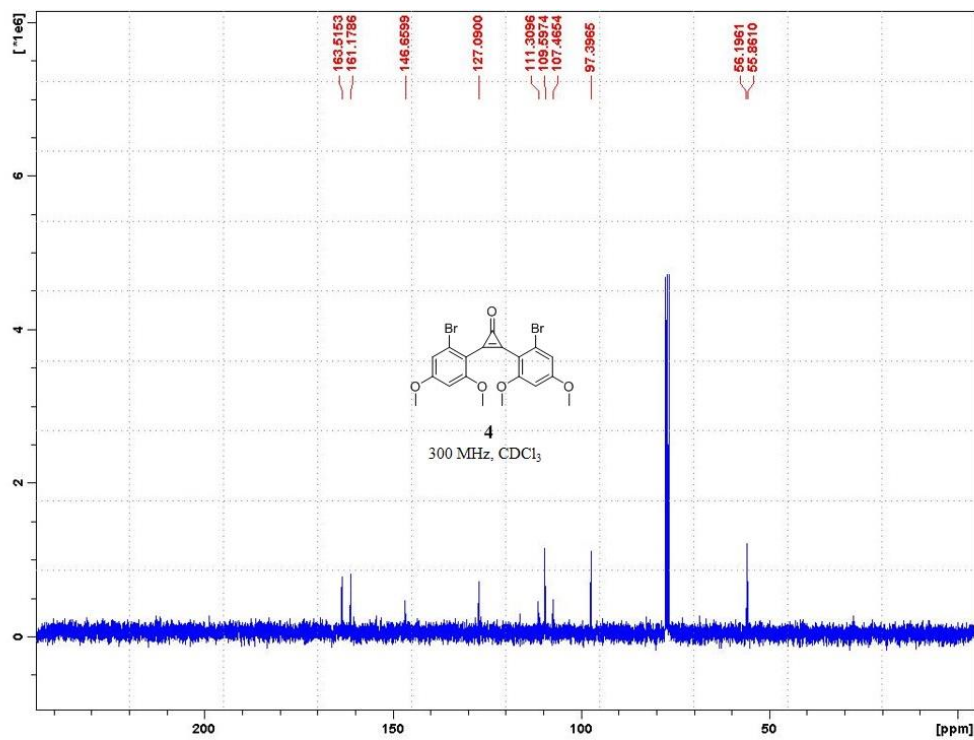
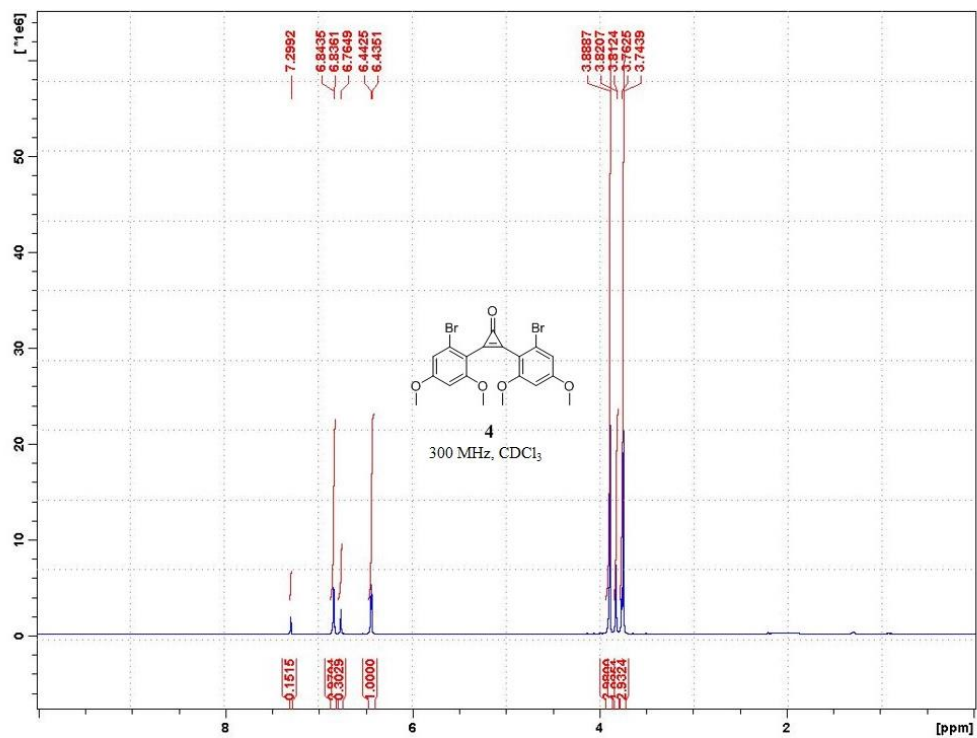


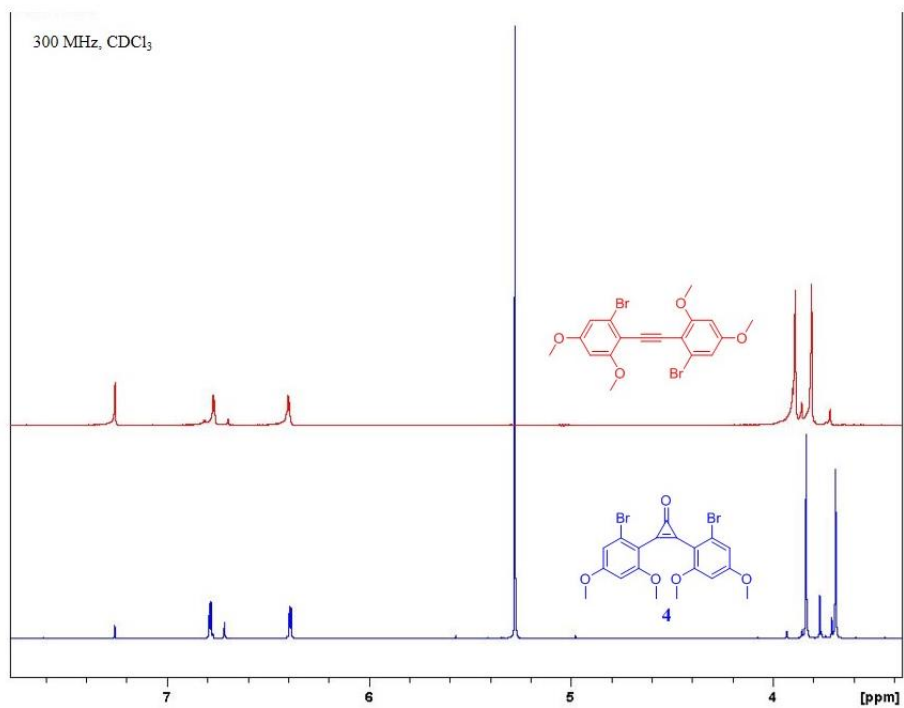
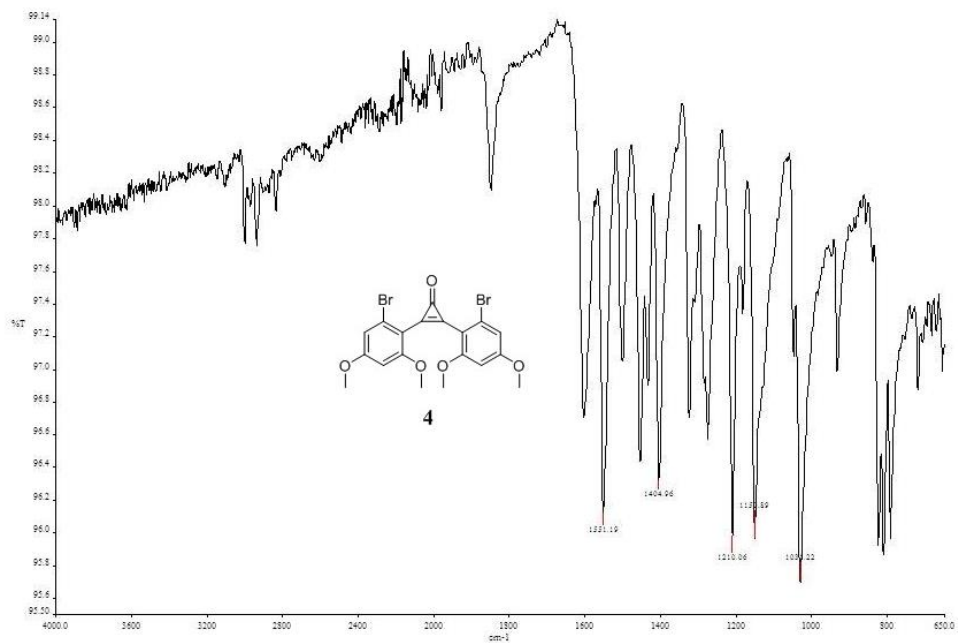


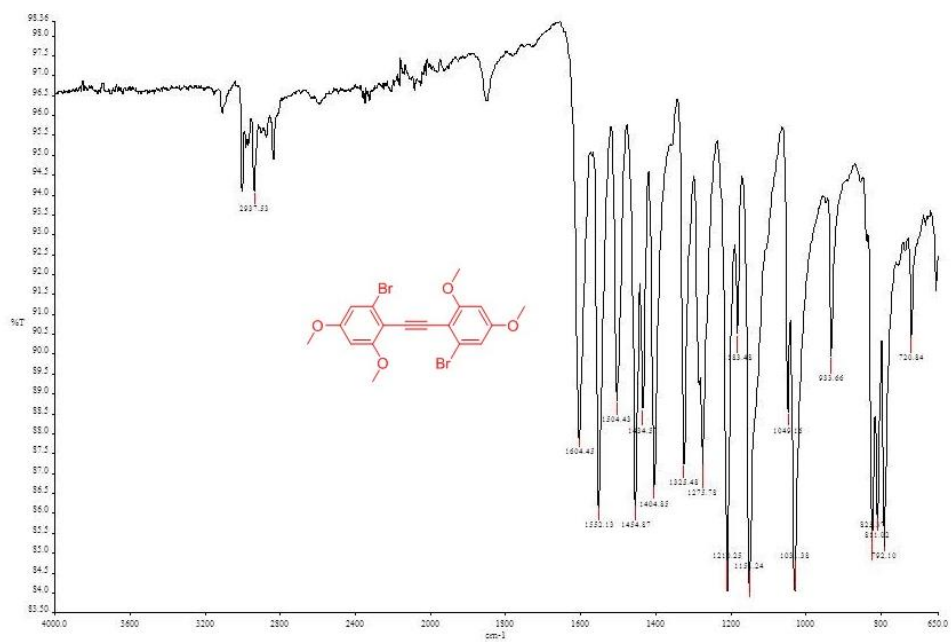




**Bis-2-bromo-4,6-methoxy phenylcyclopropenone(4).**

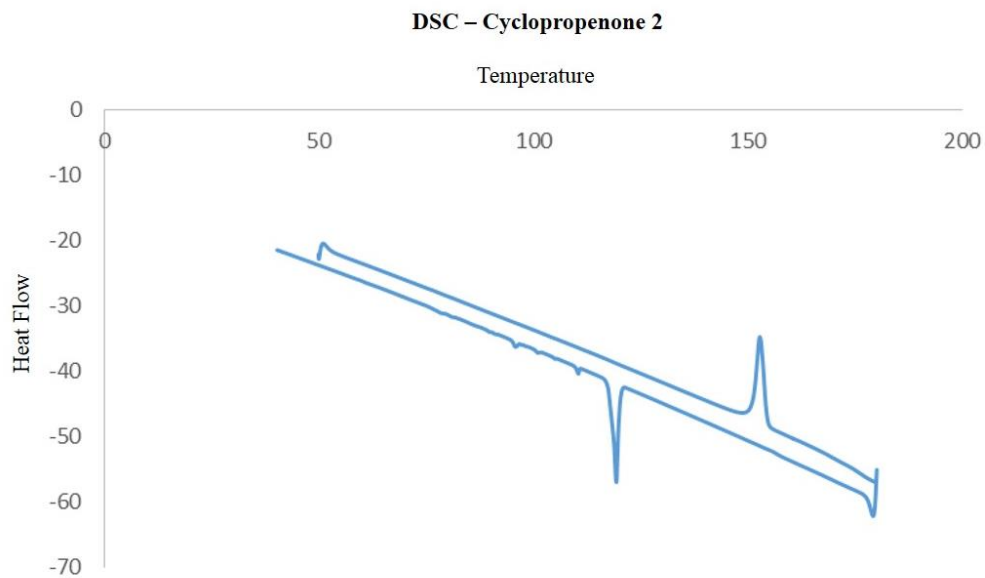




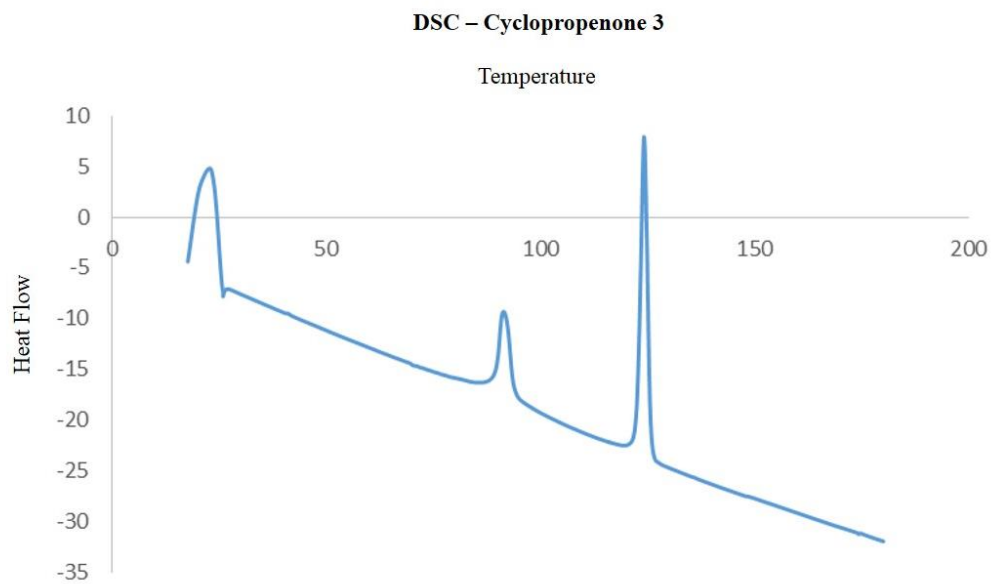


## Thermal Data

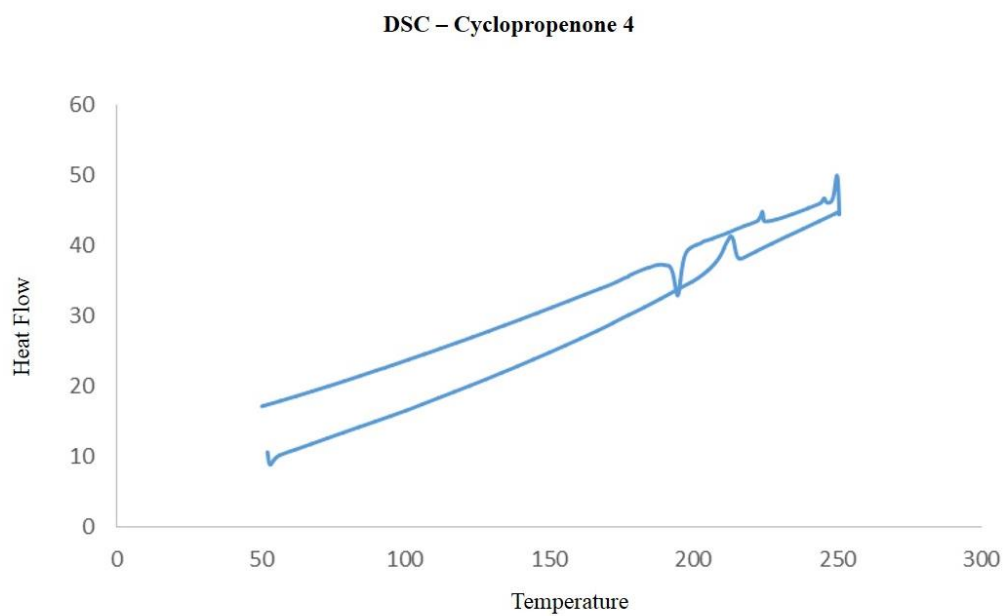
### 2-bromo-4,6-methoxy-phenylcyclopropenone (2).



### Tetrakis-1,3,5,7-(4'-(3'',3'',3''-triphenylpropynyl)-phenylene)adamantane phenylcyclopropenone(3).



**Bis-2-bromo-4,6-methoxy phenylcyclopropenone(4).**



## References

- <sup>1</sup> Trommsdorff, S. *Ann. Chem. Pharm.* **1834**, 11.
- <sup>2</sup> Ng, D.; Yang, Z.; Garcia-Garibay, M. A. *Org. Lett.*, **2004**, 6, 645-647.
- <sup>3</sup> Natarajan, A.; Mague, J. T.; Ramamurthy, V. *J. Am. Chem. Soc.* **2005**, 127, 3568.
- <sup>4</sup> Anastas, P. T.; Kirchoff, M. M. *Acc. Chem. Res.*, **2002**, 35, 686-694.
- <sup>5</sup> Fischer, H.; Paul, H. *Acc. Chem. Res.* **1987**, 20, 200.
- <sup>6</sup> Campos, L. M.; Dang, H., Ng, D.; Yang, Z.; Martinez, H. L.; Garcia-Garibay, M. A. *J. Org. Chem.* **2002**, 67, 3749-3754.
- <sup>7</sup> Kuhn, H. J., Bravlavsky, S. E., Schmidt, R. *Pure Appl. Chem.* **2004**, 76, 2105-2146.
- <sup>8</sup> Irie, M.; Kobatake, S.; Horichi, M. *Science*, **2001**, 291, 1769.
- <sup>9</sup> Cohen, M. D.; Schmidt, G. M. *J. Am. Chem. Soc.* **1964**, 53, 1996.
- <sup>10</sup> Ginsburg, D.; Schmidt, G. M. in *Reactivity of the Photoexcited Organic Molecule*, Ginsburg, D., Ed.; Wiley Interscience: New York, 1967.
- <sup>11</sup> Cohen, M. D. *Angew. Chem. Int. Ed.* **1975**, 14, 386.
- <sup>12</sup> Kohlschutter, H. W. *Z. Anorg. Allg. Chem.* **1918**, 105, 121.
- <sup>13</sup> Scheffer, J. R.; Scott, C. *Science*, **2001**, 291, 1712.
- <sup>14</sup> Mattay, J., Griesbeck, A. G. (eds) Carbonyl Compounds. In *Photochemical Key Steps in Organic Synthesis*, VCH, Weinheim, **1994**, 11-118.
- <sup>15</sup> Wagner, P. J.; Kelso, P. A.; Kempainen, A. E.; Zepp, R. G. *J. Am. Chem. Soc.* **1972**, 94, 7500.
- <sup>16</sup> Gudmundsdottir, A. D.; Lew, T. J.; Randall, L. H.; Scheffer, J. R.; Rettig, S. J.; Trotter, J.; Wu, C. H. *J. Am. Chem. Soc.* **1996**, 118, 6167.
- <sup>17</sup> Schmidt, G. M. *J. Chem. Soc.* **1964**, 53, 2014.
- <sup>18</sup> Bondi, A. *J. Phys. Chem.* **1964**, 68, 441.
- <sup>19</sup> Wagner, P. J.; Klan, P. In *CRC Handbook of Organic Photochemistry and Photobiology*, CRC Press LLC, Boca Raton, 2004.
- <sup>20</sup> Scheffer, J.R.; Scott, C. In *CRC Handbook of Photochemistry and Photobiology 2<sup>nd</sup> Ed.* Horspool, W.; Lenci, F., Eds.; CRC Press: Boca Raton, 2004.
- <sup>21</sup> Kuzmanich, G.; Natarajan, A.; Chin, K.; Veerman, M.; Mortko, C.; Garcia-Garibay, M. A. *J. Am. Chem. Soc.* **2008**, 130, 1140.
- <sup>22</sup> Kasai, H.; Nlawa, H. S.; Oikawa, H.; Okada, S.; Matsuda, H.; Minami, N.; Kakuta, A.; Ono, K.; Mukoh, A.; Nakanishi, H. *Jpn. J. Appl. Phys.* **1992**, 31, 1132.
- <sup>23</sup> Gesquiere, A. J.; Uwada, T.; Asahi, T.; Masuhara, H.; Barabara, P. F. *Nano Lett.* **2005**, 5, 1321.
- <sup>24</sup> Kuzmanich, G.; Spanig, F.; Tsai, C. K.; Um, J.; Hoekstra, R. M.; Houk, K. N.; Guldi, D. M.; Garcia-Garibay, M. A. *J. Am. Chem. Soc.* **2011**, 133, 2342.
- <sup>25</sup> de Loera, D.; Stopin, A.; Garcia-Garibay, M.A. *J. Am. Chem. Soc.* **2013**, 135, 6626-6632.
- <sup>26</sup> Choi, T.; Cizmeciyani, D.; Kahn, S.I.; Garcia-Garibay, M.A. *J. Am. Chem. Soc.* **1995**, 117, 12893.
- <sup>27</sup> Mattay, J., Griesbeck, A. G. (eds) Carbonyl Compounds. In *Photochemical Key Steps in Organic Synthesis*, VCH, Weinheim, **1994**, 11-118.
- <sup>28</sup> Yang, N. C., Yang, D., H. *J. Am. Chem. Soc.* **1958**, 80, 2913-2914.
- <sup>29</sup> Wagner, P. J. *Acc. Chem. Res.* **1971**, 4, 168-177.
- <sup>30</sup> Rubin, M. B. In *CRC Handbook of Photochemistry and Photobiology 2<sup>nd</sup> Ed.* Horspool, W.; Lenci, F., Eds.; CRC Press: Boca Raton, 2004, 430-436.
- <sup>31</sup> Norrish, R. G. W., Appleyard, M. E. S., *J. Chem. Soc.* **1934**, 874-880.
- <sup>32</sup> Norrish, R. G. W. *Trans. Faraday Soc.* **1937**, 33, 1521.
- <sup>33</sup> Laue, T.; Plagens, A. In *Named Organic Reactions*, John Wiley & Sons: Chichester, England, New York, **2005**.
- <sup>34</sup> Mikami, K.; Shimizu, M. *Chem. Rev.* **1992**, 92, 1021.
- <sup>35</sup> Wagner, P. J., Park, B. S. In *Organic Photochemistry*, Vol 11 Padwa, A. (ed) Marcel Dekker: New York, 1991, 227-366.
- <sup>36</sup> Wessig, P., Muhling, O. In *Synthetic Organic Photochemistry*, Vol 12 Griesbeck, A. G., Mattay, J. (eds) Marcel Dekker: New York, 2005, 41-87.
- <sup>37</sup> Scaiano, J. C. *Tetrahedron* **1982**, 38, 819.
- <sup>38</sup> Hesse, R. H. *Adv. Free-Radical Chem.* **1969**, 3, 83.
- <sup>39</sup> Grob, C. A., Baumann, W. *Helv. Chim. Acta* **1955**, 38, 594-610.



- <sup>40</sup> Nau, W. M.; Greiner, G.; Wall, J.; Rau, H.; Olivucci, M.; Robb, M. A. *Ber. Bunsen-Ges. Phys. Chem.* **1998**, *102*, 486-492.
- <sup>41</sup> Wagner, P. J.; Chiu, C. *J. Am. Chem. Soc.* **1979**, *101*, 7134-7135.
- <sup>42</sup> Kloek, J. *J. Org. Chem.* **1981**, *46*, 1951-1954.
- <sup>43</sup> Wagner, P. J.; Chiu, C. *J. Am. Chem. Soc.* **1979**, *101*, 7134-7135.
- <sup>44</sup> Geise, B.; Wettstein, P.; Stahelin, C.; Barbosa, F.; Neuberger, M.; Zehnder, M.; Wessig, P. *Angew. Chem. Int. Ed.* **1999**, *38*, 2586-2587.
- <sup>45</sup> Wagner, P. J.; Klan, P. In *CRC Handbook of Organic Photochemistry and Photobiology*, CRC Press LLC, Boca Raton, 2004.
- <sup>46</sup> Wagner, P.J.; Kelso, P.A.; Kempainen, A.E.; Zepp, R.G. *J. Am. Chem. Soc.* **1972**, *94*, 7500.
- <sup>47</sup> Gudmundsdottir, A. D.; Lew, T. J.; Randall, L. H.; Scheffer, J. R.; Rettig, S. J.; Trotter, J.; Wu, C. H. *J. Am. Chem. Soc.* **1996**, *118*, 6167.
- <sup>48</sup> Ramamurthy, V., *Tetrahedron* **1986**, *42*, 5753-5839.
- <sup>49</sup> Gilmore, J.G.; Neiser, J.D.; McManus, K.A.; Roh, Y.; Dombrowski, G.W.; Brown, T.G.; Dinnocenzo, J.P.; Farid, S.; Robello, D.R. *Macromolecules* **2005**, *38*, 7684-7689.
- <sup>50</sup> Ng, D.; Yang, Z.; Garcia-Garibay, M.A. *Org. Lett.* **2004**, *6*, 645-647.
- <sup>51</sup> Nielsen, A.; Kuzmanich, G.; Garcia-Garibay, M.A. *J. Phys. Chem. A* **2014**, *118*, 1858-1863.
- <sup>52</sup> Kuzmainch, G.; Gard, M.; Garcia-Garibay, M. A. *J. Am. Chem. Soc.* **2009**, *131*, 11606-11614.
- <sup>53</sup> Wagner, P.J.; Zhou, B. *Tetrahedron Lett.* **1989**, *30*, 5389-5392.
- <sup>54</sup> Wagner, P.J. *Accs. Of Chemical Research* **1989**, *22*, 83-91.
- <sup>55</sup> (a) Turro, N.J.; Weis, D.S. *J. Am. Chem. Soc.* **1968**, *90*, 2185. (b) Ounsworth, J.; Scheffer, J.R. *J. Chem. Soc. Chem. Commun.* **1986**, 232.
- <sup>56</sup> Garcia-Garibay, M. A.; Houk, K. N.; Keating, A. E.; Cheer, C. J.; Leibovitch, M.; Scheffer, J. R.; Wu, L. C. *Org. Lett.* **1999**, *1*, 1279-1281.
- <sup>57</sup> Scheffer, J.R.; Scott, C. *Science*, **2001**, *291*, 1712.
- <sup>58</sup> Veerman, M.; Resendiz, M.J.E.; Garcia-Garibay, M.A. *Org. Lett.* **2006**, *8*, 2615-2617.
- <sup>59</sup> (a) Resendiz, M.J.E.; Taing, J.; Garcia-Garibay, M.A. *Org. Lett.* **2007**, *9*, 4351-4354. (b) Chin, K.K.; Natarajan, A.; Gard, M.; Campos, L.M.; Johansen, E.; Shepherd, H.; Garcia-Garibay, M.A. *Chem. Commun.* **2007**, 4266.
- <sup>60</sup> Wagner, P.J.; Zhou, B.; Hasegawa, T.; Ward, D. *J. Am. Chem. Soc.* **1991**, *113*, 9640-9654.
- <sup>61</sup> Grassa, G.A.; Colacot, T.J. *Organic Process Research & Development* **2008**, *12*, 522-529.
- <sup>62</sup> (a) Kaminsky, W.; Claborn, K.; Kahr, B. *Chem. Soc. Rev.* **2004**, *33*, 514. (b) Nye, J.F. *Physical Properties of Crystals*, Oxford University Press: Oxford, 1985. (c) Burns, G. *Solid State Physics*, Academic Press: San Diego, 1985.
- <sup>63</sup> Kohlshutter, H. W. *Z. Anorg. Allg. Chem.* **1918**, *105*, 121.
- <sup>64</sup> Wagner, P.J.; Klan, P. In *CRC Handbook of Photochemistry and Photobiology 2<sup>nd</sup> Ed.* Horspool, W.; Lenci, F., Eds.; CRC Press: Boca Raton, 2004.
- <sup>65</sup> (a) Vura-Weis, J.; Abdelwahed, S. H.; Skukla, R.; Rathore, R.; Ratner, M. A.; Wasielewski, M. R. *Science*, **2010**, *328*, 1547. (b) Pettersson, K.; Kyrychenko, A.; Rönnow, E.; Ljungdahl, T.; Mårtensson, J.; Albinsson, B. *J. Phys. Chem. A* **2006**, *110*, 310. (c) Faure, S.; Stern, C.; Guillard, R.; Harvey, P. D. *J. Am. Chem. Soc.* **2004**, *126*, 1253. (d) Yeow, E. K. L.; Ziolk, M.; Karolczak, J.; Shevyakov, S. V.; Asato, A. E.; Maciejewski, A.; Steer, R. P. *J. Phys. Chem. A* **2004**, *108*, 10980.
- <sup>66</sup> (a) Savolainen, J.; Dijkhuizen, N.; Fanciulli, R.; Liddell, P. A.; Gust, D.; Moore, T. A.; Moore, A. L.; Hauer, J.; Buckup, T.; Motzkus, M.; Herek, J. L. *J. Phys. Chem. B* **2008**, *112*, 2678. (b) Nakano, A.; Osuka, A.; Yamazaki, T.; Nishimura, Y.; Akimoto, S.; Yamazaki, I.; Itaya, A.; Murakami, M.; Miyasaka, H. *Chem. Eur. J.* **2001**, *7*, 3134. (c) Nakano, A.; Yasuda, Y.; Yamazaki, T.; Akimoto, S.; Yamazaki, I.; Mirasaka, H.; Itaya, A.; Murakami, M.; Osuka, A. *J. Phys. Chem. A* **2001**, *105*, 4822. (d) Damjanović, A.; Ritz, T.; Schulten, K. *Phys. Rev. E* **1999**, *59*, 3293. (e) Krueger, B. P.; Scholes, G. D.; Jimenez, R. *J. Phys. Chem. B*, **1998**, *102*, 2284.
- <sup>67</sup> (a) Yeow, E. K. L.; Ziolk, M.; Karolczak, J.; Shevyakov, S. V.; Alsato, A. E.; Maciejewski, A.; Steer, R. P. *J. Phys. Chem. A* **108**, 2004, 10980. (b) Yeow, E. K. L.; Steer, R. P. *Chem. Phys. Lett.* **2003**, *377*, 391.
- <sup>68</sup> Ichimura, K. *J. Photochem. Photobio. A* **2003**, *158*, 205-214.
- <sup>69</sup> Pitts, J.; Hammond, G.; Golnick, K. In *Advances in Photochemistry Volume 11*, John Wiley & Sons: Chichester, England, New York, **2009**.
- <sup>70</sup> (a) Hirata, Y.; Okada, T.; Mataga, N.; Nomoto, T., *J. Phys. Chem.* **1992**, *96*, 6559. (b) Hirata, Y.; Mataga, N., *Chem. Phys. Lett.* **1992**, *193*, 287. (c) Terazima, M.; Hara, T.; Hirota, N. *Chem. Phys. Lett.* **1995**, *246*, 577. (d) Takeuchi, S.; Tahara, T. *J. Chem. Phys.* **2004**, *120*, 4768.

- <sup>71</sup> (a) Poloukhine, A.; Popik, V. V. *J. Phys. Chem. A* **2006**, *110*, 1749. (e) Urbadayev, N. K.; Poloukhine, A.; Popik, V. V. *Chem. Comm.* **2006**, *4*, 454. (f) Poloukhine, A.; Popik, V. V. *J. Org. Chem.* **2003**, *68*, 7833.
- <sup>72</sup> Pump-probe experiments with diarylcyclopropenones described in reference 7a have shown that the transient formed upon adiabatic decarbonylation is not identical to the transient formed upon excitation of diarylacetylene to its second excited state.
- <sup>73</sup> Hirata, Y.; Okada, T. *Chem. Phys. Lett.* **1993**, *209*, 397.
- <sup>74</sup> (a) Bally, T.; Matzinger, S.; Pawel, B.; *J. Am. Chem. Soc.* **2006**, *128*, 7828. (b) Ferrar, L.; Mis, M.; Dinnocenzo, J. P.; Farid, S.; Merkel, P. B.; Robello, D. R. *J. Org. Chem.* **2008**, *73*, 5683. Norton, J. E.; Leif, P.; Houk, K. N. *J. Am. Chem. Soc.* **2006**, *128*, 7835. (c) Tu, W.; Floreancig, P. E. *Org. Lett.* **2007**, *9*, 2389. (d) Vazquaz, C. P.; Joly-Duhamel, C.; Boutevin, B. *Macromol. Chem. Phys.* **2009**, *210*, 269. (e) Winkelmann, K.; Calhoun, R. L.; Mills, G. *J. Phys. Chem. A* **2006**, *110*, 13827. (f) Kerezsi, I.; Lente, G.; Fabian, I. *J. Am. Chem. Soc.* **2005**, *127*, 4785.
- <sup>75</sup> Powel, R. C.; Soos, Z. G. *J. Lumin.* **1975**, *11*, 1.
- <sup>76</sup> Doan, S.C.; Kuzmanich, G.; Gard, M. N.; Garcia-Garibay, M.A.; Schwartz, B.J. *J. Phys. Chem. Lett.*, **2012**, *3*, 81.
- <sup>77</sup> García-Martínez, A.; Osío-Barciana, J. *Encyclopedia of Supramolecular Chemistry*; Marcel Dekker: New York, 2004, pp 452-456.
- <sup>78</sup> Förster, T. *Naturwissenschaften* **1946**, *33*, 166.
- <sup>79</sup> Dexter, D. L. *Chem. Phys.* **1953**, *21*, 836.
- <sup>80</sup> Oikawa, H.; Nakanishi, H. In *Single Organic Nanoparticles*; Springer-Verlag: Berlin Heidelberg, 2003; pp17-31.
- <sup>81</sup> Zachariasse, K. A.; Macanita, A. L.; Kuehnle, W. *J. Phys. Chem. B* **1999**, *103*, 9356.
- <sup>82</sup> Rettig, W.; Paepow, B.; Herbst, H.; Müllen, K.; Desvergne, J.-P.; Bouas-Laurent, H. *New. J. Chem.* **1999**, *23*, 453.
- <sup>83</sup> Although the parent diphenylacetylene compound has a highly structured emission, **13** shows a less structured emission in benzene. This is due to bulk properties of benzene and not to a specific interaction with the solvent and the chromophore. See Figure S3
- <sup>84</sup> Veerman, M.; Resendiz, M.J.E.; Garcia-Garibay, M.A. *Org. Lett.* **2006**, *8*, 2615.
- <sup>85</sup> Clegg, R. *Fluorescence Imaging Spectroscopy and Microscopy*; John Wiley & Sons, New York, 1996; pp 179.
- <sup>86</sup> (a) Jordanides, X. J.; Scholes, G. D.; Shapley, W. A.; Reimers, J. R.; Fleming, G. R. *J. Phys. Chem. B*, **2004**, *108*, 1753. (b) Beljonne, D.; Curutchet, C.; Scholes, G. D.; Silbey, R. J. *J. Phys. Chem. B*, **2009**, *113*, 6583. (c) Hsu, C.-P.; You, Z.-Q.; Chen, H.-C. *J. Phys. Chem. C* **2008**, *112*, 1204. (d) Czader, A.; Bittner, E. R. *J. Chem. Phys.* **2008**, *128*, 5101.
- <sup>87</sup> Scholes, G. D.; Ghiggino, K. P. *J. Phys. Chem.* **1994**, *98*, 4580.
- <sup>88</sup> Guimarães, C. R. W.; Cardozo, M. J. *Chem. Inf. Model* **2008**, *48*, 958.
- <sup>89</sup> Frisch, M. J.; et al. Gaussian 03, revision C.02; Gaussian, Inc.: Wallingford, CT, 2004
- <sup>90</sup> Given that the decarbonylation reaction is completed within 200 fs and the lifetime of S<sub>2</sub> is 8 ps we assume that this is not enough time for conformational equilibrium to occur within the tether.
- <sup>91</sup> Wadsworth, D. H.; Donatelli, B. A. *Synthesis*, **1981**, 285.
- <sup>92</sup> Kuhn, J. J.; Braslavsky, S. E.; Schmidt, R. *Pure Appl. Chem.* **2004**, *76*, 2105.
- <sup>93</sup> Park, S. B.; Alper, H. *Chem. Comm.* **2004**, *40*, 1306.
- <sup>94</sup> Goeldner, M.; Givens, R. S. *Dynamic Studies in Biology: Phototriggers, Photoswitches and Caged Molecules*, Wiley-VCH, New York, 2005.
- <sup>95</sup> Pettersson, K.; Kyrychenko, A.; Rönnow, E.; Ljungdahl, T.; Mårtensson, J.; Albinsson, B. *J. Phys. Chem. A* **2006**, *110*, 310.
- <sup>96</sup> Reiser, A. *Photoactive Polymers: The Science and Technology of Resists*, John Wiley & Sons, Inc., New York, 1989.
- <sup>97</sup> Yeow, E. K. L.; Ziolk, M.; Karolczak, J.; Shevyakov, S. V.; Asato, A. E.; Maciejewski, A.; Steer, R. P. *J. Phys. Chem. A* **2004**, *108*, 10980.
- <sup>98</sup> Turro, N. J.; Ramamurthy, V.; Scaiano, J. C. In *Modern Molecular Photochemistry of Organic Molecules*, University Science Books, Sausalito, 2010
- <sup>99</sup> Faure, S.; Stern, C.; Guillard, R.; Harvey, P. D. *J. Am. Chem. Soc.* **2004**, *126*, 1253.
- <sup>100</sup> (a) Vura-Weis, J.; Abdelwahed, S. H.; Skukla, R.; Rathore, R.; Ratner, M. A.; Wasielewski, M. R. *Science*, **2010**, *328*, 1547. (b) Pettersson, K.; Kyrychenko, A.; Rönnow, E.; Ljungdahl, T.; Mårtensson, J.; Albinsson, B. *J. Phys. Chem. A* **2006**, *110*, 310.
- <sup>101</sup> Damjanović, A.; Ritz, T.; Schulten, K. *Phys. Rev. E* **1999**, *59*, 3293.
- <sup>102</sup> Yeow, E. K. L.; Ziolk, M.; Karolczak, J.; Shevyakov, S. V.; Alsato, A. E.; Maciejewski, A.; Steer, R. P. *J. Phys. Chem. A* **2004**, *108*, 10980.
- <sup>103</sup> Saliel, J.; Townsend, D. E.; Sykes, A. *J. Am. Chem. Soc.* **1983**, *105*, 2530-2538.

- 
- <sup>104</sup> (a) Yeow, E. K. L.; Ziolk, M.; Karolczak, J.; Shevyakov, S. V.; Alsato, A. E.; Maciejewski, A.; Steer, R. P. *J. Phys. Chem. A* **2004**, *108*, 10980. (b) Yeow, E. K. L.; Steer, R. P. *Chem. Phys. Lett.* **2003**, *377*, 391.
- <sup>105</sup> Cordes T.; Malkmus S.; DiGirolamo J.A.; Lees, W.J.; Nenov, A.; de Vivie-Riedle, R.; Braun, M.; Zinth, W. *J. Phys. Chem. A* **2008** *112*(51):13364-71.
- <sup>106</sup> Takeuchi S.; Tahara T. *J. Chem. Phys.* **2004**, *120*(10):4768-76.
- <sup>107</sup> Hyndman H. L., Monroe, B. M., Hammond, G. S. *J. Am. Chem. Soc.* **1969**, *91*, 2852.
- <sup>108</sup> Faure, S.; Stern, C.; Guillard, R.; Harvey, P. D. *J. Am. Chem. Soc.* **2004**, *126*, 1253.
- <sup>109</sup> (a) Dexter, D. L. *Chem. Phys.* **1953**, *21*, 836. (b) Forster, T. *Naturwissenschaften* **1946**, *33*, 166.
- <sup>110</sup> García-Martínez, A.; Osío-Barciana, J. *Encyclopedia of Supramolecular Chemistry*; Marcel Dekker: New York, 2004, pp 452-456.
- <sup>111</sup> Bryce-Smith, D.; Gilbert, A. In *Photochemistry Volume 25*; Royal Society of Chemistry: London; 1994, pp 190-200.
- <sup>112</sup> Kohlschutter, H. W. Z. *Anorg. Allg. Chem.* **1918**, *105*, 121.
- <sup>113</sup> (a) Cohen, M.D.; Schmidt, G.M.J. *J. Chem. Soc.*, **1964**, 1996. (b) Cohen, M.D.; Schmidt, G.M.J.; Sonntag, F.I. *J. Chem. Soc.*, **1964**, 2000. (c) Schmidt, G.M.J. *J. Chem. Soc.*, **1964**, 2014.
- <sup>114</sup> Cohen, M.D.; Schmidt, G.M.J.; Sonntag, F.I. *J. Chem. Soc.*, **1964**, 2000.
- <sup>115</sup> Cohen, M.D. *Angew. Chem. Int. Ed.* **1975**, *14*, 386.
- <sup>116</sup> de Loera, D.; Liu, F.; Houk, K. N.; Garcia-Garibay, M.A. *J. Org. Chem.* **2013**, *78*, 6626–6632.
- <sup>117</sup> (a) Garcia-Garibay, M.A. *Acc. Chem. Res.* **2003**, *36*, 491; (b) Garcia-Garibay, M.A.; Shin, S.; Sanrume, C. *Tetrahedron* **2000**, *56*, 6729.
- <sup>118</sup> Stopin, A.; Garcia-Garibay, M. A. *Crystal Growth & Design*, **2012**, *12*, 3792-3798.
- <sup>119</sup> de Loera, D.; Garcia-Garibay, M.A. *Org. Lett.*, **2012**, *14*, 3874.
- <sup>120</sup> Choi, T.; Cizmeciyan, D.; Kahn, S.I.; Garcia-Garibay, M.A. *J. Am. Chem. Soc.* **1995**, *117*, 12893.